2-1-2017

Vitamin a palmitate-loaded NLCs vs. SLN for cosmetic application with a study of their controlled release, skin permeation and characterization.

Sham Mohamad Ayman AlZahabi

The American University in Cairo

School of Science and Engineering

Vitamin A Palmitate-loaded NLCs vs. SLN for Cosmetic Application with a Study of their Controlled Release, Skin Permeation and Characterization

A Thesis Submitted to the

Chemistry Graduate Program

In Partial Fulfillment of the Requirement

For the Degree of Master of Science in Chemistry

By Sham AlZahabi

Bachelor of Chemistry

Under the Supervision of Professor Adham R. Ramadan

Acknowledgements

This thesis has not only been an academic journey, but one spurred with working with the most fascinating people who have been great support, and source of inspiration. This work was a challenge, as it involved many pharmaceutical aspects I was not previously acquainted with, and without the support of the many who contributed, it would not have been possible. The first person I would like to acknowledge is my endless source of inspiration, and the motive behind carrying out this project. A woman who believed in me, regardless of the fact I was not a pharmacist, and gave me the privilege to undergo a project that is of industrial importance to her: Dr. Yasmine Armaneous, CEO of EVA cosmetics. This project, however, would not have been carried out if it was not to the greatest Professor Dr. Adham Ramadan. I would like to thank him deeply for taking his time, effort, and support, and providing me with an academic idol that I have always and will always look up to.

There are so many people to thank and acknowledge, as this project has only come to life with their support. Dr. Osama Samuel, R&D Director at Eva Cosmetics is one of the most helpful, kind, and inspiring industrial scientists. I am very grateful for all his support, and time amidst his busy schedule. Furthermore, one man that has been pivotal, and a pillar stone in guiding me through all the technicalities of my practical work, is the brilliant Dr. Omar Sakr, CEO of NAWAH Scientific. He has been my savior in many aspects, and an endless source of support. Furthermore, there are many others who have contributed in the most beautiful way. I have learned from them, and got inspired by them as well. These include Mr. Romany (EVA), Dr. Nermin Salah (GUC), Dr. Hala Masoud (FUE), Dr. Hatem ElAyat (Statistics) and my dearest friend and colleague Omar Khairy.

Last but not least, I would like to dedicate this work to my great mother, who has been my pillar and back bone in everything I do. She has given me a very high role to look up to; a woman that is so dedicated, passionate, ambitious, and courageous, not afraid to explore with endless challenges, I have learned so much from you (mama)… and am very grateful to God for you, and everyone around me that has added so much to my life…

List of Abbreviation

Differential Scanning Calorimetry	DSC
Franz Diffusion Cell	FDC
High Pressure Homogenizer	HPH
Nanostructured Lipid Carrier	NLC
Prickly Pear	PP
Polydispersity Index	PDI
Retinyl Palmitate	RP
Trans Epidermal Water Loss	TEWL
Scanning Electron Microscope	SEM
Stratum Corneum	SC
Solid Lipid Nanoparticle	SLN
Transmission Electron Microscopy	TEM
Zeta Potential	ZP

Abstract

Nanostructured lipid carriers (NLC) are a new generation of Solid Lipid Nanoparticles (SLN), with improved drug loading capacity, stability, skin permeation, and sustained release of the encapsulated active. The encapsulation of vitamin A, a chemically labile cosmetic ingredient for anti-aging therapy, is ensued for effective delivery of the active. The method used for the production of the lipid nano-carriers is the hot homogenization technique. Furthermore, this study entailed a 2^3-factorial model design of experiment, where the three factors changed in the eight NLC formulation were surfactant to solid lipid ratio, Vitamin A Palmitate (RP), and prickly pear (PP) oil. The purpose of this study was to investigate the formulation and characterization of the NLCs, in an aim to find trends in changing the three factors constituting the matrix of the carrier on their exhibited characteristics, in order to arrive at an optimal formulation for the delivery of vitamin A to the skin in terms of particle size, polydispersity index (PDI), zeta potential (ZP), entrapment efficiency (EE%), *in-vitro* release and *ex-vivo* skin permeation.

The results attained from the parameters investigated were further analyzed using a statistical program, Design Expert. The particle size for the eight NLC carriers were in the range of 197.6 nm to 240.2 nm. The overall PDI for most of the formulations was lower than 0.3. The SLN had a much bigger particle size of 296.7 nm and PDI of 2.47. The release patterns in both *in-vitro* and *ex-vivo* showed differences in trends for the two types of carriers. The ZP of the formulations was not indicative of their predicted stability. Instead, the relative constitution of the solid to liquid lipid was pivotal in assessing the variation witnessed in both particle size and PDI upon storage for 6 weeks. The EE% showed a close dependence on the amount of PP oil in the matrix, where an equal or higher composition to the RP is required for effective incorporation. The thermal behavior assessed using Differential Scanning Calorimetry (DSC), of the 9 formulations

showed a similar trend for 7 NLC, where minimal transitions suggesting amorphous characteristics were observed. The remainder NLC formulation exhibited similar transitions to that of the SLN, suggesting a higher order of crystallinity. The lower melting point of the NLCs in comparison to the pure solid lipid is an indication to the incorporation of the RP within the matrix.

The total release of the *in-vitro* trials showed a close dependence on the amount of RP, where a higher composition of the latter lead to enhanced diffusion, and total release for the NLCs. The initial diffusion flux, however, was different and showed a close relation to the EE%. Formulations with high EE% showed a more sustained release, as opposed to more pronounced burst release exhibited by formulations with low EE%. The formulations that exhibited the highest *in-vitro* release were further assessed for skin permeation studies across a natural, rat skin membrane using Franz Diffusion Cell (FDC). The formulation with the higher surfactant ratio has shown higher permeation across the membrane, but lower skin retention. This was confirmed by slicing and extracting RP from various skin sections after the *ex-vivo* experiment. Imaging using Scanning Electron Microscopy (SEM) has also been performed on the SLN and NLC. Finally, changes in the constituting matrix of the nano-lipidic carrier gives wide variation in its properties, and hence allows it to be tinkered and adjusted for a particular use.

Finally, the NLC formulations, in general, exhibited differences in their respective assessed parameters, all showing an improvement compared to the SLN. The optimal formula consisted of a higher composition of all lipidic constituents, namely Vitamin A and PP oil content, and a lower surfactant to solid lipid ratio. Its choice was based on stability and EE% as the most important parameters. The exhibited particle size and PDI of this formulation was 236.8 nm, and 0.24 upon formulation, and 265.3 nm and 0.27 after storage for 6 weeks, respectively. The EE% was 95.1 ± 1.1%, ZP -32.87 ±0.25 mV and total *in-vitro* release was 43 ±7.3%.

Table of Contents

List of Figures

List of Tables

List of Equations

Chapter 1

Introduction

1. Introduction

Cosmeceuticals, a word coined by Dr. Kligman in 1984, is a new branch of cosmetic products aimed specifically to deliver functionally active ingredients via topical delivery, mainly for enhancing the skin's function, radiance, and look overall.[1] Bioactives derived from natural sources, include antioxidants, antimicrobial, ω-3 fatty acids, phytosterols, flavors and many more, are being used extensively in functional foods, cosmetics, and pharmaceuticals due to their added health benefits and safety as compared to synthetic materials. However, most bioactives happen to be lipophilic in nature, rendering themselves insoluble in water, as well as possess certain instabilities upon environmental stimuli such as light, oxygen and temperature variations during manufacture, storage, transport and/or utilization.[2] Consequently, certain measures have to be applied whilst handling of such bioactives in order to overcome their lack of solubility, stability and bioavailability. One of the prominent measures that can be applied to ensure the surpassing of the former drawbacks is nano-encapsulation of the bioactive in a Lipid Nanoparticulate systems such as Solid Lipid Nanoparticles (SLN) and Nanostructured Lipid Carriers (NLC).

Topical application of bioactives for various therapeutic purposes has been common since the time of the Pharaohs, where the application of oil extracts from plants, such as the lotus flower, was commonly used for moisturizing and skin protection effects.[3] However, the skin does provide an effective barrier against exchange of material with the surrounding, posing difficulties for formulating an effective formula that could penetrate to fulfill the required therapy. Therefore, the need for devising a successful formula for enhancing the permeation of the actives across the barrier has become of great importance in the cosmetic, and pharmaceutical field, for effective treatment.[4,5]

1.1 The Human Skin and Routes for Topical Therapeutic Delivery

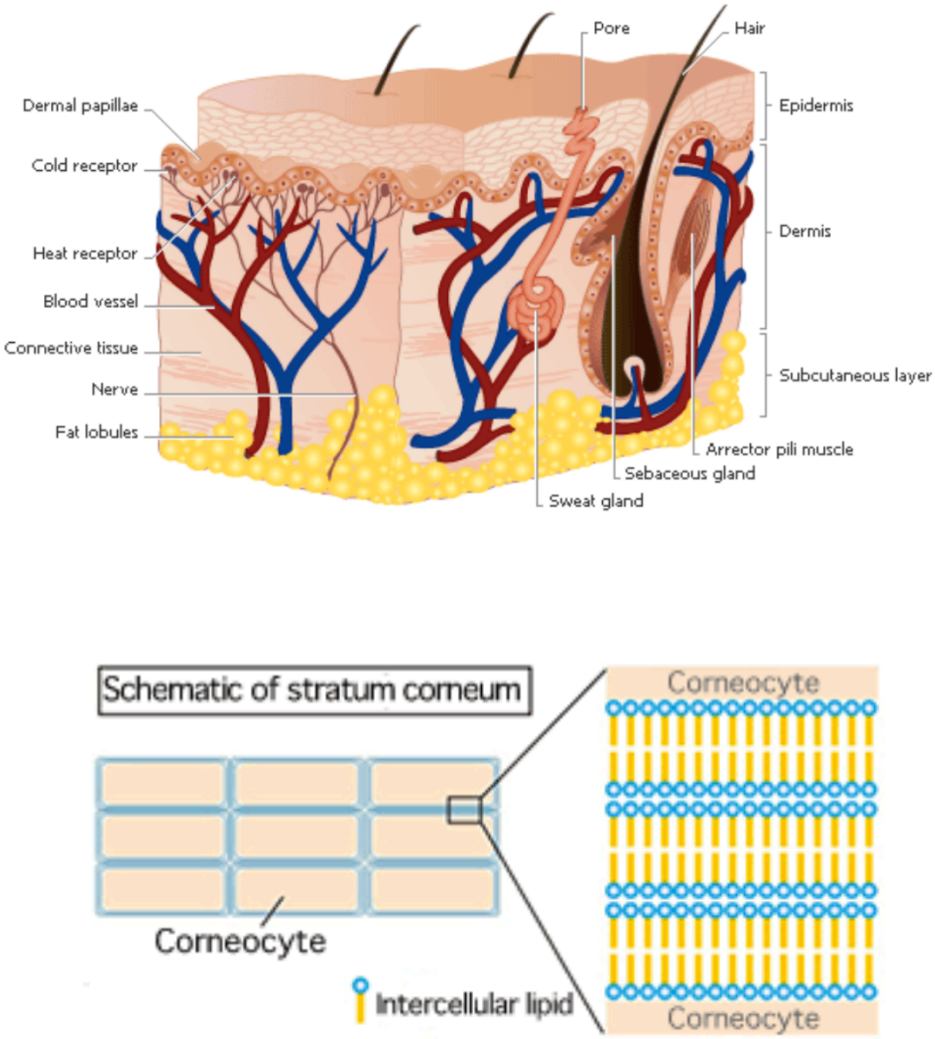

Figure 1. Skin Anatomy (top) and SC Composition.[6]

In order to devise an appropriate carrier system to deliver the actives successfully across the skin, an indepth understanding of the role of the skin and its anatomy must follow. Human skin is the largest organ of the body, constituting a remarkable surface area of 1.8-2.0 m^2, and therefore transdermal delivery of therapeutic ingredients either across the skin's barrier in case of systemic target, or within its copious layers for dermatological therapy, is a major target for optimizing drug delivery.[6] The skin constitutes three layers, the outermost epidermis, intermediate dermis and

innermost subcutaneous layer, as shown in Figure 1. Therapeutic actives or drug aimed to traverse the epidermis ought to diffuse through the intact stratum corneum (SC), which poses a challenge due to its inherent "brick and mortar" structure composed of cornceocytes and lipids,[7] making it difficult for actives to pass.[8]

There are three main routes recognized for permeation across the SC barrier, one is permeation across follicular pathways in the skin such as hair follicles and sweat glands. Although such a route offers a facilitated means of entry via the SC due to its openings at the surface, they only consistute 0.1% of the total skin surface area.[6] The second route is through the intercellular lipid region of the skin, which consists of a more flexible lamellar structure of amphiphilic molecules between corneocytes, allowing for transepidermal diffusion of lipophilic or amphilic moieties across. Hydrophilic structures can also diffuse, laterally, along the polar heads, or travel in between the corneocyte and lamella, as illustrated in the Figure 1. The third route consists of a less examined pathway because of its limited effect. It is the route across the hydrophilic cores of epithelial cells, traversing intracellularly across. This route only becomes meaningful in areas of poor lipid packing, which coincides with wrinkles on the surface, that can allow for a meaningful way to transport hydrophilic moieties across. The role of topical delivery mainly functions for the first two layers, inherent to the skin's barrier function, whereas the subcutaneous layer is responsible for body temperature insulation. Although protection of the skin from harmful UV rays can be accomplished by targeting the external epidermis layer, more elaborate functions such as those required to alleviate acne and aging signs require the actives to penetrate deeper layers of the epidermis and dermis. Nanocarriers offer a possible mechanism to facilitate permeation due to their inherent lipid based surface and small size. They allow more effective intercellular access

through the stratified epithelial layer,[9] as well as offer other benefits such as protection from degradation[10], and better control over release.[11]

1.2 Lipid Nano-Based Structure Delivery Systems

For many years, solid lipid matrices as a means of better controlled release of drugs, have been used.[11] It was a matter of time until such delivery matrix caught up with modern technology, and gradually become more and more optimized, with decreasing size and higher surface area to volume ratio, by moving from bulk, to micropellets,[12] up to the latest nano-particles. Almost twenty years ago, nanopellets were replaced with a more evolved generation of nanoparticles, SLNs.[13] They quickly became very popular as their means of production was relatively simple, hence industrial scaling up caught on quickly after. The techniques that were at first established include the use of high pressure homogenization, or microemulsion precipitation,[14] however the present state of the art for their production includes a wider variation that includes emulsification-solvent diffusion, solvent injection method, phase inversion, multiple emulsion technique, ultrasonication, and membrane contractor techniques.[11] SLNs led the way as a delivery vehicle due to their circumvention of difficulties posed by previous vehicles, such as the limitations incurred in liposomes and posed toxicity of polymeric nanoparticles (NP). This had to do with many advantages brought about by SLNs, such as their food grade excipients, and facilitated means of production. Furthermore, as with all technologies, there were drawbacks of SLNs such as limitations on drug loading capacity[15], drug expulsion by lipid polymorphic transition[16] and an inherently high aqueous constitution of the SLN dispersion (70-95%).[14] This resulted in a more evolved generation of nano-carriers, NLCs, where a mixture of solid and liquid lipids are used to allow higher EE%, prolonged stability, and finally higher particle concentration dispersion.[14]

1.3 PP Oil and Vitamin A Bioactives

Plant extracts have been widely used as topical applications for wound-healing, anti-aging, and disease treatments.[17,18] What all these plants share in common is that they are rich in flavonoid compounds with phenolic structures.[19] These phytochemicals, commonly referred to as antioxidants, possess a high reactivity with other compounds such as ROS (Reactive Oxygen Species), considered accelerators of the aging process,[20] in order to neutralize free radicals and deter aging symptoms. PP seed oil is rich in vitamins and antioxidants, remarkably in larger doses than the Argan oil that has been an attractive and popular ingredient in many cosmetic applications. These include linoleic acid, which is essential in stimulating healthy cell production and turn over, as well as vitamin E which provides protection and helps skin retain moisture, and flavonoids which are anti-inflammatory.[21] The added light feel and high skin absorption of PP seed oil contributes further to its aesthetic attributes. When interviewed by Elle magazine, Dr. Joshua Zeichner, dermatologist at Mt. Sinai Hospital in New York City confirms that PP seed oil "soothes, hydrates, and reduces inflammation that damages collagen, explaining why it's used to prevent skin aging".[22]

On the other hand, vitamin A is a promising active for the treatment of anti-aging, and plays many important roles in skin therapy for various skin disorders.[23] These include epidermal cells renewal, extracellular matrix production, inhibition of UV-induced extracellular matrix degradation, cytokine modulation, oxidant/antioxidant, sunscreen effect, prevention of UV-induced vitamin A deficiency, and malonocyte function modulation.[24] All these benefits should make vitamin A a superior bioactive in dermatology, and anti-aging cosmetic applications. However, its poor water solubility, high chemical/photochemical instability, and induced skin irritation, render it less practical in cosmetic and medical formulations.[23] Different possible

approaches are conducted to overcome these limitations, such as the use of less irritating and more stable retinoid derivatives or using a low concentration in the formulation.[21] One effective possibility is its encapsulation within a lipidic carrier, such as SLN or NLC, resulting in higher stability, improved targeting and enhanced efficacy for skin disorder treatments.[23]

The admixture of PP oil to vitamin A could generate several advantages to the formula. In many reports, the addition of liquid oil in the SLN formulation has shown a remarkable improvement of the drug loading capacity. Consequently, the stability of the formulation will also increase since less of the vitamin A is exposed to the aqueous dispersing medium.[26] This could also be explained by the fact that oil solubilizes bioactives to a greater extent than solid lipids.[27] Other studies have shown enhancement in both photostability and encapsulation efficiency of the SLN-vitamin A when adding antioxidants, such as vitamin E.[28] The radical scavenger, antioxidants, prevent the degradation of vitamin A by oxidation.[29] PP oil, which is rich in antioxidants such as tocopherols, with a high content of linoleic acid, is aimed to improve the encapsulation, stability, and drug localization of the NLC formulation on the epidermis.[30]

1.4 Leading Brands in Nanocosmetics

In 1987, the first cosmetic product constituting nanotechnology was introduced to the market by the famous French brand, Christian Dior, in their cream named *Capture*, an anti-aging face gel. Lancôme, a luxury sister company of the cosmetic giant L'Oréal,[108] later followed with the first nanoparticle product, an anti-aging cream consisting of pure vitamin E nanocapsules, for maximizing the bioavailability and stability of the active. Ever since, a boom in the field followed due to the ascertained efficiency of such optimized, nano-delivery systems, where L'Oréal designated an unmatched budget of $600 million dollars to further research, making it rank as one of the top patent holder in the field.[4] Figure 2 enlists some of the leading brands in nanocosmetics,

and their corresponding market share as estimated by the number of patents issued, as revealed by Espacenet.[12] Starting with anti-aging gels and creams, nanotechnology has now become applied in almost all of its products, such as nail polish, perfumes, aftershave, sunscreens, shampoos, make-up and more.[31]

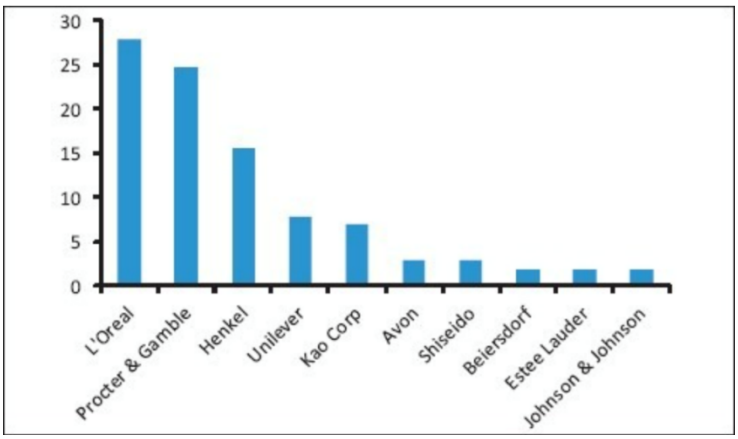

Figure 2. Ranking of Top 10 Cosmetic Companies based on Nano-related Patents.[4]

Nanocosmetics achieve two imperative benefits simultaneously: aesthetic appeal, and high efficiency. Due to the intrinsic nature of the small sized particles, an increase in surface area for the same quantity is achieved, which means an improved delivery of the actives in the formula while minimizing the risks of compromising the formula's sensory attributes. The pursuit of any topical therapy formulation is to either assist in the regulation of the barrier function of the skin, or to deliver an active to one within, with minimal systemic engagement.[5] The barrier function of the lipid layer in the SC traps water molecules within to prevent their loss, so as to minimize skin dehydration (trans epidermal water loss, TEWL) while retaining other natural moisturizing factors from leaching out, as well as preventing chemical or biological irritants from entering. Nano-carriers used for topical therapy can lead to consumer perceivable benefits such as skin cleansing, hydration, protection, care or enhancement.[5] Optimizing the formula intended for cosmetic use

means studying the optimal release rate, control over release, encapsulation efficiency, skin permeation and its stability.

Chapter 2

Literature Review

2. Literature Review

2.1 SLN/NLC as Effective Carriers of Drugs and Bioactives

Lipid nanoparticles (SLN, NLC) have shown escalating interest in pharmaceutical applications since the beginning of their development in the early 1990s. They are now considered good candidates in parenteral, peroral, dermal, occular, and pulmonary administration, where Parkeike, Hommoss, and Müller, review their various potential applications.[13] Their possible application in dermal delivery for both pharmaceutical and cosmetic intentions had significantly increased over the past decade, with several reviews devoted to elucidating their potential as dermal carriers for therapeutic agents. In one review, Müller, a leading scientist in the field of lipid nanoparticle delivery, highlighted the advantage of using SLNs for controlled drug delivery as a replacement for traditional colloidal carriers, namely emulsions, liposomes and polymeric micro- and nanoparticles.[11] He went on further to expose the biocompatibility of the lipidic excipients used in the vehicle, along with their cost-efficient mechanism of production using high pressure homogenization. Other advantages specific to SLN topical application as in cosmetics, is their small particle size that adheres to the skin surface forming a thin film that prevents TEWL, consequently increasing hydration. In his review, Müller also explained the mechanism of drug incorporation and how it relates to the degree of crystallinity of the lipid carrier, clarifying the link between increase in packing density and thermodynamic stability, with decrease of drug incorporation rate. However, he also added that the addition of emulsifiers and the inherent small size of the particles does work in favor of the formula, impeding drug expulsion.

In another review devoted to SLN, Menhert and Mäder presented the modes of production, means for characterization and application.[32] The key advantages of SLN are highlighted in their possibility to control drug release, by locking them in within the solid matrix and hence

immobilizing them, along with their biocompatibility and ease in large-scale production. The general ingredients are also specified, such as fatty acids, waxes, and steroids as options, along with any type of surfactant, noting a prolonged stability if a combination surfactant system is used. Characterization of the SLN in terms of particle size and ZP, degree of crystallinity and lipid modification as well as investigation on the possible coexistence of additional colloidal structures such as micelles, liposomes, and such are highlighted as key factors in understanding the stability and release kinetics of the formula. In the case of coexisting colloidal species, lecithin, a possible excipient in lipidic carriers and a key ingredient in the investigation reported in this thesis, is said to form liposomes. Furthermore, they also mentioned a personal account on a study conducted on their part on SLNs which revealed that the drug, nitroxide, was being incorporated in micellar structures instead of within the wax of the SLN carrier.

The potential of encapsulating bioactives as caretonoids, a precursor of vitamin A, omega-3 and phytosterols, has been investigated in another review by Weiss et al., as a means of enhancing nutraceuticals, specifically functional foods.[33] The SLN vehicle is highlighted as a prominent candidate in delivering lipophilic bioactive compounds, as they get solubilized within the solid lipidic core of the carrier. An increase in the bioavailability of the encapsulated bioactive is feasible due to the nanosized particles with a high surface area to volume ratio, thus increasing their adsorption capacity onto the targeted site. The composition of the lipid matrix is shown to play a decisive role in determining the properties and structure of the SLN. The choice of lipid can influence the manufacturing process in terms of temperature during homogenization, post cooling rates and the crystallization temperature of both the bioactive and lipidic matrix. This in return will play a pivotal role in the overall structure of the final SLN matrix along with its respective loading capacity. The crystallinity of the matrix can be decisive in determining the capacity of the SLN

formula of withholding the bioactive, where a lower expulsion rate is claimed for heterogeneous lipids.

SLN for topical drug delivery has been specifically tackled in another review by Zang, Purdon and Smith where they illustrated the current understanding of the SLN-mediated skin penetration and proposed possible mechanisms for the SLN-skin interactions.[35] There are three mechanisms illustrated, as shown in Figure 3. The first one includes an intact penetration of the SLN through the SC, although suggested to be a less probable case, but more so in follicular and gland duct openings, as shown in (a). This mechanism is claimed to have an advantage in releasing the bioactive or drug in a controlled manner, maintaining a threshold concentration in the epidermis and dermis layers of the skin for a set period of time. This thereby eliminates the need for repeated dosage intake, as it reaches the same target therapeutic dose over a prolonged period of time. A second mechanism uses the inherent features of the SLN matrix, such as surfactants and lipidic structure, that act as penetration enhancers, and thus allow for the permeation of the SLN lipids into the SC where they may release the active then, as shown in (b). The last mechanism conveys a gradual disintegration of the SLN carrier to release the bioactive on the surface of the SC, without permeating within, as the drug partitions away from the lipid matrix and into the skin independently, as shown in (c).

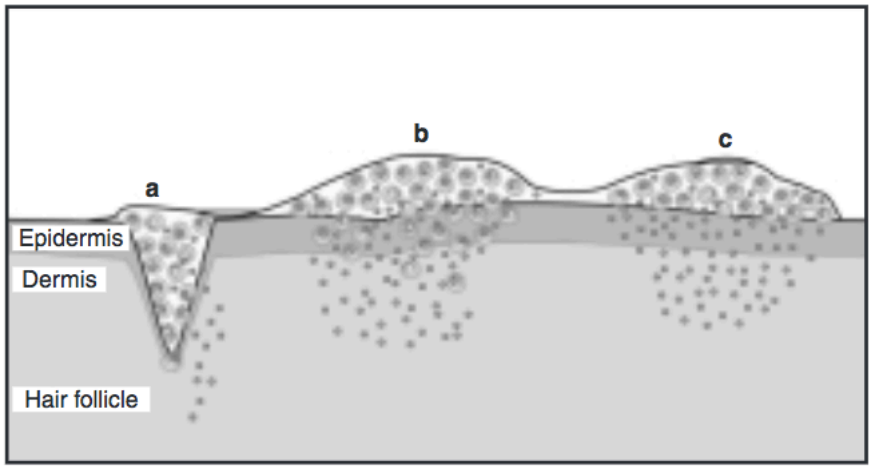

Figure 3. Skin penetration mechanism of SLN.[35]

The dermal application of lipid nanoparticles, both SLN and NLC, for cosmetic and pharmaceutical products was reviewed by Parkeike, Hommoss, and Müller.[13] The two carriers are distinguished from one another by the constituting lipids in the solid matrix, where NLCs possess a less crystalline order by the incorporation of liquid oil, enhancing the loading capacity of the carrier. The way to incorporate the SLN or NLC dispersion in existing commercial products as creams, gels, or lotions, is depicted by substituting a percentage of the water phase of the product with the dispersion. An increase in hydration due to the reduced TEWL induced by the carriers is also noted, which is attributed to the occlusion factor of the lipid nano-carriers. The strength of the occlusion of the carrier is related to both the particle size and lipid concentration, where an increase of occlusion is noted with decreasing particle size and increasing lipid concentration. Finally, lipid nano-carriers are claimed to be "nanosave" carriers as they do not exhibit any cytoxicity as confirmed by several studies reported.

The occlusive effect and penetration ability of SLN and NLC were further studied by López-Garcia and Ganem-Rondero.[36] An *in-vitro* set-up to measure the occlusive effect was used, where the procedure entailed the measurement of the amount of water evaporated through a filter

paper that had empty nano-lipid dispersions, in comparison to a reference blank. The difference in the occlusion effect of both SLN and NLC was reported to be statistically insignificant, as well as the difference in their respective induced TEWL. The film formation of the nanoparticles was examined on pig skin using SEM, as shown in Figure 4. Furthermore, SLN/NLC encapsulating Nile Red, a lipophilic stain, was ensued for the measurement of penetration into pig skin following a FDC set-up. The results showed a 2.7 fold increase in penetration for NLC, concluding that the occlusive factor cannot be indicative for the efficiency of the drug permeation. They also note that the composition of the lipid matrix plays a key role in drug permeation, due to the difference in interactions between the lipids and skin components. Finally, it was argued that ZP was pivotal in determining the stability of lipid nanoparticles. The determining factor for these carriers is the specific molecular arrangement that the lipids exhibit in the external layer of the carrier, along with their interaction with stabilizers, such as surfactants. For their samples, the ZP was reported to be lower than the threshold value of $\pm$30 mV required for stability, with values of -7.5 and -11.1 for SLN and NLC, respectively. There was no significant increase in PDI and ZP noted upon storage. This conferred stability was related to the steric hindrance induced by the stabilizer used, a non-ionic block co-polymer, preventing the lipid particles from coalescing.

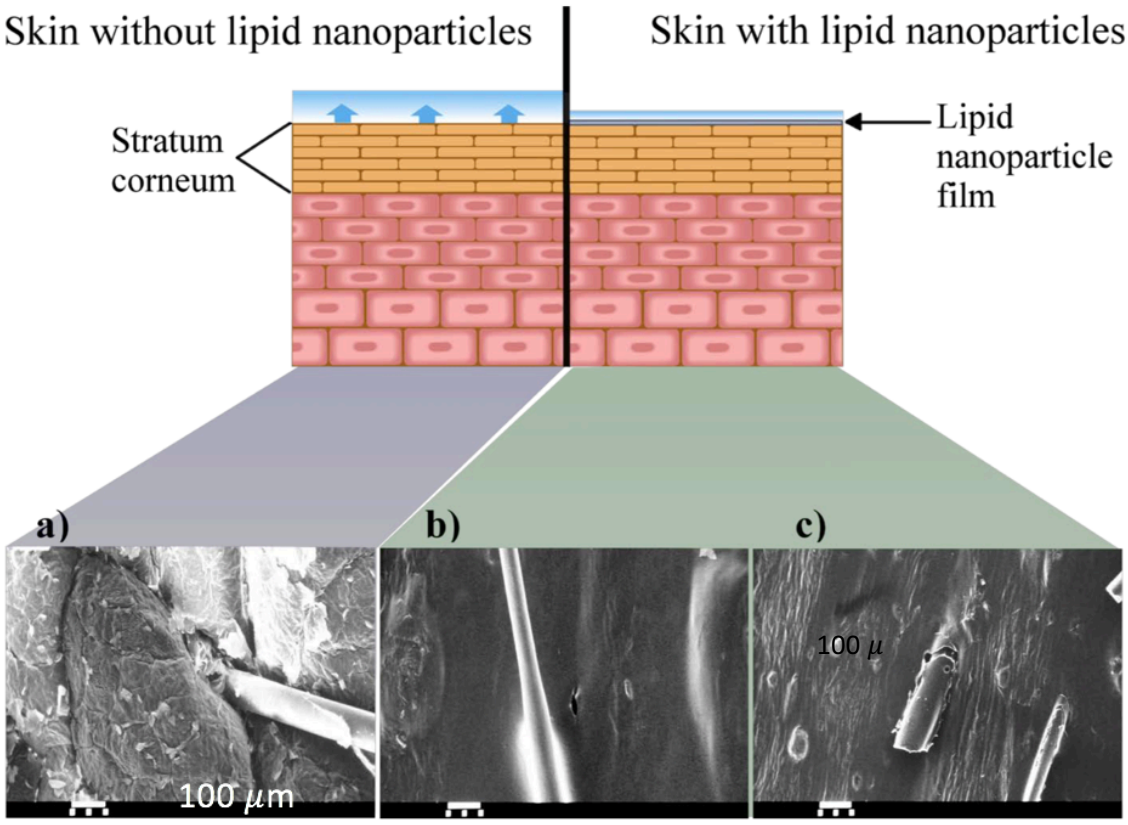

Figure 4. SEM images of untreated pig skin (a), with SLN (b) and with NLC (c).[36]

In a study conducted by Liu, Wu and Fang, vitamin K1 was delivered using SLN nanoparticles for peroral administration.[37] The formula of the SLN was optimized by screening different types of lipids, and surfactants, both hydrophilic and hydrophobic, where the highest stability and smallest size of the resulting lipidic nano-carrier is pivotal in the choice of the best formulation. Statistical analysis of the experimental design was ensued to obtain a regression equation for describing the relationship between the surfactant system and the particle size of the SLN. The combined system of emulsifiers was used to stabilize the dispersion by forming a film around the particles. The method of production of the SLN included ultrasonic emulsification, and the relationship between the time needed for the melt to be homogenized on one hand, and the EE% and particle size of the optimal formula on the other, was also investigated. The higher time

in homogenization showed a decrease in particle size, but no correlation to EE% was found. Further characterization was carried out using TEM and DSC, where the latter helped in the evaluation of the lipid crystallinity. The values of the crystallinity of the SLN with and without vitamin K1 showed no significant differences, thus indicating that the encapsulation did not affect the lattice arrangement in this case.

The drawbacks of SLN have been addressed by the evolution of a new generation of lipid nanoparticles, namely NLC, with several reviews devoted to discussing the difference between the two. In a review by Müller, he explains the cosmetic and dermatological preparations of the two carriers, along with other features intrinsic to the carriers such as the occlusion factor induced due to the film formation upon applying the dispersion on skin.[38] Müller explains the reason behind the higher loading capacity and increase in stability of the NLC compared to SLN, which he specifies as pertaining to the nanostructured feature induced in the former by mixing a liquid lipid within the solid matrix. The lack of crystallinity of the NLC can be confirmed by DSC analysis. Müller goes further to explain an important active in pharmaceutical application, retinol, a derivative of Vitamin A. He states that since the solubility of the hydrophobic retinol is higher in liquid oil, when incorporated into a solid matrix, it will form oil nano-compartments. These nano-compartments would still be able to control the release of the vitamin through being surrounded with a solid matrix. Furthermore, he depicts an increase from 1-5% retinol in the formula when using NLC carriers instead of SLN, for successful incorporation and stability.

In an effort to illustrate the enhanced stability of the SLN carriers, Ghanbarzadeh et al. conducted a study for encapsulated hydroquinone active for dermal delivery.[39] The bioactive is of a hydrophilic nature, which retards the absorption through the lipidic skin layer. The encapsulation using SLN has shown successful incorporation of the bioactive within the vehicle. The optimized

formula exhibited a particle size of 86 nm and EE% of 89.5%. *Ex-vivo* permeation studies with rat skin mounted on a FDC revealed a significant deposition of drug localized on the skin, with minimal systemic absorption. The latter was correlated with the amounts of drug analyzed in the receptor compartment of the diffusion cell. About 3% release was found for the drug from the SLN formulation, compared to almost 3-fold higher concentration for the hydroquinine gel control. The amount of drug localized onto the skin is also quantified, where the permeated skin area is excised after the incubation, cut into smaller pieces, and added in methanol for drug extraction. The results show a significant improvement in drug localization in the case of SLN, compared to the control, with twice the concentration of drug found in the former case. The SLN has also shown an occlusive effect due to the small size and lipidic nature of the carrier that adheres to the skins surface. Other factors mentioned include solubility and permeation enhancement. This effect improves skin delivery of actives, and effectiveness of intended therapy by the formula.

Another study was conducted by Kushwaha et al. to encapsulate hydrophilic moieties using SLN carriers.[40] The drug, raloxifene hydrochloride, is aimed for oral use, and functions in a similar fashion to hormonal estrogen as means of alleviating menopausal symptoms. An optimization procedure was ensued to arrive at the best formulation, where different surfactants were screened and the final formulation was assessed based on its particle size, PDI index and ZP. The EE% was all within the range of 55 to 66%, showing a relatively lower value than the previous work on hydroquinone, which can be attributed to the increasing hydrophilicity of the raloxifene hydrochloride. The SLN nanodispersion separation from the supernatant solution was conducted using ultra-filtration nanosep centrifuge tubes, with membrane having a weight cutoff of 100KD. Centrifugation was carried out at 5,000 rpm for 15 minutes, at a temperature of 4°C. Further characterization was conducted such as *in-vitro* release using a dialysis bag diffusion technique.

The release of the SLN exhibited an initial burst release in the first three hours, followed by a more sustained pattern onwards. This behavior is attributed to drug being adsorbed on the surface of the SLN in the former case, which quickly gets released, as opposed to the ones encapsulated within, immobilized by the surrounding solid lipids. Other techniques used included FTIR and DSC in an effort to assess any possible interaction between the lipid and drug as a result of encapsulation, which was shown to be none-existent in the former case, but did show a broadening of peak in the latter case. This is explained by the transformation of the drug from crystalline to amorphous as a result of drug encapsulation.

In another review by Müller devoted solely to NLC carriers in cosmetic dermal products, he elaborates on their effectiveness as cosmetic excipients.[41] Their benefits include prolonged stability of the active, inherent film formation upon application that can lead to improved skin hydration due to the occlusion factor, as well as improved bioavailability. Müller specifies that the nature of the crystalline lipid in SLN as being a limiting factor for a high loading capacity for the active. This is due to tendency of the SLN for drug expulsion as a means of transforming it into a more crystalline form. Hence, the imperfect crystalline nature of the NLC is a pivotal factor in its improved loading capacity compared to the more crystalline SLN. The stability of the SLN and NLC matrices can be directly inferred from DSC measurements along various time intervals, where a comparison between the initial enthalpy measurement and that after a period of time can give an indication to the percentage of particle remaining intact. Furthermore, NLC concentrates as cosmetic excipients are reported to be commercially available. The essential fatty acids in the oil, such as linoleic acid, is said to exhibit improved skin appearance, elasticity and barrier functions.

An extensive study was conducted to illustrate the various features of SLN and NLC carrying psoralen drug, used for treatment of skin disorder, by Fang, Liu and Su.[42] The study presented an optimization procedure used to assess the best formula, with the type of surfactant being the independent variable. The aim was to devise a formula with the best permeation and release kinetics for effective therapy of Psoriasis. The SLN and NLC carriers were produced using the hot homogenization method where the lipid and aqueous phase were prepared separately, heated to about 85°C before adding the latter onto the former and dispersing them using a high-shear homogenizer, followed by sonication for 10 minutes. Upon particle size characterization, it was confirmed that SLN exhibited a significantly higher size than NLC particles, where the SLN had a size of 296.6 nm in comparison to 210.2 and 172.7 nm of the two NLC dispersions formulated constituting different surfactants. An increase in viscosity was also witnessed for the SLN formulation, correlating this effect with an improved strength of the film forming due to the crystalline nature of the solid lipid. An enhancement of drug delivery was explained by the increase in contact between the lipid carriers and SC as a result of the fine-particle size and high surface area. Surfactants are also claimed to fluidize the SC, acting as permeation enhancers, to allow more drug to permeate through the brick and mortar barrier like SC, and into the intended site of delivery. Finally, NLC did show an improved drug permeation and release kinetic profile, with a higher total release, almost two folds as much released from SLN, and higher permeation flux, indicating that it is a superior vehicle to SLN.

The development of both carriers, SLN and NLC, to encapsulate clotrimazole, a lipophilic drug, was carried out by Souto et al. in an effort to assess their respective physical stability, EE% and *in-vitro* release kinetics.[43] The lipid carriers were produced using the hot homogenization technique with a High Pressure Homogenizer (HPH). For EE% measurements, the lipidic particles

were separated using centrifugation. This was followed by spectrophotometric analysis of the drug in the supernatant at a previously known λ_{max}. The release was carried out using a FDC with artificial membrane, cellulose nitrate, placed between the receptor and donor compartment. The number of total formulations were three, where the first two were SLN structures with varying lipid and drug content, and the third an NLC with an added oil constituent that replaced 30% of the solid lipid content of the SLN with higher lipid content. The results of the *in-vitro* release showed a dependence on the drug concentration in the lipidic carrier, where a higher release was observed for lower drug concentration. This was attributed to the drug-enriched shell model that formed, as compared to an enriched core, when low drug concentration was used. Furthermore, the fastest release was observed for the NLC formula, which is related to its liquid component, and found to be 26% in comparison to 24% and 22% of the two SLN formulations. Finally, NLC showed higher EE% and stability, maintaining an EE% greater than 60% which is not the case for SLN, although a lower occlusive capacity in comparison to SLN with the same lipid content was found.

2.2 Vitamin A loaded SLN/NLC

Vitamin A is a highly effective therapeutic bioactive that exerts beneficial treatments against several skin disorders, such as acne, dermatitis, and aging, hence enabling its use as an effective cosmetic ingredient. The poor solubility of vitamin A, however, makes it less available for skin targeting, along with its chemical fragility against oxidation. Lipid based carriers have been subject to increasing interest due to their potential in addressing all the previous exhibited drawbacks. In one study aimed at further increasing the stability of all-trans retinol (AR), a vitamin A derivative, Jee et al. accomplish their aim by adding another excipient to the formula, namely lipophilic antioxidants.[27] Initially, an optimization procedure was used where both the amounts

and ratio of the surfactants were altered, until reaching an acceptable ZP and particle size, about -30 mV and 100 nm, respectively, for prolonged physical stability of the dispersion. The optimized formulations were then irradiated with a 60-W bulb and the extent of vitamin A degradation was monitored with HPLC measurements. Very surprisingly, however, the rate of degradation of the AR was higher when encapsulated in the SLN vehicle, as opposed to the intact AR control. This was claimed to have contradicted previous works, as well as overall assumptions of SLN protective functions. In light of their contradicting results, the investigators attributed their findings to the lipid system used in the SLN that might have been more prone to auto-oxidation, forming lipoperoxyl radicals that would be scavenged by AR and consumed in the process. Finally, the stability of the AR-SLN system was shown to be substantially improved when co-loading antioxidants, such as BHT-BHA, and tocopherol.

In an investigation by Argnimón et al. the effect of the carrier on the improvement of the chemical stability of the vitamin was concluded.[44] The SLN-RP dispersion was formulated with hot homogenization, using HPH, where three cycles at 1000 bar were ensued. The dispersion was then freeze dried, and the powder used for further characterization. EE% was determined by dissolving SLN-RP in isopropyl alcohol, and further analyzed using UV-vis spectroscopy to determine the concentration of SLN with respect to the total RP added, where a mean EE% of 90.7% was found. The investigation of the conferred protection of the SLN was then studied by monitoring the concentration of RP over 10 days at room temperature, in comparison to free-vitamin A suspension in surfactant media, with 50% degradation found for the former in comparison to a higher rate of 80% for the control. Thus, the SLN showed an improved protection on the vitamin with less degradation compared to the latter.

In another effort to convey the conferred protection of SLN vehicles against photo- and thermally induced degradation, Sapino et al. prepared RP loaded SLN in an ethyl cellulose gel for evaluation.[10] Three types of solid lipids were used, namely, cetyl palmitate, glyceryl behenate, and palmitic acid, using the hot homogenization technique for production of the SLNs. The RP was added to the lipid phase after melting, and the temperature was maintained throughout the procedure at 65°C to prevent RP degradation. The SLN dispersion was then added to the hydroxyethylcellulose gel, which was then irradiated with UVA and UVB lamps for photo-degradation studies. A controlled RP dispersed in the same gel was used for comparison. The samples withdrawn were first diluted with methanol, centrifuged, and then analyzed using UV-vis spectrophotometer at λ=323 nm. The results of the irradiation tests showed a significant improvement in protection of the SLN against degradation, in comparison to the free RP gel dispersion. However, differences in the percentage degradation of the vitamin were observed for the different lipid constituents, which was explained by the difference in polarity between the lipidic core and the aqueous medium. This results in variations at the interface between the two moieties, increasing the partitioning of the vitamin into the aqueous dispersion in cases of reduced interfacial tension of the more polar lipid, and hence increasing their degradation. The order in increasing protection against degradation conferred by the lipid constituents was cetyl palmitate > glyceryl behenate > palmitic acid. This protective action induced by the SLN vehicle was attributed to possible light scattering effects by the carrier lipid matrix. It was also noted that the addition of radical scavengers such as vitamin E, and anti-oxidants can help impede the photo-degradation process of the RP, as they consume the oxygen radicals that could possibly react to degrade the vitamin. Furthermore, the degradation of the three SLNs and the control at 25 and 40°C after 30 days incubation in the dark was investigated. The results revealed an improved protection, with

higher concentration of RP found after the incubation period, where only 20-40% degradation was witnessed in all three SLN formulations as compared to a 70-80% loss of the RP in the control. Finally, it was confirmed that a higher loading capacity of the retinoids was observed when mixing a small amount of liquid oil in the solid lipid matrix, and that a higher EE% improves stability as less RP is exposed to the aqueous medium.

Vitamin A-loaded SLNs for topical use were synthesized by Jenning, Korting and Gohla, where the drug release properties were the main focus of the preparation.[16] Since vitamin A is an irritant, its sustained and prolonged release is a target for cosmetic formulators. The EE% of vitamin A, due to its high insolubility in water, was assumed to be 100%. The release set-up consisted of a FDC, with artificial membrane, cellulose nitrate, soaked with a lipophilic surfactant, isopropyl myristate, which is used to simulate the properties of the SC. Samples from the receptor cell were withdrawn in 6 hour intervals over one day, and later analyzed using HPLC, to study the release profile of the SLN. A nano-emulsion of similar size to the SLN dispersion was used as a reference, and the release profile did show significant variations between the two. A burst release was observed for the nano-emulsion, releasing higher amounts of vitamin A for the first 6 hours in comparison to SLN. On the other hand, the SLN did show a more consistent and controlled release profile at first, followed by a higher flux that exceeded that of the nano-emulsion after 12 hours, confirming the previously claimed high EE% of the carrier. This high flux in the release profile in comparison to the nanoemulsion was explained in relation to polymorphic transitions that took place in the lipidic excipients of the SLN, which were monitored using X-ray diffraction and DSC studies. This SLN dispersion underwent an initial gelation process as water evaporated, followed by polymorphic transitions that eventually lead to drug expulsion, since the latter crystalline form cannot accommodate the drug as well as the previous. This now expelled vitamin

A will be in contact with water in the receptor phase, causing an increase in thermodynamic activity due to its inherent hydrophobicity, and resulting in a higher diffusion velocity. This was confirmed when the SLN nanoparticles were dispersed in a buffered solution instead of distilled water as in the original formulation, showing a similar release profile to that of the nano-emulsion. Retinyl Palmitate (RP) loaded SLN were synthesized in order to compare with other investigations conducted on retinol, and a higher stability of the dispersion for the former was observed, that could explain the slower flux in release. However, it was noted that SLN-RP dispersions exhibited prolonged stability in storage, as they were less sensitive to aggregation.

In another study, Jenning, Gohla, Gysler and Schäffer-Korting studied the drug targeting mechanism of SLN dispersions on the upper skin along with their occlusive properties.[45] The use of lipid carriers to encapsulate irritant drugs such as vitamin A reduced their irritancy due to their controlled release profile, along with minimizing their uptake by the blood. Penetration studies were conducted on a Franz flow-through cell using adult Yucatan pig skin. After the 24h incubation, the skin was frozen and then sliced horizontally into different sections so the retinol can be extracted from different skin depths. The highest content of retinol was found at the upper most layer of the skin, which represented the SC and higher layer of epidermis. The amount of retinol detected in deeper parts of the skin increased with time for the SLN dispersion, as opposed to nanoemulsions that gave no change in the extent of their permeation with time. This was explained by the mechanism of the SLN forming a film, and gelling as a result of water loss. This gel-film forming on the surface would act as a barrier to prevent TEWL, and by enhancing occlusion, allow for the retinol to permeate deeper into the skin. Simultaneous polymorphic transitions of the lipid carrier take place, expelling the retinol at a higher pace, which is witnessed by a loss of controlled release from the carrier. Furthermore, light microscopy was used for

confirmation of any structural changes in the epidermis as a result of applying the SLN-retinol dispersion. A comparative study was ensued on the morphology of skin following application of SLN enriched cream, SLN-free cream, and untreated skin as reference, for further evaluation of occlusive effects. The images retrieved from light microscopy, in Figure 5, showed a thickening of the SC as the nanoparticles perturbed the lamellar arrangement of the skin's lipid structure. Swelling was also observed, due to the occlusive effects that led to increased hydration for the SLN applied skin (C) in comparison to the untreated skin (A) and SLN-free cream treated skin (B). Finally, SLN dispersions in an oil in water emulsion showed an improvement in retaining the drug by impeding the polymorphic transition of the lipid, the driving factor behind drug expulsion.

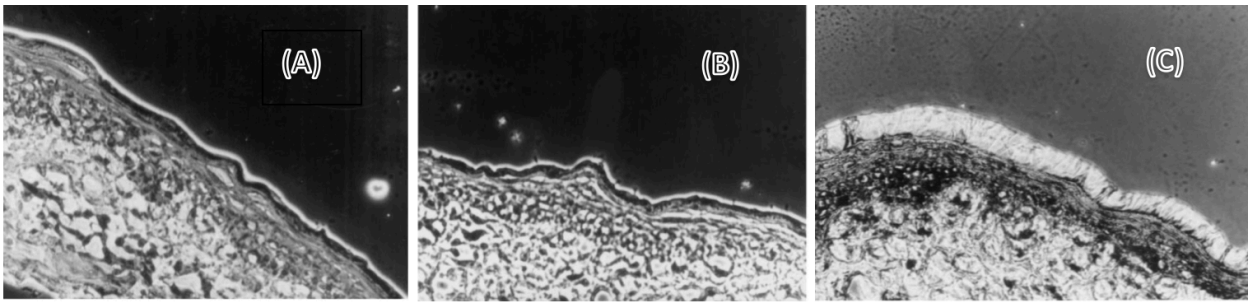

Figure 5 Images of vertical section of skins using light microscopy where (A) is untreated (B) treated with SLN-free cream and (C) treated with SLN containing cream.[45]

Jenning and Gohla attempted to compare the three main derivatives of vitamin A, namely: tretinoin, retinol and RP in terms of encapsulation efficiency in SLNs.[46] This was ensued in an effort to get a deeper understanding of the underlying mechanism of drug incorporation within the SLN. The study also included an attempt for devising a new method to evaluate EE%. This method included kinetic analysis of the decomposition rate of the different forms of retinoids in water and in an oil phase. Other methods included polarized light microscopy for detecting expelled drug crystals, and the use of DSC for determining variations in the melting point of the lipids as a result of drug expulsion. Although all three methods, DSC, light microscopy and kinetic study, do not

give a quantifiable percentage on the loading capacity, as this is only possible by actual separation of the lipid from the supernatant, however, they were conducted in an effort to understand the inclusion mechanism of the retinoid within the SLN matrix. A mechanism proposed for low melting point drugs in comparison to that of the solid lipid, such as RP, is that they tend to distribute on the surface of the carrier, forming a shell enriched type SLN. Furthermore, a correlation between the lipid's crystallinity and its EE% was also explored, where the metastable polymorphic β' is claimed to have a higher capacity for incorporating drugs due to more defects in its crystalline structure in comparison to the more crystalline β form. Finally, the addition of a liquid lipid component in the formula allowed for a higher loading capacity of the retinoids.

With an aim to compare the effect of different carriers encapsulating RP on skin permeation, Clares et al. went about developing three carriers, namely nanoemulsions (NEs), liposomes (LPs), and SLNs.[47] The study focused on highlighting the features of these three carriers in terms of skin permeation, stability against photo-degradation, and biocompatibility. Further characterization was ensued to assess particle size, ZP, pH, EE%, and morphology. The permeation was conducted using a Franz-type diffusion cell, with a mixture of alcohol and ether as the receptor medium, and human skin as the membrane. The amount of RP remaining on the skin was quantified by sonicating the skin exposed in the donor cell with the same receptor medium mix as the extracting solvent, followed by centrifugation, and finally HPLC measurements of the supernatant. The results showed a much more pronounced flux of permeated RP for NEs compared to the LPs and SLNs. This was explained by the comparably small size of the NEs, giving higher surface area for interfacial interaction, which facilitates the drug absorption through the skin. Another reason is the presence of surfactants in the emulsion system, as this fluidizes the lamellar lipidic structure of the SC. In addition, the NEs themselves exhibit intrinsic fluid-like behavior,

thus acting as permeation enhancers. It was also noted that formulations with negative charge are less easily permeated into the skin due to the inherent alike charge of the mammalian skin induced by the presence of anionic molecules as cholesterol sulfate. This could be another reason for the increased flux of less negative NEs in comparison to SLNs and LPs. Furthermore, the retention of RP on the skin showed a significant reduction for NEs and SLNs as compared with LPs. The biocompatible phospholipids as main constituents of LPs are claimed to be the reason behind their more likely retention on the skin. Furthermore, SLNs did exhibit improved photo-protection along with higher EE% as compared to LPs. The reason for the higher EE% was attributed to the vesicular structure of the LP carrier, with aqueous chambers within it that hinder the proper incorporation of the highly hydrophobic RP. Finally, it was noted that in the light of cosmetic delivery carriers, a high flux across the skin barrier is not needed as for percutaneous drug delivery, where an improved skin retention property is instead needed for effective therapy.

Mélot et al. investigated the penetration enhancers in delivering retinol through the SC.[48] Chemical penetration enhancers alter the barrier properties of the SC by either disrupting the lipid structure of the membrane or by enhancing the drug solubility within the skin. An *in-vivo* monitoring of the permeation of trans-retinol was quantified for treatments of trans retinol in a highly soluble oil, myritol, with and without penetration enhancers. The results showed an improved penetration in case of the former, where lipid fluidizers, such as oleic acid, increase the partitioning effect into the membrane, allowing a higher diffusion into the SC. On the other hand, retinol in myritol is highly solubilized, with a much lower tendency to partition into the skin.

The permeation of RP in nanocarriers was also demonstrated through *in-vitro* studies on human skin with confocal laser scanning microscopy (CLSM) by Teixeira et al and others.[49] A FDC set up was used, where the skin exposed to the formula was incubated for 24 hours. Similar

to SLN and NLC carriers, polymeric nanoparticles exhibited film formation on the skin, where a deep penetration was revealed, suggesting intercellular permeation of the drug. Along with sample withdrawals from the receptor compartment of the cell, the skin itself was analyzed for the quantification of RP in both the SC and the deeper epidermis/dermis layer. The extraction from the SC was conducted by a tape stripping test, after the skin was initially dried with a cotton swab. The RP on the tape was then extracted in methanol, and analyzed using HPLC. As for the other layers of the skin, RP was extracted with ethyl acetate. The results showed that the permeation of the RP in the dermis/epidermis was the highest, which was later confirmed with CLSM. The fluorophore in RP allowed its excitation without prior attachment of a fluorescent probe, as was the case for the polymeric capsule. The labelled polymer and RP were distinguished in the images retrieved by their different fluorescing colors. Namely, RP fluoresced green whereas the Nile blue probe on the nanocapsule gave red fluorescence, as shown in Figure 6. The excitation wavelength of RP was 740 nm, and its emission was in the region of 419-548 nm. The images showed a deeper permeation of the RP, leaving behind the nanocapsules at the upper layers upon their release. The conclusion made from the images regarding the penetration of the RP is that it took place via intercellular routes provided by openings in the skin, allowing for the uniform penetration observed.

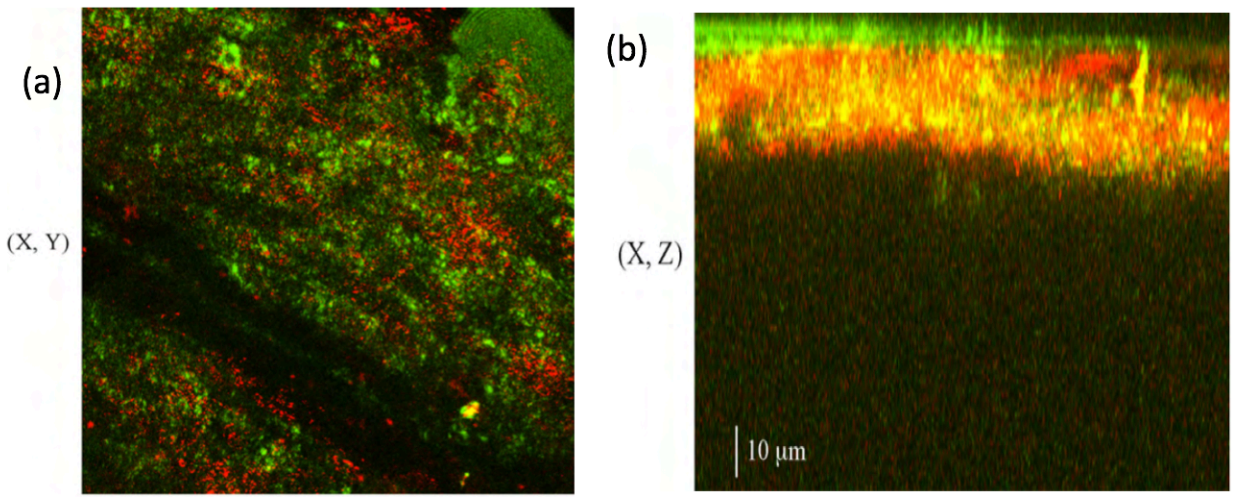

Figure 6. Confocal images (a) (x,y) on the surface (b) (x,z) deeper cross section of the skin where red is Nile-blue labelled polymeric nanocapsules and green is RP.[49]

In an effort to use RP-loaded nanocarriers for therapy on skin aging, Oliveira et al. studied the *in-vitro* profile of liquid crystalline systems (LCS) loaded with RP, in comparison to free LCS.[50] The study demonstrated the capacity of the LC carriers to prolong the antioxidant activity of the RP active. This was quantified by measuring the inhibition capacity of the formulations on 2,2-diphenyl-1-picrylhydrazyl (DPPH). The control consisted of free RP, showing a much lower inhibition rate with time due to a faster loss of antioxidant activity of the unprotected vitamin. Furthermore, the confirmation of the biocompatibility of the formulations was conducted by an *in-vitro* cytoxicity assay. This test constituted of using red blood cells to reflect any possible changes in the lipids, enzymes or proteins of the membrane. The results showed a tolerable extent lysis of the red blood cells, against a positive control that exhibited 100% hemolysis. Finally, it was concluded that LCS encapsulating RP for therapeutic application show very low toxicity and can be considered potential carriers.

The encapsulation of RP in NLC carriers were investigated by Pezeshki, et al., where the effect of surfactant concentration on the particle size, particle size distribution, encapsulation

efficiency and stability of the vitamin upon storage, were explored.[51] The NLC-RP carriers were synthesized using a hot homogenization technique, with four formulations ensued. The solid lipid and liquid oil composition was fixed, with only the surfactant changing in a level of 2%, starting with 2% till 8%. EE% were measured by centrifugation and separation of the NLC carriers by solvent extraction, which was then dried under liquid nitrogen and dissolved in a known volume of the mobile phase for HPLC measurements. The physical stability of the lipid dispersion was evaluated by measuring the particle size distribution after storage for two months at room temperature, along with quantifying the remaining amount of RP in the dispersion. The effect of the surfactant concentration on the particle size revealed at first a decrease in size up to 6%, followed by a significant increase for the formulation with 8%. The formulations with lower surfactant concentration showed lower stability upon storage with a pronounced increase in particle distribution and size, as a result of particle agglomeration. This phenomenon was explained by interfacial tension between the lipid and aqueous constituents that increase with increasing surface area of the smaller sized particles, and hence require higher amounts of surfactant concentration to off-set their tendency to coalesce. However, the pronounced particle size enlargement upon increasing the surfactant concentration to 8% was reasoned to be the excess surfactant molecules forming micelles, that remained in the continuous phase of the dispersion, flocculating with time. Finally, an optimal surfactant concentration is necessary for the success of the formulation in terms of stability.

The effect of SLN-RP on skin permeation *in-vitro* and *in-vivo* anti-wrinkle effect was studied by Jeon et al., where a modification of the carrier's surface was also ensued for positive permeation behavior.[52] This modification included dicetyl phosphate (DCP), which is a surface modifying agent that renders a negative charge onto the carrier. Since the skin is negatively

charged, the absorption of the carriers into the skin will not take place, instead, they will accumulate and localize on the skin. This effect is required for cosmetic therapy, as systemic penetration is not favored. Furthermore, the distribution of the negatively charged carriers enhanced the permeation of RP, although not to the receptor compartment in the FDC set-up. This increase in mobility of the RP was explained by the film formation of the SLN and the prolonged interaction between the carrier and the skin, allowing for material exchange between the SLNs and the lipids in the intercellular region of the skin. The diffusion of RP showed modifications in the SC in terms of lipid enthalpy and lamellar stacking, which is another plausible mechanism for the observed enhancement in RP penetration. As for anti-wrinkle effects assessed *in-vivo*, 50 female hairless mice were used, divided into 5 groups. Two of the groups were given DCP-SLN-RP, with varying concentrations. The third was a positive control, given a commercial product containing vitamin A. Finally, the last two were not given any vitamin A, one was irradiated with UV (negative control) while the other was not. The UV radiation is meant to promote skin degradation by inducing reaction oxygen species (ROS) that damage DNA and cell membranes through free radical reaction, diminishing the skin's elasticity and promoting wrinkle formation. Finally, the results showed a significant improvement in anti-wrinkle behavior for the first two groups in comparison to the positive control, although the effect was dose dependent with improvements in the higher dose RP in SLN. The higher dose SLN-RP also showed improvement over the commercially available product. This anti-wrinkle phenomenon of the formulation was hypothesized to follow the following mechanism. First, the DCP anchored on the surface of the SLN allowed for improved skin hydration, resulting in promoted delivery of the RP into the viable dermal layer and not in the blood, which was confirmed by *in-vitro* studies where no RP was detected in the receptor cell after 12 hours of application. Since RP exhibits antioxidant activity

by quenching radical reactions possibly triggered by UV, it would function as an anti-aging agent by impeding the loss of elastin, the protein responsible for the skins elasticity.

Improvement of photo-aged facial skin by topical application of vitamin A derivative, retinol, was also studied *in-vivo* by Kikuchi et al. on middle-aged Japanese females.[53] A randomized double blind clinical study on 57 subjects was first ensued for 6 months using 0.075% retinol creams and its base cream as control for each half of the face. Three of the subjects experienced irritation effects, but the remaining exhibited a significant improvement on the half part of the face where retinol was applied. The assessment of wrinkle diminishment was assessed by a dermatologist, that examined both deep and fine wrinkles, where improvements noted in both were 28% and 50% of the subjects, respectively. Another trial was conducted with lower concentration retinol for a shorter period of time, namely 0.04% retinol for 13 weeks. The improvements in the latter case were not as significant, however.

In a review article by Babamiri and Nassab on cosmeceuticals, mainly tackling "the evidence behind the retinoids", they illustrated the mechanism of action of vitamin A against skin aging.[54] One mechanism involves the retinoids diffusing through cellular membranes, propelled by their lipophilic nature, to bind to specific nuclear receptors that help in modulating gene expression responsible for cell proliferation and differentiation. Other non-genomic actions include UV absorption, antioxidant activity, along with possible changes in pigmentation. Vitamin A was shown to exhibit UV protection by its ability to absorb such frequency of light due to its inherent chromophore, the conjugated system of double bonds, where RP demonstrated an equivalence of SPF 20. The mechanism employed in antioxidant activity of the retinoids involves the scavenging of free radicals, and hence minimizing loss of elastin.

A comparative study was conducted on different nano-lipoidal carriers encapsulating the acid derivative of vitamin A, isotrinoin, based on skin permeation, photostability, biocompatibility and anti-psoriatic activity.[55] The lipidic carriers includes SLNs, NLCs, liposomes, and ethosomes which were compared to a commercially available product containing the active. Characterization included quantifying the EE% of the vehicles. This was found highest for NLCs followed by SLNs, ethosomes and liposomes. The highest conferred stability was also for the NLCs, followed by SLNs, and least for the ethosomes. The stabilities of liposomes and the commercial product were equivalent. Permeation studies on mice skin mounted on FDC showed permeation to be highest for isotrinoin in ethanolic media, followed by NLCs > SLNs > ethosomes > liposomes > commercial product. The ethanolic solution was highest due to the lack of barrier for the diffusion of the vitamin along with alchohol's intrinsic penetration enhancement capabilities. However, the biocompatibility of the phospholipidic shell of the vesicular liposomes was claimed to be the reason for its retention in the skin. Finally, it was concluded that for deep skin targeting, as in the case of acne located in the sebaceous gland, lipidic carriers as NLCs, SLNs or ethosomes are recommended. However, superficial treatments such as those necessary for psoriasis, liposomes would be a more effective vehicle due to their high skin retention capacity.

Chapter 3

Theoretical Background

3. Theoretical Consideration

3.1 Nanocosmetic Vehicles

Topical delivery of bioactives, such as vitamins and naturally derived antioxidants, for skin therapy poses a major challenge due to the limited stability, and bioavailability of phytochemicals.[59] Other possible challenges include poor drug solubility, which primarily stems from the bioactives' intrinsic hydrophobic nature in many cases, pertaining to the presence of the organic alkyl chain.[60] This led scientists to develop new delivery systems that both solubilize the drug and protect it from damage. There are, however, required properties for the nano-vehicles used in drug delivery. These include the following: no illicit toxicity of any of its ingredient; high loading capacity of the active; specificity in drug targeting; and a controlled release behavior.[34] A common method for attaching the active to the nanostructured carrier is encapsulation. There are several well established systems developed to fulfill this purpose, which includes vesicular, emulsion, and particulate based vehicles.

3.1.1 Vesicular Systems

A vesicular system contrives a bilayer lamellar structure constiting of amphiphilic molecule assembling into a concentric sphere in the presence of water. These molecules can be of several origins, both organic and inorganic, and are able to encapsulate both hydrophilic and hydrophobic drugs, the former within the interior of the vehicle, and the latter in between the polar hydrocarbon lamellar bilayer, as shown in Figure 7. A common example of such system are liposomes, which are used extensively in pharmaceuticals as well as cosmetics.[61] As the name suggests, liposomes are composed of lipids, commonly phospholipids, cholesterol or glycolipids. The main advantage of liposomes is their lipid membrane, which makes them optimal for penetrating through the non-polar lipid layer of the SC, reaching the site intended for the release of the active. Extensive bio-

disposition studies has shown that liposomes are able to deliver a much higher concentration of drug and keep it localized at the epidermis, with almost 7 to 8 folds that of conventional matrices as in gels, lotions, and creams, and minimal intravenous penetration and accumulation in internal organs.[62]

Synthesis of liposomes occurs simultaneously when dispersing phospholipids in a water medium, at a temperature above their phase transition, where both small unilamellar as well as multilamellar vesicles form.[63] These vesicles can be transformed to smaller, nano-vehicles by methods such as high-pressure homogenization, ultra-sonication, etc.[64]

There are other vesicular systems such as niosomes, which were developed to bypass some of the drawbacks of liposomes such as their chemical instability, triggered by the possibility of the oxidation of unsaturated fatty acids and the hydrolysis of the ester bindings in the phospholipids.[65] Niosomes circumvent such obstacles by replacing the moieties of the amphiphilic molecules with saturated hydrocarbon chains and intramolecular ether linkages.[66,67]

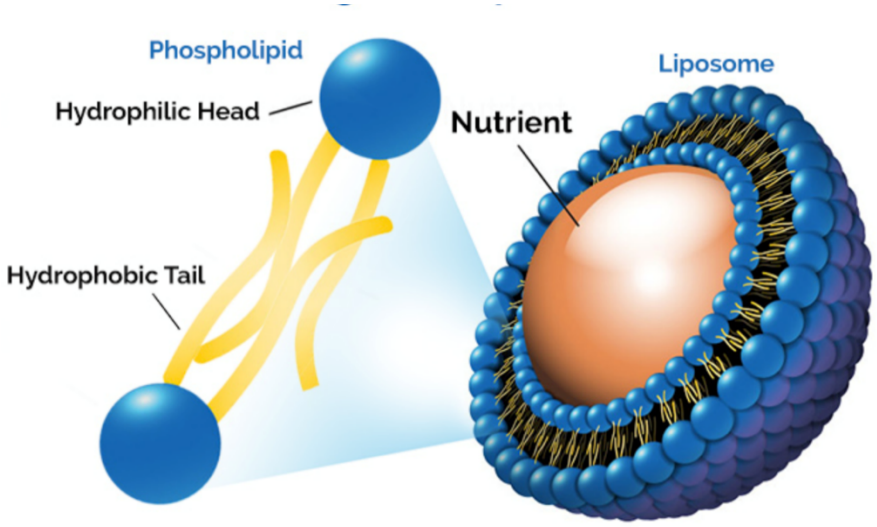

Figure 7. Amphiphilic molecules in liposomal vesicular delivery vehicles.[68]

3.1.2 Emulsions

The lipophilic nature of many bioactives poses a disadvantage in their incorporation into cosmetic formulation, as they can only be solubilized in organic solvents. The use of non-aqueous solvents can be both costly and toxic, and thus the search for an alternative mode of delivery for these actives was required. Emulsions allows the latter's' delivery in appropriate aqueous media, as well as grant the possibility of delivering the optimal concentration by dilution.[69] There are several different systems of emulsions being used, each with their respective advantages and limitations. Examples of systems include micro-emulsions, multiple emulsions, nano-emulsions and pickering emulsions.

The main difference between micro-emulsions and nano-emulsions is their thermodynamic stability, where the latter is less stable due to the increased surface area as a result of the decrease in size, leading to more contact between the two immiscible phases and hence resulting in an increase in surface tension[70]. Micro-emulsions, however, constitute solubilizing molecules, such as surfactants and co-surfactants, that help diminish the surface tension, rendering the overall system optically isotropic, and single-phased.[71]. The presence of micro-domains of opposite polarity within the same phase allows for a high capacity for solubilizing both hydrophilic and hydrophobic moieties.[72] Figure 8 illustrates the difference in Gibbs free energy between each emulsion and its counterparts separated. Although nano-emulsions are thermodynamically unstable, they are kinetically stable making them less prone to respond to changes in temperature and composition, as opposed to micro-emulsions.[73] However, rapid drug release was observed to be a limiting factor in the case of nano-emulsions, which stems from the nature of the system that allows for a higher mobility of the drug solubilized in the lipid phase in comparison to cases of where the drug is encapsulated within the vehicle.[5]

Pickering emulsions are similar to nano-emulsions. They do not require surfactants, and are instead stabilized by the presence of amphiphilic solid particles, such as zinc oxide coated with aluminum stearate. This decreases the surface tension at the interphase of the two immiscible liquids and solubilizes the dispersed moieties within the continuous phase.[75] The main advantage of substituting conventional emulsions with pickering emulsions stems from the dismissal of surfactants in the latter.[76] However, there are concerns regarding the stability of the emulsion, claiming a mesostable state, but a study conducted confirms the opposite, where a particularly high stability against coalescence was observed, compared to surfactant stabilized emulsions. This increased stability can be stemming from the presence of solid particles enveloping the oil droplets that decrease the mobility of the droplets.[76,77]

Another type of emulsion based carriers for bioactives are multiple emulsions, based on the concept of separating the continuous phase from the dispersed, where the latter encapsulates within it a portion of the former. This system is thermodynamically unstable although uses two system surfactants to solubilize the three phase emulsions (W/O/W or O/W/O). Chances for emulsion breakdown can take place via several routes, such as osmotic swelling or shrinking, internal phase expulsion, or coalescence of either internal or external droplets.[75] These multiple system emulsions can have their stability improved by means of having a polymerized gel in either the internal or external phase, reducing their mobility, and hence prolonging stability.[5] The application of this system in cosmetics is effective due to its sustained release, which is optimum in cases of prolonged skin moisturizers, or aerosol fragrances with a better sustained release, etc.[78]

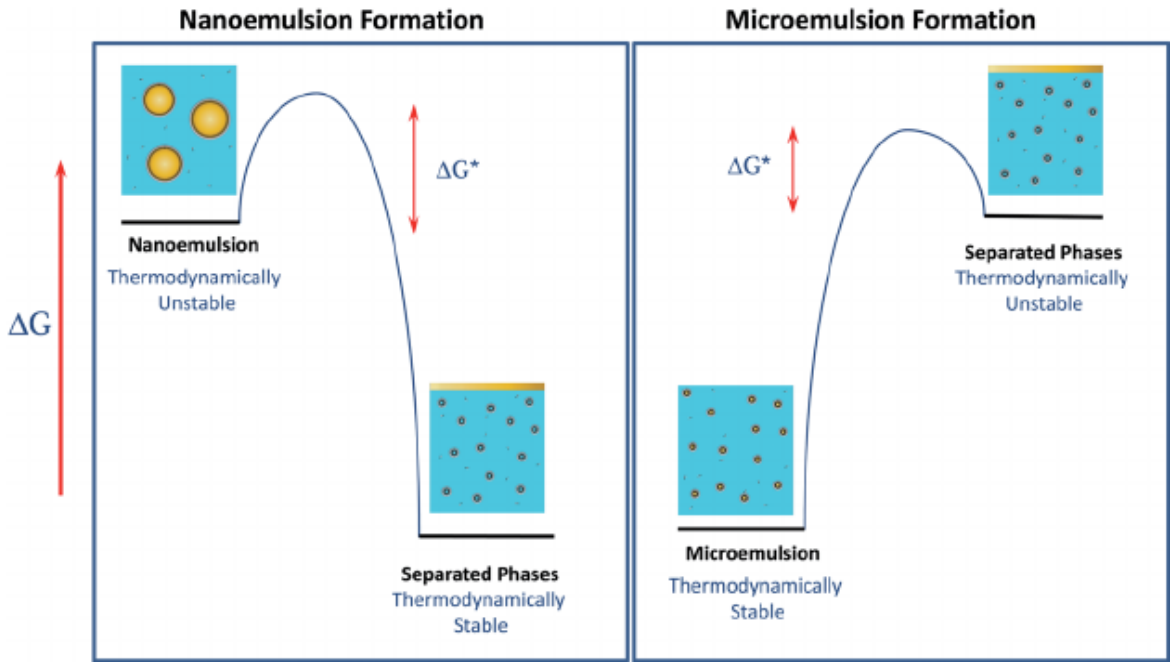

Figure 8. Thermodynamics of nanoemulsions vs. microemulsions.[79]

3.2 Lipid Nanoparticles

Over the past decade, much research has been conducted to validate the efficacy of colloidal nano-vehicles encapsulating bioactives for therapeutic targets in the cosmetic realm.[80] Although particulate drug carriers showed remarkable improvements in drug targeting, and chemical stability, their limitations outweighed their progress to large-scale production. These include a lack of physical stability, difficulty in up-scaling for commercial use due to their complex synthesis, as well as their cytotoxicity, especially for polymeric carriers.[27] The evolvement of lipid based carriers overcomes these drawbacks, particularly toxicity, where now all excipients are biodegradable solid lipids forming the matrix, dispersed in an aqueous medium in the form of a suspension.[81]

3.2.1 SLN

SLNs are dispersions synthesized by replacing the liquid lipid in an o/w emulsion with solid lipids or a blend of solid lipids.[82] The main feature of lipid carrier is their characteristic solidity that can withstand body temperature.[11] In comparison to other vehicles, such as emulsions and liposomes, these solid-based systems can provide higher protection for the active against chemical degradation, as well as impede its mobility once entrapped within the defects of the solid lipid's crystalline matrix.[46] The choice of lipid used influences the characteristics of the carrier by several means such as the particle size, stability upon storage, EE%, and release profile.[83] Another advantage of these nano-vehicles is the biocompatibility and biodegradability of their components. The inherent solid nature of the SLN has also been shown to prolong stability.[84] The mechanism for this process was discussed by Patravale, showing a relationship between the lower mobility of the vehicle as a result of its solid nature, hence preventing coalescence as well as providing better control over the release of the encapsulated actives.[5] Another advantage of SLNs is their mode of production, which is relatively cheap and simple in comparison to other vehicles.[85] A common method is by using a High Pressure Homogenization technique, where the possibility of both a hot and a cold homogenization process can be incurred, as demonstrated in Figure 9.

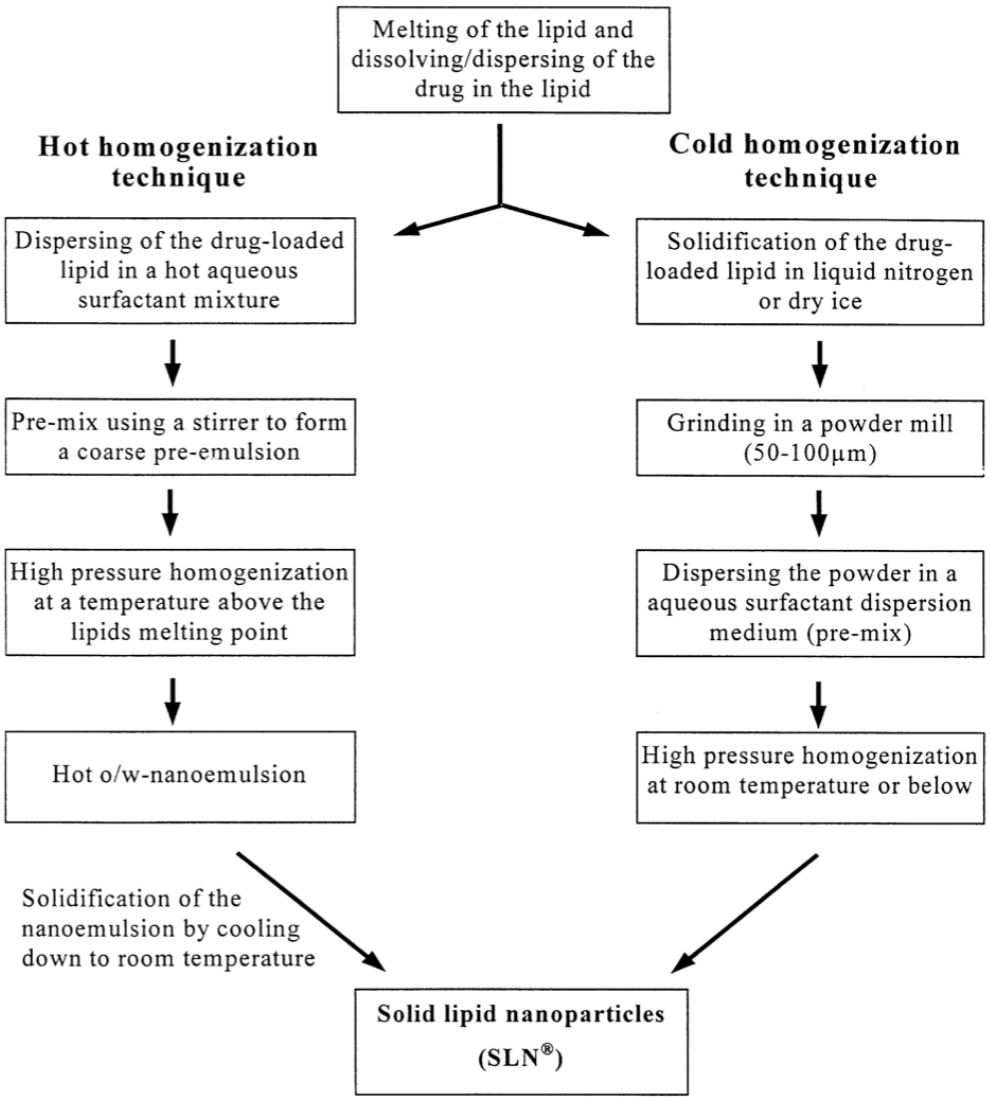

Figure 9. Schematic procedure of hot and cold homogenization techniques for SLN production.[32]

SLNs are capable of encapsulating both hydrophilic and lipophilic moieties, although risk of partitioning of hydrophilic drugs renders the system more effective towards the latter type.[86,85] The average size of SLNs can range from 50 to 1000 nm, with solid lipids such as triglycerides, glyceryl monosterarate, glyceryl behenate, glyceryl palmitostearate, or wax cetyl palmitate, and other biodedgradable lipids forming the matrix. To ensure physical stability of the dispersion, a

surfactant or a combination of surfactants must be used. Typical examples of common emulsifiers include lecithin, polysorbate 80, sodium cocoamphoacetate, or sacchrose fatty acid esters.[87]

A. SLN Structure and Drug Loading Mechanism

There are three types of SLNs categorized according to the embedment of the drug within the matrix, as follows:[88]

1) Type I SLNs are derived from a homogeneous mixture of the drug and solid lipids, with the former being well dispersed in the latter.
2) Type II SLNs pertain to drugs that enrich the shell of the matrix.
3) Type III SLNs consist of a drug loaded core, taking place when the drug crystallizes prior to the lipids.

The addition of oil or drug in a liquid form can decrease the crystallization tendency of the system, whereas the addition of long chain fatty acids, or surfactant molecules with long, saturated alkyl chains is a possible mean to overcome this effect. The crystallized solid lipid carrier will then allow for better control over release for the bioactive by impeding its mobility within the suspension, as well as protect it from the surrounding media, hence improving its stability.[34]

B. Drug Expulsion Mechanism

The crystalline nature of the lipids constituting the matrix of SLN imposes an inevitable drawback of gradual drug expulsion as a result of polymorphic transitioning to a more stable form.[89] This phenomenon can take place either within a few days or a few weeks after the date of formulation. Each type of lipidic excipient used in the matrix possesses an inherent type of polymorphic form. Polymorphic transitioning, which are higher in nano-material as compared to their bulk form, results in a more densely packed matrix, which can change the shape of the SLN. This in turn disfavors the incorporation of drugs within its highly ordered crystalline matrix,

resulting in drug expulsion. Therefore, the EE% of the system depends on the chemical and physical nature of the drug, as well as type and crystalline form of the lipids constituting the matrix, where a mixture of lipids was shown to have a higher incorporation capacity than using one pure form.[37,13,88]

The major advantages of SLN carriers include: controlled release due to their solid matrix; increased skin permeation pertaining to their small size that allows for a closer contact to incur with the SC; and occlusive properties resulting from their inherent film formation upon application on the skin.[46] However, SLN carriers suffer from low EE% and gradual drug expulsion. This occurs because of the inherent crystalline nature of the lipid matrix, with the drug encapsulated within the defects, expelling the drug as a result of the crystallographic transitioning to a more stable polymorphic form.[46] Other disadvantages include tendency to gelation and lipid particle growth.[88] Challenges pertaining to loading capacity is addressed by inducing more defects to the lipid matrix, and increasing the solubility of bioactives by adding an oil component, leading to a new generation of lipid vehicles, namely NLCs.[90]

3.2.2 NLC

NLCs improve on some of the major limitations of the SLNs. Although both belong to the same class of lipid carriers and follow an identical synthetic approach, the main difference stems from the composition of the solid matrix, where in NLCs liquid lipids are used along with crystalline solid fatty acids to build the core. This compositional difference has resulted in pronounced differences in EE%, with much higher loading capacity for NLCs. This has been attributed to the induced imperfections in the NLCs structure arising from the two phased lipids, as opposed to the more perfectly crystalline SLNs. This allows larger amounts of actives to be encapsulated within the NLCs. NLCs also exhibit enhancements in stability, also explained by the

induced imperfections in its core, overcoming the higher tendency to expel the actives.[91] This is illustrated in Figures 10 and 11 below, where the perfectly crystalline matrix of the SLN is shown to entrap less actives as compared to the less perfect composition of the NLC on the right, as well as possess higher stability.

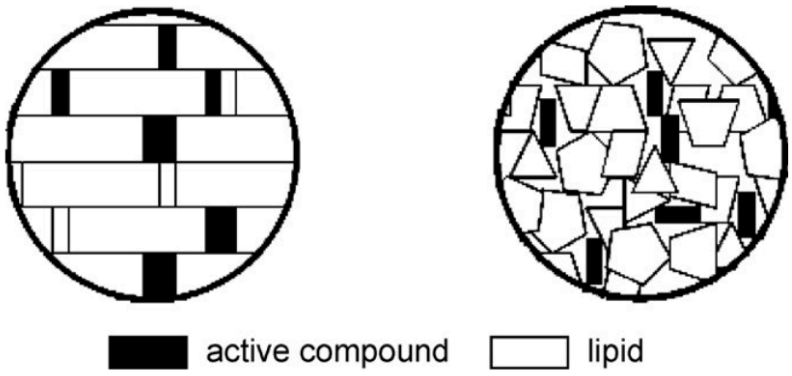

Figure 10. Perfectly crystalline SLN (left) vs. the imperfect NLC (right).[92]

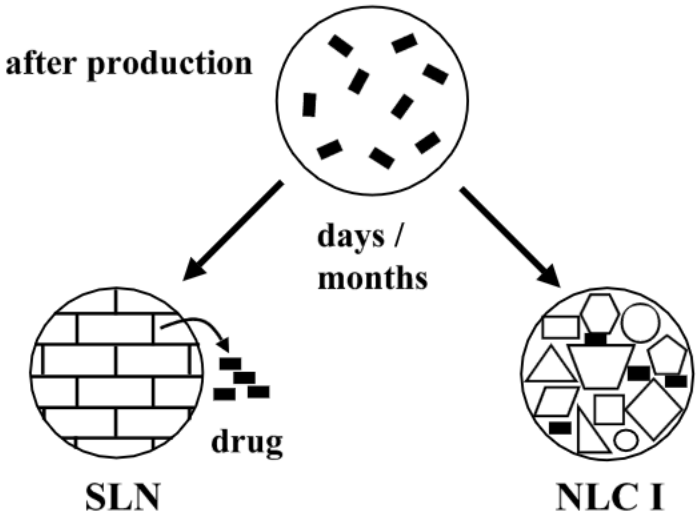

Figure 11. Drug expulsion as a result of polymorphic transition in SLN and unchanged structure in NLC due to imperfect crystalline structure.[14]

Similar to the SLNs, there are three types proposed for NLCs depending on the structure of the matrix:[88]

1) Type I, as shown in Figure 11, are similar to the composition of SLNs, but with the addition of oil to yield an imperfect crystal structure. These induced imperfections in the lattice can now accommodate a higher capacity of drug. This can be attributed to the varying lengths of alkyl chains in the fatty acids present and the mixtures of mono-, di-, triacylglycerols that allows for larger gaps between adjacent molecules. Such structures also possess a lower tendency for polymorphic transition, and hence impede the process of drug expulsion over time.[88]
2) Type II consists of an amorphous structure, resulting from the mix of solid and liquid lipids that do not recrystallize after homogenization. This is shown in Figure 12.

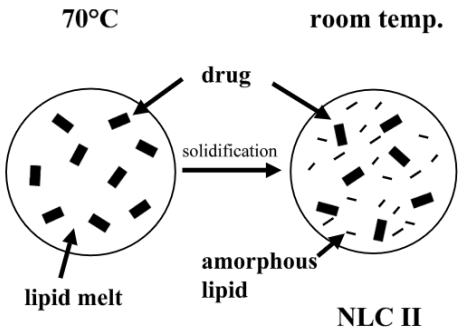

Figure 12. Amorphous NLC type II model.[14]

3) Type III, known as the multiple model, is composed of an oil-in-fat-in-water dispersion, as illustrated in Figure 13. The solid matrix of the NLCs is composed of tiny oil compartments within where the entrapped drug resides.

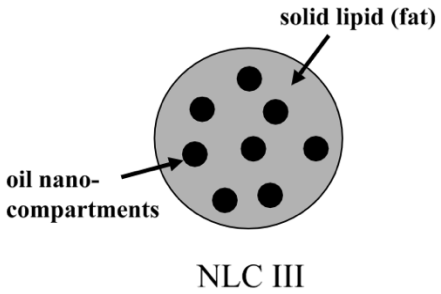

Figure 13. Oil-in-solid fat-in-water (O/F/W) NLC III structure.[14]

3.3 Vitamin A

Retinoids, also referred to as vitamin A, are an important class of actives necessary for the healthy functioning of the epithelial tissue, such as the skin, and has been found to be responsible for the coordination and regulation of important functions such as keratinization and cell division. They have conveyed control over cell proliferation and differentiation,[48] and are reported to promote epidermis thickening.[93] Other important dermal benefits witnessed of vitamin A is their ability to stimulate fibroblast cells to secrete collagen, elastin and hyaluronic acid, hence acting as a powerful anti-wrinkle agent.[94] This paved the way for their incorporation into many dermatologic and cosmetic products where they have shown to treat severe skin conditions such as acne, disorders of keratinization as in psoriasis and ichthyosis, as well as reduce signs of aging.

3.3.1 Chemistry of Retinoids

The chemical structure of vitamin A consists of isoprene units, similar to other vitamins such as E, K and cholesterol, all categorized as isoprenoids. Just like many essential nutrients, vitamin A has to be consumed in one's diet, where it is either derived from retinyl esters in animal products or synthesized from β-carotene in plants.[95] The primary derivative of vitamin A is retinol, constituting an alcohol group at the end of the hydrocarbon chain, as shown in Figure 14. The

hydroxyl group can be oxidized to an aldehyde, or to a carboxylic acid, yielding retinal or retinoic acid, respectively, which are the biologically active derivatives.[54] Furthermore, esterification of retinol with palmitic acid yields RP. Since this organic molecule possess several chirality centers, optical isomerism results, where the three most common are all-trans-retinol, 11-cis-retinal, and 13-cis-retinoic acid, which has the generic name of isotretinoin, an anti-acne drug.[96]

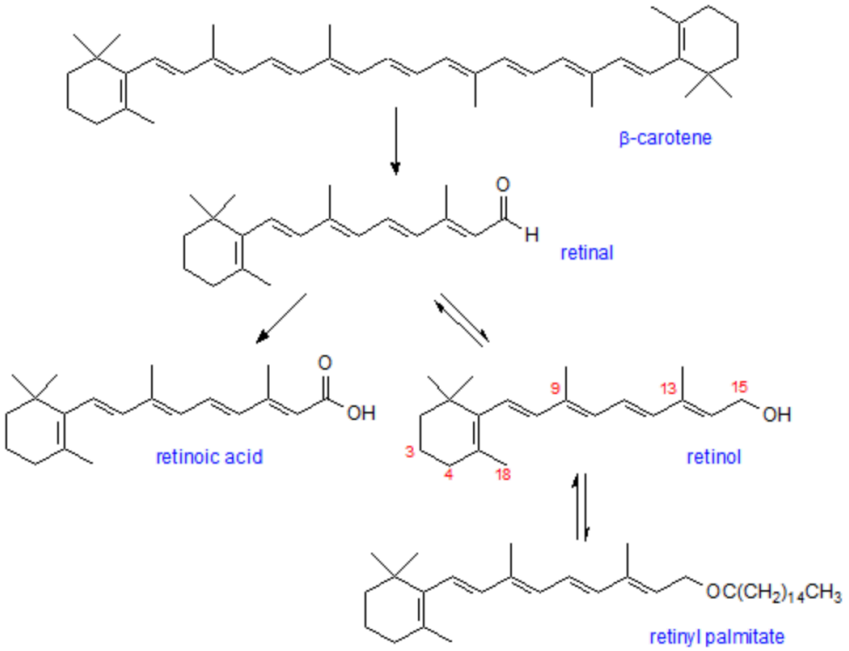

Figure 14. Various forms of Retinoids.

3.3.2 Photodecomposition of Retinoids

Albeit its effective use as a cosmetic active agent, vitamin A's chemical instability makes it easily prone to oxidation,[97] along with its pronounced irritation to the skin when directly applied,[98] limiting its potential in topical therapeutic applications. A more stable, esterified, form of retinol, namely: RP, has shown lower irritancy, and hence higher acceptability by consumers.[50] RP, however, follows an indirect path for therapy. Upon skin absorption, RP must be first

converted to retinol by enzyme hydrolysis, cleaving the ester linkage,[50] and by further oxidative metabolic action, converted further to retinoic acid, the active that initiates skin therapy.[94] The different derivatives of vitamin A and the reactions required for their conversion is illustrated in Figure 15 and 16. RP, as with other forms of retinoids, can be further stabilized, and made available for skin absorption by incorporation within a nano-vehicle as in SLNs and NLCs.[98] Furthermore, RP has been reported to have an increased entrapment in SLN vehicles compared to other more polar derivatives, namely retinol and retinoic acid.[46]

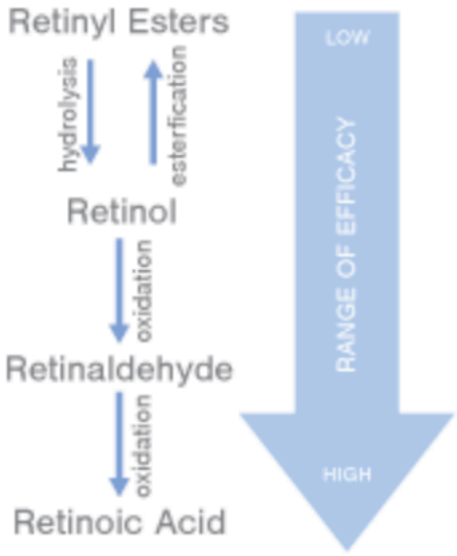

Figure 15. The Mode of Reaction in Retinoid derivatives Interconversion.[99]

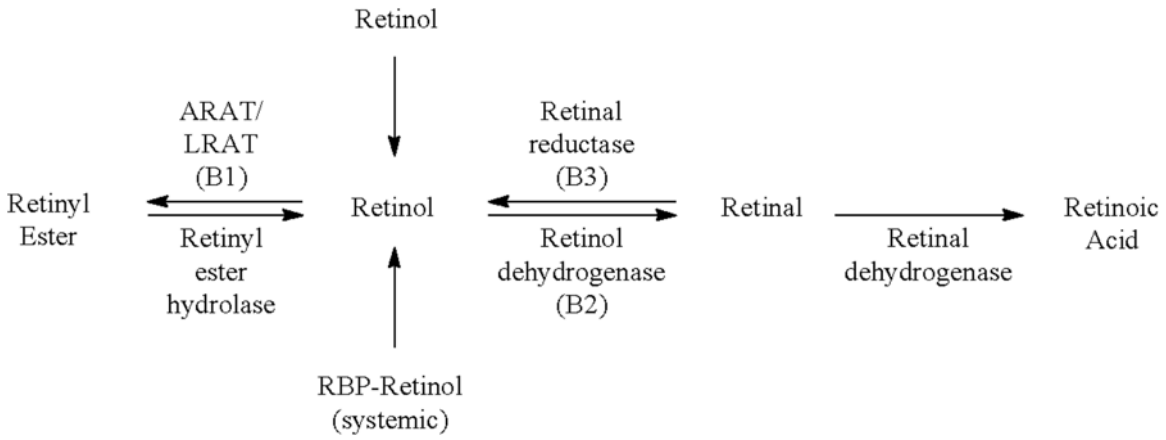

Figure 16. RP metabolism in Epidermis through Enzymatic action.[99]

The chemical instability of retinoids is highly dependent upon the conditions of the formulation such as type of solvent, temperature, and availability of oxygen. In general, photo-induced reactions of retinoids take place via several routes, including isomerization, polymerization, oxidation, or degradation, depending on the surrounding environmental stimuli. These may include the type of carrier, concentration of the retinoid, energy and amount of radiation, and nature of surrounding species as in impurities or other excipients.[100]

3.4 PP Oil

PP (*Opuntia ficus indica* L) is a tropical or subtropical plant originally grown in South America and cultivated in dry regions as an important nutrient and food source.[101] The seed oil properties of PP fruits were investigated during the maturation period.[102] The seeds and pulp were also compared in terms of oil composition.[2] In addition, researchers have agreed that PP seed oil was rich in polyunsaturated fatty acids. A study was executed to study the nutritive value and chemical composition of PP seeds growing in Turkey.[103] A Multi-ingredient fruit such as PP holds promising answers for tailor-made nutraceuticals and functional foods by embracing essential ingredients, such as taurine, amino acids, readily absorbable carbohydrates, minerals, vitamin C

and soluble fibers.[104] From a study conducted to determine some of the mineral contents of PP seeds, it was found that many important minerals such as Ca, K, Mg and P were present at high level.[103]

The fatty acid (FA) composition of PP seed oils was assessed by Monia, Evelyne Laurence and Hamadi, for two species of PP from Tunisia.[56] The analysis took place using GC-MS after derivatization of the FA by methylation to yield their respective esters. The four major FA found in both species were palmitic, stearic, oleic, and to a higher extent, linoleic acid, making up almost 70% of the total oil content. The rich FA composition of PP oil allows for their use as a valuable nutritive source, one of which possesses an economic value in regions where they could be effectively cultivated.

The characterization of phenolic compounds in PP seed oils as well as fatty acid content was carried out in a collaborative study between the University of Bejaia in Algeria and two other institutions in France, namely University of Bordeaux, and University of Lorraine UMR.[57] Phenolic compounds are claimed to exhibit high anti-oxidant activity, which is attributed to their effectiveness at scavenging free radicals and chelating metal cations involved in the radical initiation. Therefore, they quench any oxidative stress that could lead to skin aging, or even cancer. The phenolic extraction from the oil was done by ethanol, and later analyzed using HPLC. The characterization of the various phenolic forms was carried out using NMR. Antioxidant activity was evaluated by correlating the quenching of DPPH free radicals with varying amounts of phenolic content of the extracts. A significant correlation was found between the antioxidant dose and the free radical activity. Finally, a high composition of linoleic acid in the FA content was recorded, ranging between 58-63%.

In a review on PP, El-Mostafa, Kharassi, Badreddine and others illustrated the potential of the plant in terms of nutrition, health and disease prevention.[58] This is attributed to the plant's rich composition in polyphenols, vitamins, polyunsaturated fatty acids and amino acids. Biological activities of various extracts from the plant is claimed to possess anti-inflammatory, antioxidant, hypoglycemic, antimicrobial and neuroprotective potential. Vitamin K1 and various derivatives of vitamin E was documented, where 52.5 and 106 mg/ 100 g total is reported, respectively. The mineral content of the seed oil is also tabulated, with calcium, magnesium, sodium, potassium, iron, phosphorus, zinc, copper and manganese included. Amino acid content is also revealed for all the 25 various forms, with Glutamic acid being the major form.

3.5 Principle for the Production of SLNs and NLCs

3.5.1 HPH

The homogenization technique is a fluid mechanical process involving the breaking down of droplets or particles into smaller sizes in the micro or nano-range, depending on the power of the equipment.[106] It is used in cases where two or more immiscible constituents are needed to be well mixed in one another to give a homogeneous consistency in the form of a dispersion or emulsion, where one involves solid particles dispersed in a liquid media and the latter constitutes liquids only. The need for such consistency is a quality of vital need in the food and cosmetic industry as it improves not only the aesthetic appeal of the product, but its stability, shelf life, bioavailability of active constituents, as well as digestion and taste in case of food.

There are two commercial types of HPH, the jet-stream and the piston-gap based homogenizer. In the case of the jet-stream set up, the breaking of the macroparticles or droplets coming in from the suspension takes place by the shear momentum of two high velocity streams. As for the piston-gap, it is the same set up of the instrument used at EVA factory, where the high pressure induced when the macro-suspension enters the narrow gap of a few millimeters allows for their diminution.[54]

3.5.2 Principle for Quantifying Amount of RP Loaded in SLN/NLC Formula

A means to separate nanoparticles suspended in a fluid can be strenuous due to their extremely small particle size. Various methods have been adopted for separation, such as chromatography[55], precipitation,[110] solvent extraction,[111] and ultra-centrifugation.[51,46] A technique that has proven to be efficient is physical separation by ultra-filteration.[112] This technique is based on separating molecules or small particles (micro or nano), by the use of a polymeric membrane with a tunable pore size, such as polyethersulfones.[113] Species larger than the pore size will be

retained on the surface, and not within the porous polymer framework as in the case of microporous membranes.

There are many advantages for using ultra-filtration compared to other non-membrane processes, which include:[112]

- Molecules are handled more gently, hence less damage is incurred as a result
- Does not interfere chemically with the system being processed; does not induce changes in the ionic or pH environment
- Relatively rapid, inexpensive, and efficient

3.6 UV-vis Spectroscopy

Spectrophotometry is an invaluable tool in both quantitative and qualitative molecular analysis. The main underlying principle behind this technique entails an irradiating beam pertaining to a particular region in the electromagnetic spectrum where, depending on its nature, will induce a particular excitation in the sample. These excitations can be rotational in case of microwave, vibrational in case of Infrared, or electronic in case of UV-visible radiation.[114] These excitations are translated to an absorption in the spectrum at a wavelength intrinsic to the nature of the molecule in the sample.

3.6.1 Beer-Lambert Law

A means to quantify the spectrum pattern of a particular molecular specie is by applying the Beer-Lambert Law.[115] This mathematical relation depicts the basic and direct relationship between the extent of absorption of the system with the number of absorbing species present, and their inherent capacity to absorb efficiently, at a particular wavelength. The amount of molecules present is related to the molar concentration, c, as for the molecule's efficiency at absorbing, it is

referred to as the molar absorptivity, ε, a constant at a particular λ_{max} for a specific type of molecule. The equation is as follows:[116]

$$A = \log\left(\frac{I_0}{I}\right) = \varepsilon cb \qquad \text{Equation 1}$$

where A is the absorbance, I_0 is the incident beam on sample cell, I the emerging beam, and b the length of the sample cell (in cm).

3.6.2 Instrumentation

The basic set up for any spectrophotometer constitutes an energy radiating source, monochromator, and detector.[115] In the case of a UV spectrophotometer, the energy source is usually a deuterium lamp, which radiates energy in the UV regions. As for the monochromator, it is a device used to resolve the impinging polychromatic beam into its various components, which is then directed to the sample cell by a series of slits.[116] The instrument can be tuned to generate monochromatic light with various wavelength to hit the sample. The emerging beam from the sample cell then hits the detector, generating the absorption spectrum. The types of detectors include photomultiplier or photodiode.[116]

Furthermore, there are two different set-ups for the UV-vis spectrophotometer, one that entails a single beam radiating one sample cell compartment, and the other that constitutes two cell compartments with a preceded splitting of the beam by mirrors. In the case of the latter, it allows for more rapid measurements to be pursued due to the simultaneous measurement of the blank reference solvent and sample.[117] A schematic representation of the composition of both types of spectrophotometers is shown in Figure 17 below. For the purpose of the work conducted for this thesis, both types were used, where the double beam was used to give an absorption pattern

over a wider range of wavelengths for the excipients involved in the formula, and the single beam used for assessing the EE% of RP.

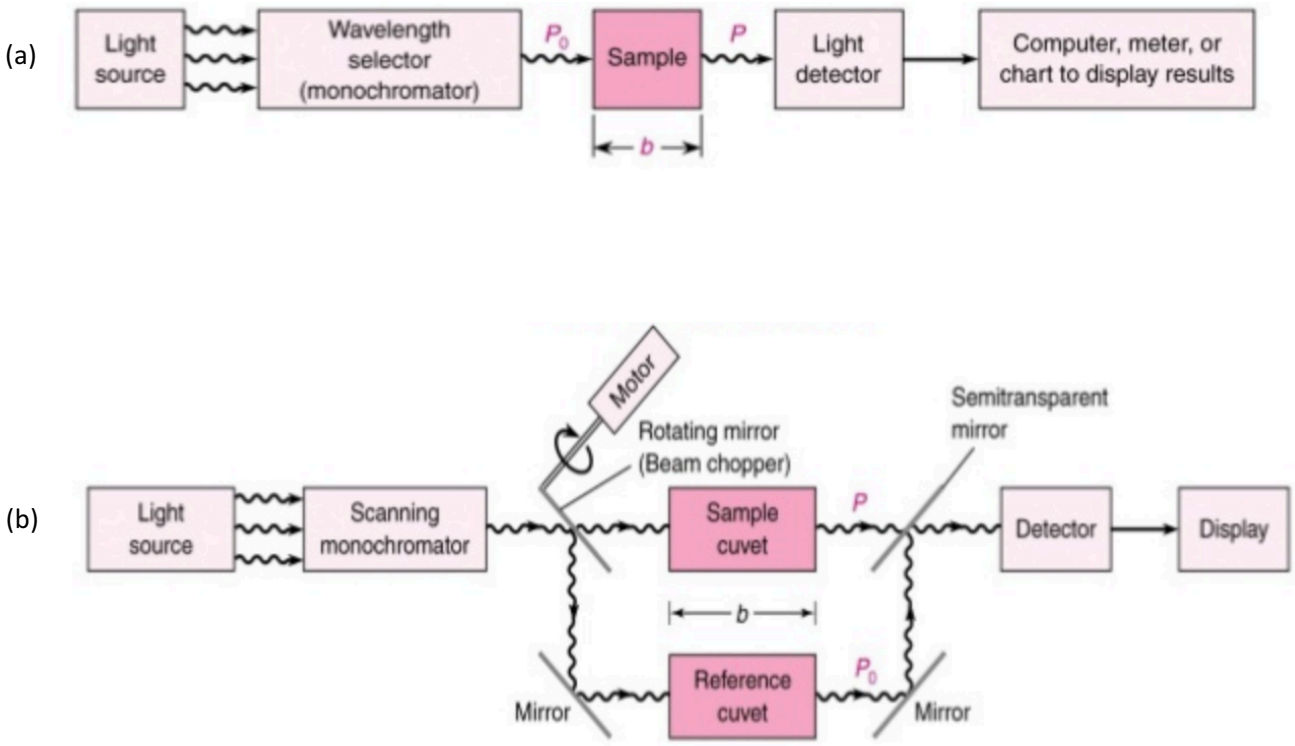

Figure 17. (a) Single beam and (b) double beam Spectrophotomers.[118]

3.7 Chromatography

Another major technique used in characterizing the various formulations of NLC/SLN was chromatography, namely Liquid Chromatography. The basic idea behind this technique is separating the various constituents of a mixture according to their varying affinity to a stationary phase, typically packed in a column, and the eluting solvent, representing a mobile phase, which can be either gas or liquid.[119]

3.7.1 Liquid Chromatography

The mode most commonly used for the purpose of pharmaceutical studies, including this research, is the reversed phase Chromatography, that includes a non-polar column, which in case of this project, was octadecyl silane (ODS). The mechanism of interaction is based on adsorption. This allows for the analyte molecules to interact with the functional groups previously grafted on the silica column. The retention time increases with increasing hydrophobicity of the constituents, where aliphatic compounds are found to be the best retained, and carboxylic acids the least, due to their polar acidic functional group that elutes faster with a like-wise polar mobile phase.[120]

Some of the advanced instruments in column chromatography, that are also used in this project, are High Pressure Liquid Chromatography (HPLC) and Ultra Pressure Liquid Chromatography (UPLC).[121] The only difference between the two is that the latter uses a more powerful pressure pump that reduces the relative retention time, and thus data are acquired more rapidly. The main components of both devices include an eluent, reservoir, a high or ultra-high pressure pump, a sample injector, the column which consists of the stationary phase, a detector and recorder.[120] The detector used for both HPLC and UPLC was UV-visible spectrophotometer

3.8 Differential Scanning Calorimetry (DSC)

DSC is a technique developed to assess the heat dependent conformational transitions of a material, against temperature. The setup includes a sample and reference cell, where the difference between the energy inflow as a function of temperature is plotted. The temperature of both the reference and sample cell are adjusted until identical, using energy in the form of power input. This energy difference inputted is quantified and can depict enthalpy or heat capacity changes of the sample relative to the reference.[122]

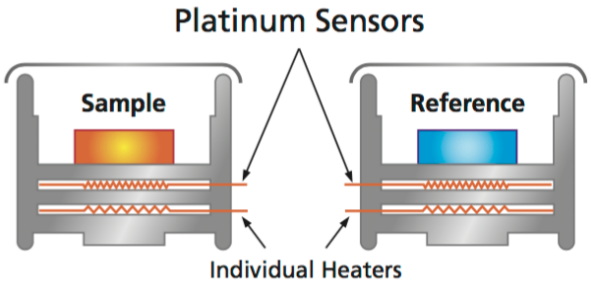

Figure 18. Double Furnace DSC.[123]

3.8.1 Data Analysis in DSC

The thermogram, specifically endotherm, retrieved from the DSC gives valuable information concerning the transition of the sample, which in the case of the project may be crystalline, depending on the formula, to an amorphous liquid (TS→TL). The maximum height of the transition is labelled Tm, and the temperature at which this transition is half complete is denoted T1/2. The thermal induced conformational changes and phase transitions can be quantified in relation to their temperature dependence by integrating the area under the peak, to give the enthalpy change, ΔH.[124] In cases of lipids, the temperature of transition represents the change from a crystalline-like ordered gel to a disordered fluid like state. Conformational changes that follows the transition include an all trans hydrocarbon arrangement to a less ordered gauge conformation. The higher the saturation level and chain length of the lipids, the higher is the enthalpy values needed for the transition to occur. Thus, the inherent structure of the lipids is pivotal in marking such a transition. Furthermore, the sharpness of the peak is relative to the purity of the lipid phase, where the sharper the peak means the purer the phase.[124]

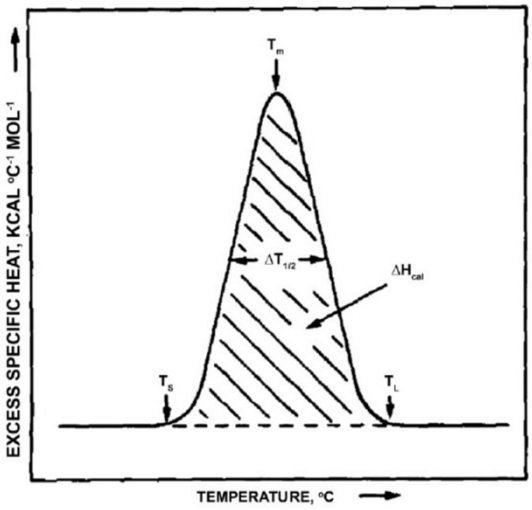

Figure 19. DSC Endotherm. [124]

3.9 Electron Microscopy (SEM & TEM)

Unlike conventional light microscopes, electron microscopes use a beam of electrons to analyze the features of a sample. Another difference is that images acquired from electron microscopes must be produced under a vacuum, since any gas particles present can hinder the electron beam movement. This use of electrons instead of light is due to the fact that the former, when accelerated to a high velocity, according to the de Broglie equation below, will possess a shorter wavelength than that of light.[75] Moreover, the smaller the wavelength of the interacting radiation, the clearer the details and resolution of the projected image. The interaction between the electron and the surface of the solid sample gives information on the external morphology, topography, its chemical composition, and arrangement of atoms in the framework (crystallinity).[76]

$$\lambda = \frac{h}{p} \qquad \text{Equation 2}$$

3.9.1 Scanning Electron Microscopy (SEM)

When an electron hits the surface of a solid sample, it can interact with the sample in different ways, and depending on whether the collision is elastic or inelastic, gives different signals.[77] The most abundant signal produced is that pertaining to inelastic collisions, where the electron loses some of its initial kinetic energy to the sample, ejecting a weakly bound electron that will hit the detector, to give information concerning the sample's topography. This ejected electron is called the secondary electron (SE), whose signal produces the SEM images, reflecting both topography and morphology of the sample surface. In case of the less frequent elastic collisions, backscattered electrons (BSE) possessing the same initial kinetic energy, but traversing a different path, can give an indication to the composition of the sample as their number is proportional to the atomic number of the sample.[77,78] The heavier the atom is, the brighter they will appear on the SEM image. Other signals that can be detected include diffracted backscattered electrons, which can give information on crystal structure of the sample, characteristic X-ray photons for elemental analysis, Auger electrons, cathodoluminescence, and heat.

A. Instrument

- The components of a SEM include the following parts, as shown in Figure 20:
- Electron Source ("Gun")
- Electron Lenses used to focus electron beam using either electric or magnetic fields
- Detector specific to the signal being examined, with at least secondary electron detector, and possibly an added scintillator for BSE, Energy Dispersive X-ray spectrometer (EDS) for X-ray photons.
- Display
- Infrastructure Regiments:

- Power Supply
- Vacuum System
- Cooling System
- Vibration-free floor
- Room free of ambient magnetic and electric fields

The sample must be dry, and conductive, with non-conducting material being sputtered with a conducting metal, such as gold, prior to analysis.

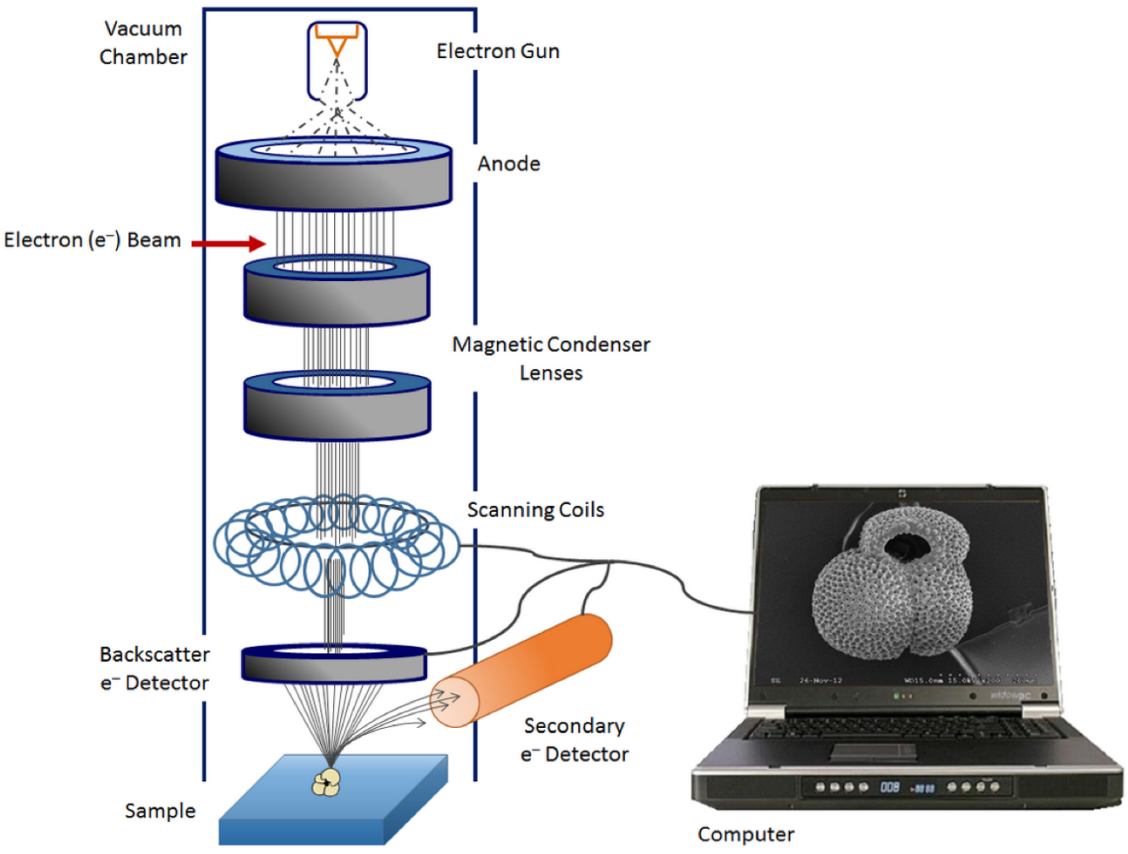

Figure 20. Schematic illustration of an SEM device.[129]

B. Advantages

SEM can produce a 3D image of the sample with rapid data acquisition. It gives a deep insight into the sample from different perspectives such as topography, morphology, crystallinity, and chemical composition.

C. Limitations

The regiments employed on the sample to be detected by SEM are extensive. Firstly, samples must be solid and small enough to fit into the microscope chamber, with a horizontal dimension in the order of 10 cm and height not exceeding 40 mm.[127] The sample must also be stable in high vacuum and low pressure environment that could reach up to 10^{-6} Torr.[127] Also, elemental analysis using EDS detectors is limited to heavier atoms, where atoms with atomic numbers less than that of carbon will not produce a readable signal. The ability for the probing electron to penetrate the sample is limited in case of dense specimens with atoms of high atomic number as more frequent collisions result that prevents the electrons from going more in depth. Although increasing the voltage of the accelerating electrons can increase their chance to go deeper into the sample, the resulting image acquired will be of a poorer resolution.[130]

3.9.2 Transmission Electron Microscopy (TEM)

In TEM microscopy, a beam of electrons is transmitted through an ultra-thin specimen, interacting with the specimen as it passes through. The electron-sample interaction as the beam is shone through gives an image that is first magnified and focused before hitting the sensor of the detector.[131] Similar to an SEM, the TEM provides information concerning the morphology, composition and crystallinity of the specimen.[87] Unlike an SEM, however, the image is in two dimension, and hence does not depict topographic details as realistically as the former, albeit the latter's superior capability in magnification and higher resolution.

A. The Components of a TEM Consist of the Following Parts

- An electron source
- Electromagnetic lenses: condensing lenses used to focus the electron beam onto sample, and objective land projector lens to later magnify and delivery beam to the fluorescent screen.
- Fluorescent screen that uses cathodoluminacence, derived from the visible light emitted when the electron beam impacts a photographic film, or charge coupled device (CCD). [131]

B. TEM Imaging

The set-up of the instrument is similar to an optical microscope, with alternative sources for the same features, such as an electron beam instead of a visible beam, electromagnetic lens instead of glass lenses, and a fluorescent screen instead of an eyepiece, as shown in Figure 21 below. The image projected onto the screen can be manipulated by changing either the speed of the electrons, which is related to its wavelength, or the strength of the electromagnetic field of the lenses. The lighter areas in TEM images reflect regions of lower density, unlike the case of SEM images where brighter parts correlate with elements of higher atomic number.[132]

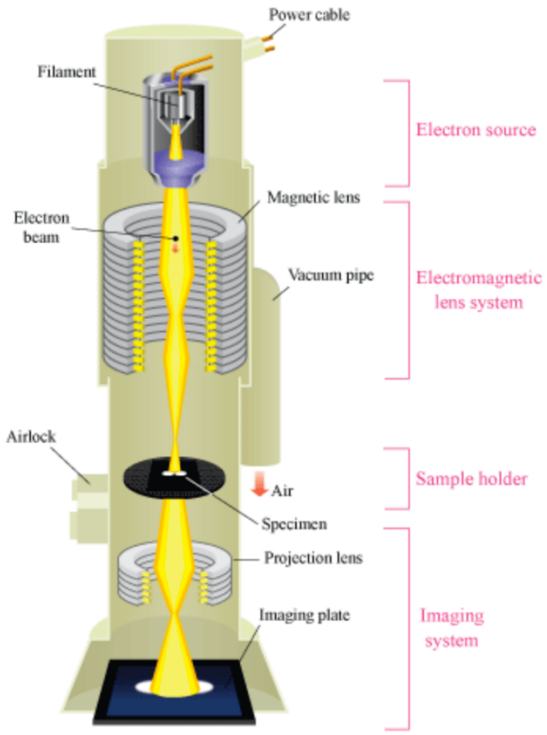

Figure 21. Diagrammatic representation of TEM.[132]

C. Advantages and Limitations

TEM images can give high-quality and detailed images of the specimen, with information including elemental composition and crystallinity. The magnification of TEM can reach the scale of 1 nm, giving a more elaborate and finely defined image to SEM.[133] However, TEM gives black and white 2-D images, at a much higher expense to SEM. Furthermore, the type of sample, and sample preparation is laborious. The samples need to possess certain properties as electron transparency, stability under vacuum chamber, and non-conductivity.

3.10 Vertical Diffusion Cell (VDC)

The VDC, also known as FDC, is an apparatus set-up widely used in the pharmaceutical industry to test the drug release kinetic profile of semisolid formulations. The basic features of the cell include a donor and receptor compartment with membrane sandwiched in the middle. The

formula is added to the donor area, where the drug can then permeate through the membrane into the receptor media. Aliquots are withdrawn either manually, or in the case of this project, automatically, every set interval of time. A critical requirement in the sampling process is the expulsion of air bubbles, as the creation of bubbles can cause adversely skew test results as they adhere to the membrane, interfering with the membrane-liquid interface.[134]

The basic features of the VDC automated sampling equipment is described in Figure 22 below. This includes six VDC placed on a plate with magnetic stirrers, a circulating waterbath that allows for thermostatic control, and a deaerated replacement media for the receptor compartment.[134]

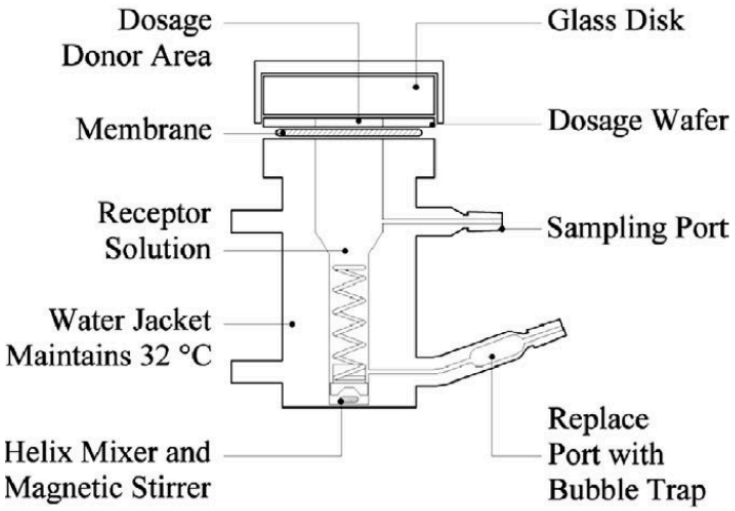

Figure 22. Automated VDC set-up.[134]

3.11 Photon Correlation Spectroscopy (PCS)

PCS is a technique used to assess the size of particles in a dispersion, and the homogeneity of their size distribution, namely their PDI.[135] The theory behind the method of the device employs the determination of the Brownian motion of the particles, which is dependent upon their hydrodynamic diameter.[136] This can be explained by the diffusion velocity of particles with respect

to their size, as larger particle tend to diffuse slower than relatively smaller ones. The set up as shown in Figure 23 below includes a laser, a thermostated sample compartment, and a photomultiplier for detecting the scattered lights at a specific angle. A monochromatic laser light is shone onto the sample cell with the suspension, while the particles are exhibiting Brownian motion, and the reflected intensity will undergo a Doppler shift as a result. This change in the frequency of the light is then correlated to the particle size distribution.

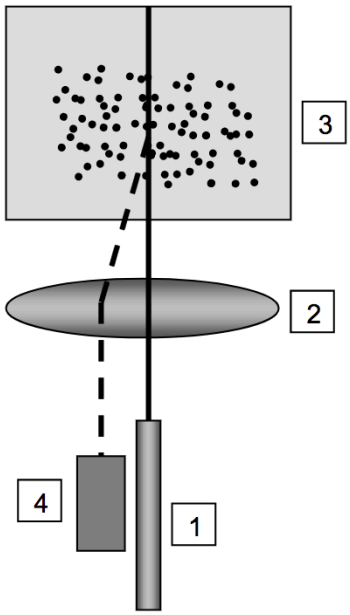

Figure 23. Schematic diagram of a typical PCS device: (1) laser (2) focusing lens (3) cuvette (4) detector.[70]

3.12 ZP

It is the potential difference between the mobile dispersion medium and the stationary layer of the dispersion medium forming a double layer at the interface of the dispersed particle.[137] Any recorded electric potential for the lipidic nano-carriers can be attributed to the surface charge of the particle, possibly from adsorbed ions or the chemical nature of the surfactants, along with the surrounding media.[70,138] This surface charge induces electrostatic repulsion between the dispersed

particles, and can hence influence the stability by impeding their aggregation. The change in velocity and direction of the lipid nanocarriers as a result of applied electric field is measured and correlated to their respective ZP values.[136]

Chapter 4
Materials and Methods

4.1 Materials

4.1.1 Solid Lipid: Emulium® Kappa[2]

It is a natural o/w emulsifier product made in France, donated by Gattefossé. No additional purification was required. It constitutes a mixture of lipids, derived from natural waxes of Candelilla, Rice bran, and Jojoba Polyglyceryl-3 Esters. The waxes are hydrophilized by transesterification with Polyglycerol-3, due to the hydrophilic character of the latter alchohol, giving a self-emulsifying ester, with surfactant properties.[82] Other ingredients added include Glyceryl Stearate, Sodium Stearoyl Lactylate, which are ester salts, and Cetearyl Alcohol, all contributing to the emulsifying capacity of the mix.[139,140]

4.1.2 Liquid Lipid: PP Oil

PP oil (Croda.), required no additional purification. In case of NLCs, an oil component was needed to be added to the solid lipid mix. PP oil is composed of a variety of fatty acid, both saturated and unsaturated, with the main component being linoleic acid, also known as omega-6, making almost 60% of all the fatty acid composition.[141]

4.1.3 Surfactants

A. Brij™ S721

Brij™ S721 (Croda, purity<99.5%). Also known as Steareth-21, it is a non-ionic ether surfactant of polyethylene glycol and Stearyl alcohol, as shown in Figure 24 below.[142,143] It has a Hydrophilic/Lipophilic balance (HLB) value of 15.5.[144] It is solid at room temperature.

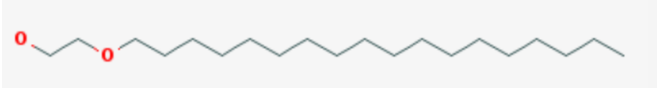

Figure 24. Brij 721 Surfactant chemical structure.[8]

B. Phospholipon 90 G

Phospholipon 90G (Lipoid GmbH, purity 96.9%). The main component is Phosphatidylcholine, which is naturally found in soy lecithin.[145,146]

4.1.4 Preservatives

Tristat, which is sodium dehydroacetate (TRI-K, purity >98%)

4.1.5 Vitamin A

Vitamin A- Palmitate derivative RP (Sigma Aldrich, purity≤100%)

4.1.6 Other Materials

Other materials used for the analysis included Ethanol (ROAJ, purity 96%), Isopropyl Alcohol (Lee Chang Yung Chemical, purity <99%) from , Methanol (Sigma Aldrich, HPLC grade) from Honeywell, and Glycerol (Piochem).

4.2 Equipment

1. Homogenizers:

There are two types of homogenizers involved in the production of SLN/NLC. The first one is the lab dispersing device, IKA T25 Ultra-Turrax® Disperser, operating at speeds reaching 24×10^3 rpm. This device is used to emulsify the melted lipid and aqueous phase together after heating them up until the lipid phase melts[46], following the hot homogenization technique.

The second, is the high- pressure homogenizer, EmulsiFlex-05 Avestin Inc. (Canada), with a pressure that can reach up to 2500 bar. It consists of a piston-gap, where the high pressure induced when the macrosuspension enters the narrow gap of a few millimeters allows for their diminution.

2. UV-vis Spectrophotometer, Jenway 6305, was used in the quantitative determination of RP in the carriers
3. An incubator shaker (Fisher Scientific), was used for the incubation of the formulations in the *in-vitro* set-up.
4. HPLC-PDA detector (Waters) was used for all analysis of RP content for in-vitro and ex-vivo release. A C18 column XTerra (3.9×100 mm) was used for the separation, with methanol as the mobile phase.
5. A Hanson Vertical FDC Vision® MicroetteTM Automated Test System was used for the ex-vivo permeation studies.
6. A Christ Alpha 2-4 LDplus lyophilizer was used to lypholize the samples prior to DSC measurements.
7. A Perkin Elmer Diamond DSC with autosampler (Hyper DSCTM) using Pyris software was used to study the thermal behavior of the lypholized lipidic-carriers.
8. Dynamic light scattering (Microtrac, NIKKISO Group, USA) is used for measurement of the average diameters of the particles in the suspension.
9. The ZP of the lipid nanoparticles was measured using a Malvern Zetasizer Nanoseries ZS90.
10. SEM images were obtained by two instruments, a JEOL 5200 Japan (2000), using Sema Four Software, and a Thermo ScientificTM QuantaTM Field Emission Gun (FEG)-250.
11. TEM images were obtained using a JEOL JEM-2010 USA instrument.

4.3 Methods

4.3.1 Production of Lipid carriers

The method employed in the development of both the SLN/NLC was the hot homogenization procedure described in several review articles.[11,32] The method entailed the following steps:

1. The Aqueous was prepared by adding a fixed amount of Tristat, namely 0.6% of the total suspension, which is soluble in water.
2. Lipid phase consists of the Emulium Kappa^2, Lecithin, Brij 721 and PP oil in case of NLC.
3. The two phases were heated to 70°C until the lipids were melted.
4. RP was then added into the lipid melt so as to prevent overexposure of the RP to heat, keeping the melt immersed in hot water beaker to prevent recrystallization, and making sure the temperature does not exceed 65°C to prevent the degradation of RP.[148]
5. The hot lipid melt is then dispersed into the hot aqueous solution which was maintained at the same temperature, using the Ultra-Turrax homogenizer, at 21×10^3 rpm for one minute.
6. The premix is then passed through a high-pressure homogenizer, where three cycles were performed at 1500 bar.[149]
7. The dispersion is then rapidly cooled in an ice bath at a temperature of 4°C for 1 hour to promote the crystallization of the lipids into spheres, by thermal shock, c.[25,150]
8. The difference in composition between the NLC and SLN was achieved by substituting the same percentage liquid oil phase, namely PP oil, with solid lipid Emulium Kappa^2 for the latter lipid nano-carrier.[41]
9. The dispersions were stored in dark glass bottles that were hermitically sealed.

4.3.2 Optimizing the formula for NLC using a 2^3 Factorial Design of Experiment

Since the SLN/NLC carriers are affected by the composition of all the excipients, which include surfactant, lipid, and drug, a way to optimize the formulation in terms of controlled release, high EE%, particle size homogeneity, and high skin permeation, a 2^3-factorial design was used to design the experiment from the start. The three factors varied in this work include the surfactant system composition, liquid oil (PP seed oil), and drug (RP) amounts. Each of the three factors had two levels. The chosen factors varied were based on previous literature reviews reporting a correlation between the constituting lipidic phase and surfactants composition on the assessed parameters.[27,37] As for the chosen levels of each factor, they are based on guidance from preliminary work conducted at EVA. The design of experiment using a 2^3-factorial design varies every one of the three factors by two levels, and produces a series of combinations, where for this specific design 8 trials were ensued. The responses considered for every trial includes EE%, particle size, PDI index, ZP and total *in-vitro* release. This design aimed to give the best combination of factors for the NLC carrier, using the SLN as the control, in terms of highest EE%, lowest PDI and particle and highest release. Statistical analysis using one-way ANOVA also allows for determining any correlation among the factors.

4.3.3 Factorial 2^3 Design for Factors X1-3

Factorial design is an experimental design that involves several factors, where each is varied at only two levels. These levels can be either quantitative or qualitative. For this work the 2^3 design entailed changing the quantitative factors of the constituting ingredients of the NLCs, for the 8 formulations that followed the design ($2^3 = 8$). In order for this design to be applied, three assumption must be validated: (1) the factors are fixed, (2) the designs are completely randomized, and (3) the residuals are normally distributed. Furthermore, the advantage of this design is that it

allows for the smallest number of runs to be studied. Therefore, in cases as this, it is optimal for screening the factors in a system.

The analysis procedure for the factorial design includes first (1) estimating the factor effects, followed by (2) formulating a model, then (3) testing the model using analysis of variance (ANOVA) techniques, and finally (4) refining the model by omitting the insignificant terms.[151] The residuals should be analyzed graphically to confirm the assumptions required for ANOVA, such as their normality and independence. These validations will be provided in the appendix for reference, as they do not contribute to the analysis of the results. Moreover, there are seven degrees of freedom between the eight treatment combinations in the 2^3 design. Three degrees of freedom are associated with the main effects of A, B, and C. The remaining four are associated with interactions amongst the factors, such as AB, AC, BC and ABC. The design matrix and the geometric view of the 2^3-factorial design is shown in the Figure 25.

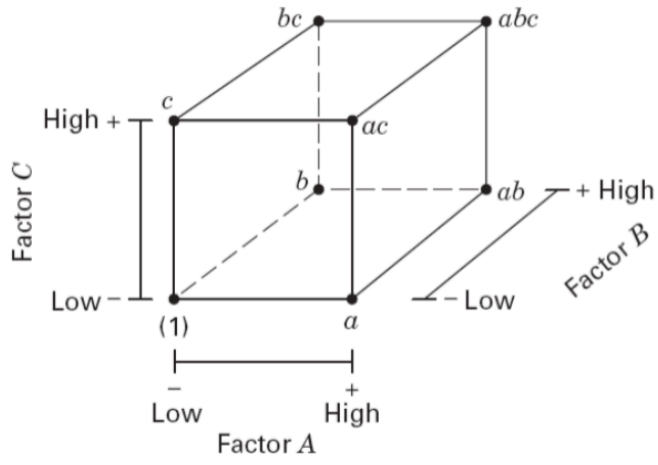

(a) Geometric view

Run	Factor A	B	C
1	−	−	−
2	+	−	−
3	−	+	−
4	+	+	−
5	−	−	+
6	+	−	+
7	−	+	+
8	+	+	+

(b) Design matrix

Figure 25. The 2^3 factorial design.[151]

The statistics software used to compute all the required values is Design-Expert. The ANOVA is retrieved for all the factors of significance, and a regression model is then derived. The general form of the model is:

$$y = \beta_0 + \beta_1 x_1 + \beta_2 x_2 + \beta_3 x_3 + \beta_{12} x_{12} + \beta_{13} x_{13} + \beta_{23} x_{23} + \beta_{123} x_{123} \quad \text{Equation 3.}$$

For the purpose of this experiment, x_1, x_2 and x_3 are the coded variables that represents the composition of RP, surfactant to solid lipid ratio, and PP oil composition, respectively. The regression coefficient for each variable, β, is calculated by the software and assessed to be statistically significant or not by the F-test carried out in the ANOVA. The first line in the ANOVA is an overall summary of the full model that consists of all the main effects and interactions. The F-test for the overall model is judged significant if at least one of the regression coefficients (β) are non-zero. The chosen significance level for this case was chosen to be at 10%.

The three factors and two levels for each are as follows:

X_1: vitamin A%

+ = 5% - = 2.5%

X_2: surfactant to solid lipid ratio

+ = Kappa^2 (5%) Brij721 (4%) - = K (4%) B(5%)

X_3: PP oil

+ = 5% - = 2.5%

The composition of the 8 formulations based on the combination of the three factors, each varied at two levels, is listed in the table 1 below, where the only two constituents that remained constant are the Phospholipon 90G at 0.5%, and Tristate at 0.6%.

Table 1. NLC Formulations Composition, %

Trial no. for NLCs	T1 (--+)	T2 (+--)	T3 (-+-)	T4 (+++)	T5 (---)	T6 (++-)	T7 (+-+)	T8 (-++)
Vitamin A	2.5	5	2.5	5	2.5	5	5	2.5
PP oil	5	2.5	2.5	5	2.5	2.5	5	5
Emulium Kappa[2]	4	4	5	5	4	5	4	5
Brij 721	5	5	4	4	5	4	5	4
Water	82.4	82.9	84.9	79.9	84.9	82.4	79.9	82.4

The SLN formulation had a slightly different composition, where the amount of solid lipid was increased to substitute for the missing oil component in the NLCS:

Table 2. SLN Composition

SLN	%
Vitamin A	5
Phospholipon	0.5
Emulium Kappa[2]	10
Brij 721	4
Tristat	0.6
Water	84.9

All percentage compositions were carried out weight/weight, where the final was 50g, about 50 mL of SLN/NLC dispersion.

4.4 Characterization

4.4.1 EE%

SLN/NLC particles were all greater than 100 nm, so a 100kDa molecular weight cut off (MWCO) was suitable, as it is equivalent to a membrane pore size of 10 nm. About 0.1g SLNA was accurately weighed directly into a clean Eppendorf, and diluted to 1 g with distilled HPLC water. Another 0.1g of the diluted SLNA was added directly into Pall Nanosep® with omega membrane (100 kDa) Eppendorf. Nanosep was inserted into a Scilogex D2012 centrifuge device for 15 mins at rpm 14000. The water came through the filter and the concentrate particles remained in the filter compartment. 0.5 mL of IPA was added volumetrically using a micropipette with slight shaking. A second round of centrifuge so that the IPA dissolves the NLCs and releases the unentrapped V.A was ensued. Finally, the IPA was diluted 100 folds in triplicates, and measured using UV-vis Spectrophotometry.

The EE% of RP was quantified using previously prepared calibrations of RP in IPA, using a UV-vis spectrophotometer. The absorbance of the dissolved SLN/NLCs carriers in IPA from the previous step was substituted in the linear equation of the calibration curve. IPA was used as blank. In order to confirm that none of the excipients of the formula absorb, a formula of NLC without vitamin A was done and the same procedure applied to it. The following was the equation used to calculate the EE%:

$$EE\% = \left(\frac{W_{initial\ RP} - W_{entrapped\ RP}}{W_{initial\ RP}}\right) \times 100 \qquad \text{Equation 4}$$

where $W_{initial\ RP}$ is the mass of the total amount of RP present in the diluted sample of the dispersion, and $W_{entrapped\ RP}$ is the mass of the RP detected in the NLC carriers after separating them from aqueous dispersion medium.

4.4.2 *In-vitro* Release

The dialysis bag was a cellophane membrane, Spectra Por® (Spectrum Medical Inc. USA) The membrane molecular weight cut off is in the range of 12-14 kD. The membrane was cut into 10 cm for each replicate, where they were first pre-soaked in distilled water to soften and open up. The bottom was tightly tight into a knot. 5 mg of V.A was added into the dialysis membrane from the top opening and sealed by folding thrice with attachment of a firm metal paper clip.

The following were the calculations for the amounts of formula used in the set-up:

For formulations with 5% V.A:

$$100\ mg\ of\ SLN\ \&\ NLC \times 0.05 = 5\ mg\ V.A$$

For formulations with 2.5% V.A:

$$200\ mg\ of\ NLC \times 0.025 = 5\ mg\ V.A$$

In order to achieve sink conditions, a minimum of 36.5 mL solution medium is required to dissolve 15 mg of the V.A. An approximate value of 50 mL ethanol/glycerol media was taken, and measured accurately using a 25mL pipette.

Two preliminary tests were conducted to confirm the validity of the method. The first was to measure the total release of a known concentration of RP solution in ethanol glycerol in the dialysis

bag, after 24 hours. The aim was to see if the membrane allows for the release of the RP to a great extent (>90%), without acting as a barrier that could be a limiting factor in the experiment.

The other experiment was to test the stability of the RP in the solvent at the same conditions of the experiment, incubated for 24 hours. A change in the initial concentration means that the RP has degraded, and the results will then have to be normalized accordingly.

Sampling for the *in-vitro* release of the formulas:

2 mL samples were withdrawn from the solution outside the membrane bag at the following intervals: 0.5h 1 h 2h 4h 6h 8h 12h 24h, which were then replaced with fresh media maintained at the same temperature inside the incubator as that of the set up. An incubator shaker was used where the temperature was adjusted to 37°C and shaking at 144 oscillations per minute. The receptor media was a mixture of glycerol in ethanol in 2:8 ratio as adopted from the study conducted by Ro et al..[93]

The samples were then analyzed using HPLC. The flow rate was 2 mL/minute, injection volume 50 μL, run time 5.0 mins, and RP retention time was in the range of 3.8-3.9 mins. RP was detected at λ_{max}= 326 nm.

4.4.3 *Ex-Vivo* Release

Rat skin was used as natural membrane for measuring the permeation of RP across the skin barrier. The rats weighed from 250-350g. A depilatory cream was first applied on the skin for hair removal, and then the rats were sacrificed. The skin was de-fattened using ether. The skin was then put in a saline medium, with the SC facing up, and store in the freezer until use.

A vertical FDC set up with automated sampling was used. The excised rat skin was placed in the donor compartment, with its SC facing up. The receptor media was the same as that for the *in-vitro* (glycerol in ethanol, 2:8), where every cell contained 7mL. The diffusion cells were maintained at a temperature of 37°C, with constant stirring at 600 rpm.

1 g of suspension of the two formulas with highest *in-vitro* release (T2 and T6) were placed on the donor cell, and 2mL samples was withdrawn at predetermined time intervals (1, 2, 4, 6, 8, 10, 12, 24h), where an equivalent amount of medium, maintained at 37°C was replaced. The samples withdrawn where then filtered through 0.22 µm filters and analyzed using HPLC. After the incubation, much of the formula still remained on the surface, showing an infinite dosing set up where the dose applied is no longer a limiting factor.[152] This was the case presented in one study used as reference for this procedure, by Teixeira et al., where the dose applied was not listed as a factor, as opposed to a finite dosing set-up conducted by Jenning et al. in their permeation study.[48,44]

4.4.4 RP Penetration Studies

The amounts of RP left behind in the SC, and deeper in the dermis and epidermis section were quantified by a similar procedure to that reported in a study conducted by Teixeira et al. on the permeation of RP in nano-polymeric capsules.[48] The following was carried out:

- For the SC, the skins used for the *in-vitro* release after 24 hour incubation were gently dried with cotton swabs and then taped 20 times.[153] The tape used was tesa film, 19 mm wide. The tapes were immersed in 10 mL methanol for extraction of the RP. The sample was then put in an ultra-sonic bath for 30 minutes at 40°C, vortexed for 3 minutes and finally filtered through 0.22 μm filters to be analyzed using HPLC.

- For the epidermis/dermis section, the remaining skin that had its SC taped off, was cut into small pieces, 2-4 mm each, using a scissor, and added to 30 mL methanol which were then homogenized using Ultra-Terrax homogenizer at 8000 rpm for 4 minutes. The extract RP solution was then filtered through 0.22 μm filters to be analyzed using HPLC.

4.4.5 DSC Thermal Analysis

Thermal behavior of the samples and pure solid lipids were investigated using DSC. DSC thermograms were conducted on the pure solid lipids (Kappa^2 and Phospholipon 90G) and all the lyophilized suspensions. Approximately 10 mg sample were weighed into hermetic crimp aluminum pan that are then sealed. An empty pan was used as a reference. The temperature rate increase was 10°C/min with a temperature range of 0-200°C, heated under N_2 gas, as adopted from Akbari et al. in their characterization of SLNs.[154]

4.4.6 Particle Size Analysis

The samples were diluted 10 folds with distilled water to prevent multiple scattering. A refractive index of 1.33 was used for the fluid characteristics, with a temperature range from 20-30°C. The instrument gave the average hydrodynamic diameter of the particles and the PDI to assess the homogeneity of the particle size distribution in the dispersion.

4.4.7 ZP

A dilution factor of 10 was ensued on the formulations prior to the analysis of their ZP.

4.4.8 Stability of RP in NLC

The stability of the control RP in the stock solution, and an RP loaded NLC carrier, namely T4, was investigated. Both were incubated at a temperature of 25°C for 38 days, and four samples were collected at time 48 hr, 120 hr, 216 hr, and 456 hr.[43] The amounts of RP in the NLC initially

was determined by dissolving the dispersion in isopropyl alcohol, and followed by measuring the content using UPLC. An equivalent amount of the stock solution was then prepared.

4.4.9 SEM Imaging

One drop of the suspension was added onto a slide, and put in a desiccator until the suspension dried. The lipid carriers were then sputtered with gold, and mounted onto the device. A skin sample incubated for 5 hours with the drug applied on it in the FDC was also analyzed, where 1 mm of the skin was cut and sputtered with gold before imaging.

4.4.10 TEM Imaging

The operating voltage was between 80 to 200 kV. The SLN/NLC suspensions were first diluted 10 folds with distilled water. A carbon coated copper grid was then dipped into the diluted suspension, and allowed to soak for about 3 minutes. It was then removed and moved onto a filter paper to allow the water to dry out. The grid was then mounted onto a holder and into the TEM where vacuum was first achieved prior to the viewing of the sample.

Chapter 5

Results and Discussion

5. Results and Discussion

5.1 Particle size and PDI analysis

Figure 26 below shows the results for the mean particle size along with the PDI values for the fresh NLCs and SLN samples. The latter value gives an indication to the homogeneity of the particle dispersion. In many works reported in the literature, a value of PDI <0.3 is considered to be pertaining to a narrow distribution size.[155,156,157] Only values less than 0.1 are considered monodisperse, however. The size of the NLC-RP formulations range from 197.6 nm to 240.2 nm. The variation in particle size for most of the formulations had a PDI <0.3, and can be considered ideal. The variation in size among the formulations can be attributed to three factors: liquid lipid amount (PP oil), surfactant composition, and vitamin A amount. The inherent chemical nature of the lipids and surfactants used, along with their chemical interactions has been reported to affect the particle size.[149] The design of experiment was used to allow for statistical analysis of the results. The graphs for the variation in particle size is shown in the Figure 27, where the surfactant composition refers to the surfactant (Brij 721) to solid lipid (Kappa^2) ratio, and level 1 implies a higher surfactant ratio than level 2.

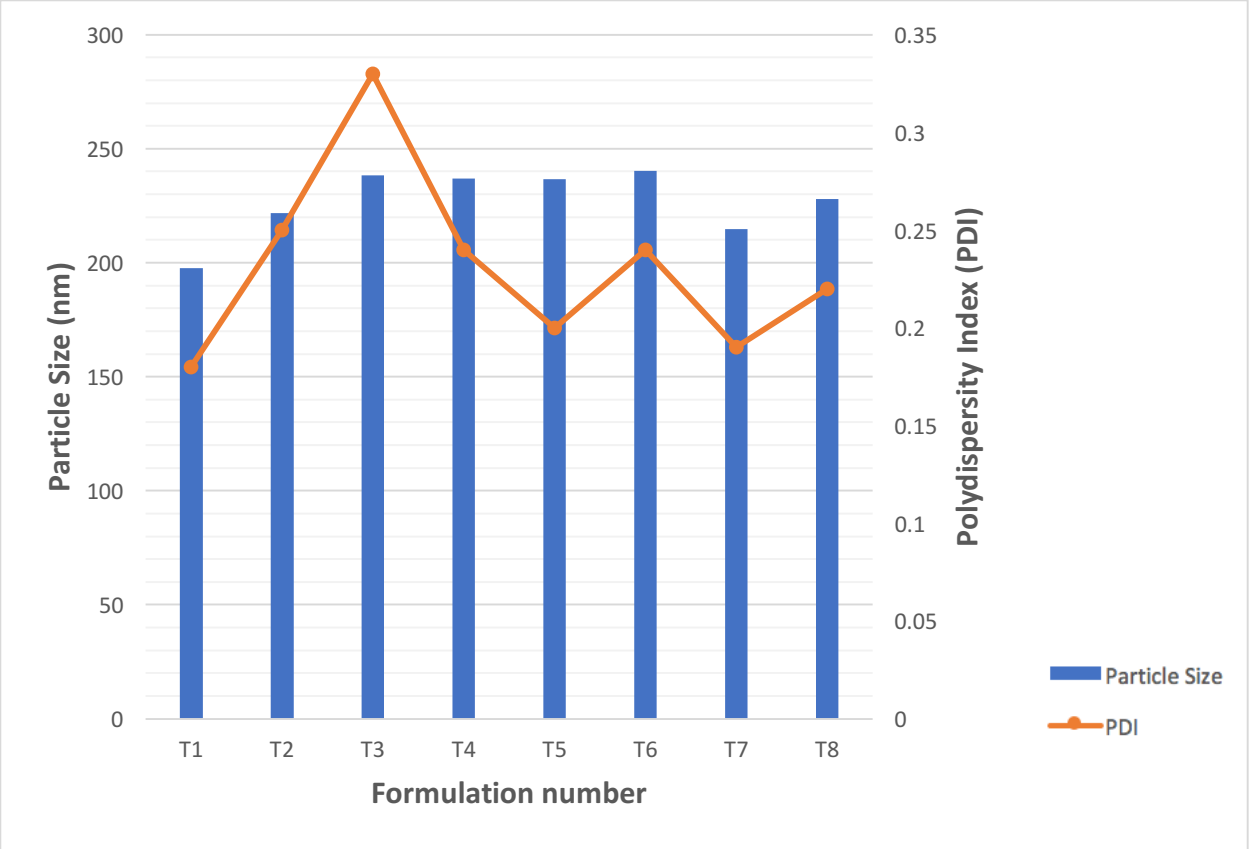

$$SLN\ Particle\ size = 296.7, \qquad PDI = 2.47$$

Figure 26. Particle size and PDI values upon formulation.

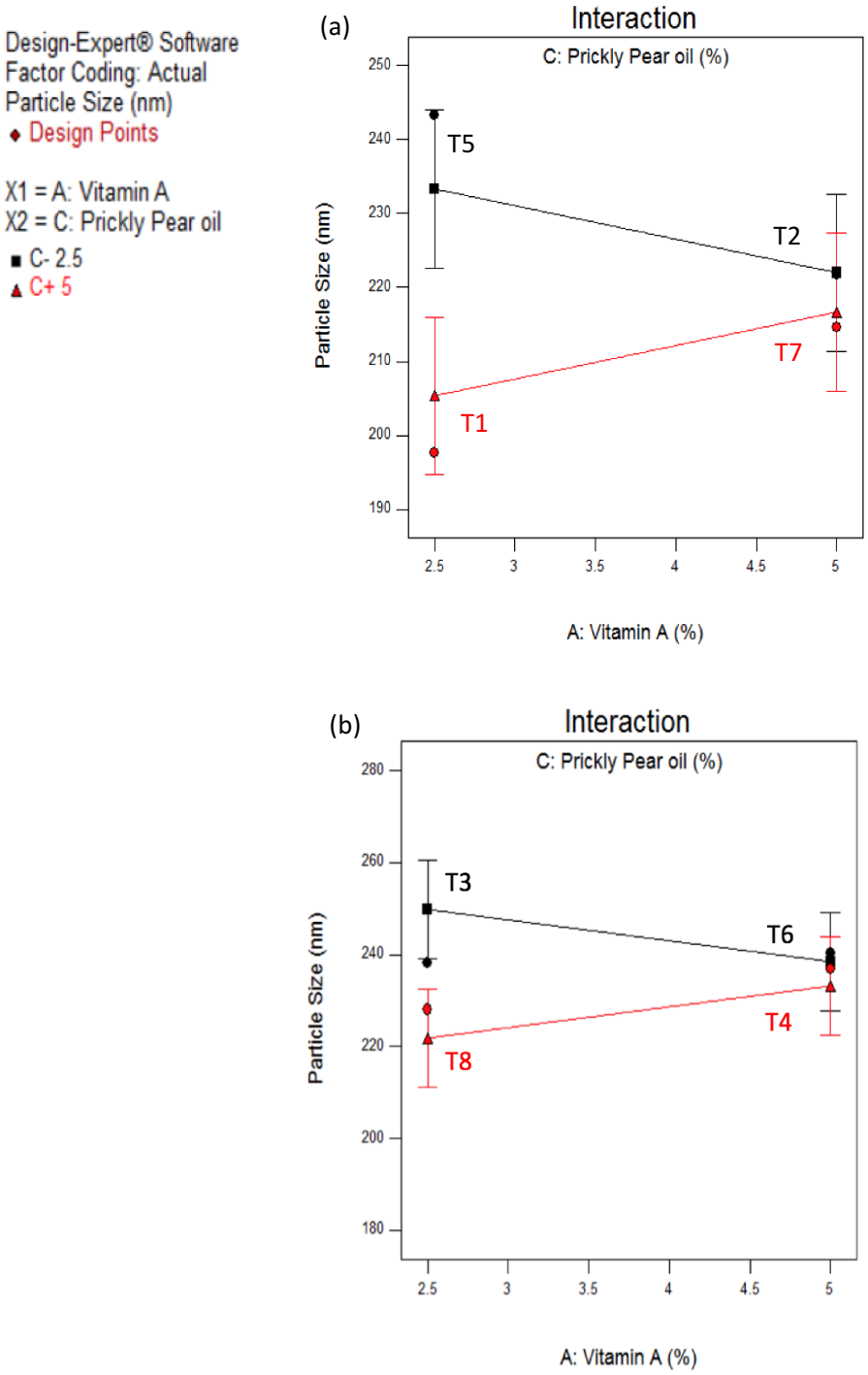

Figure 27. Interaction plots of the factors on Particle Size with (a) high surfactant and (b) low surfactant to solid lipid ratio showing the trend in formulations with increasing Vitamin A%.

The change in the particle size for the 8 formulations is divided into two parts. Figure 27 (a), shows the response of particle size with respect to change in vitamin A and PP oil composition, fixing the surfactant composition at level 1, which is equivalent to a high surfactant to solid lipid composition. These formulations (T1, T2, T5 and T7) have a higher amount of surfactant Brij, and a lower amount of Kappa^2, a self-emulsifying solid lipid. In part (b), the response is illustrated for formulations (T3, T4, T6 and T8) with surfactant composition at a low, when lower amount of surfactant Brij is compensated by a higher amount of lipid Kappa^2. The composition of water in each formulation was dependent upon the lipids and surfactant composition in each respective formulation, as it is a mixture based experiment.[149] In both Figure 27 (a) and (b), a similar trend is seen for formulations with higher and lower amounts of PP oil. A lower particle size is seen when the amount of oil is high (PP oil = 5%), and vitamin A is low (RP = 2.5%). The particle size for the four formulations (T1, T4, T7 & T8) show an increase with an increasing amount of vitamin A. This result is reported in several previous works, where an increase in lipid concentration, which is in this case the RP, is associated with an increase in particle size, keeping all other factors constant.[158,154] The surfactant to lipid ratio was also reported to influence the particle size, where smaller size is correlated with higher surfactant composition.[158,154] This is seen in the results here, where part (a), with a higher surfactant to solid lipid ratio, shows a relatively smaller particle size for all four formulations, as compared to part (b). This can be explained by the fact that surfactants decrease the surface tension between the two interphases, and hence facilitate the formation of particles with higher surface area and smaller size.[159] Surfactant molecules envelope the lipid droplets, and impede coalescence by steric hindrance, as in this case, or repulsive interactions in the case of ionic surfactants. The surfactant used here, a polyoxyethylene fatty ether, however, is nonionic, with a structure given in the Figure 24. The polar head of the ether, which is given by

the two electronegative oxygens, allows for emulsification in the aqueous dispersing medium, and the alkyl chain provides steric hindrance between the carriers.

Furthermore, in both part (a) and (b) a larger overall particle size is seen for the 4 formulations T2, T3, T5 and T6. This increase can also be attributed to a less viscous dispersion as a result of the lower composition of PP oil in all four, leading to a less proper diffusion during homogenization. This contributes to a larger particle size.[149,160] The decrease in particle size as a result of increasing RP in that case can be attributed to an increased viscosity of the lipidic active's low melting point.[158]

T3 has shown a relatively significant polydispersity in particle size, which can be attributed to its high solid lipid content with respect to all other factors. This highly viscous lipid could have diffused slowly, allowing time for flocculation of particles into larger aggregates prior to stabilization by surfactant absorption on their surface.[159] T1, on the other hand, had a lower viscous lipidic phase, due to the high amount of PP oil with respect to the solid lipid. This change in composition was reflected in its much smaller particle size, and PDI index, which can also be attributed to the stabilization of the higher surfactant to lipid ratio of the formulation.

The SLN showed the highest particle size and PDI, which can be assumed to be due to the poor solubility of the RP since there was no PP oil to solubilize it. This could lead to limited diffusion of the lipids at the interface, resulting in a poorly, highly polysdispersed dispersion.[158]

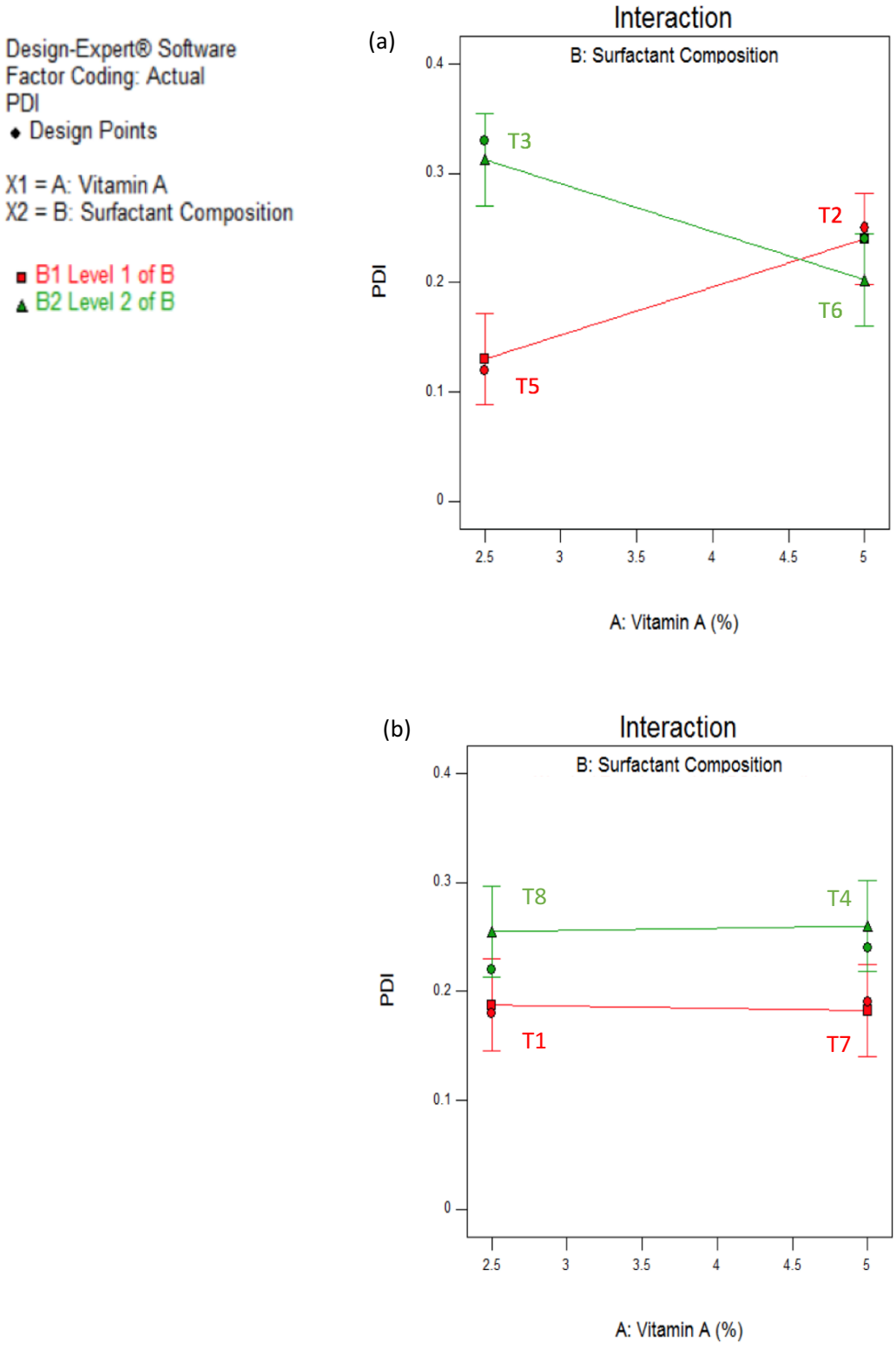

Figure 28. Interaction plots of the factors on PDI with (a) low PP oil% and (b) high PP oil% showing the trend in formulations with increasing Vitamin A%.

Figure 28 (a) and (b) show the effects of the factors on the PDI response for the 8 NLC formulations. As can be seen in part (a), a change was recorded with variations in composition as opposed to part (b). In part (a), formula T3 and T6 both had a low surfactant to solid lipid ratio and high PP oil amount. The only factor that changed was the composition of vitamin A, which led to a decrease in PDI with the increase in its concentration. The decrease in PDI could also be related to the change in viscosity of the lipid phase, which becomes more viscous with the increase of the oily RP, facilitating diffusion into the aqueous melt and thus resulting in a more effective homogenization. T5, on the other hand, showed the lowest PDI, which could be attributed to its low composition of all three lipidic constituents, that could be more easily dispersed in the aqueous medium. An increase in only the vitamin A composition in T2 shows a significant increase in PDI. This could be due to insufficient lipids, both solid and liquid, to form NLCs, allowing for the formation of other colloidal carriers such as micelles and liposomes.[32] In part (b), however, where all 4 formulations were of a higher composition of PP oil, the change in both vitamin A composition, and surfactant to lipid ratio (red and green lines), did not show a change in the PDI for each pair. Formulations T1 and T7 did show a lower PDI compared to T8 and T4, where the higher surfactant to solid lipid ratio of the former was the key factor in this change. This result confirms the previous claim on surfactant role in particle size, where T1 and T7 exhibited both the lowest particle size and PDI, showing an optimized formulation in this respect when surfactant composition is high relative to the solid lipid. However, this phenomenon is only observed in part (b), when a high composition of PP oil was used. This means that more than one factor is responsible for this phenomenon, as the PP oil level is decisive in the trend that follows. One may conclude that a higher amount of PP oil allows for a lower PDI with increasing surfactant to solid lipid ratio, since the vitamin is now better solubilized.

5.1.1 Analysis of Variance for particle size and PDI

Table 3. ANOVA for particle size response

Response Particle Size

ANOVA for selected factorial model

Analysis of variance table [Partial sum of squares - Type III]

Source	Sum of Squares	df	Mean Square	F Value	p-value Prob > F	
Model	1352.14	3	450.71	5.11	0.0745	not significant
B-Surfactant	*542.85*	*1*	*542.85*	*6.15*	*0.0682*	
C-Prickly Pe	*552.78*	*1*	*552.78*	*6.27*	*0.0665*	
AC	*256.51*	*1*	*256.51*	*2.91*	*0.1634*	
Residual	352.90	4	88.22			
Cor Total	1705.04	7				

Table 4. ANOVA for PDI response

Response PDI

ANOVA for selected factorial model

Analysis of variance table [Partial sum of squares - Type III]

Source	Sum of Squares	df	Mean Square	F Value	p-value Prob > F	
Model	0.023	3	7.546E-003	8.27	0.0344	significant
B-Surfactant	*0.011*	*1*	*0.011*	*11.52*	*0.0274*	
AB	*5.513E-003*	*1*	*5.513E-003*	*6.04*	*0.0699*	
ABC	*6.612E-003*	*1*	*6.612E-003*	*7.25*	*0.0545*	
Residual	3.650E-003	4	9.125E-004			
Cor Total	0.026	7				

The chosen level of significance for the purpose of this model was 10%, meaning $p<0.10$. This level was chosen based on the chance of random error, that could mount up to 10% due to

limitations in the experimental set up. The significance of the model implies that at least one of the three factors have a coefficient different from zero. In the case of the response on particle size by the 8 formulations, the model is shown to be significant at 10%. Factor A, B, and C stand for vitamin A, surfactant to lipid ratio, and PP oil composition, respectively. The possible interaction of any two or three factors together is reported as well (e.g. AB, ABC, etc). In table 3 the two factors that had a significant relative effect at the chosen level of 10%, were that of the PP oil and the ratio of the surfactant to the solid lipid. This confirms the claims made previously pertaining to the lower viscosity of the lipid melt and stabilization of the surfactants in achieving smaller particles. The ANOVA for the PDI, however, showed a higher significance in the variation among the formulations as a result of changes in the factors. The most significant factor is the surfactant to solid ratio (surfactant composition), which further confirms the interaction Figure 28 of the PDI. Vitamin A (A) and PP oil (B) composition were irrelevant in this case. However, their respective interaction (AB and ABC) were significant.

5.1.2 Regression model for Particle Size

The regression equation for the particle size response includes only the surfactant to solid lipid ratio and PP oil composition, since the other factors, such as vitamin A % (w/w), had a zero coefficient. The following is the coded regression equation from Design Expert:

$$particle\ size = 227.54 + 8.21X_2 - 8.29X_3 \qquad \text{Equation 5.}$$

The R^2 of the model gave a value of 0.6406, which is not a good fit. However, a qualitative interpretation can be deduced from the above equation between the composition in PP oil, surfactant ratio and predicted particle size. The equation in terms of coded factors can be used to make predictions about the response for given levels of each factor. By default, the high levels of the factors are coded as +1 and the low levels are coded as -1. The coded equation is useful for

identifying the relative impact of the factors by comparing the factor coefficients. From the above equation, one may see that the absolute value of the coefficients for both factors, X_2 and X_3, are almost the same. This is expected since their relative p-values was also close, in the previous ANOVA table 3. Their impact on the particle size response, however, varies with the level chosen. For instance, when X_2 and X_3 are both at level 1, one may substitute for their variables with -1, which will give a higher particle size in comparison to fixing X_2 and changing X_3 to level 2 (+1). This is clarified in the calculations below:

$X_2(-1)\ and\ X_3(-1)$:

$$particle\ size = 227.54 + 8.21(-1) - 8.29(-1) = \ 227.59\ nm$$

$X_2(-1)\ and\ X_3(+1)$:

$$particle\ size = 227.54 + 8.21(-1) - 8.29(+1) = \ 211.04\ nm$$

Thus, one may conclude from all the previous graphs, and above equation that in general increasing surfactant composition with respect to the solid lipid (X_2=-1), and incorporating higher amounts of PP oil (X_3=+1), leads to a reduction in the average particle size.

5.1.3 Regression Model for PDI

The regression equation for the PDI response includes the surfactant ratio, X_2, its interactions with vitamin A% (w/w), X_{12}, and interaction between all three factors, X_{123}. The following is the coded equation that includes all significant factors that affect the PDI:

$$\boldsymbol{PDI = 0.2213 + 0.0363X_2 - 0.0262X_1X_2 + 0.0287X_1X_2X_3} \qquad \textbf{Equation 6.}$$

The R^2 of the model gave a value of 0.8612, which is significantly higher than the value for the particle size model. This is expected, since the model's significance was also higher in case of the

PDI, with a p-value of 0.0344, in comparison to 0.0745 for the particle size model. Furthermore, from the above equation, the relative significance of X_2 is the highest, due to its high relative coefficient's magnitude.

5.1.4 Validating the Assumption of ANOVA

The validation of the assumptions of the ANOVA are provided in Appendix B for each of the 5 responses (particle size, PDI, ZP, EE% and *in-vitro* release). The first two assumptions include the normality and independence of errors, which is the variation of each value around its own group mean. This eliminates any bias in the results, which if present, would not allow for the use of ANOVA claims. The third assumption includes the homogeneity of the variances, where each group, in this case each of the three factors, must have commons variances among their respective residuals.[151]

5.1.5 Stability of NLCs and SLN Formulations based on Particle Size and PDI

The stability of SLN/NLC systems is controlled by two processes related to both the suspension, and the matrix of the nano-carrier. The former relates to the system's ability to remain homogeneously dispersed, where a failure in this aspect results in irreversible particle coalescence.[161] As for the latter, an inherent polymorphic transitioning of the crystalline lipid can lead to a gelling effect resulting from the network formation of the, now, thermodynamically stable crystalline forms.[41] Hence, the composition of the SLN/NLC is pivotal in optimizing the stability of the lipidic carriers, as shown in Figure 29, where the stability of the NLCs in this case is shown to be dependent on the formulation composition.

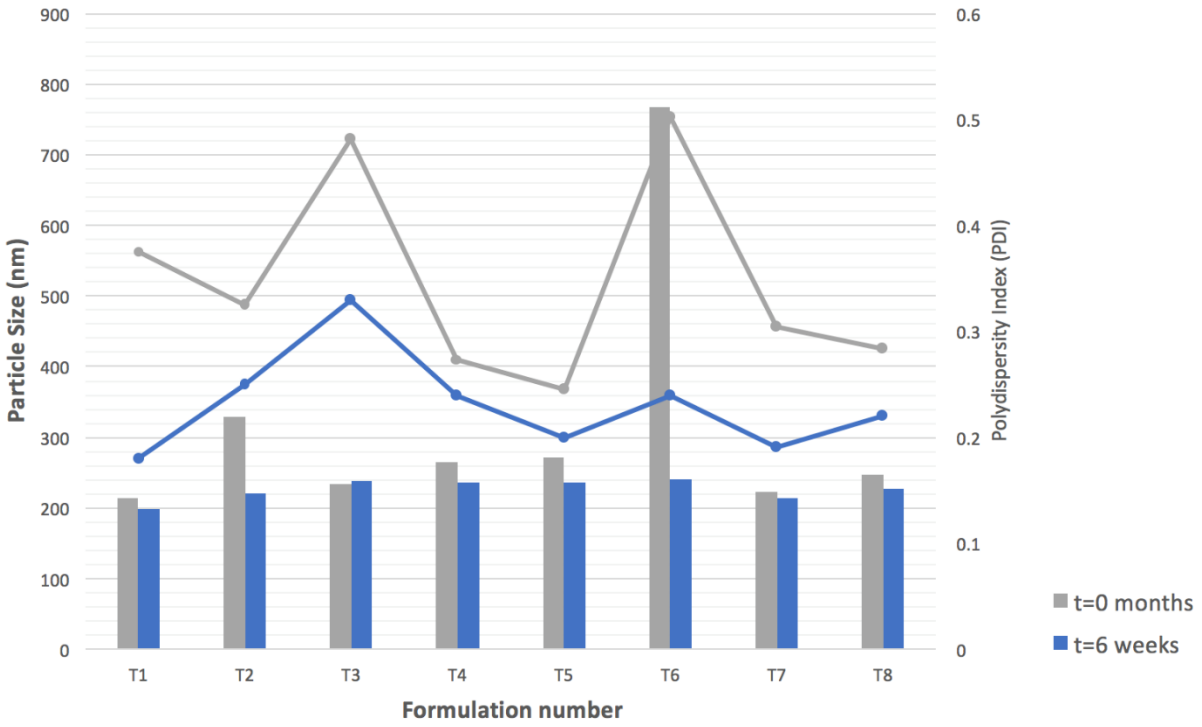

$$SLN\ Particle\ size = 203.7, \qquad PDI = 2.05$$

Figure 29. Comparison of Particle size and PDI values at t=0 and after 6 weeks.

The SLN has shown better stability in comparison to the less stable NLCs, with much more pronounced increase in PDI. This is due to the SLN's immediate particle growth upon formulation, a tendency of the carrier to form a gel. This phenomenon is previously reported to be one of the main drawbacks of SLN.[37] This can be explained by the lipids' tendency to transition into a more stable polymorphic form.[136] The lack of an oil component in the SLN allowed for a less stable polymorph, which prompted an early transitioning of the solid lipid crystals. This transition is reported to result in a change in the shape of the nanoparticles, from spherical into a platelet-like forms with higher surface area.[162] The TEM image of the SLN, Figure 30, also shows this variation in particle size.

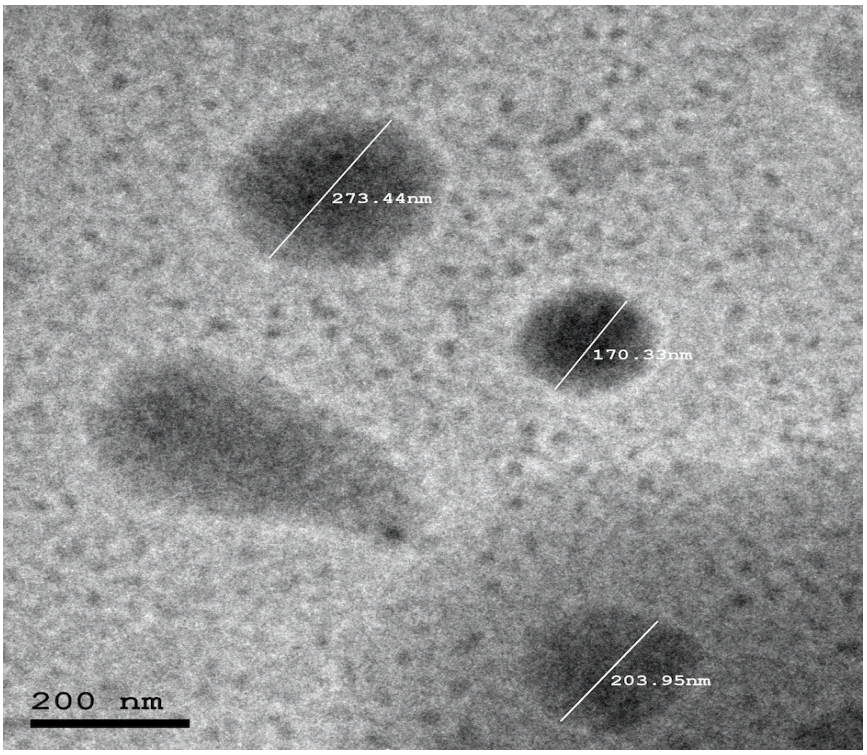

Figure 30. TEM image of SLN showing heterogeneous size distribution.

The particle size distribution of all formulations is shown in Figure 32. As can be seen in the SLN plot, large particles were forming at the onset of the formulation. This could allow for an Ostwald ripening process to occur, which can be confirmed with the increase in the distribution of particles with larger sizes, as a consequence of smaller particles dissolving and re-precipitating on the larger particles.[163] This process is thermodynamically driven due to the saving in lattice energy in larger particles, and reduction in surface energy of the smaller particles by redistributing them on the former. A similar explanation can be given to T6, which did exhibit a change in viscosity upon storage, unlike the remainder NLC formulations. However, this increase in viscosity, was less pronounced for T6, as well as took place at a much slower rate than the SLN. This was confirmed when withdrawing the dispersion using a micropipette, where less amounts of SLN were withdrawn in comparison to T6, due to its more condensed gel like structure. A similar argument could be made when comparing the viscosity of T6 with the remaining NLC

formulations. An SEM image showing the variation in particle size for T6 is shown in Figure 31 below.

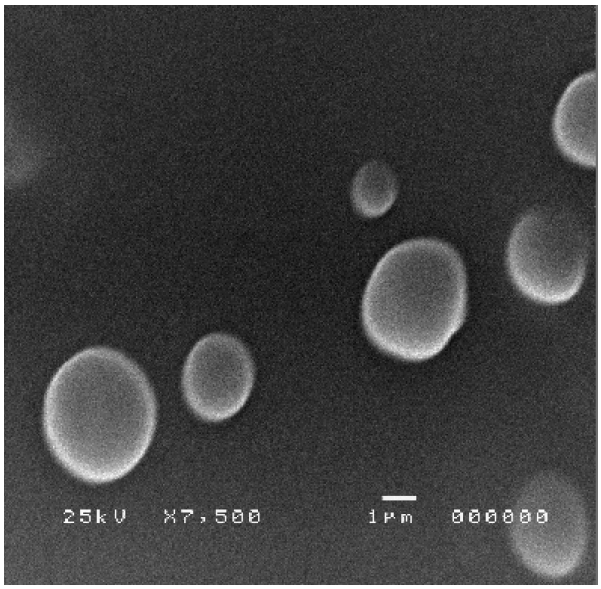

Figure 31. SEM image of T6.

NLCs/SLN	$t = 0$	$t = 6\ weeks$
SLN	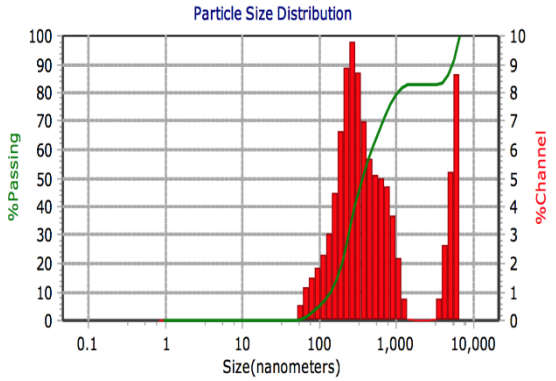	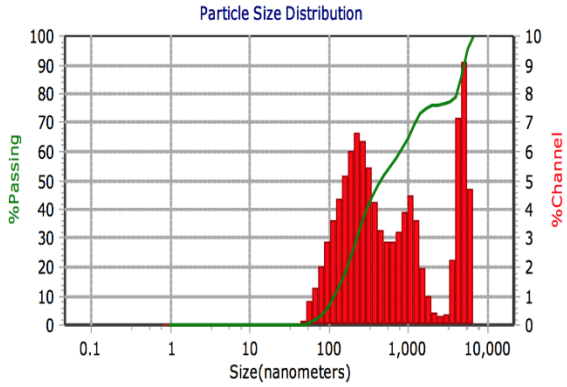
T1	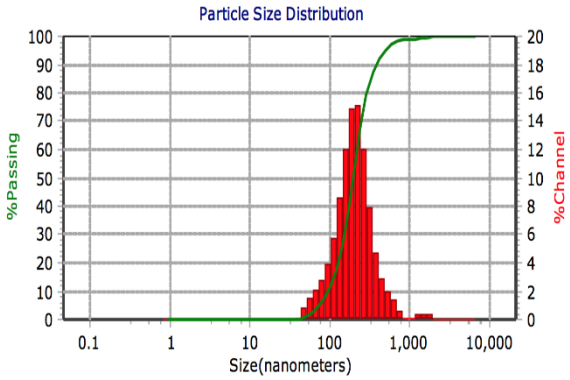	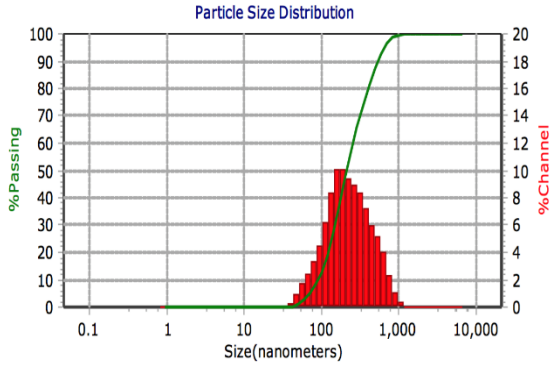
T2	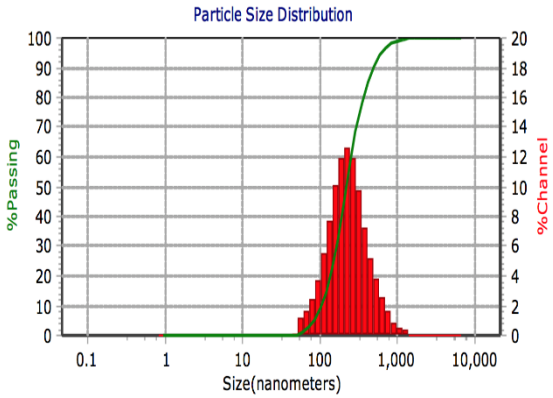	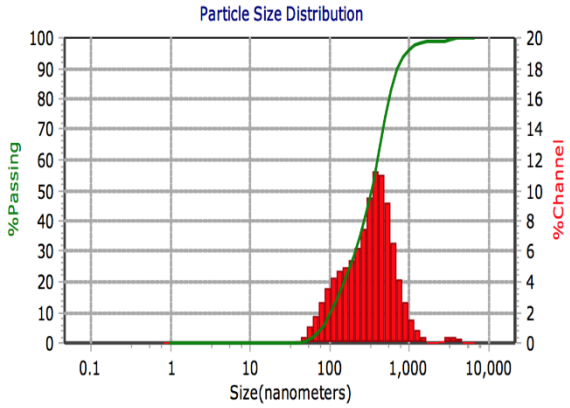

NLCs/SLN	$t = 0$	$t = 6\ weeks$
T3	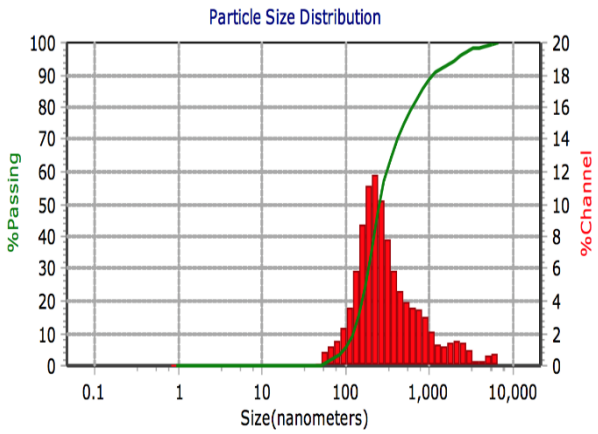	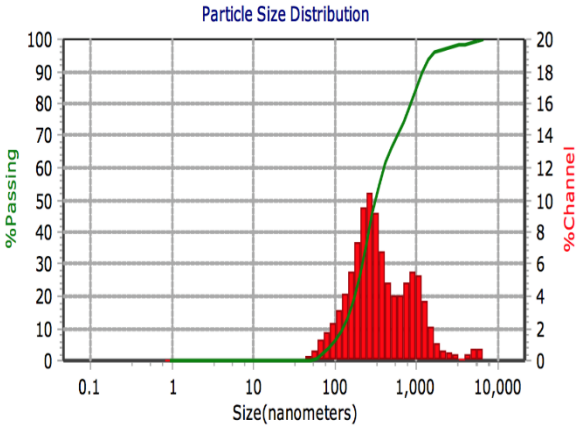
T4	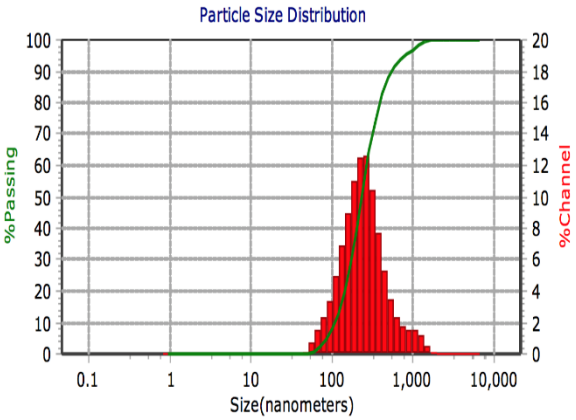	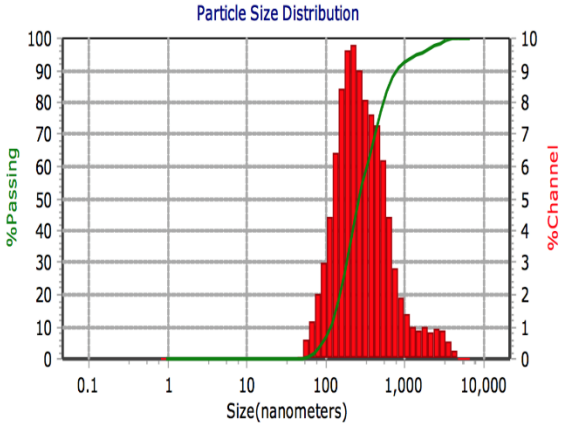
T5	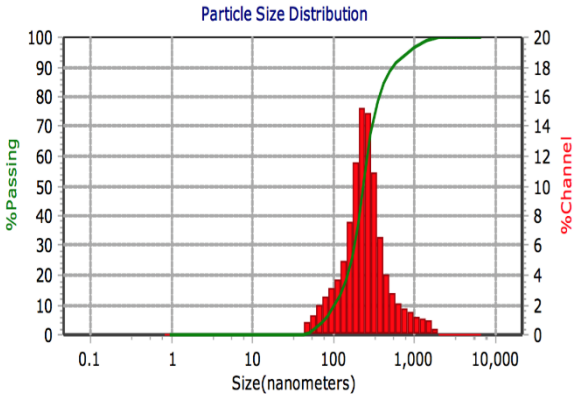	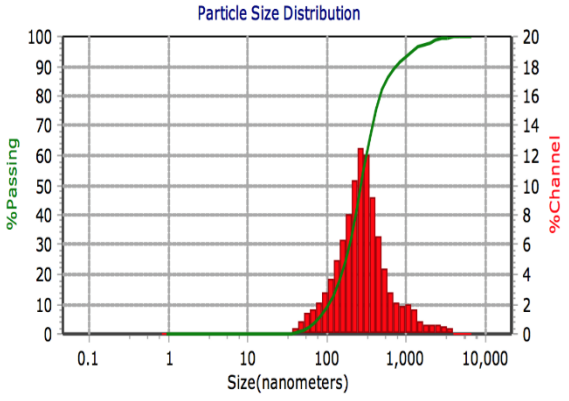

NLCs/SLN	$t = 0$	$t = 6\ weeks$
T6	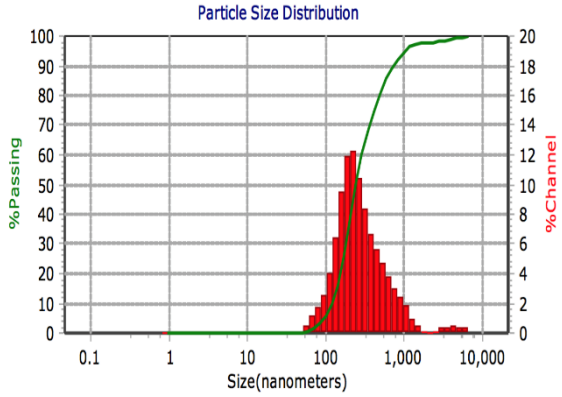	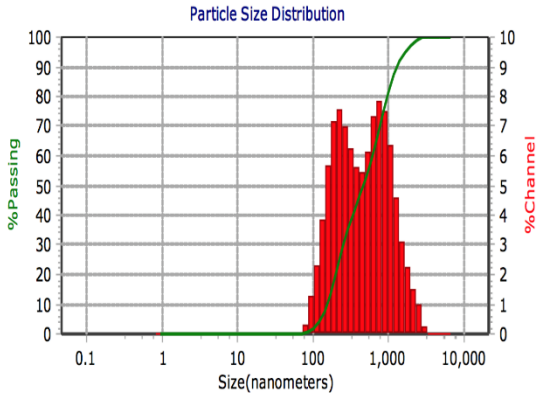
T7	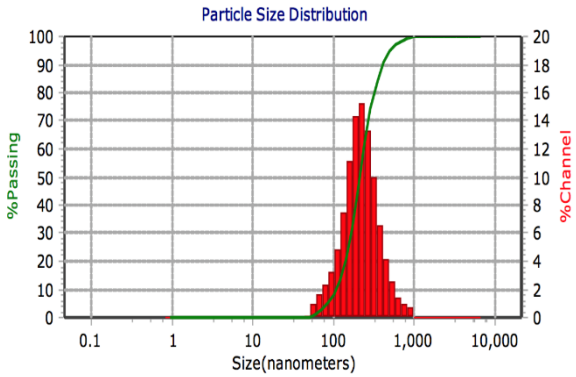	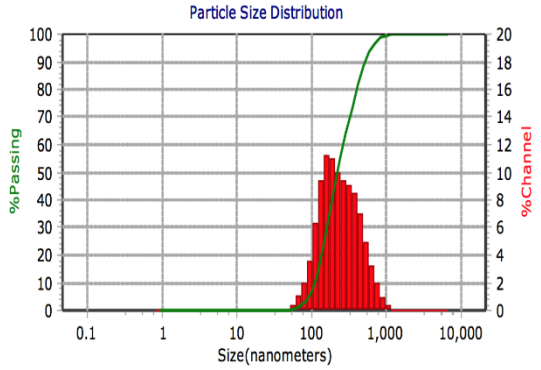
T8	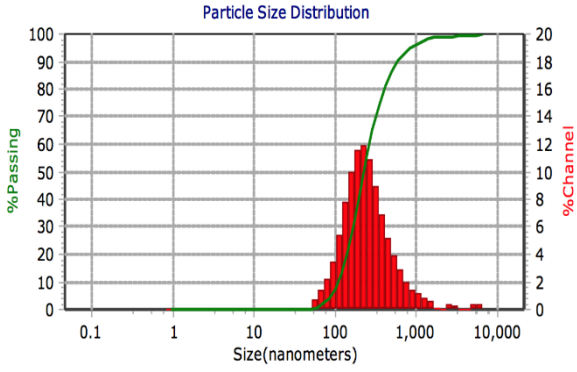	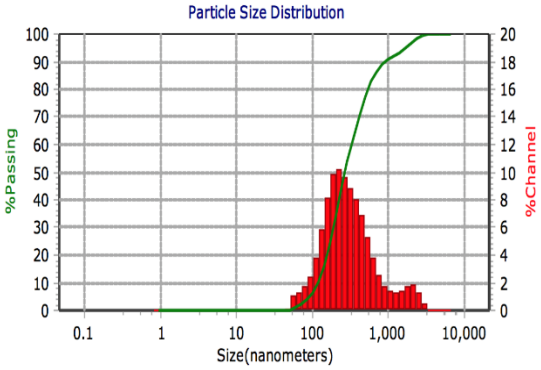

Figure 32. Particle size distribution of NLCs/SLN at (a) t=0 and (b) t=6 weeks.

The formulations that showed a relatively higher stability based on their ability to retain a narrow particle distribution, with a PDI lower than 0.3, are T4, T5, and T8. Two out of the three formulations, namely T8 and T4, exhibited the highest EE% among the formulations. Therefore, less aggregation is expected for these formulations since the RP is mostly localized within the matrix of the carrier. The composition of T4 and T5 were opposite in all three factors. This shows that the relative proportion of the constituents is critical, since a high vitamin A concentration required a high PP oil content in T4. A similar argument could be made for T5, where the low composition of both vitamin A and PP oil allowed for a stable dispersion. However, the surfactant to solid lipid ratio, which was at a low in T4 and a high in T5, does not appear as significant. This is confirmed by T4, where a lower surfactant amount was able to stabilize the formulation with the higher total lipidic composition. The TEM images of T4 and T5 are shown in Figure 33 below, showing a smaller size for T5 compared to T4, as confirmed by particle size analysis.

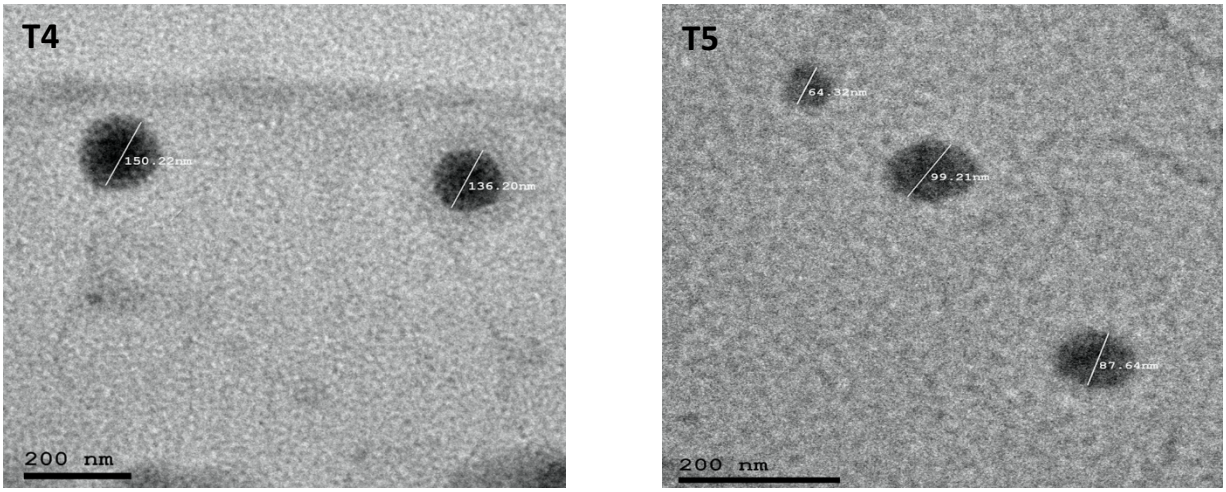

Figure 33. TEM image of T4 and T5

Moreover, T8, which constituted a lower amount of vitamin A, lower surfactant to solid lipid ratio, and a higher amount of PP oil, still showed relative stability. What these three formulations had in common was that in all of them the increased amount of solid lipid (Kappa^2)

required an increase in the PP oil amount and vice versa. There is no direct explanation for this phenomenon in the literature. A possible explanation, however, is as follows: In cases where the oil content is higher than the solid lipid, as in T1 and T7, the formation of micelles and liposomes by the phospholipids present in the formula is likely to happen,[32] which could easily flocculate through hydrophobic interaction, and have their particle size increase with time. T1 has shown a more significant increase in the PDI index, which could possibly be attributed to the higher composition of the oil relative to the two other factors. In this case, the possibility of the formation of carriers that do not require a solid core, such as liposomes, becomes likely. These carriers are less stable than SLNs and NLCs as they easily coalesce, by hydrophobic interactions.[164]

Finally, although surfactant concentration was reported to improve the kinetic stability of the formed lipid carriers by steric hindrance, even in cases where the respective crystalline form of the lipid is not stable, this does not seem to be the case in this study. A high surfactant to lipid ratio did give a smaller particle sizes, as in T1, T2 and T7, but could not prevent subsequent aggregation. Two out of the three formulations that were relatively stable constituted a lower surfactant to lipid ratio, namely T4 and T8. The results show that the relative amounts of solid lipid to the oil lipid is pivotal in understanding the NLC's stability.

5.2 Stability in Terms of RP Degradation

The stability of the control RP in the stock solution, and an RP loaded NLC carrier, namely T4, was investigated. The results retrieved showed a higher degradation rate for the NLC in comparison to the free vitamin A stock, which is found in the Appendix A. This finding relates to a previous work conducted by Jee et al. where they claim that the lipid system in the nano-carrier is prone to auto-oxidation, forming lipoperoxyl radicals that would be scavenged by the vitamin and consumed in the process.[27] Furthermore, two other studies reported an increase in RP

degradation as a result of incorporation in either NLC or SLN, suggesting an incorporation of antioxidants and chelating agents, as means to further enhance stability.[148,165] However, antioxidants provided by the PP oil did not confer the protection needed in this formulation.

5.3 ZP

ZP of the lipid nanoparticles can also be used to evaluate the dispersion's stability, where an absolute value above 30 mV is generally considered stable, even though stability of formulations of smaller ZP values could be achieved through steric hindrance of non-ionic surfactants.[43] The high electrostatic repulsion forces exhibited by the particles in the system can avoid aggregation, coalescence or flocculation.

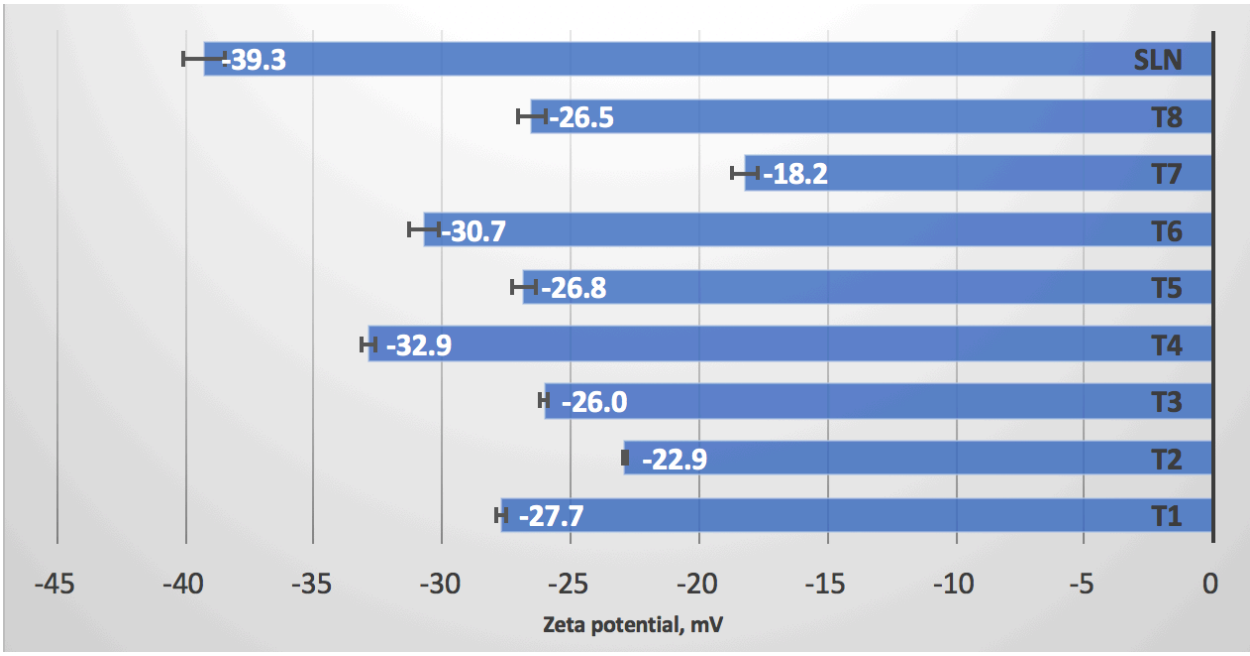

Figure 34. ZP for NLCs (T1-T8) and SLN.

As can be seen in Figure 34, the largest ZP value was for the SLN formulation. This could be due to the high composition of solid lipid, Kappa^2, which includes polar species such as sodium stearoyl sactylate, cetearyl alcohol and polyglyceryl-3 esters. However, although the ZP is

considered acceptable for a stable colloidal system with sufficient electrostatic repulsion, it did not overcome the gelling effect which was reflected in the particle size change upon storage. This is probably due to the solid lipid's tendency to transform into a stable polymorph, and increase the lattice energy saving by growing larger in size,. Moreover, the SLN did contain a smaller ratio of surfactant to solid lipid, and this could probably be the reason for the lack of sufficient steric hindrance between the nano-lipids, where their tendency to aggregate exceeded their interfacial electrostatic repulsion. In a similar light, T6 has also exhibited size and PDI increase with time, in spite of having a relatively large ZP. Similar to the SLN, T6 also had a lower surfactant to solid lipid ratio, which could be a contributing factor to the temporal changes in size and PDI.

In a different light, T4, which did show a high zeta potential, did also exhibit colloidal stability with time. This could be attributed to two main factors. The first factor was the electrostatic repulsion which was strong enough to prevent particle aggregation. The second factor was that the higher composition of oil in comparison to T6, which had identical compositions in the remaining factors, could have resulted in a more stable crystalline form that prevented further transformation, and hence consequent gelling.[11,37] This phenomenon was exhibited by T6, unlike the remainder NLCs, and could be related to its lower ratio of PP oil to solid lipid. Unlike T4, T2 with similar composition of both solid lipid and PP oil, did exhibit instability as observed in the relatively significant particle growth. This could be related to two factors, one is the high composition of RP with respect to both solid and liquid lipids, resulting in inadequate amounts to solubilize and withhold all the RP. Another is the relatively low ZP. However, the second reason is less likely since the surfactant is at a higher composition than the lipids, and can provide adequate steric hindrance to stabilize the formulation. Furthermore, T7 exhibited higher stability than T1, T2, and T3, although they had a higher ZP. This could be attributed to the higher surfactant

to solid lipid ratio, as well as higher oil composition, that decelerated aggregation by steric hindrance, and stabilized the polymorph, respectively, for T7. Finally, as confirmed in another study, the specific molecular arrangement that the lipids exhibit in the external layer of the carrier, along with their interaction with stabilizers, such as surfactants, is a determining factor in the evaluation of the stability incurred by nano-lipidic carriers.[35]

The interaction plots from Design Expert for the 8 formulations is shown in Figure 35. In both parts (a) and (b), the red line shows a decreasing ZP with increasing vitamin A% (w/w). This is expected since RP is non-polar, and hence increasing its concentration decreases the electrical potential of the carriers. However, these formulations, namely T5, T2, T1 and T7, also possess a higher surfactant to solid lipid ratio. This plays a critical factor in affecting the ZP, as the trend for decreasing ZP with increasing vitamin A%(w/w) fails in the remainder formulations. The latter formulations, which lie on the green line, have a higher solid lipid amount, showing an increasing ZP with higher vitamin A% (w/w). This could possibly be due to a specific arrangement induced by the latter composition, namely that of T6 and T4, that allows for the polar heads of the constituting lipids to re-orient in the external layer of the carriers. Consequently, the ionic atmosphere surrounding the carrier will increase, along with its induced ZP. The solid lipid's higher melting point allows it to first crystalizes upon cooling, holding in a part of the oil within its matrix, and allowing the remaining to distribute on its surface. The oil's short chain fatty acids, and polar phenolic compounds[56], redistribute on the surface and add to the ionic charge of the carriers.[35] In case of T6, which is identical in composition to T3, but with a higher vitamin A% (w/w) than the latter, the significant increase in ZP could be understood in the same light. The higher amount of vitamin A in T6 could have pushed out the PP oil more onto the surface, as it accommodates within the solid lipid's lattice defects. Finally, T6 also exhibited a visually observed

gelling effect, which confirms the claim of the core of the NLC being mainly composed of solid lipid.

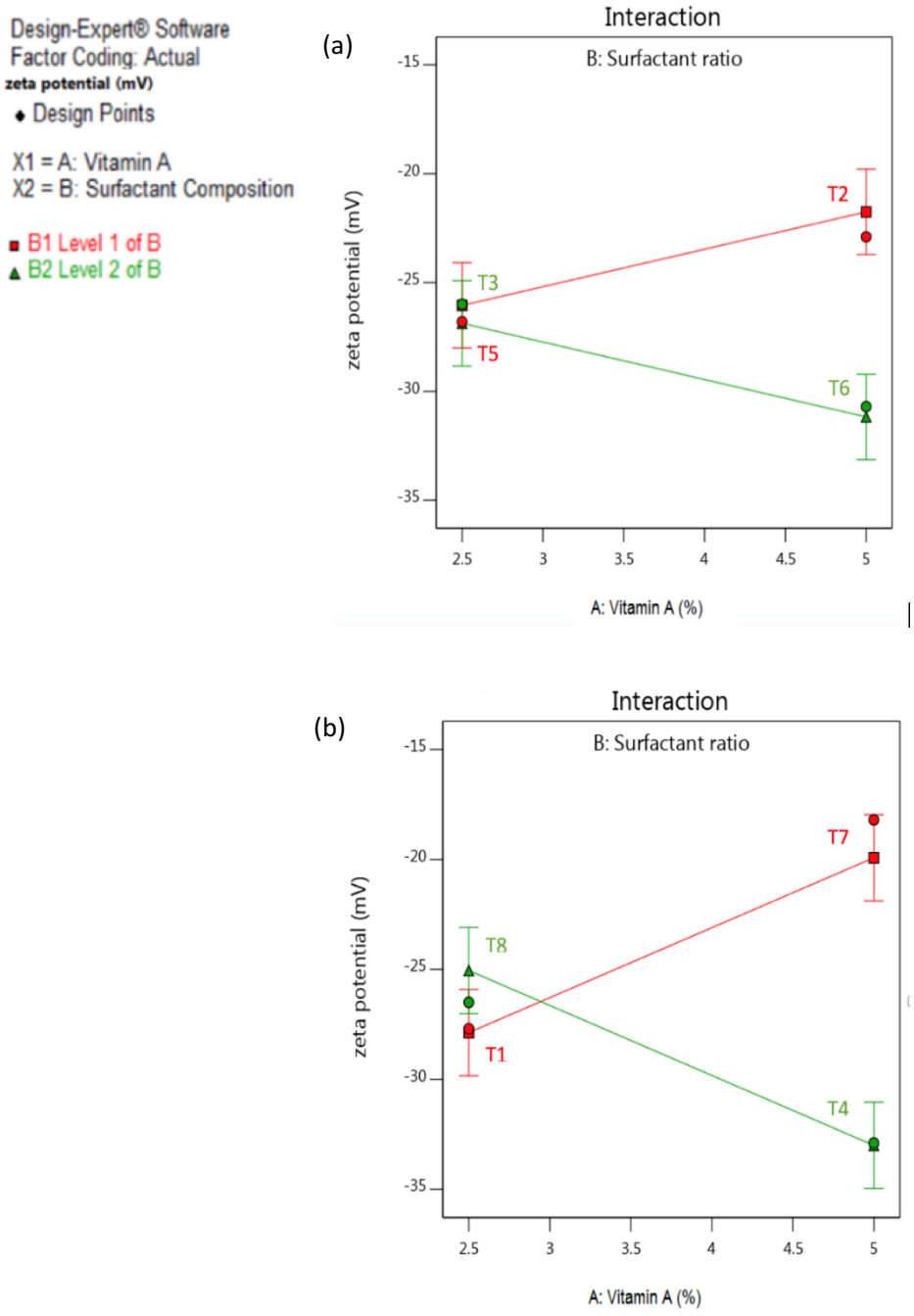

Figure 35. Interaction plots of the factors on ZP with (a) low PP oil% and (b) high PP oil% showing the trend in formulations with increasing Vitamin A%.

5.3.1 ANOVA for ZP

Table 5. ANOVA for ZP

ANOVA for selected factorial model

Response zeta potential

Source	Sum of Squares	df	Mean Square	F-value	p-value	
Model	134.22	3	44.74	22.38	0.0058	significant
B-Surfactant	52.53	1	52.53	26.28	0.0069	
AB	75.03	1	75.03	37.54	0.0036	
ABC	6.66	1	6.66	3.33	0.1420	
Residual	8.00	4	2.00			
Cor Total	142.22	7				

The above ANOVA for the ZP shows a significant model compliance. The level of significance, <<5%, is unlike the previous cases for the particle size and PDI. In this case, the coefficients of the variables, namely surfactant to solid lipid ratio, and interaction AB and ABC, is significant. This means that the variables listed in table 5 contribute to a large extent to the ZP of the formulations. The highest coefficient is that of the AB interaction, which is the interaction between the vitamin A composition and the surfactant to solid lipid ratio. This confirms the previous claims, where a decrease in ZP was observed for formulations with lower solid lipid ratio, and increasing vitamin A composition. These contrast the formulations with higher solid lipid ratio, that showed increasing ZP with increasing vitamin A composition. Finally, one may conclude that the interaction between the surfactant to solid lipid ratio and vitamin A composition is pivotal in predicting the ZP.

5.3.2 Regression Model of the ZP

The regression equation for the ZP includes the surfactant to solid lipid ratio and interactions AB and ABC. The following is the coded regression equation from Design Expert:

$$ZP = -26.46 - 2.56X_2 - 3.06X_1X_2 - 0.9125X_1X_2X_3 \qquad \text{Equation 7.}$$

The R^2 of the model gave a value of 0.9438, which is significantly higher that those for the previous models. This means that the regression equation can be considered a better predictor for ZP values. The above equation shows that a higher vitamin A% (w/w), relative solid lipid to surfactant composition, and PP oil% (X_1=X_2=X_3=+1,), give an increasing ZP. However, since the coefficient of the last term of the equation is relatively small, the impact of PPoil% can be conclude to be minimal.

5.4 DSC Thermograms

The degree of crystallinity and thermal behavior of the formulations, along with the solid lipid and phospholipid used were investigated. The dispersions were first lyophilized as the broad water peak (~100°C) in the thermograms may interfere with that of the sample.[41]

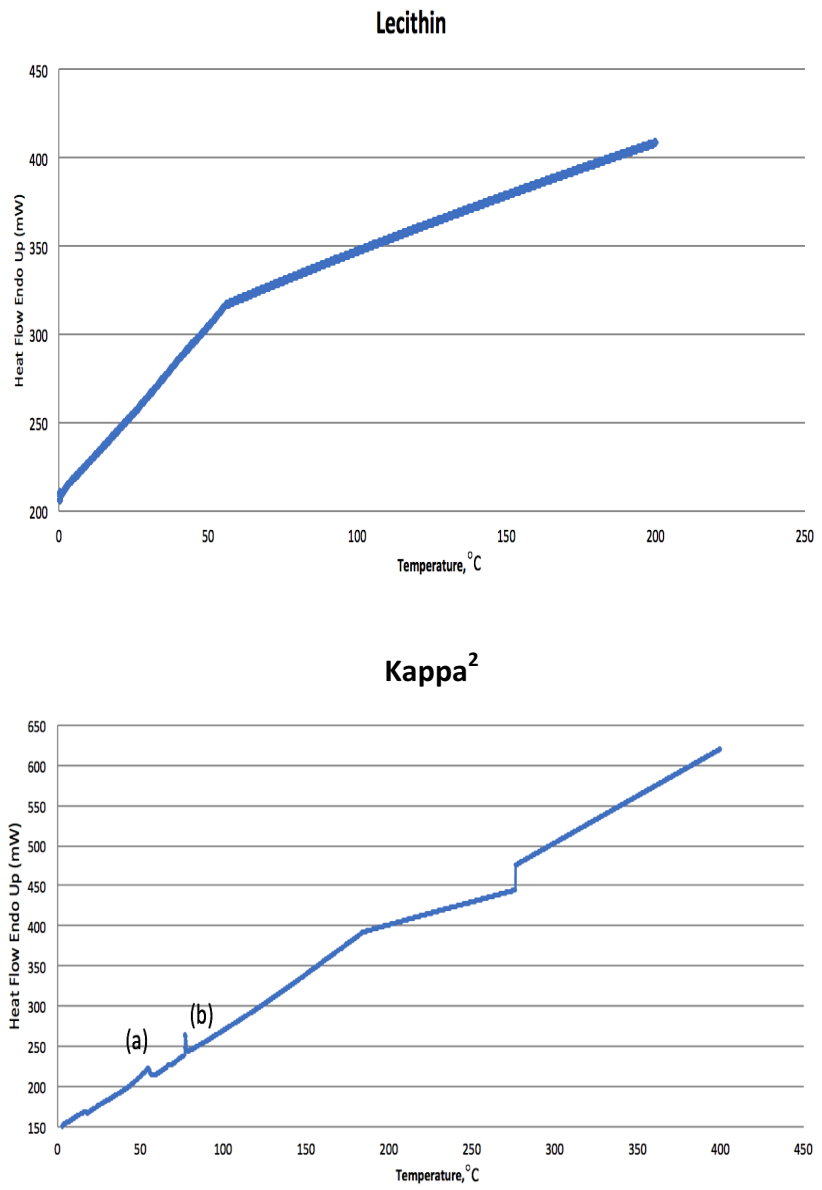

Figure 36. DSC Thermograms of Solid lipids.

As can be seen in the Figure 36, the solid lipid Kappa^2 showed multiple peaks, prior to it reaching a plateau, which signals the transition from a gel to liquid. However, lecithin did not show peaks which meant that it was in an amorphous state. On the other hand, the solid lipid Kappa^2 did exhibit crystalline transitions, where a change in the subcell packing from $\beta' \rightarrow \beta$, the latter being a more crystalline form, with lower number of defects in the packing. This was observed in the

DSC thermogram by the sharper peak (b) proceeding a broader peak (a).[16] In cases where the drug is located inside the defects, the transitioning to a more ordered crystalline lattice will result in its expulsion.

The DSC of the formulations reveals more insight into the phase transition that takes place upon heating, along with insight on the crystallinity of the solid lipid. From the DSC of the pure solid lipids in Figure 36, one can see a transition in the lecithin that takes place at around 53°C which is also seen in T1-8, apart from T4. In case of these formulations, a similar transition is observed at the inflexion point, which is slightly shifted to the left. This could be attributed to the presence of other constituents, and their interactions with the lecithin that accounts for this depression.[41] In these formulations, one may also see small peaks that can be attributed to the presence of the Kappa^2. These peaks are also shifted to lower temperatures with respect to the original found in the lipid's pure form. This could be attributed to the reduction in particle size and consequent increase in surface area, which now require less energy to melt in comparison to the bulk state of the pure lipids.[111] The depression of the melting temperature in SLN loaded with RP was also reported by Sapino to be an indication for the drug's inclusion in the lattice of the lipid.[10]

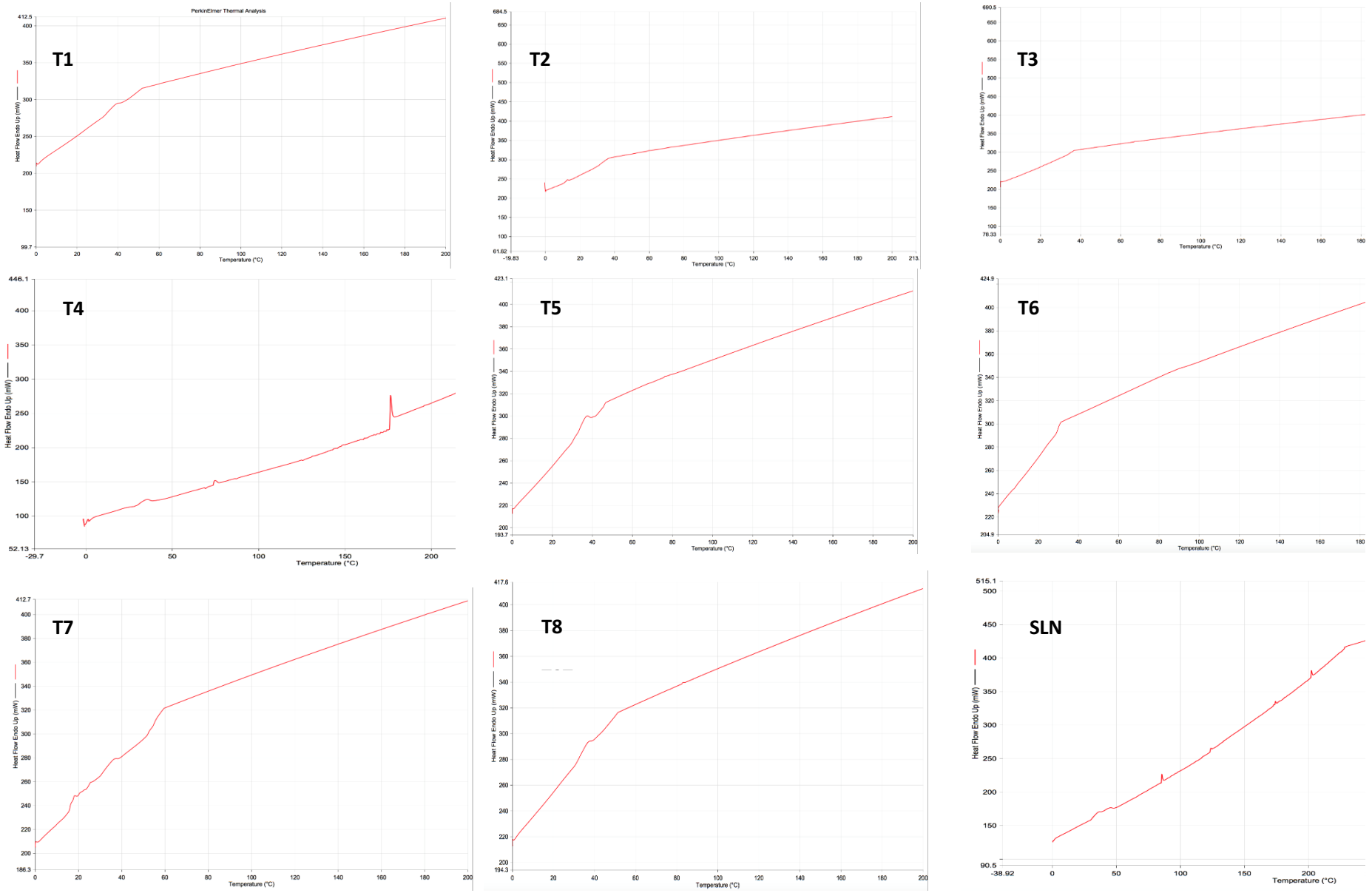

Figure 37. DSC Thermograms for NLCs (T1-8) and SLN.

From the peaks observed in the formulations, namely T1-T8, excluding T4, one can see that the first peak observed is that pertaining to T2. In this particular formulation, a high composition of drug was used, with relatively lower solid and liquid lipids. This lowering of the melting point as a result of adding RP was reported to be linked with the drug's preferential distribution onto the surface of the lipid nano-carriers, rather than the core, which also relates to RP's lower melting point in comparison to the solid lipids.[148] Although it was noted previously that a higher drug composition favors a core rather than shell distribution of the drug, in this specific case, a saturation of the drug in the lipid could have been ensued due to the lower composition of the solid lipid. In general, all the peaks observed were shifted to lower temperatures, suggesting an incorporation of the RP within the NLCs, where Jenning et al. reported a direct relation between lower melting temperature and higher drug loading.[45]

Moreover, T4 shows a lower shift in melting temperature in comparison to the SLN, suggesting a higher incorporation of the RP, also confirmed by the EE% measurements. The multiple peaks observed for both T4 and SLN is probably due to the various polymorphic forms the carrier exhibits with increasing temperature. The first peak can be attributed to the metastable α-subcell, which is characterized with many disordered regions and a hexagonal structure, as shown by the broader peak observed in the thermogram. Upon heating, a transformation into a more stable polymorph, β', is observed by a relatively sharper peak in both the SLN and T4. The orthorhombic β' subcell undergoes another transition into a highly ordered triclinic β structure, which is seen much more pronounced in T4 in comparison to SLN.[16] This could be explained by the smaller size of the T4 formulations that allows for easier attainment of higher order crystallinity in comparison to the SLN that has already begun to form networks by the gelling effect observed. The various polymorphs exhibited by the fatty acid chain of the lipids is shown in the Figure 39

below. Finally, it has been reported in a review on SLN that the lipid composition is decisive in determining the type of crystal polymorph that will form upon cooling.[33]

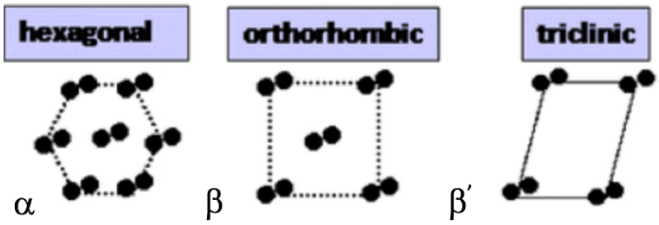

Figure 39. Polymorphs of fatty acid chains.[33]

Furthermore, the area under the peaks for T5 is shown below in Figure 40, in comparison with T4, SLN and pure Kappa[2]. The peak area of T5 is significantly smaller than the rest, namely 2.37 mJ in comparison with 67 mJ, and 64.1 mJ for T4, and SLN, respectively. This can be attributed to the lower crystallinity of T5, which is expected since it possessed a lower composition of Kappa[2] with respect to the two others. In comparing T4 with SLN, a sharper peak is observed for the latter in Figure 40, which is also shifted to a higher temperature. This confirms the assumption that SLN is transformed into a more crystalline polymorph, since a higher ordered crystalline form requires more energy to overcome the lattice forces, in comparison to a lattice with numerous defects and amorphous regions, that is already disordered.[111] Moreover, in comparing the peaks in both the SLN and the Kappa[2] for the β transition, one may observe an expected higher enthalpy for the pure, but an unexpected shift to a higher temperature in case of the SLN, which is unlike the other formulations

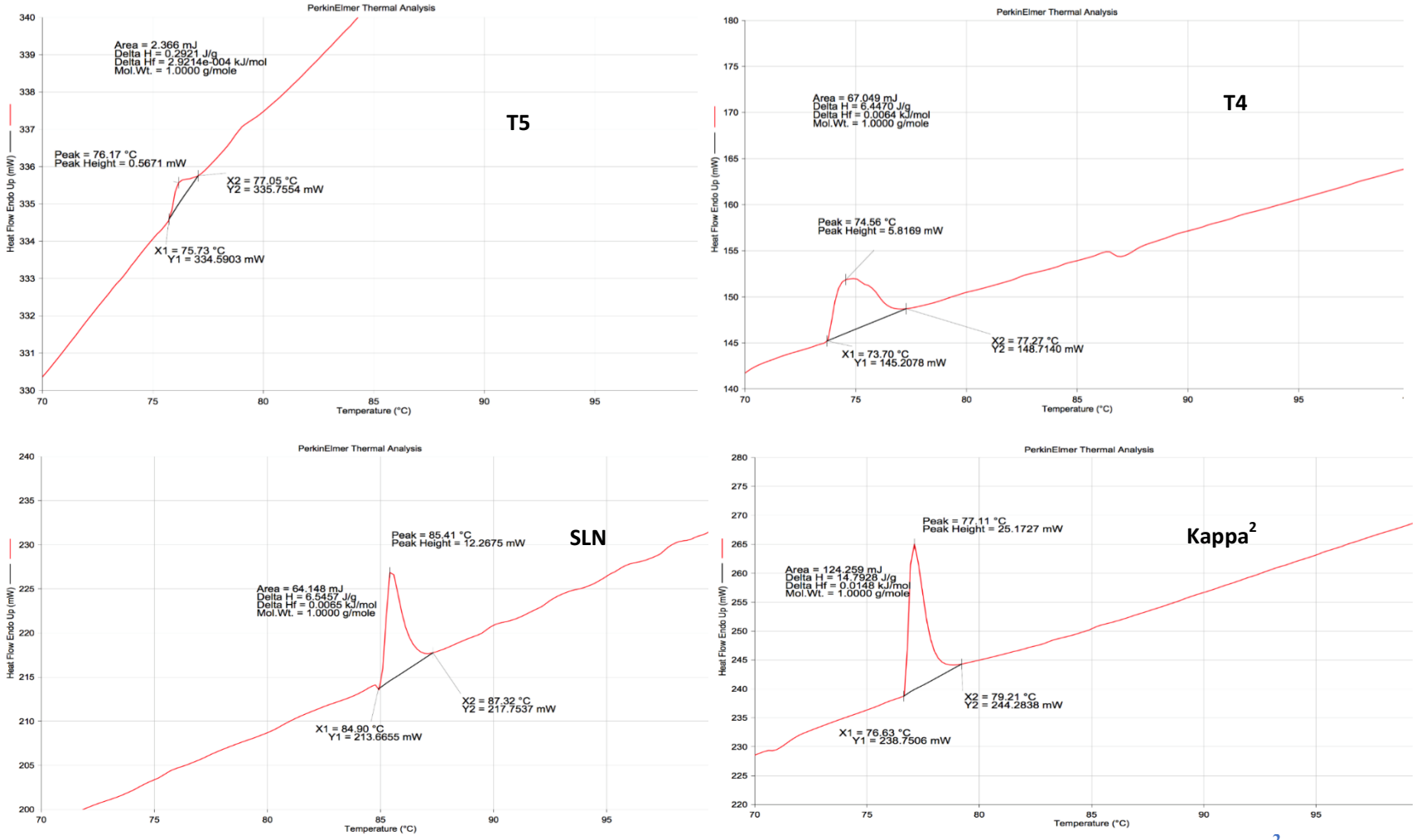

Figure 40. DSC Thermograms with Peak Area and Transition Temperature for T5, T4, SLN and Kappa[2].

5.5 EE%

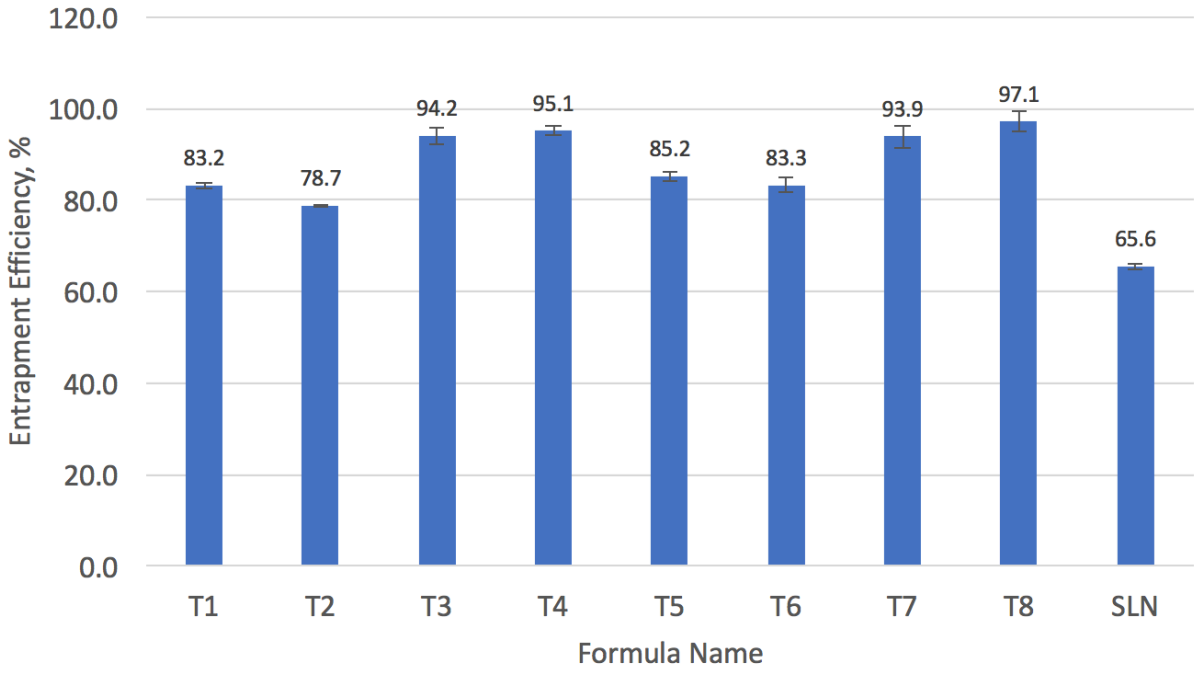

Figure 41. EE% for NLCs and SLN.

As shown in Figure 41, the EE% showed a variation of results, from 65.6% to 97.1%. The lowest value was for the SLN, which is reflected in the literature.[11] This could be attributed to the oil lipid constituent that allows for higher solubility of the RP in its phase, and hence improvement in the overall EE%. This was confirmed in studies claiming an improved incorporation capacity when using a mixture of lipids rather than using a single form.[36,13,87] The low EE% of SLN could be attributed to two mechanisms. One is the gradual drug expulsion as a result of polymorphic transitioning of the lipid from an α to a more stable β subcell form.[16,88] The other is attributed to the synthesis process, where the highly viscous lipid melt diffuses at a slower rate into the aqueous medium, expelling any drug during the crystallization process.[166,154]

The NLCs showing the highest EE% were T3, T4, T7 and T8. Three out of these four formulations, all except of T3, incorporated higher amounts of lipid oil. T8 and T4 exhibited the highest two, and both consisted of identical composition for the surfactant to solid lipid ratio, and PP oil, with varying amounts of RP. The higher composition of the solid lipid and oil lipid in these two formulations can be the reason behind their higher EE%, as reported by Jung in his study for the optimization of vitamin A in SLN.[149] The former, T8, had a lower amount of vitamin A, and showed a higher EE%. This means that the amount of vitamin influences the EE%, with lower amounts being encapsulated more efficiently. This is further observed in T2 and T6, where a low EE% could be attributed to the increased vitamin A% and lower amount of PP oil. This lower amount of PP oil relative to the vitamin's composition could have allowed for the lack of its proper incorporation.

The DSC thermograms in some formulations could also be used to support the observations inferred from the EE% results. In case of T2, which possessed the lowest EE%, a small peak was observed, before all the remaining NLC formulations, which could be related to the RPs initial melting, which was not well incorporated within the matrix. In comparing the high T5 and T8, with similar trends in their thermal behavior, the latter had a broader peak, also shifted towards a lower melting temperature. This is an indication to a higher incorporation of the RP within the matrix of T8, as confirmed by the EE% results.[45] Furthermore, in comparing SLN with T4, which also exhibited similar trends in their thermal behavior, a shift towards a lower temperature was observed in T4. This increase in melting temperature for the SLN can be explained by lower drug loading of the RP, which was also confirmed by the significantly lower EE% value in comparison to the rest of the formulations. In case of both T3 and T6, no peaks was observed, only an inflexion in the thermogram that is attributed to the lecithin. However, the steepness of the thermogram in

case of T6 was much more pronounced, which could be related to the higher crystallinity of the formulation, induced by the higher ratio of solid to liquid lipid content. Thus, a higher temperature is required to overcome the lattice forces in the crystalline T6, which confirms its much lower EE% in comparison to T3, where now the RP has fewer places to accommodate within the more rigid lattice framework. Furthermore, the thermogram of T7 reveals several peaks, as opposed to the more smooth and subtle ones present in the remaining formulations. Although T7 possessed a high EE%, its low content of solid lipid with respect to both the RP and PP oil composition could have contributed to the observed phenomenon. The RP, although well incorporated within, can now migrate easier to the surface and melt, as observed by the first peak in the thermogram, at about 20°C. This is a similar phenomenon to the early peak observed in T2, although the EE% was much lower. Finally, all NLC formulations, apart from T4, exhibited an amorphous behavior in comparison to SLN. This has been reported by Jenning et al. to result in a very weak crystallization as a result of combining a binary mixture of solid and liquid lipid.[16] This lowering in crystallinity can be related to the higher EE% exhibited by the NLCs with respect to the SLN.

The analysis of the three factors on the EE% of the respective 8 NLC formulations was further analyzed using Design of Expert. The Interaction plots in Figure 42 (a) and (b) show a similar trend in formulations with varying surfactant to solid lipid composition. This confirms the claim above that the relative amounts of oil lipid to vitamin composition is the main factor in the analysis of the EE%. A higher value of EE% is shown for formulations with higher amounts of PP oil, namely T4, T7 and T8. In case of T3, the higher EE% could be attributed to the solid lipid's high composition. This effect can be further evaluated by comparing T3 with T5, both having identical composition, apart from the solid lipid to surfactant ratio. In T5, the lower solid lipid content could be the reason for the lower EE% observed. However, in comparing T3 with T8,

where the only factor change between the two is the amount of PP oil added, the higher EE% exhibited by T8 could be attributed to the increased amount of PP oil in the formulation. Furthermore, part (a) shows an increase in EE% when increasing the amount of vitamin, namely from T1-T7. This is not the case, however, in part (b), where T4 showed a lower EE% than T8. This could be attributed to the variation in the surfactant to solid lipid ratio of the parts (a) and (b). The higher surfactant composition has been reported to improve the EE% by increasing the solubility of the drug within the carrier.[167] A similar argument could be made in this case, where in T7 the higher surfactant composition allowed for a better incorporation of the RP as opposed to T4. This was not the case when the amount of PP oil was decreased, as can be seen in formulations lying on the black lines of both parts in Figure 42. This is probably due to a lack of sufficient solubility of the vitamin A and hence its expulsion during the crystallization process. This was also seen in part (b), where the lower surfactant to solid lipid ratio did not offset the trend illustrated in part (a) in the formulation lying on the black line (T5 – T2 in (a), T3 – T6 (b)). The overall values for the EE% were lower for formulations with a higher surfactant to lipid ratio in part (a) as compared to a higher solid lipid content in part (b). Unlike particle size, where the effect of surfactant was pivotal in allowing smaller sized particles, the solid lipid content in this case outweighs the latter effect. A higher lipid content was reported in a previous study to improve EE%, but the ratio between solid and liquid lipids could not be explained due to insufficient studies.[149] In this study, however, their respective ratios was assessed, showing an increased drug loading capacity when a higher amount of oil was incorporated.

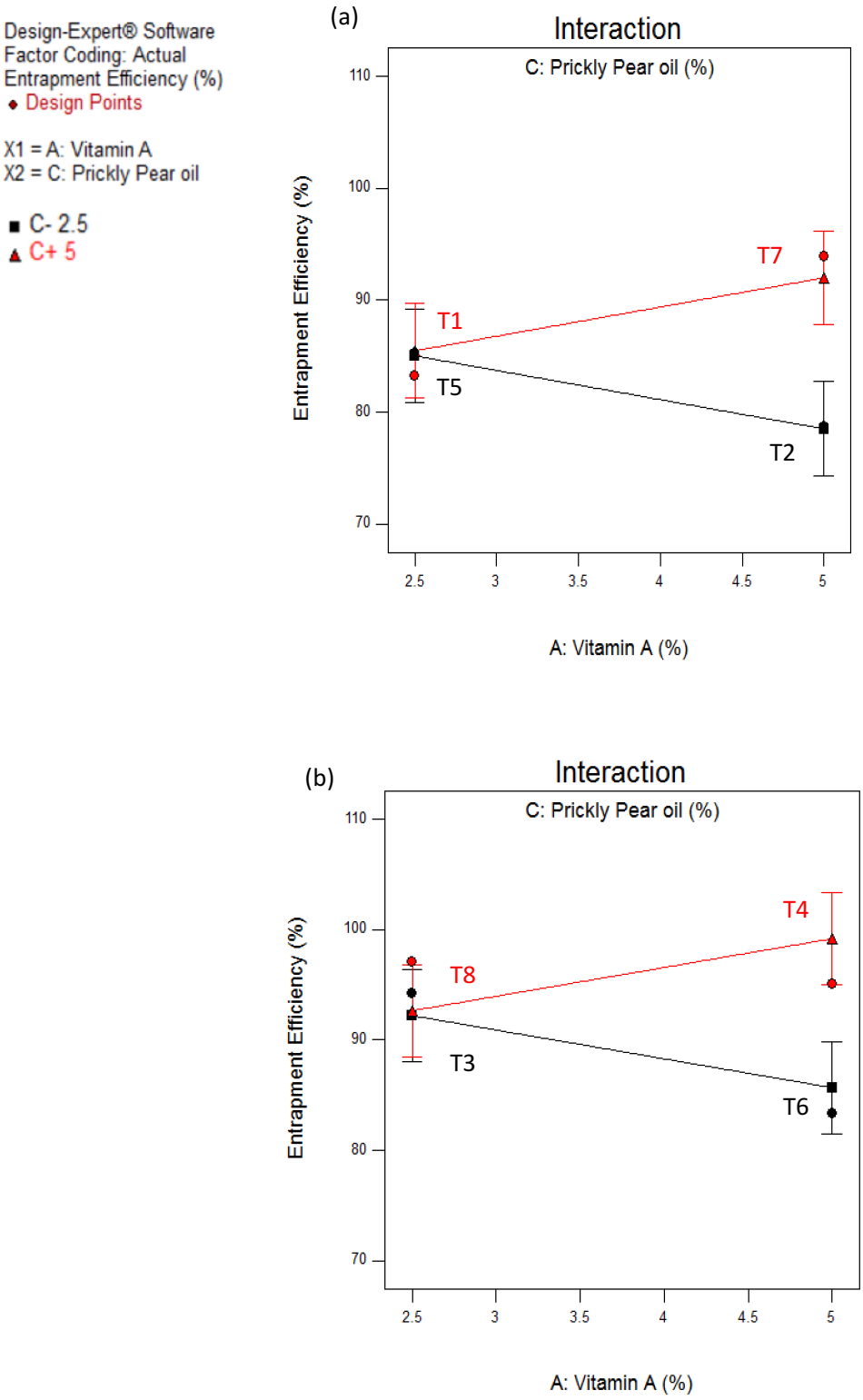

Figure 42. Interaction plots of the factors on EE% with (a) high surfactant and (b) low surfactant to solid lipid ratio showing the trend in formulations with increasing Vitamin A%.

5.5.1 Analysis of Variance of EE%

Table 6. ANOVA for EE% of NLCs

Response	Entrapment Efficiency					
ANOVA for selected factorial model						
Analysis of variance table [Partial sum of squares - Type III]						
Source	Sum of Squares	df	Mean Square	F Value	p-value Prob > F	
Model	285.41	3	95.14	6.93	0.0461	significant
B-Surfactant	*102.96*	*1*	*102.96*	*7.50*	*0.0520*	
C-Prickly Pe	*97.30*	*1*	*97.30*	*7.09*	*0.0562*	
AC	*85.15*	*1*	*85.15*	*6.20*	*0.0674*	
Residual	54.91	4	13.73			
Cor Total	340.32	7				

In table 6, the model was shown to be significant. The factors that did show an impact on the EE% response were the surfactant to solid lipid ratio, PP oil composition and the interaction between it and the amount of vitamin A% (AC). This confirms the claims previously made where the surfactant to solid lipid ratio affects the overall EE%, giving a higher value when higher relative amounts of solid lipids constituted the matrix. This is reflected in the low p-value of factor B, showing a significance at 5%. Furthermore, the amounts of PP oil was also shown to influence the EE%, which was seen in formulations with higher amounts of PP oil with respect to the other factors, giving a higher value.

5.5.2 Regression model for EE%

The regression equation for the EE% response includes the surfactant to solid lipid ratio, X_2, PP oil composition, X_3, and the latter's interactions with vitamin A%, X_{13}. The following is the coded regression equation which includes all the significant factors that affect the EE%:

$$EE\% = 88.84 + 3.59X_2 + 3.49X_3 + 3.26X_1X_3 \qquad \text{Equation 8}$$

The R^2 of the model gave a value of 0.8387. Although not a perfect fit, it can be used to qualitatively assess the variation in EE% as a result of changing the three factors. In this case, it can be directly inferred that a low surfactant to solid lipid ratio (X_2=+1), and a high PP oil and RP composition (X_1=+1, X_3=+1), will give a higher EE%.

5.6 *In-Vitro* Release

The *in-vitro* release of all the 8 NLC formulations and the SLN, along with a control which consisted of RP dissolved in the dispersing medium (Glycerol:Ethanol; 2:8), is shown in Figure 43. The results show an expected high release for the control, due to the absence of any barrier in the formulation that could impede the RP's release.[54] In contrast, the lowest release was administered by the SLN formulation. The lower mobility of the RP in this case could be justified by the presence of solid lipids in the carrier that come in the way of the vitamin's release. Furthermore, NLCs showed varying extent of release, depending on the formulation composition, but overall a higher total release than the SLN. This pertains to the presence of an oil component, that lowers the viscosity of the system, and allows for increased mobility.[16] The chromatograms are provided in Appendix C.

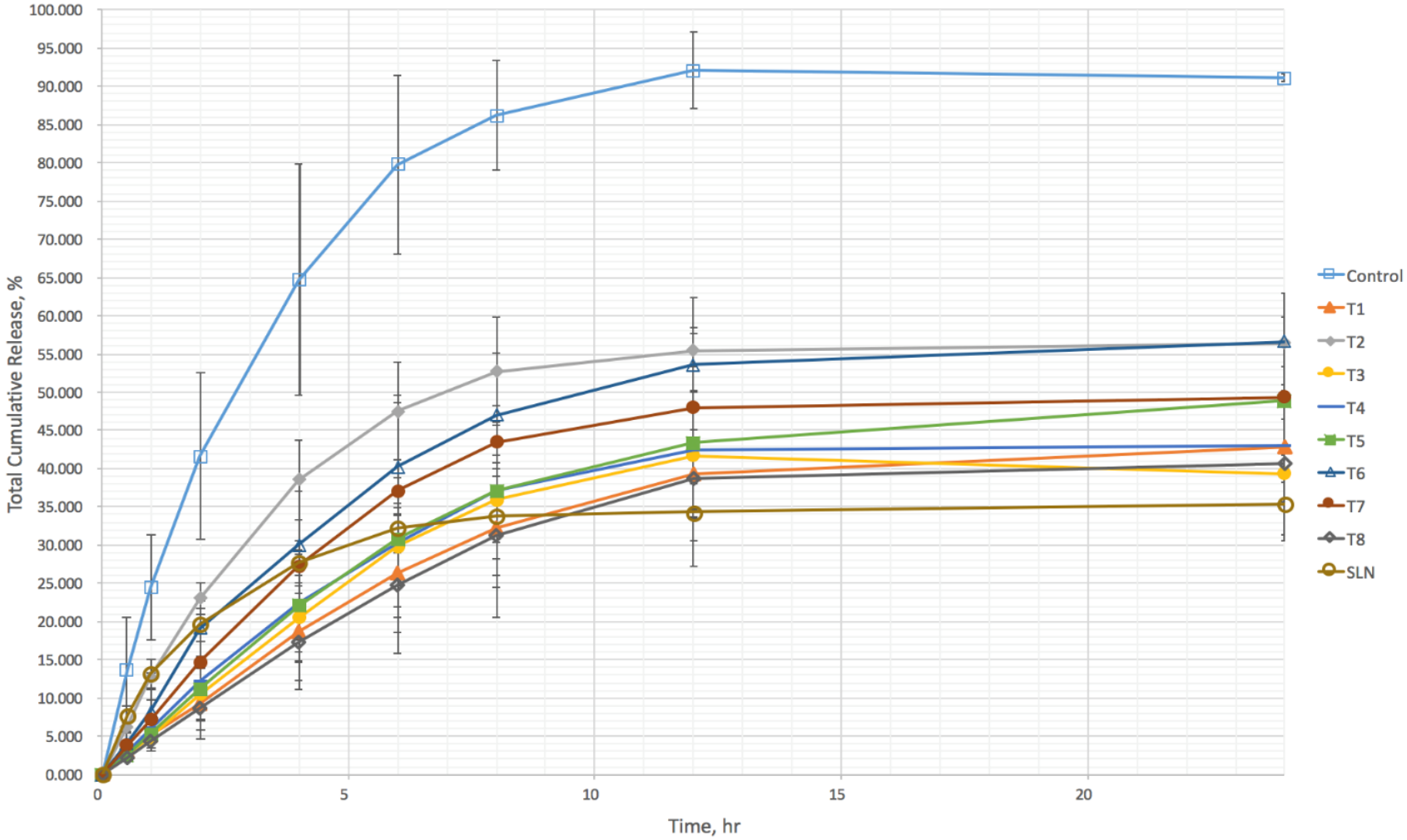

Figure 43. *In-Vitro* release profile for all formulations and control tested.

The release from the SLN at first occurred at a faster rate than all NLC formulations, apart from T2, namely in the first hour. Afterwards, the flux slowly depreciated, and reached a plateau after 8 hours, 4 hours before all the NLC carriers did reach theirs. The observed high initial flux of the SLN could be attributed to polymorphic transitioning taking place within the solid lipid's matrix, which is also confirmed in the multiple peaks observed in its thermogram, expelling the RP in the process.[16] In general, both nano-lipidic carriers, SLN and NLC, allowed for a prolonged and relatively controlled drug release, which could be explained by the drugs localization within the solid lipid matrix of the carriers.[111]

The release for every formula did vary, however, with some showing a higher flux in the first hours than others. The control showed the highest flux, which is expected since the RP is free in the solution, and not bound in a matrix as in the case of both NLC and SLN formulations. The initial flux of T8 < T1 < T3 < T5 showed a slower, and more controlled release than the rest. T5 did not reach a plateau during the time expected, and continued to release RP after 12 hours incubation, the same time most of the formulas reached their maximum release. This observed phenomenon for T5 could be attributed to the crystalline behavior observed previously in the thermogram, where a peak was observed inherent to the β polymorph. When viewed under an SEM, T5 exhibited a needle-like shaped structure, as shown in Figure 44 below, which confirms the previous claim, as the β crystals are now undergoing directional growth. As they do so, they expel more RP as they transform into a more crystalline form.[33]

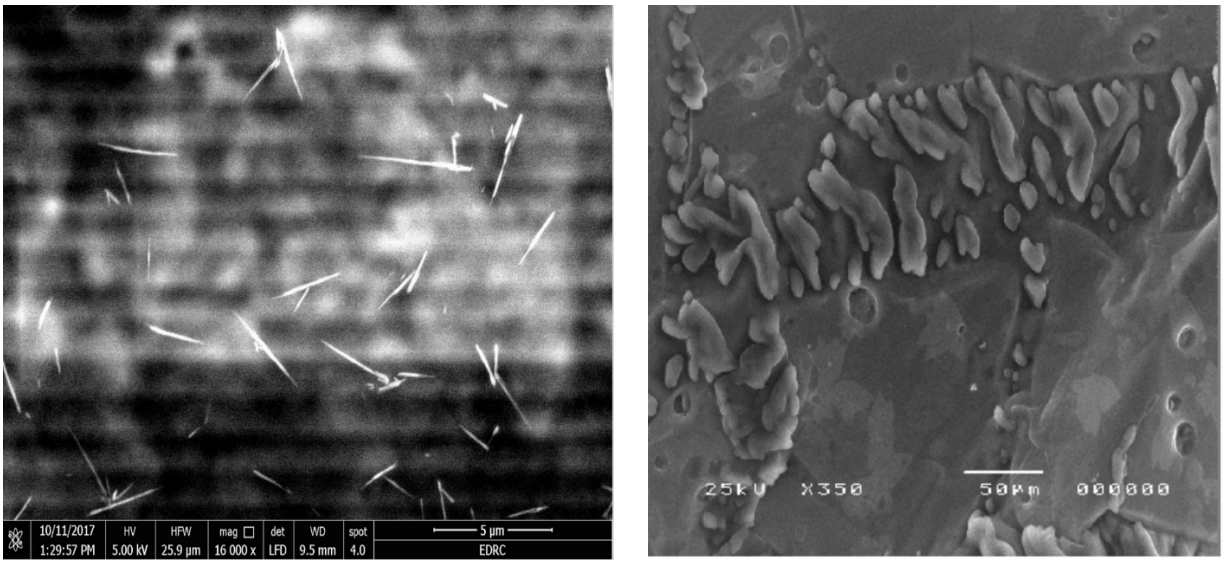

Figure 44. SEM images of T5.

The concentration of the drug in the lipid matrix can influence its embedment within, where an enriched shell model was attributed to SLN/NLC formulations with lower drug dose, as opposed to an embedment of the drug within the core of the matrix at higher drug concentration.[42] This phenomenon was explained by Müller, where he noticed that concentration of the drug with respect to the solid lipid can influence its distribution within the matrix.[14,37] In case the drug in the lipid melt is well below its saturation solubility, the solid lipid will first crystallize, leaving the drug to distribute on the surface (shell-enriched model). This contrasts the case where the drug concentration is close to its saturation solubility, which as a consequence of cooling, becomes supersaturated, and crystallizes prior to the solid lipid (core-enriched model). In a similar light, although not typical to the previous argument, the NLC formulation with the lowest EE%, instead of RP% (w/w), showed the highest diffusion flux. This high initial flux of T2 could also be related to the DSC measurements, where a small peak was observed well before all the remaining NLC formulations. This is attributed to the RP's preferential distribution onto the surface of the carrier, as the respective ratio of both solid and liquid lipid was lower, confirmed by the low EE%

observed. On the other hand, T8 which exhibited the highest EE%, although with a low composition of RP, showed the slowest release flux. This could be attributed to the now drug enriched core of T8 that allows for a prolonged release of the RP, due to the surrounding solid lipid matrix that impedes its mobility. The relatively higher stability for T8 further confirms the claim of a core enriched model, where its less likely for the RP to partition into the aqueous dispersion and form aggregates that can vary the PDI value with time.

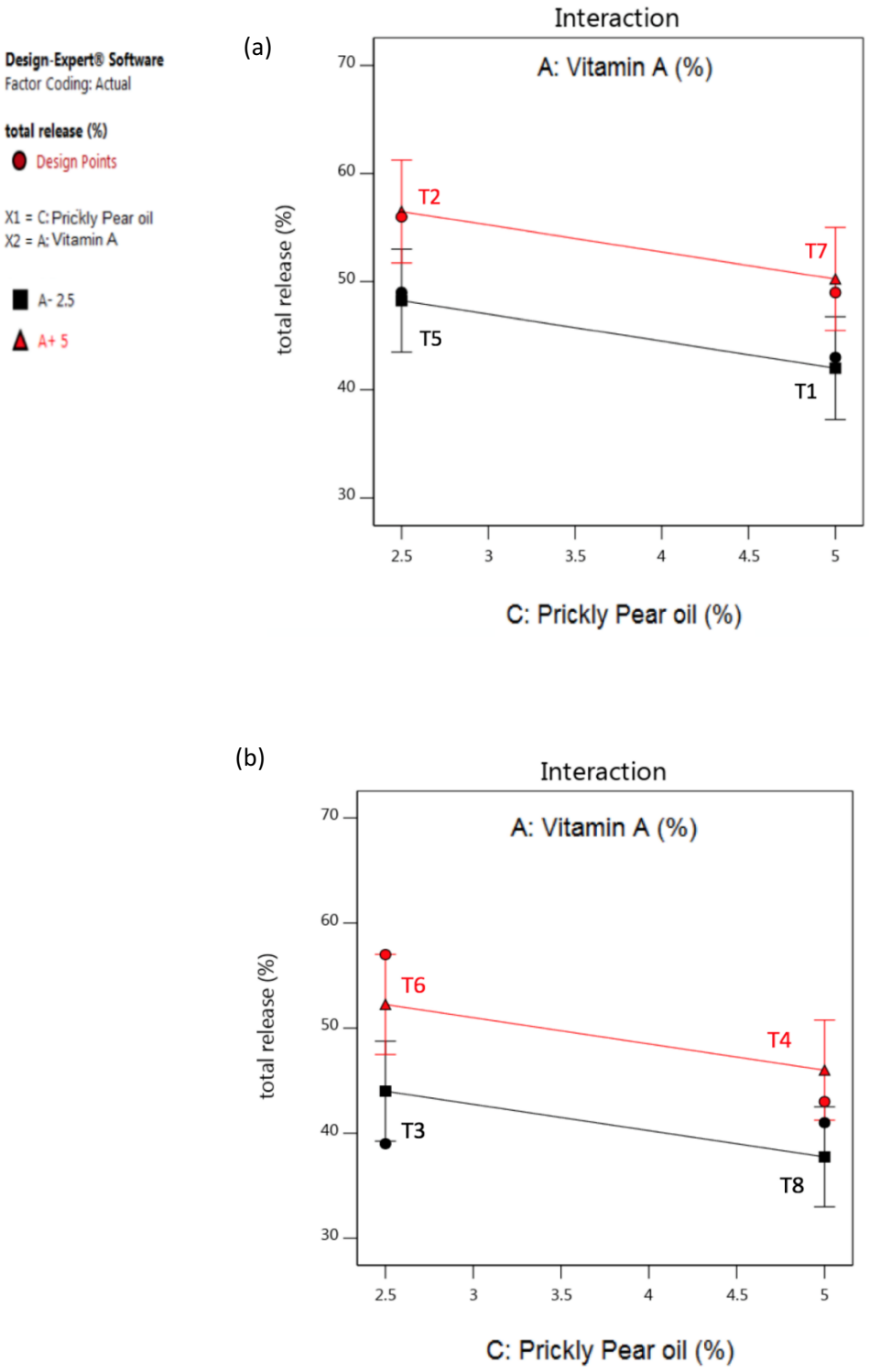

Figure 45. Interaction plots for Total release of NLCs with lower (a) and higher (b) surfactant to solid lipid ratio showing the trend in the formulations with increase PP oil.

The interaction plots, Figure 45, for the 8 formulations show a dependence of the total release on the amount of PP oil incorporated. The increase in PP oil allowed for lower RP to be released into the medium. This could be explained by the fact that PP oil is a better solvent for RP than is the solid lipid matrix. The RP when well dissolved with higher amount of oil will tend to localize in the carrier, rather than partition into the medium. The oil will solubilize the RP, and increase its thermodynamic stability, impeding its tendency to migrate out and into the polar, ethanolic media. This trend is seen in all formulations, which is then confirmed in the significant level of the PP oil factor of the ANOVA later. A higher total release is also witnessed for formulations with higher composition of vitamin A. This is explained by the increased diffusion capacity of the system.

5.6.1 Analysis of Variance of *In-vitro* Release

Further statistical investigation on the *in-vitro* release was done by Design Expert for the total release for all the 8 NLC formulations. Table 7 shows the ANOVA of the effects of the three factors on the release profile, showing statistical significance for the model at 10%. Vitamin A shows the highest relative significance, at 5%, which relates to the dependence of drug concentration to the extent of diffusion, and thus the total release. This is attributed to the dependence of the diffusion constant on the concentration of the drug, where a higher drug concentration results in a higher diffusion coefficient.[168] Finally, although all the *in-vitro* release had the same amount of initial RP, the total amount of their respective total release was not all the same. It was shown that formulations with a higher composition of RP showed a higher release, such as T2, T6 and T7. Furthermore, the amount of PP oil did show a significant effect at 10%. This is shown in the formulations with the highest release, such as T2, and T6. These two formulations had a low composition of PPoil, which could have allowed for higher release. This

could be explained by the fact that less of the RP is now dissolved in the matrix, and hence could be made easier to partition out of the carrier and into the skin.

Table 7. ANOVA on the response of total *in-vitro* release of NLCs

ANOVA for selected factorial model

Response total release

Source	Sum of Squares	df	Mean Square	F-value	p-value	
Model	250.38	3	83.46	4.74	0.0836	not significant
A	136.12	1	136.12	7.72	0.0499	
B-Surfactant	36.13	1	36.13	2.05	0.2255	
C-PPoil%	78.13	1	78.13	4.43	0.1030	
Residual	70.50	4	17.63			
Cor Total	320.88	7				

5.6.2 Regression Model for Total Release

The regression equation for the total release response includes the vitamin A%, X_1, surfactant ratio, X_2, and PP oil composition, X_3. The following is the coded equations that includes the factors that affect the total release:

$$Total\ release = 47.13 + 4.13X_1 - 2.13X_2 - 3.13X_3 \qquad \text{Equation 9}$$

The R^2 of the model gave a value of 0.78. Although not a perfect fit, it can be used to qualitatively assess the variation in total release as a result of changing the three factors. The relative significance of the factors can be evaluated by the absolute value of their respective coefficient. This is seen in the first factor, that of the vitamin A% (w/w), which confirms the previous claims that it is pivotal in determining the total release. The second significant factor is that of the PPoil%, and to a lower extent the surfactant to solid lipid ratio. In the latter case, it can be directly inferred

that a low surfactant to solid lipid ratio (X_2=+1), will give a lower total release. This is seen in the formulation pairs T3 and T5, and T4 and T7, where all factors were identical apart from the surfactant to solid lipid ratio. The lower release of the formulations with lower surfactant ratio is seen in T3 and T4, with respect to their pairs T5 and T7, respectively. This could be attributed to the lower tendency of the RP to partition into the medium since there is now lower amounts of amphiphilic surfactant molecules to facilitate their release. This could be related to the results of the EE%, where a lower value was exhibited in formulations with higher surfactant to solid lipid ratio. The low EE% means that more RP is freely available in the dispersion, contributing to a higher release.

5.6.3 Preliminary Trials for RP Degradation in Chosen Media (Ethanol/Glycerol)

In an attempt to confirm that the RP in both the media and the *in-vitro* setup, does not degrade, a control solution of RP in ethanol/glycerol solution was incubated for 24 hours. The graph below shows the change in RP concentration with time, which was shown to be statistically insignificant (i.e. < 5%). Therefore, the amounts of RP documented in the release are not affected by degradation, as the RP is relatively stable in the media for the time required in the incubation period as shown in Figure 46.

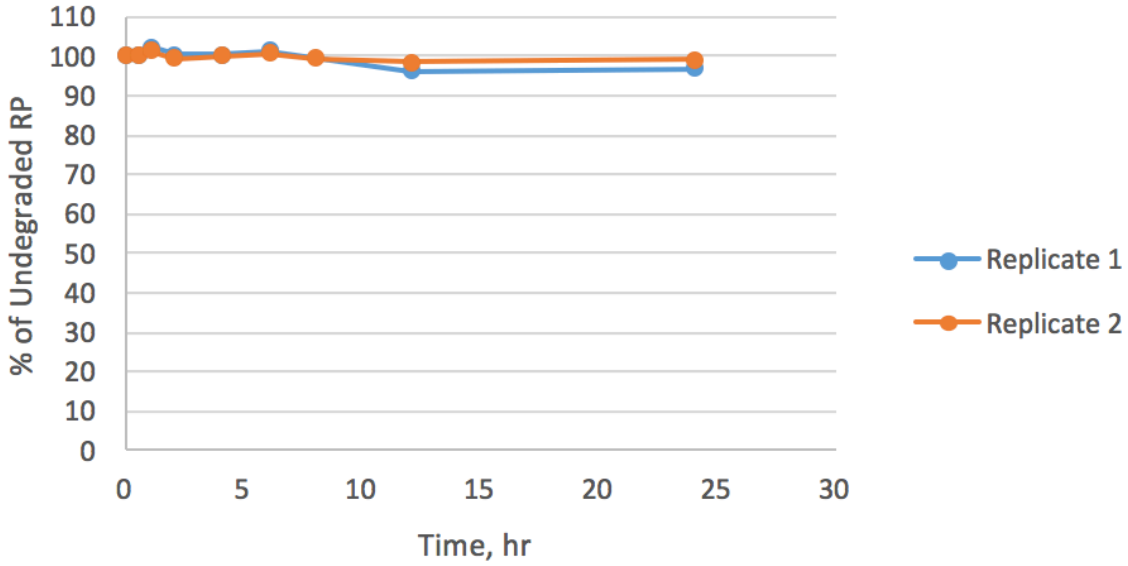

Figure 46. RP degradation in Ethanol/Glycerol Media.

5.7 *Ex-Vivo* Skin Permeation

After conducting the *in-vitro* release of the formulations, the two formulas that exhibited the highest total release, namely T2 and T6, with 56% and 57%, respectively, were evaluated for skin targeting potential. The total release in the receptor compartment of the FDC over a 24-hour incubation period is shown in Figure 47. The lower amount of RP released could mean that there is a lower chance of systemic absorption, as the drug has a higher tendency to localize on the skin.[111] Since RP is highly hydrophobic, it is expected that skin retention will exceed its tendency to partition into the blood, as the RP will be better accommodated within the lipidic lamellar structure of the skin, rather than the aqueous media of the blood. From results in the literature, one study has added 0.5g of a gel enriched with SLN-RP dispersion and reported a release of about 10 $\mu g/cm^2$ in the receptor compartment using human daver skin as the membrane.[111] In comparison, the results in this experiment gave a total release of 285.4 and 116.0 $\mu g/cm^2$ for T2 and T6, respectively. The significantly higher release in this case is probably due to the different receptor

medium used. In the study, they used PBS buffer solution, which has shown very poor solubility for the RP in preliminary trials conducted when selecting the optimum receptor medium. The ethanol/glycerol solution used showed much higher solubility for the RP, as well as possibly contributed to the enhanced permeation due to the alcoholic media. Ethanol has been reported to act as a penetration enhancer by several mechanisms, one is by extracting lipids and proteins from the skin, and hence increasing its porosity. Another includes increasing the drugs solubility in the lipid lamellar layers of the skin due the presence of alcoholic enhancers.[169] The chromatograms are provided in Appendix C.

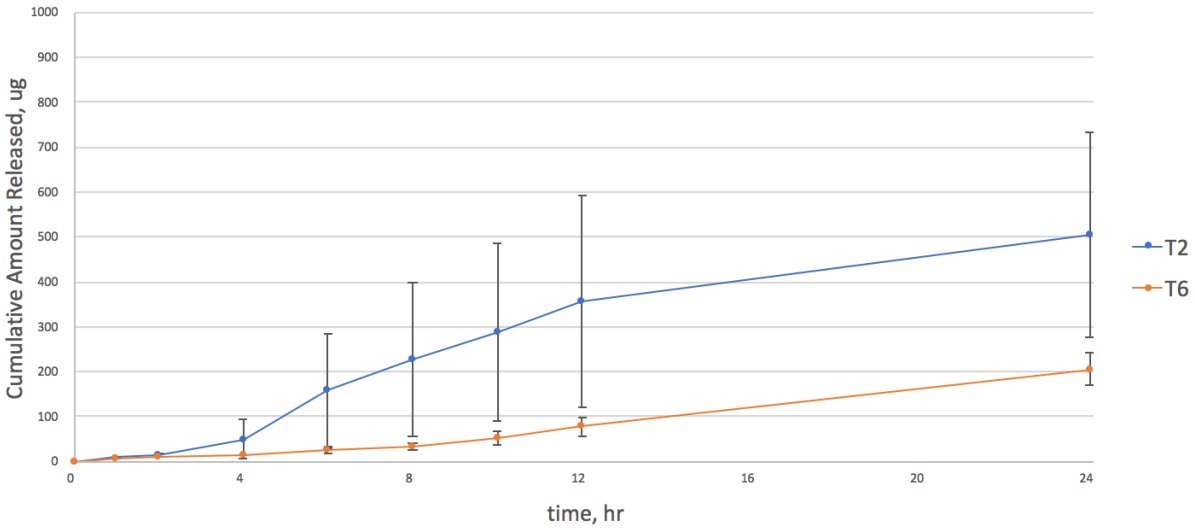

Figure 47. *In-vitro* skin deposition profile of RP, error bars are too small to scale for T6.

Furthermore, T2 has shown higher tendency to permeate through the skin than did T6. This could be explained by the relative viscosity, which is lower for T2, since it has a lower composition of solid lipid compared to T6. This has resulted in the observed gelling effect in T6, forming networks in the dispersion that increases its viscosity. Furthermore, in one previous study conducted by Raza, Singh and Lohan, the skin permeation of the NLC has shown to exceed that of the SLN.[54] The high permeation of NLC was explained in the study by the addition of isopropyl

myristate as the oil component. A similar argument can be made in this case, where the higher viscosity of T2 that had a lower ratio of solid lipid to oil, showed an enhanced permeation effect. An oil component has a higher content of unsaturated fatty acids, in comparison to higher saturation in solid lipids. This has been reported to improve the degree of permeation through the SC, where the unsaturated chains form kinks that further disrupt the lipid lamellar layers of the skin.[170,169] As a result, a higher flux in permeation is then observed.

From another light, the ZP of T6 exceeded that of T2, which could be another contributing factor to its lower penetration, which has been reported to decelerate penetration due to the inherent negative charge of the skin.[171] However, the permeation through the skin and into the receptor compartment of the FDC does not necessarily correspond to the drug found in the blood. This means that not all of the RP migrating across the skin barrier in this set-up should be equated to an *in-vivo* behavior. This is confirmed in a case reported, where the drug permeated from an SLN vehicle, and into the receptor compartment, was characterized as the drug deposited on the skin rather than absorbed in the blood.[41] Therefore, more in depth analysis was ensued on the skin sample to extract the total amount of RP in its various layers, namely, SC and Dermis/Epidermis.

5.8 *In-vitro* Skin Distribution Study

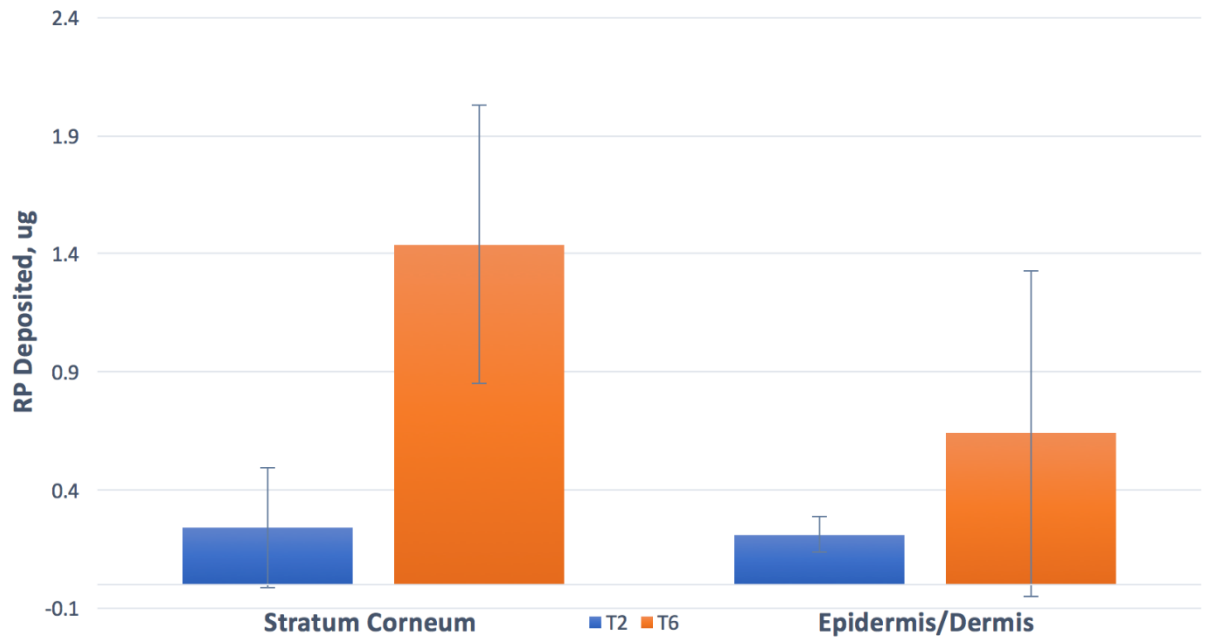

Figure 48. *In-vitro* Skin Deposition Profile of RP in Rat Skin with Error Bars showing Standard Deviation in Triplicates.

The distribution of RP in the rat skin layers was analyzed by extraction using methanol after the 24 hour incubation period. Figure 48 illustrates the amount of RP deposited in the upper layer, the SC, and the deeper tissue, the Epidermis/Dermis layers, for both T2 and T6. A more pronounced deposition was found for T6 in both sections of the skin. This resonates with the previous findings in the *in-vitro* release, showing a higher permeation through the skin for T2, and thus lower skin deposition. The higher viscosity in T6 was claimed to be linked with a stronger interfacial film forming on the surface, which could be due to the crystalline state of the solid lipid core.[41,172] This film has been suggested to increase the permeation of vitamin A through the skin by the consequent occlusion factor that takes place as a result of decreased TEWL which results in increased skin hydration.[44] An SEM image of one of the rat skin incubated over night with T6 is shown in Figure 49. The image shows the coverage and adsorption of the nanoparticles on the

skin, which is explained by their inherent film formation, and small size that adsorbs onto the skin. In comparison to a similar study reported in the literature, the cumulative amount of vitamin A, namely isotretinoin, in the all three layers of the skin was extracted and found to be in the range of 2.5-3.6µg.[109] In this study, the total of both SC and epidermis/dermis layers for T2 and T6 are 0.45, and 2.1µg, respectively. In the case of T2, it shows a poor skin retention as opposed to T6. The chromatograms are provided in Appendix C.

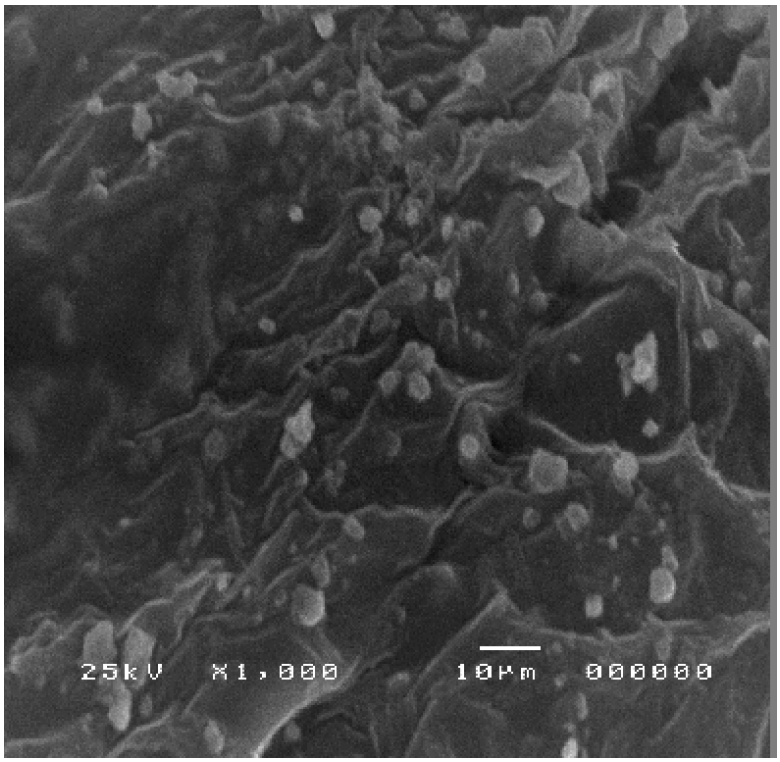

Figure 49. SEM image of rat skin with T6 from *ex-vivo* experiment.

Furthermore, drug expulsion as a result of polymorphic transitioning of the solid lipid matrix can also account for the increased amounts deposited in T6.[45] From another perspective, T2 does have a higher surfactant to solid lipid ratio, which could attribute to its enhanced permeation through skin and into the receptor compartment. This is due to the surfactant nature that has been reported to fluidize the lipid lamellar matrix of the skin, thus acting as a penetration

enhancer.[41] Finally, since the purpose of this formulation is to allow for higher skin retention for the RP in order to maximize its anti-wrinkle activity, T6 is more desired in this case.

In terms of ZP of the two formulas, T6 having a higher negative charge will not be absorbed by the skin as much, instead, will accumulate and partition into its various layers as observed in the results above. Another study confirmed similar findings, showing a correlation between the increased surface charge of the SLN with negatively charged surface modifying agents, and an enhanced RP permeation.[51] The higher skin deposition and permeation into the deeper layers of the skin, namely SC and Epidermis/ Dermis, is due to the film formation of the lipidic carriers, that forms more strongly in case of T6 due to the increased solid lipid constituent, and its tendency to accumulate on the skin rather than permeate. This film will now allow for a prolonged interfacial interaction between the carriers and the skin, that can pave the way for material exchange between the SLNs and the lipids in the in the intercellular region of the skin.

5.8 Summary

Table 8. Summary of Responses of all 9 formulations.

Formula	Particle Size, nm	PDI	ZP, mV	EE%	Total release %
T1	197.6	0.18	-27.7 ±0.2	83.2 ±0.7	43 ±4
T2	221.8	0.25	-22.9 ±0.1	78.7 ±0.2	56 ±7
T3	238.2	0.33	-26.0 ±0.2	94 ±2	39 ±1
T4	236.8	0.24	-32.9 ±0.3	95 ±1	43 ±7
T5	243.3	0.12	-26.8 ±0.5	85 ±0.9	49 ±7
T6	240.2	0.24	-30.7 ±0.6	83 ±2	57 ±3
T7	214.6	0.19	-18.2 ±0.5	94 ±2	49 ±7
T8	228	0.22	-26.5 ±0.5	97 ±2	41 ±10
SLN	296.7	2.4	-39.3 ±0.8	65.6 ±0.6	35 ±4

The main factors that affected the particle size is the amount of PP oil, and surfactant to solid lipid ratio. When the two were at a relatively high constitution, a small size resulted. The importance of the PP oil in assessing the particle size is as important as the role of the surfactant, a phenomenon that has not been addressed previously in literature. This could be explained by two mechanisms. One, is that the presence of the oil allows for a lower viscous lipid melt, that is easier to diffuse during the homogenization process, and thus form smaller sized particles. The second is the oil's superior ability to solubilize RP, which allows for the RP to be localized within. The mechanism of the surfactant's role, on the other hand, in reducing particle size is well document.

This was explained by the latter's ability to decrease the surface tension between the two immiscible phases, and hence allow for the formation of smaller particles with higher surface area.

The ratios of the factors to one another is important in assessing the PDI. The most significant factor found, however, was the surfactant to solid lipid ratio, where a high constitution leads to a more homogeneous dispersion with lower PDI. The interaction of the three factors together, and that of the vitamin constitution and surfactant ratio has also shown to be significant in the PDI's assessment. In terms of PDI, T5 exhibited the narrowest particle distribution. This could be attributed to its overall low lipid composition in all three components.

After storage for 6 weeks the formulations showed different stabilities. The ones with higher stability, based on their ability to retain a narrow particle distribution, had a lower surfactant to solid lipid ratio. This means that the stability is not so much affected by the amount of surfactant, as much as it is by the relative constitution of all the factors making the matrix. In addition, the relative amount of PP oil to the solid lipid seems to also play a significant role. The three formulations with the highest stability, namely T4, T5 and T8, had equal ratios of solid lipid to PP oil. ZP was not pivotal in determining the dispersions' stability.

The EE% for all NLC formulations generally exceeded that of the SLN. The highest value was for T8, with a value of 97.1%. This formulation had a relatively low composition of RP with respect to both solid and liquid lipids. The mixture of both types of lipids in equal ratios, but high composition, allows for effective incorporation of RP.

Another phenomenon observed was the effect of the relative constitution of the RP to the PP oil, giving a low EE% when a relatively lower oil composition is used. This is due to the RP's lack of proper solubility in the matrix. The importance of the oil in the EE% can be further

confirmed by evaluating the significantly lower value attained for the SLN. The lack of an oil component in the former formula is pivotal in explaining its decreased ability to retain the RP. Finally, the most significant factors in assessing the EE% is the relative constitution of the lipids, where a high solid and lipid composition results in improved incorporation of the RP within the matrix.

To confirm the crystalline behavior of the solid lipids in relation to their EE%, DSC measurements were executed on all 9 formulations. The thermograms, however, were not consistent in the trend they depicted. Finally, in concluding one may use the DSC as supplementary tools to give insight into the polymorphs and crystallinity exhibited by the carriers, but must not be on its own to predict EE%.

In assessing the *in-vitro* release of the 9 formulations, a relationship was observed between the diffusion flux and the EE%. Since the amount of RP influences its embedment within the carrier's matrix, this in turn influences its ability to migrate out of the matrix, and partition into the receptor medium. This was confirmed with the highest diffusion flux observed for the SLN and T2 formulations, that also exhibited a relatively low EE%. This is contrasted in formulations having high EE%, as in T8, and as a result exhibiting a more controlled and sustained release. This phenomenon is attributed to the embedment of the RP in the core when a sustained release is observed, as opposed to a shell enriched model in cases of burst release. The total amount of RP released from the carriers did vary, however, with T2 and T6 showing the highest total release with 56% and 57%, respectively. What these two formulations had in common is their relatively high composition of RP, that in return prompts its diffusion from the matrix and into the receptor medium.

The results indicated that the composition of the formulation was paramount in the skin retention, namely the solid and liquid lipid ratio. The skin permeation of the formulations with the highest total *in-vitro* release, T2 and T6 , was further examined, along with their distribution in the upper most SC and deeper epidermis/dermis layers of the skin. The results showed an enhanced permeation in T2, as opposed to a higher skin retention in the various layers for T6. This is attributed to the difference in the solid lipid composition between the two, where the more viscous T6 allows for the formation of a stronger interfacial film. This in return allows for occlusion and decrease in TEWL, favoring material exchange between the carrier and the skin.

Chapter 6

Conclusion and Future Work

6.1 Conclusion

PP oil has shown to be a valuable ingredient not only because of its high antioxidant activity and nutritive content, but most importantly its effect on the lipidic carrier's attributes. The admixture of PP oil into the solid lipid matrix has contributed significantly in influencing the measured responses, such as particle size, PDI, ZP, EE% and *in-vitro* release. Variation in the composition of the lipidic carriers resulted in significant changes in the measured attributes, Different factors, such as amounts of RP incorporated, solid lipid to surfactant ratio, and PP oil composition, played varying significance in each response measured. In all cases, the NLCs formulations have shown superior attributes to the SLN carriers.

In evaluating the various particle size of the NLCs, a new trend was found, which has not been previously identified. It was shown that the amount PP oil plays a role, as significant as that of the previously reported role of the surfactant, in determining the particle size. This was seen as smaller sized NLCs were achieved with formulations consisting of higher PP oil composition. In assessing the PDI, the higher amount of surfactant to solid lipid ratio was the main factor that led to a narrow particle size distribution. However, this phenomenon could not predict the formulations stability upon storage. A new trend was now observed, where the relative proportion of the solid lipid to PP oil, when in equal ratios, gave the highest stability based on their ability to retain a narrow homogenous particle size distribution (PDI < 0.3). This observed phenomenon is also novel. Furthermore, the ZP of the formulations could not predict its stability, as particle aggregation was observed in formulations with an acceptable value (ZP < -30 mV).[43]

The amounts of PP oil incorporated showed significant effects on the EE% of the NLCs. Higher amounts of PP oil improved the incorporation capacity of the carrier significantly when combined with a similar composition of solid lipid. This phenomenon has been reported

previously, where a mixture of lipids is seen to enhance the EE%.[36,13,87] DSC measurements gave further insight onto the incorporation of RP within the matrix, where an overall shift to lower melting temperature of the lyophilized carriers, as compared to the pure solid lipid, was seen in all NLC formulations. A strong correlation was also seen between the EE% and diffusion flux in the first few hours of the *in-vitro* results. Generally, lower EE% showed higher diffusion flux, as the RP is more readily available on the surface of the carrier, rather than embedded within. The total amount released, however, was strongly affected by the amount of PP oil constitution the carrier. The highest release consisted of a low PP oil composition. This confirms the ability of NLCs to provide a more controlled and sustained release of the RP.

Ex-vivo studies conducted using natural membrane comprising rat skin for the two formulations that exhibited the highest *in-vitro* release, both had a low PP oil composition. RP extracted from the two layers of the skin, SC and epidermis/dermis, showed a higher retention for the formulation with higher solid lipid composition. On the other hand, higher permeation capacity for the formulation with lower solid lipid composition was observed. Since the work entails a cosmetic application of the formulation, skin retention is favored. Finally, the NLC formulations showed a variation in their exhibited assessed aspects. The choice of the optimal formula, is thus, a compromise where one must choose the formulation that entails or achieves the main targets required. The aim of this work entailed the investigation of different factors in order to reach a formulation with the most effective delivery of RP. In this respect, and based on the findings of this investigation, and the need for the different trade offs, formulation T4, consisting of high composition of all lipidic constituents, including RP, is the formula that has shown the best overall attributes, as shown in Table 9.

Table 9. Optimized Formulation, T4.

Optimized Formula	T4
Particle Size, nm	236.8
PDI	0.24
ZP, mV	-32.9 ±0.3
EE%	95 ±1
Total release %	43 ±7

6.2 Future work

Suggestions for future work for a better understanding and optimization of the NLC-RP for cosmetic application include the following:

- Different types of solid lipids, as well as surfactant must be used in the formulation. This will allow for a more comprehensive understanding, as well as pave the way for reaching a more effective carrier for RP.
- *In-vivo* studies to assess irritation, a main drawback of vitamin A derivatives, for comparison between conventional, direct application versus nano-encapsulation.
- Studies on the characterization and release profile of NLC-enriched creams and gels versus the original dispersion. This will allow for assessment on the final form of the cosmetic product in terms of stability, EE%, ZP, and release patterns.

- Since PP oil has shown improved attributes in the NLC-RP carriers, its use could be further assessed in encapsulating other lipophilic bioactives and vitamins.
- More detailed molecular studies on the arrangement of the lipidic and surfactant constituents should also be pursued, which will allow for a better understanding of the observed trends exhibited by the NLCs.

Appendix A

Calibration Curves and RP Degradation Study

Calibration Curves

Calibration curve using UV-Vis Spectroscopy for EE% measurements:

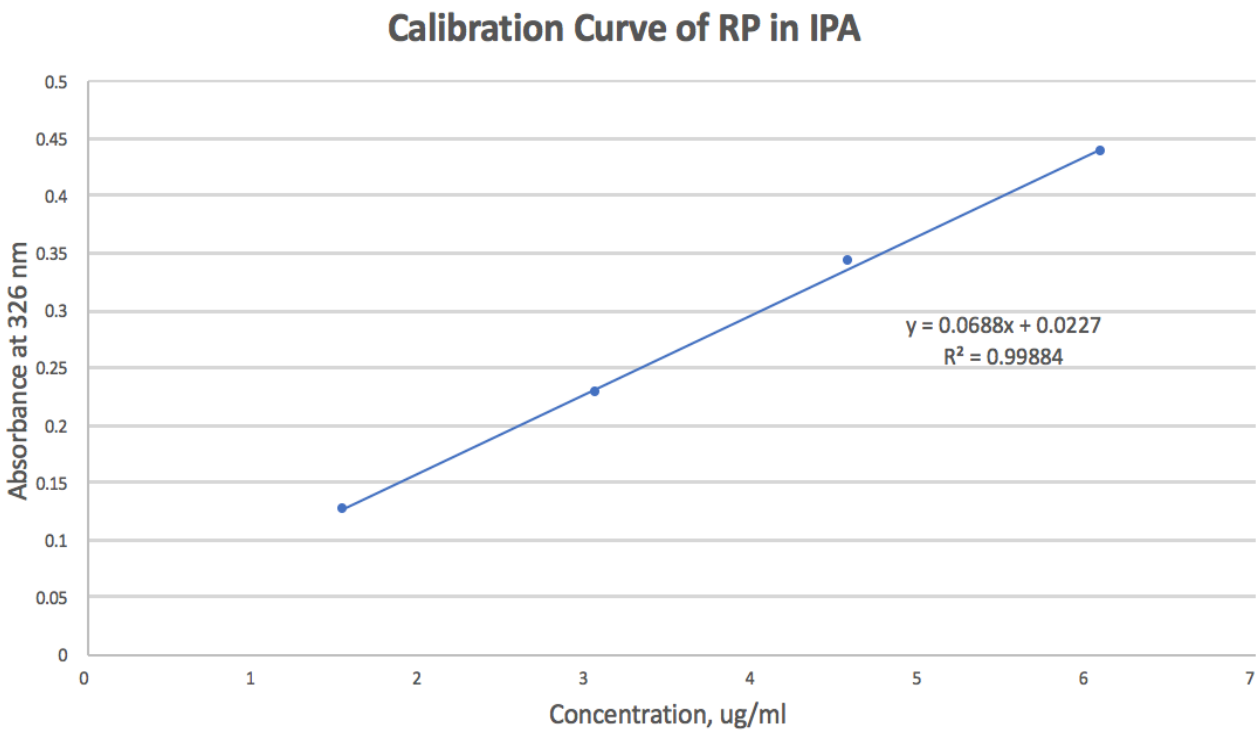

Calibration Curves using HPLC for (a) *In-vitro* Release and *Ex-vivo* Permeation (b) Skin Retention and Distribution studies:

(a)

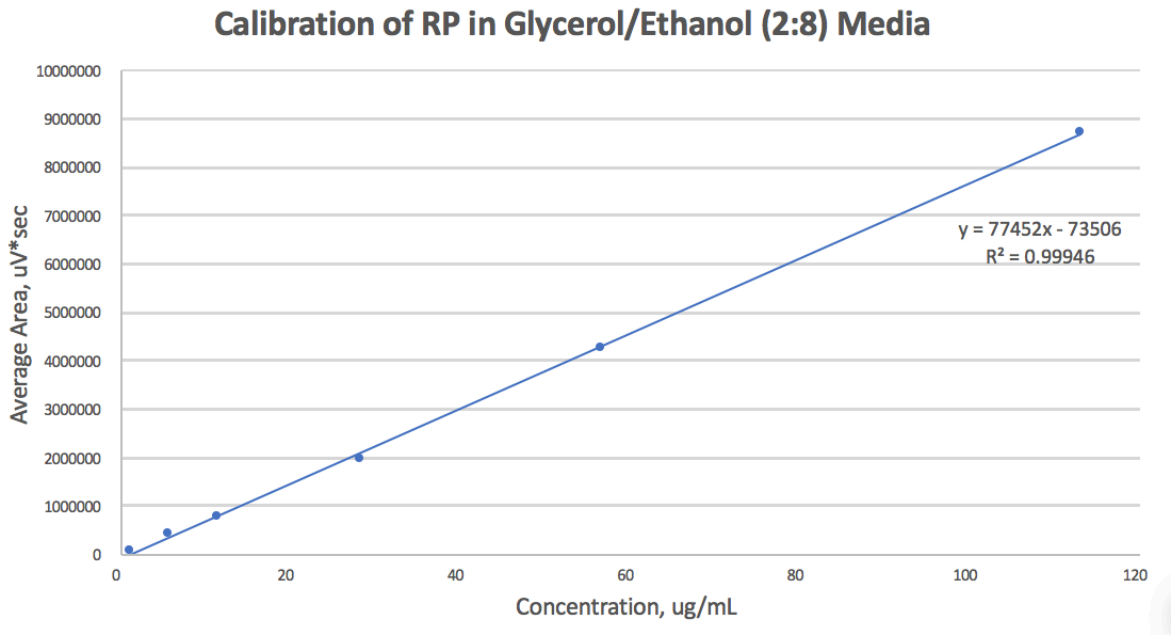

(b)

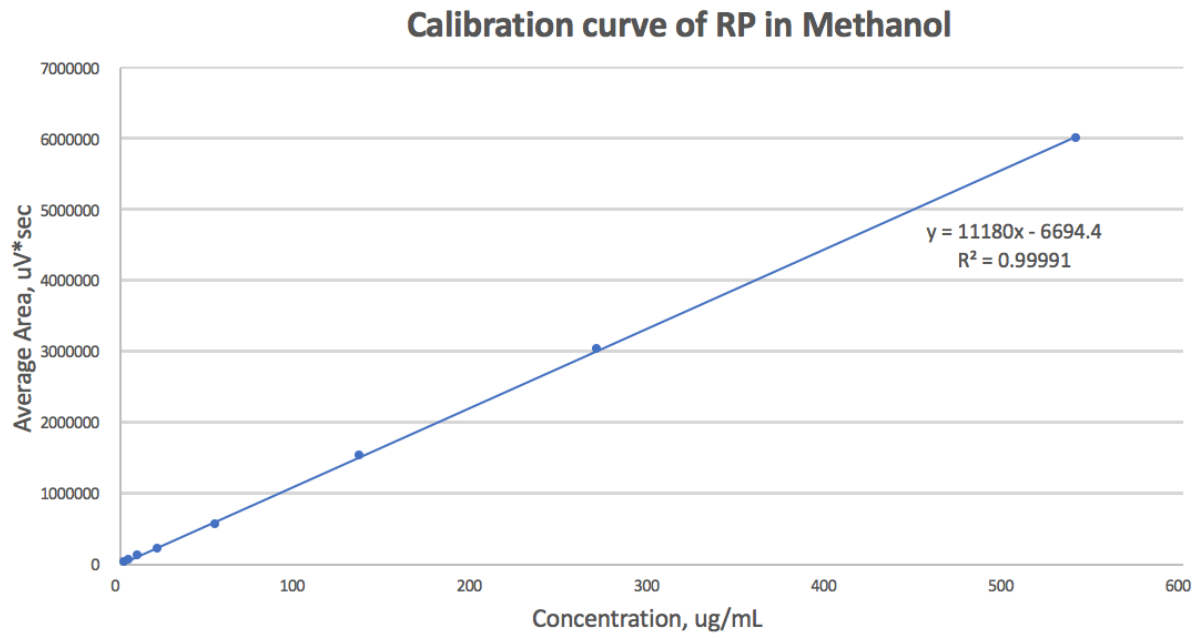

RP Stability Curve done using UPLC:

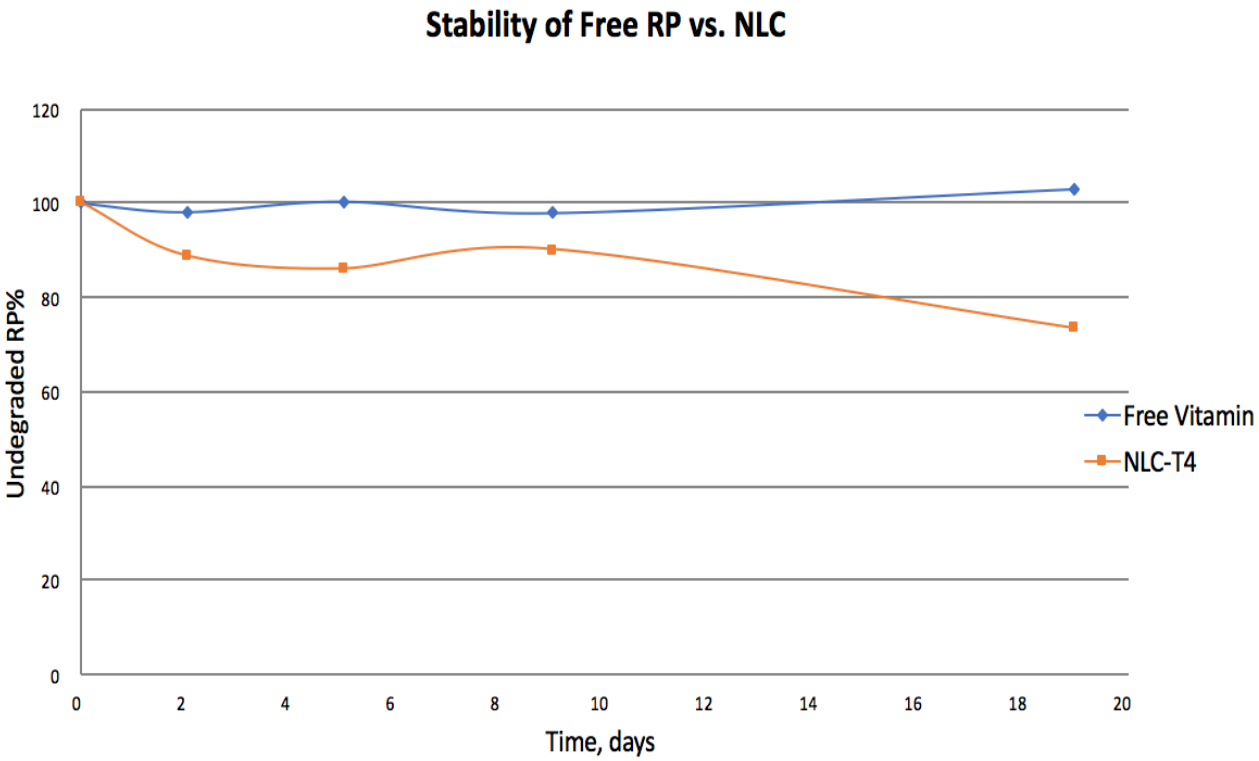

Appendix B

Validation of ANOVA Claims

Validating Claims of normality, independence and equal variance of residuals

Particle Size:

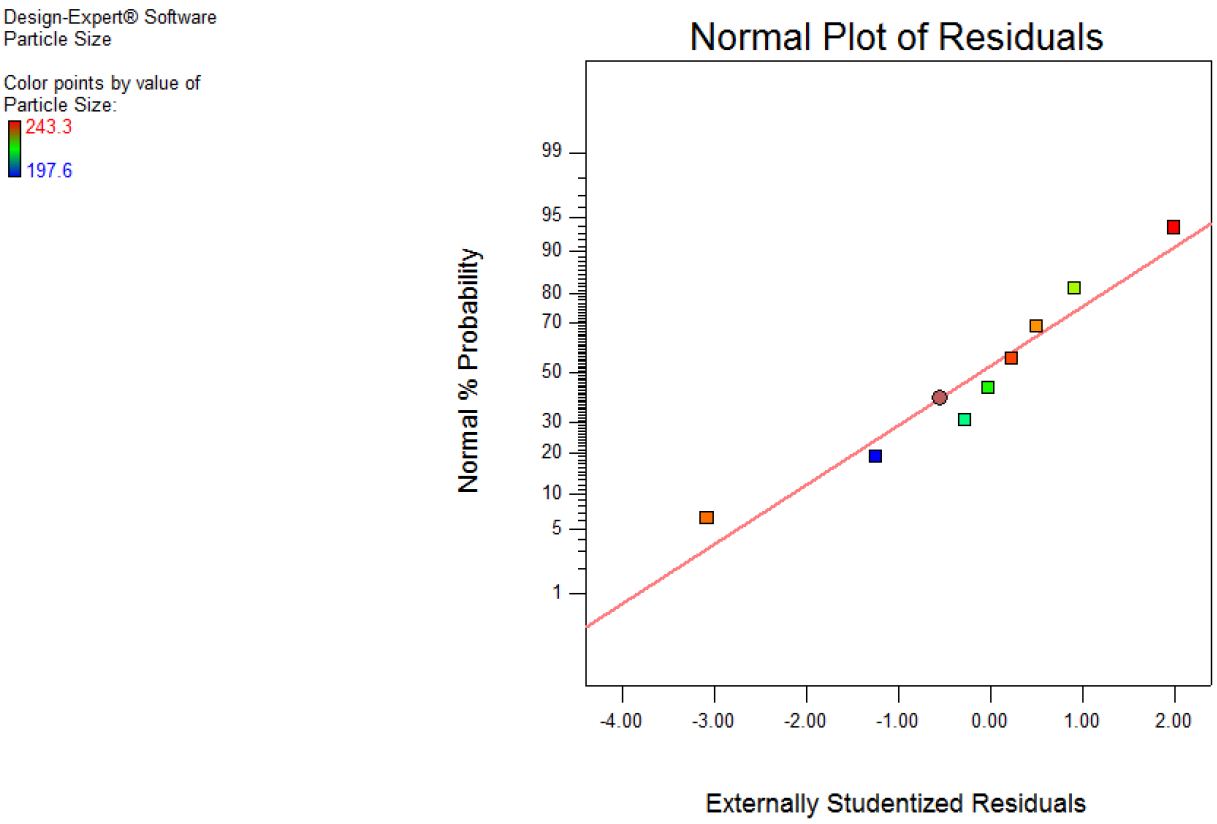

From the above plot, the residuals appear to be normal, as they mainly coincide on the line or in close proximity to it, without major deviations.

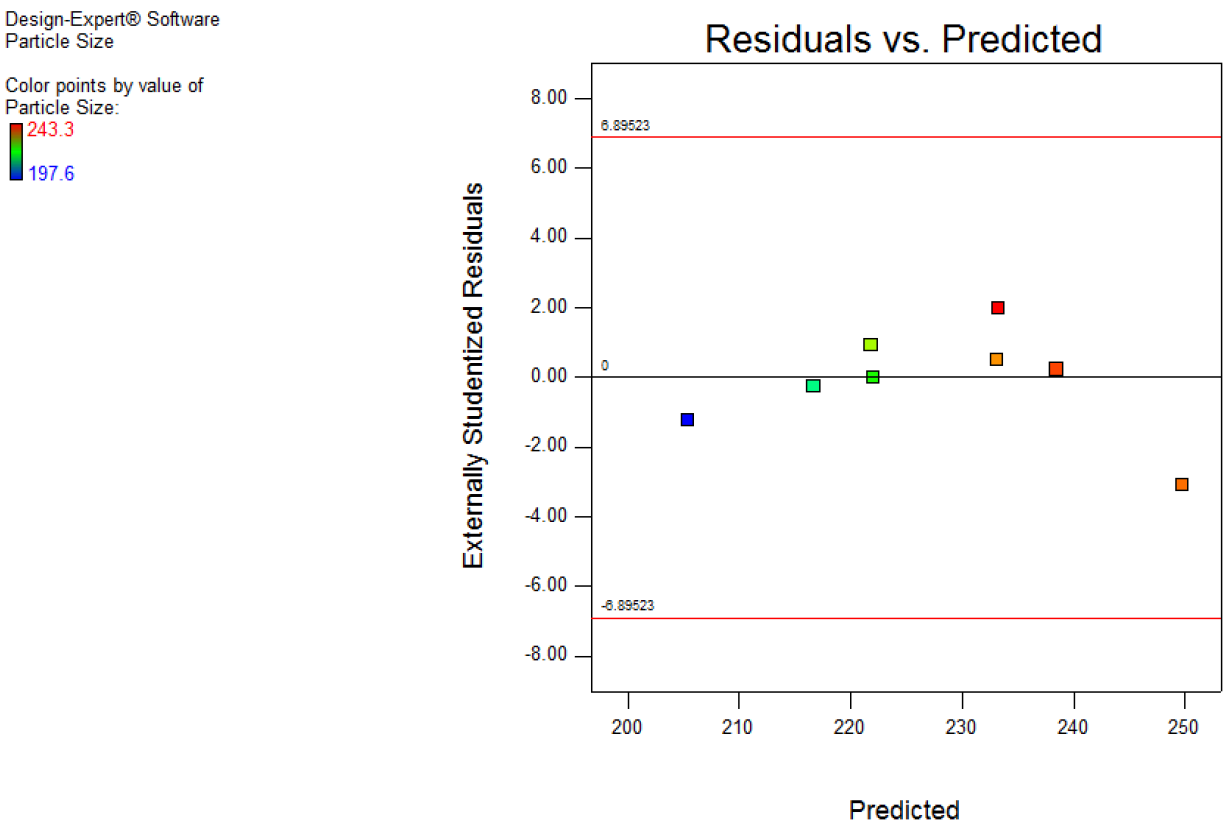

From the above plot of residuals versus predicted, the values lie between the two red lines, indicating homoscedasticity, or constant variance among residuals.

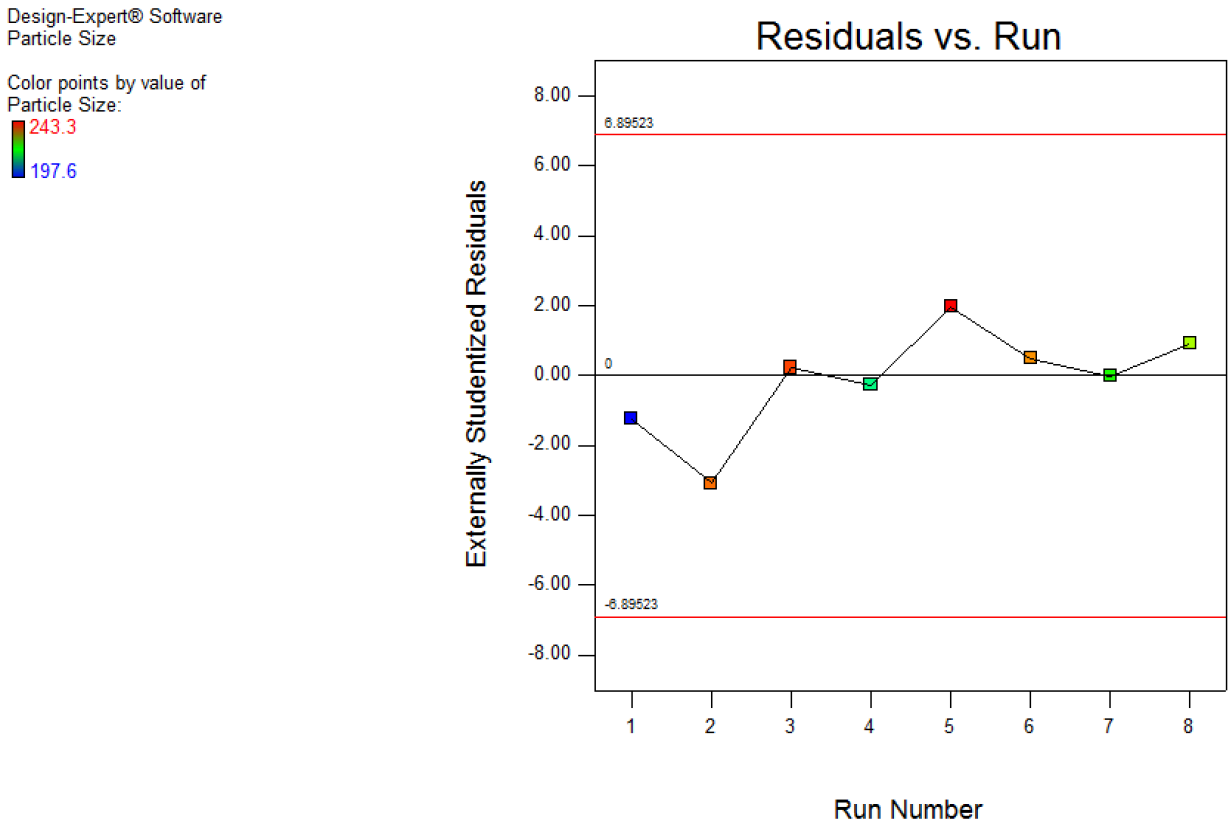

From above plot of residuals vs run, they appear randomly distributed and independent.

PDI:

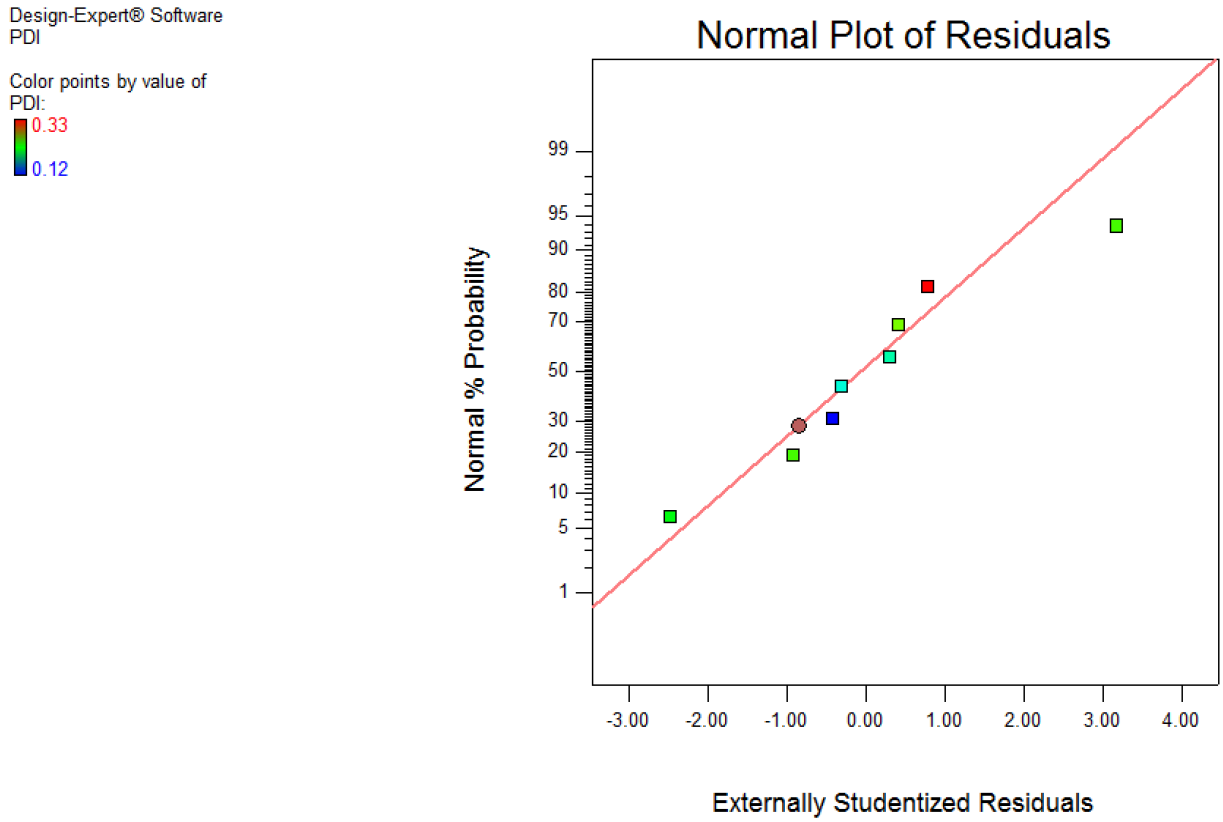

From the above plot, the residuals appear to be normal, as they mainly coincide on the line or in close proximity to it, without major deviations.

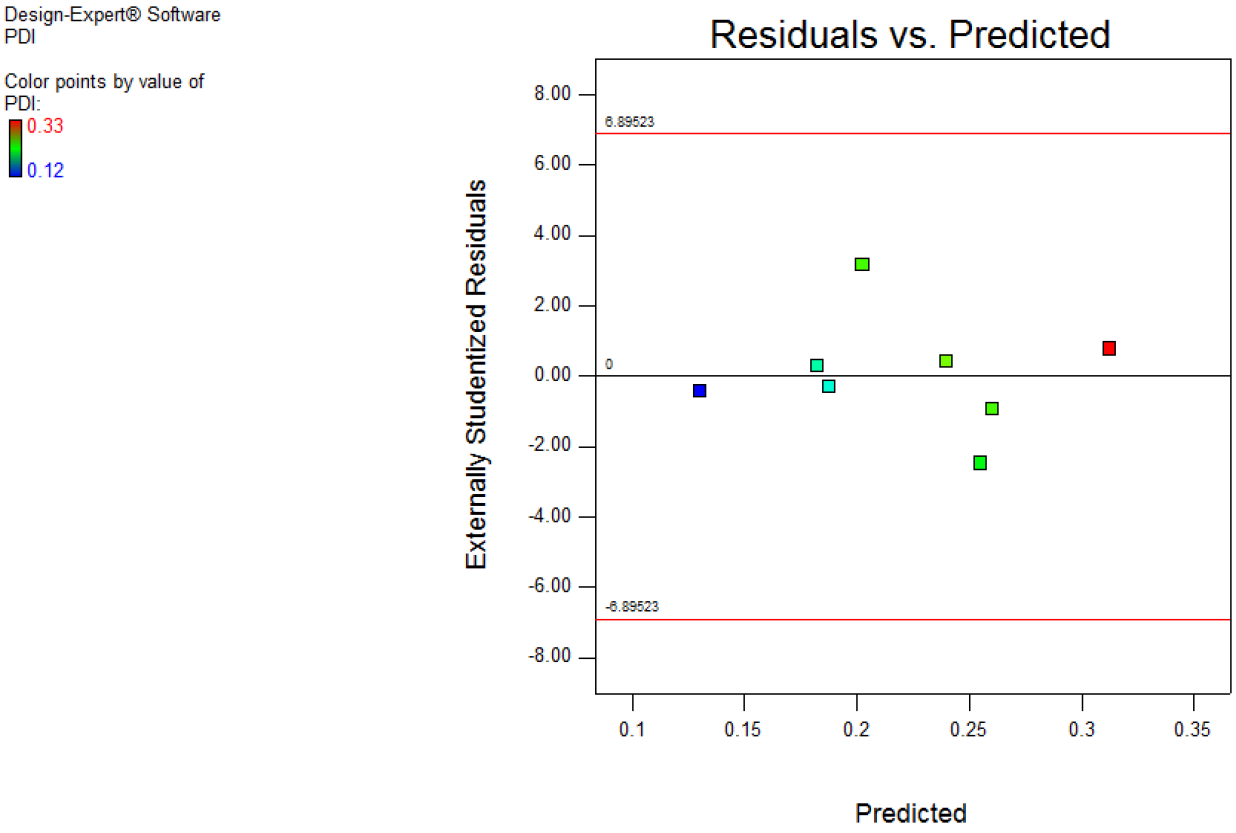

From the above plot of residuals versus predicted, the values lie between the two red lines, indicating homoscedasticity, or constant variance among residuals.

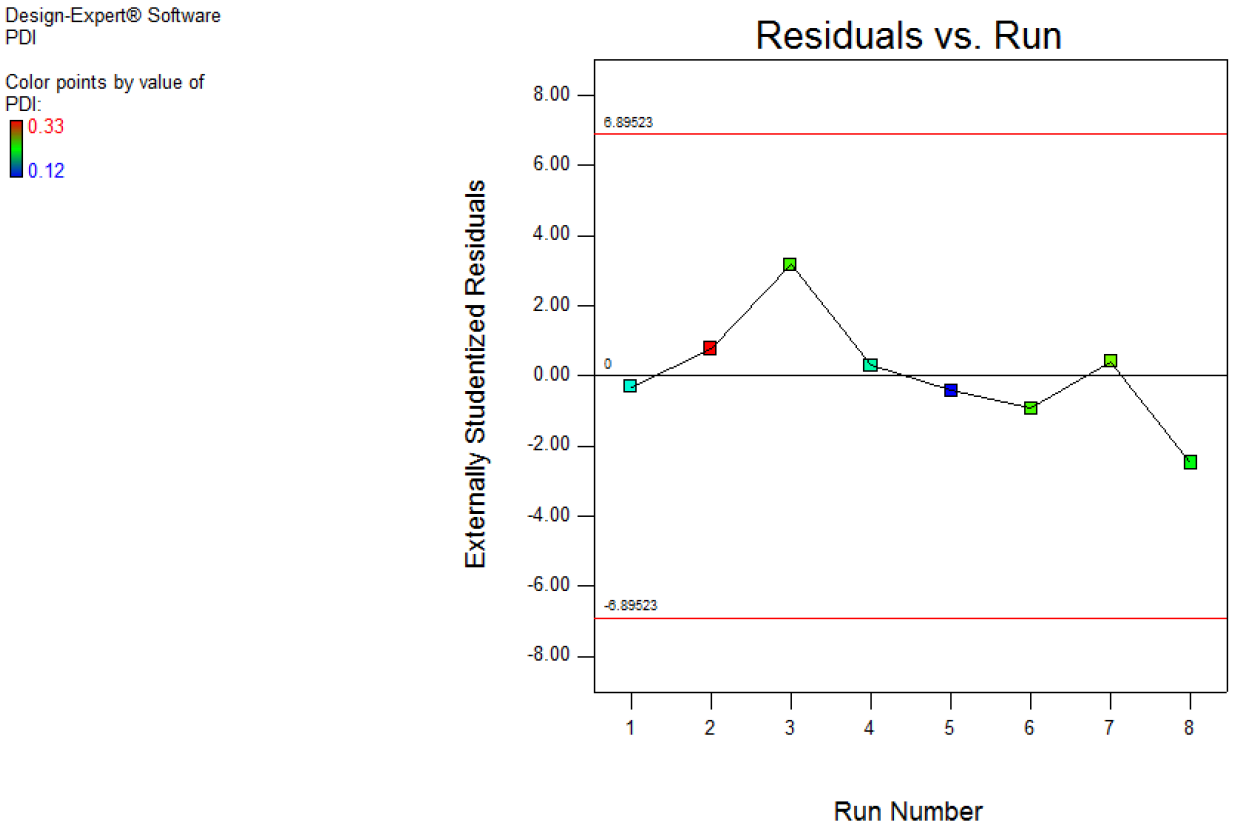

From above plot of residuals vs run, they appear randomly distributed and independent.

ZP:

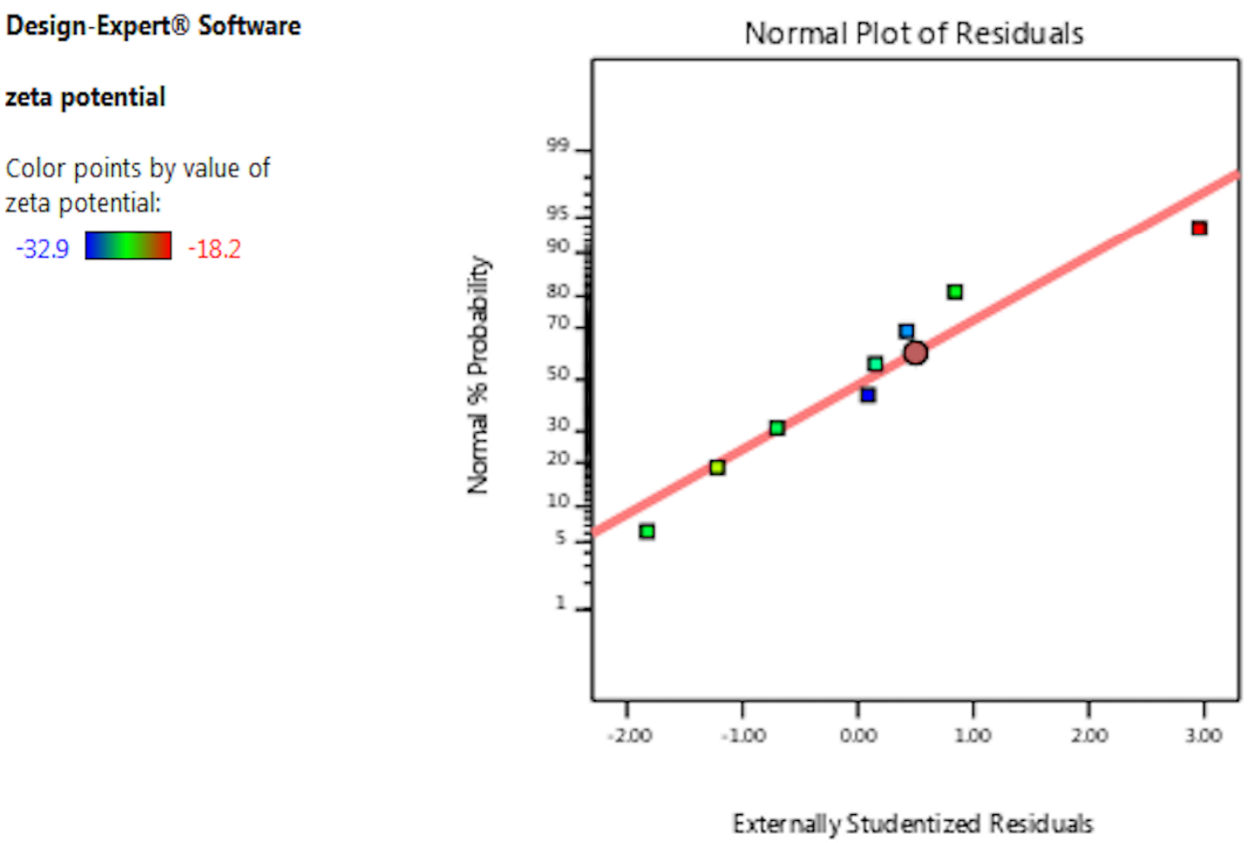

From the above plot, the residuals appear to be normal, as they mainly coincide on the line or in close proximity to it, without major deviations.

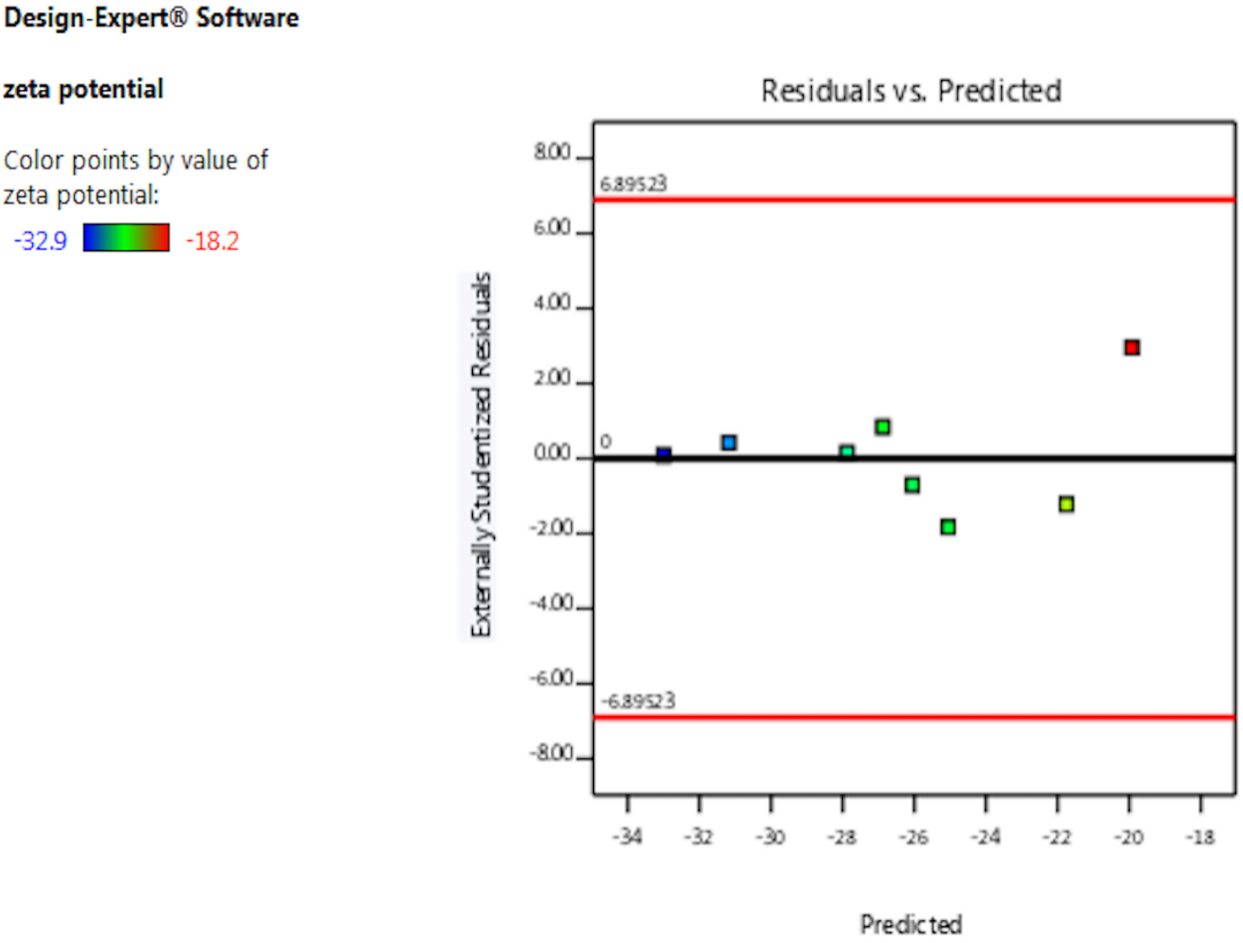

From the above plot of residuals versus predicted, the values lie between the two red lines, indicating homoscedasticity, or constant variance among residuals.

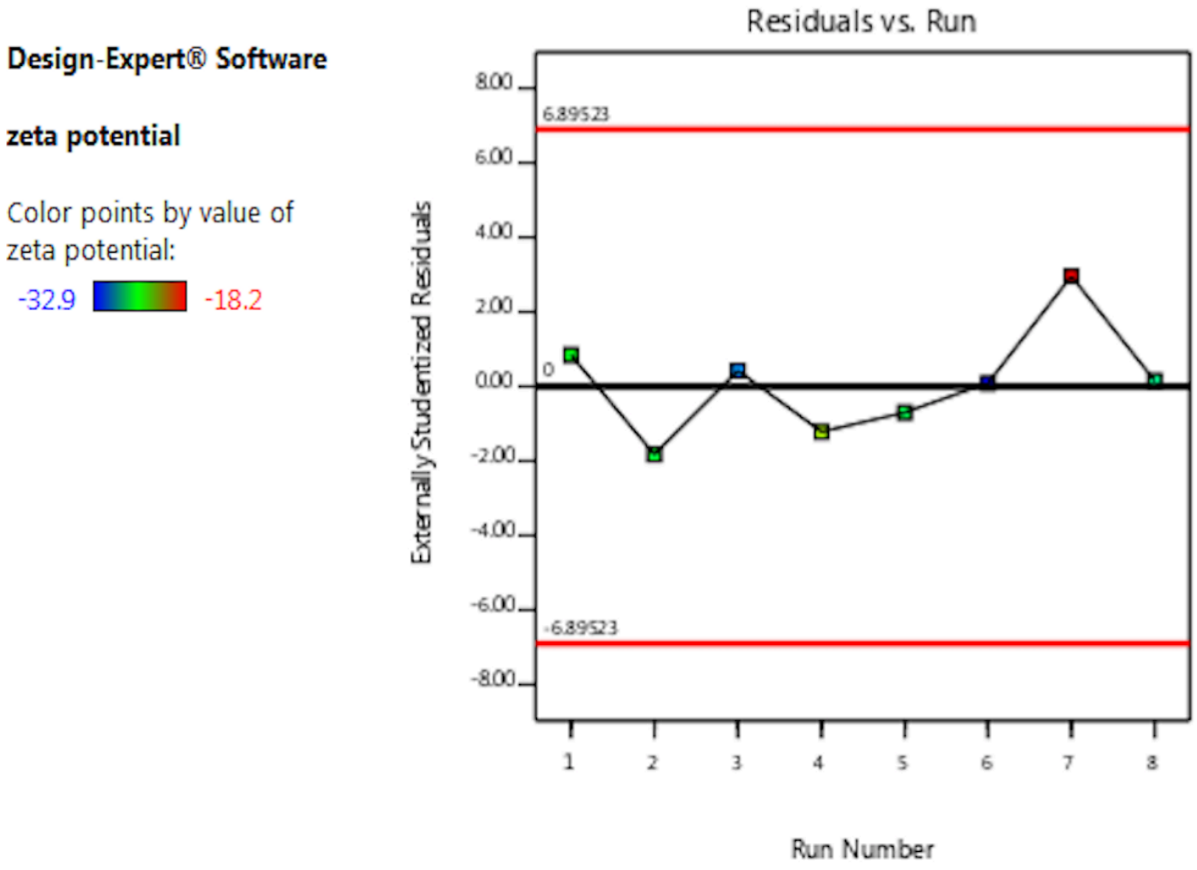

From above plot of residuals vs run, they appear randomly distributed and independent.

EE%:

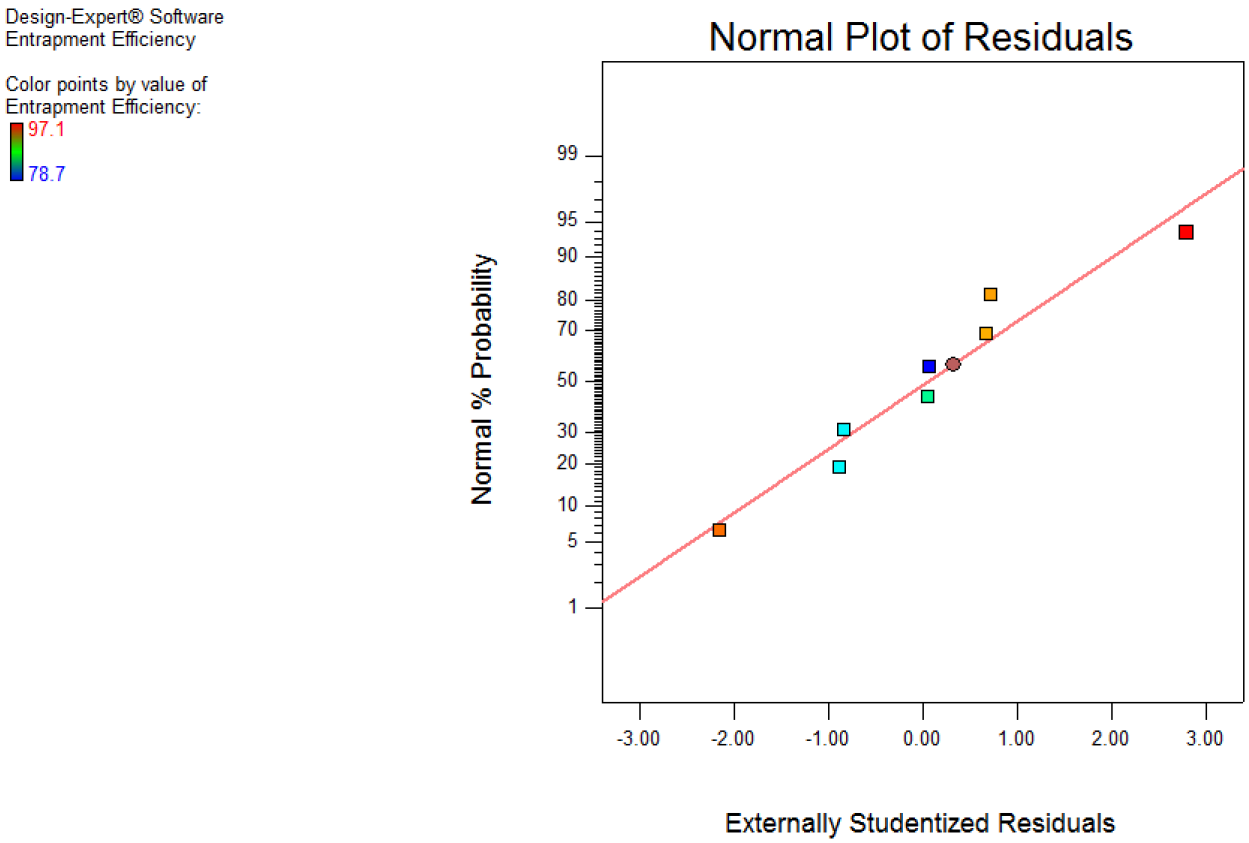

From the above plot, the residuals appear to be normal, as they mainly coincide on the line or in close proximity to it, without major deviations.

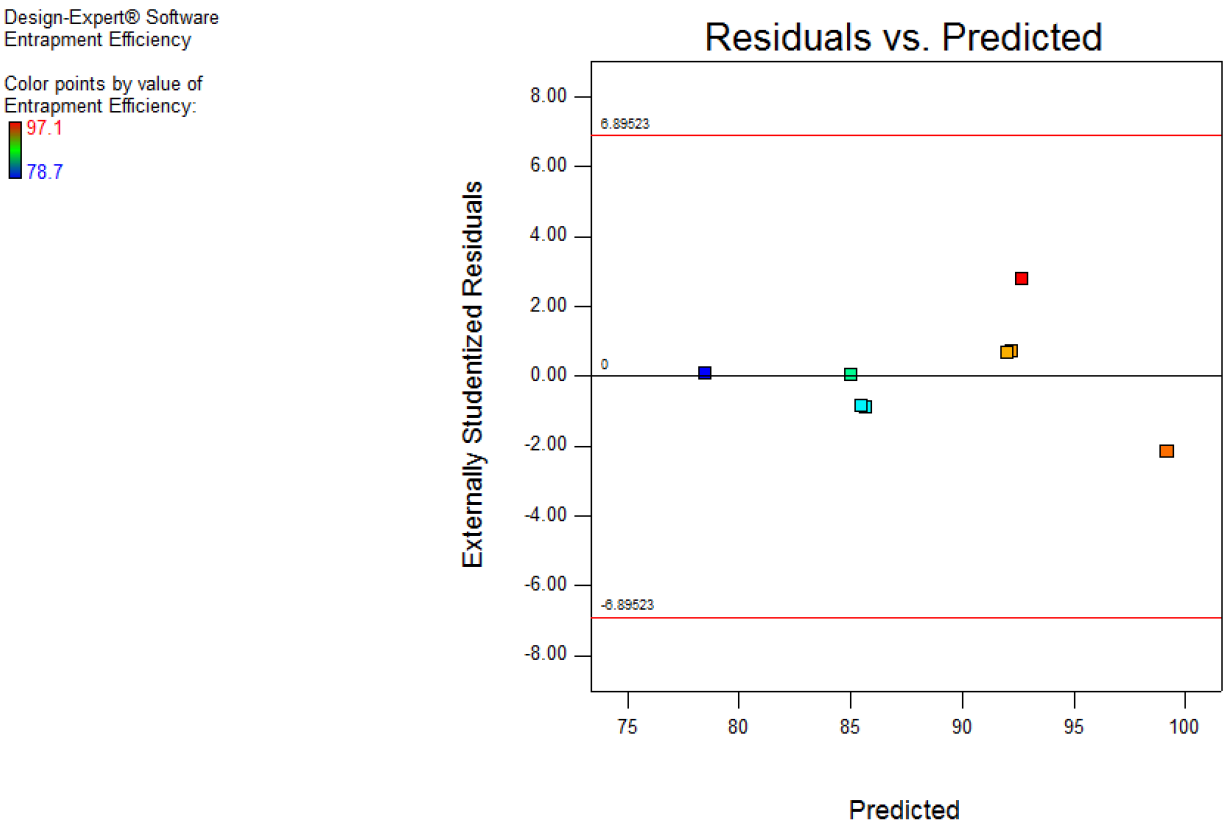

From the above plot of residuals versus predicted, the values lie between the two red lines, indicating homoscedasticity, or constant variance among residuals.

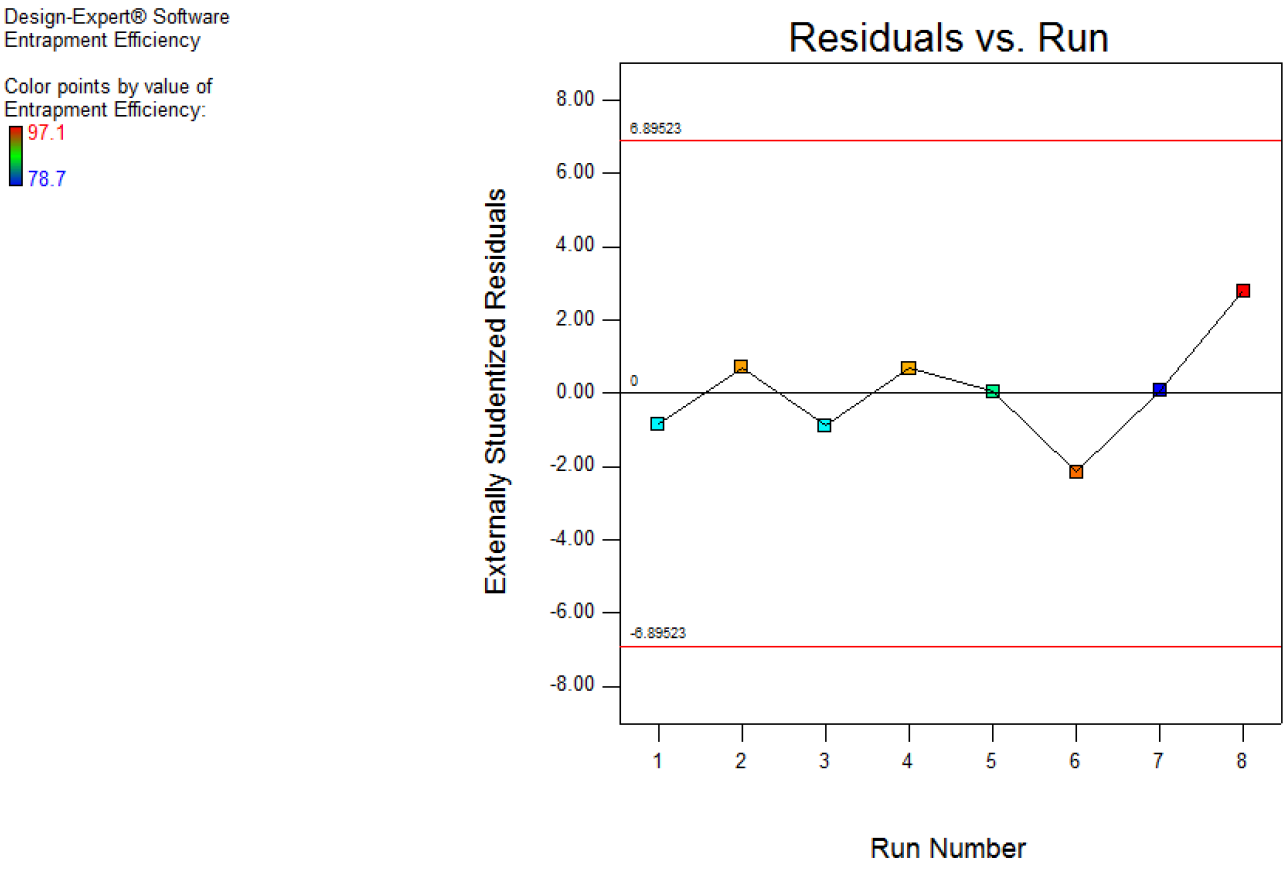

From above plot of residuals vs run, they appear randomly distributed and independent.

In-vitro Total Release:

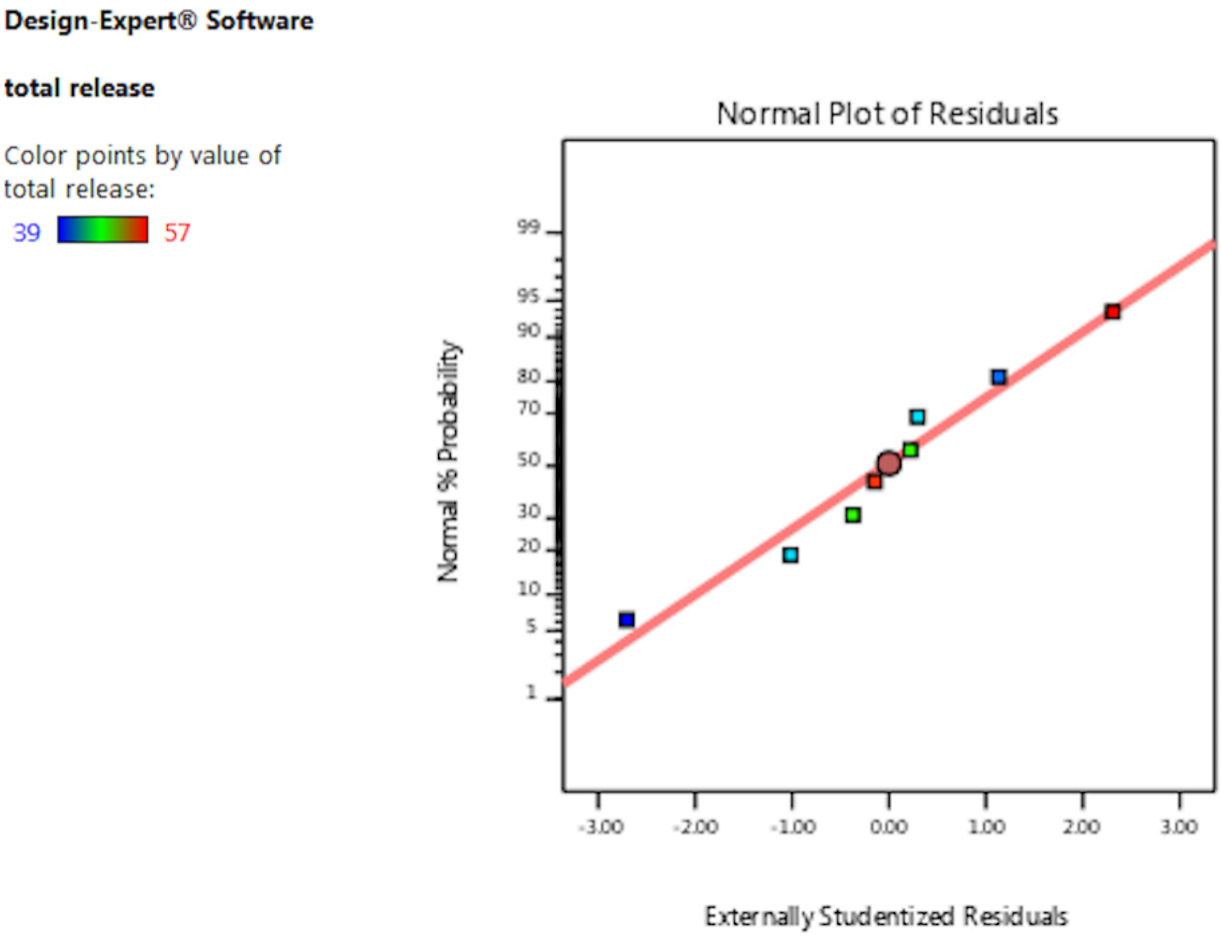

From the above plot, the residuals appear to be normal, as they mainly coincide on the line or in close proximity to it, without major deviations.

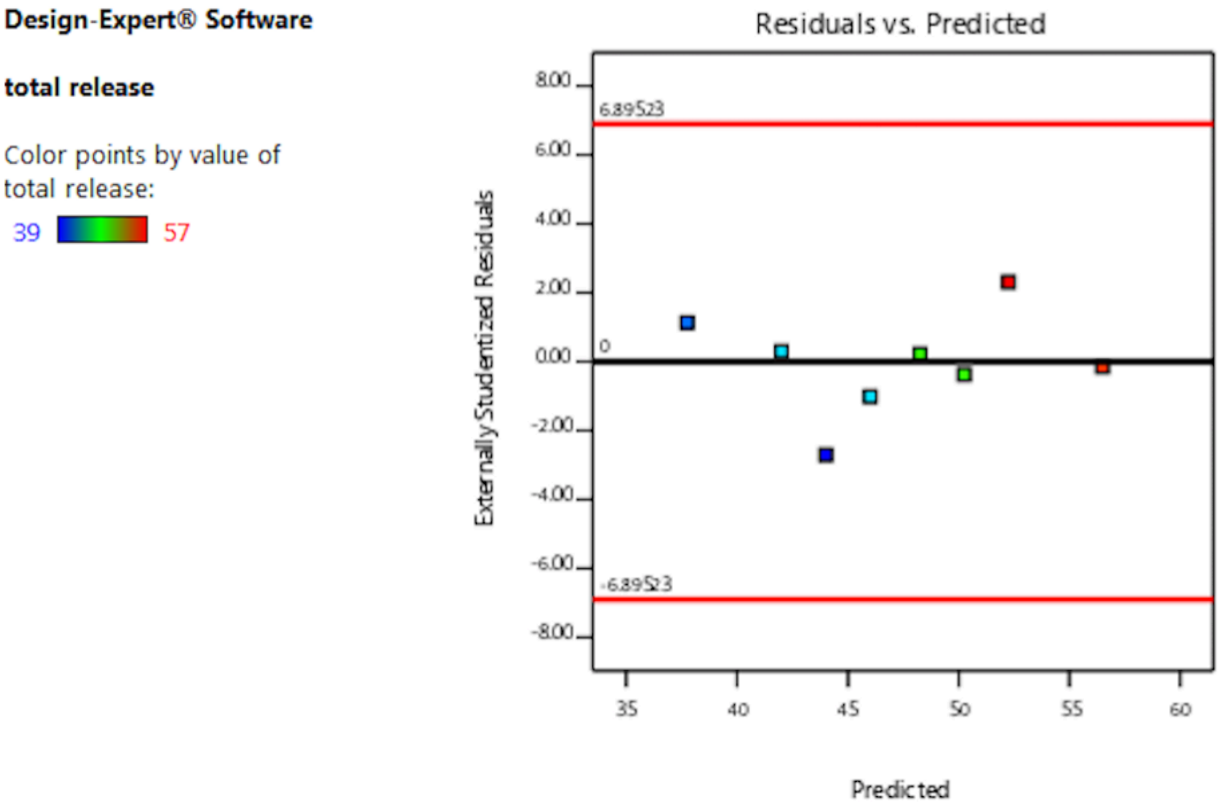

From the above plot of residuals versus predicted, the values lie between the two red lines, indicating homoscedasticity, or constant variance among residuals.

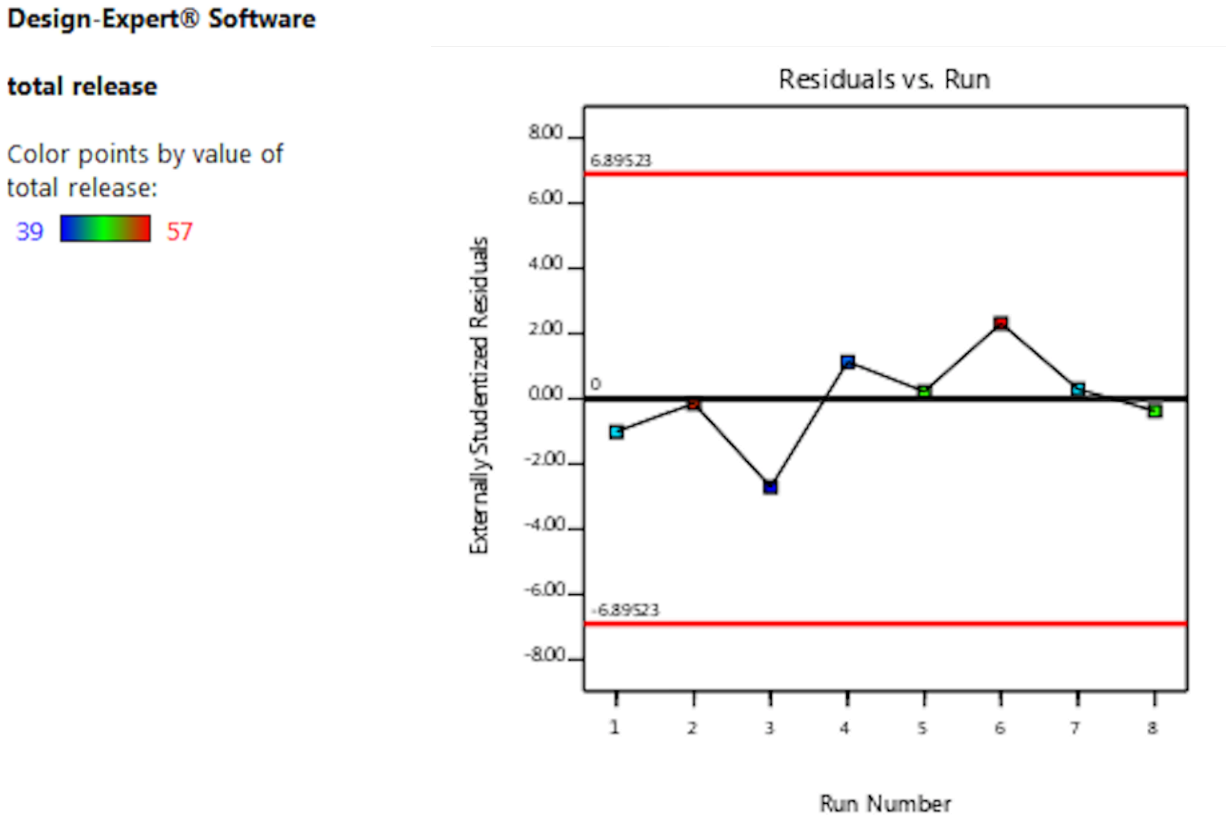

From above plot of residuals vs run, they appear randomly distributed and independent.

Appendix C
HPLC Chromatograms

Chromatograms of *in-vitro* release for T1:

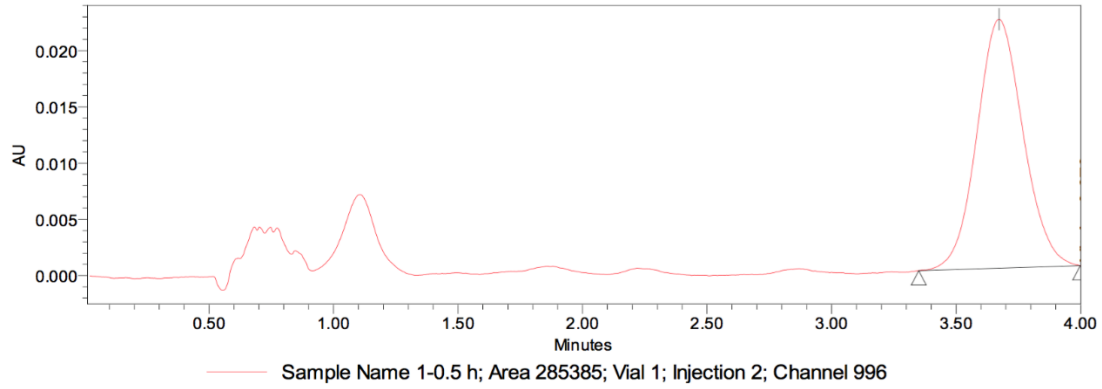

Sample Name 1-0.5 h; Area 285385; Vial 1; Injection 2; Channel 996

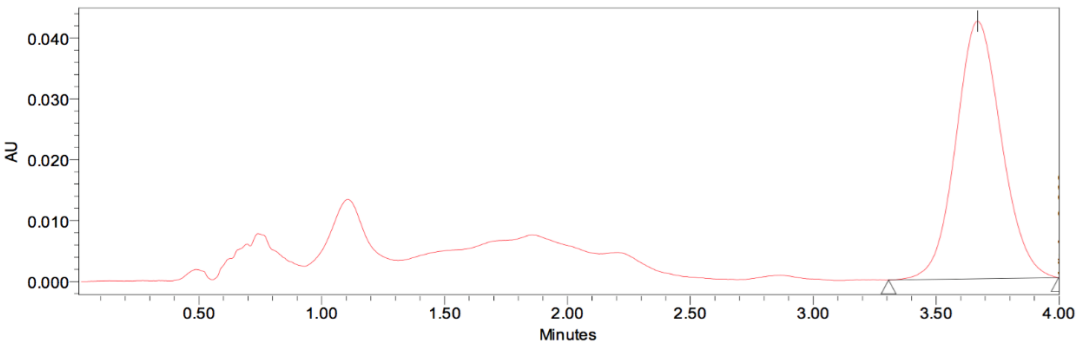

Sample Name 1-1 h; Area 546245; Vial 2; Injection 1; Channel 996

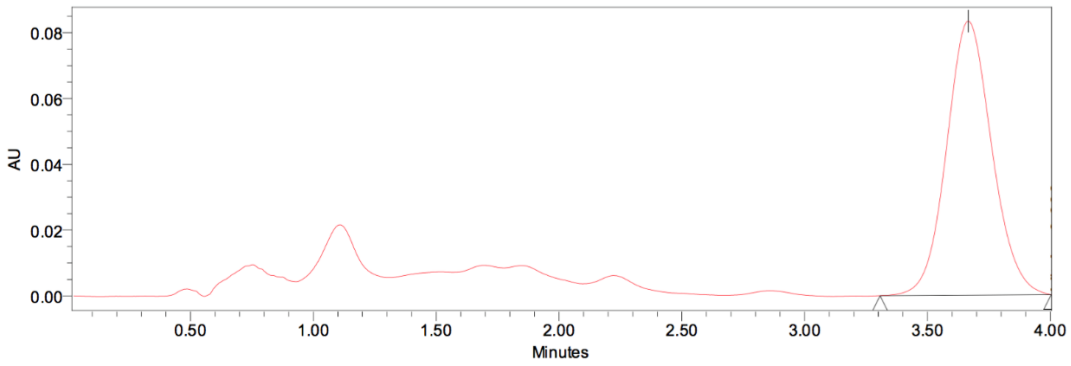

Sample Name 1-2 h; Area 1068236; Vial 3; Injection 1; Channel 996

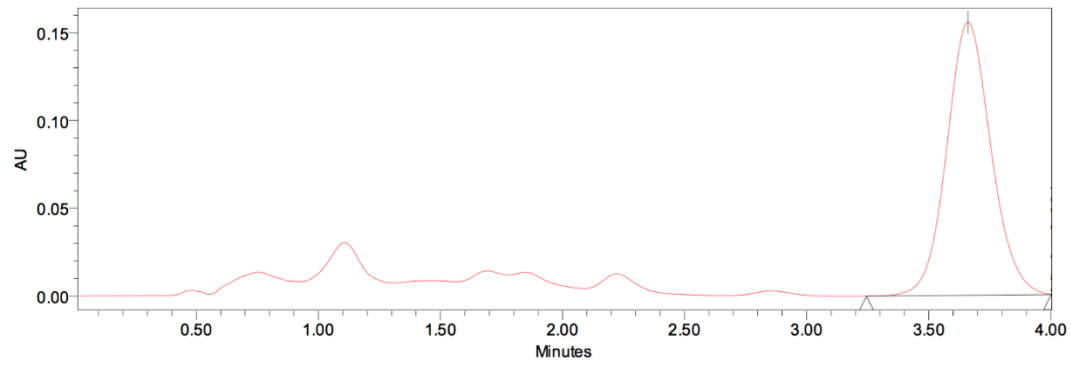

Sample Name 1-4 h; Area 1965592; Vial 4; Injection 1; Channel 996

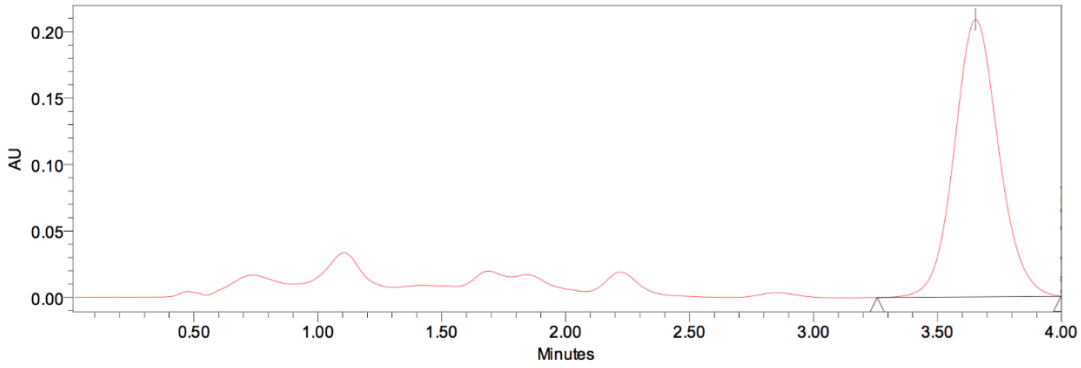

Sample Name 1-6 h; Area 2600969; Vial 5; Injection 2; Channel 996

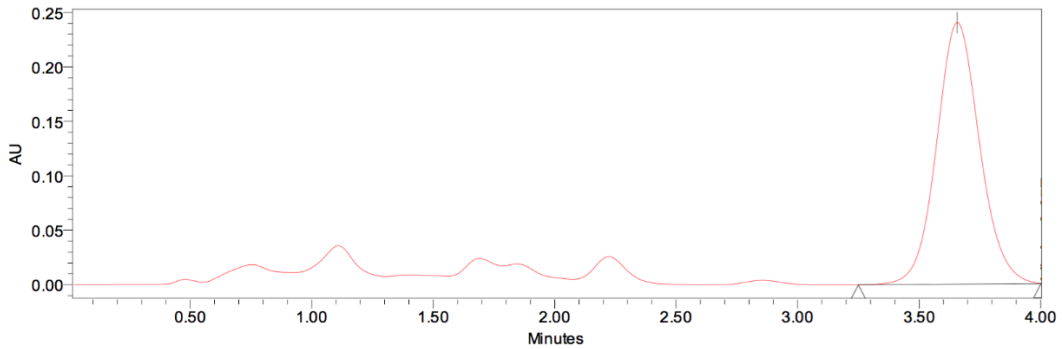

Sample Name 1-8 h; Area 2963686; Vial 6; Injection 1; Channel 996

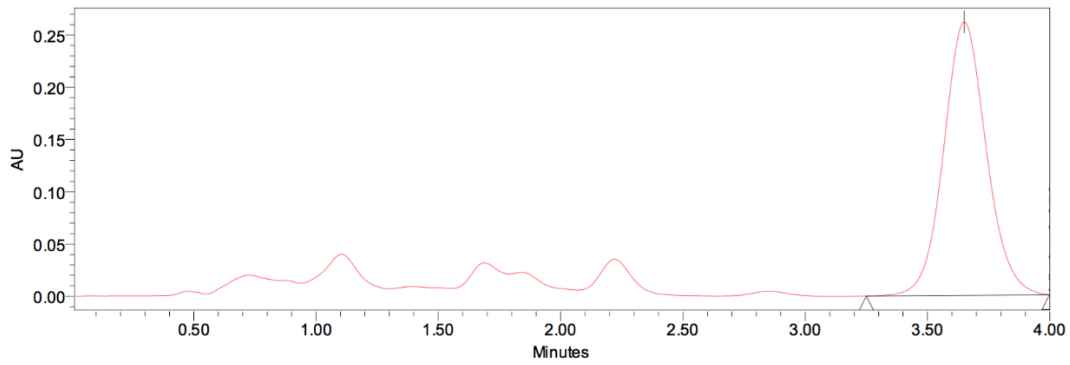

Sample Name 1-12 h; Area 3177632; Vial 7; Injection 2; Channel 996

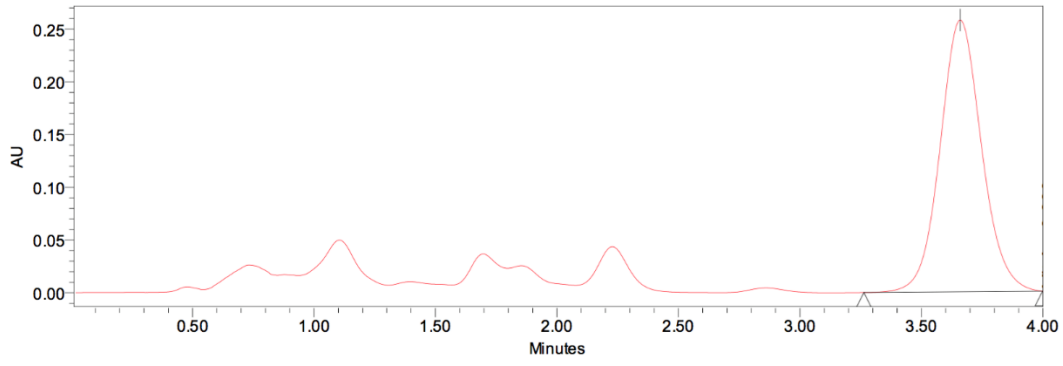

Sample Name 1-24 h; Area 3063099; Vial 8; Injection 1; Channel 996

Chromatograms of *in-vitro* release for T2:

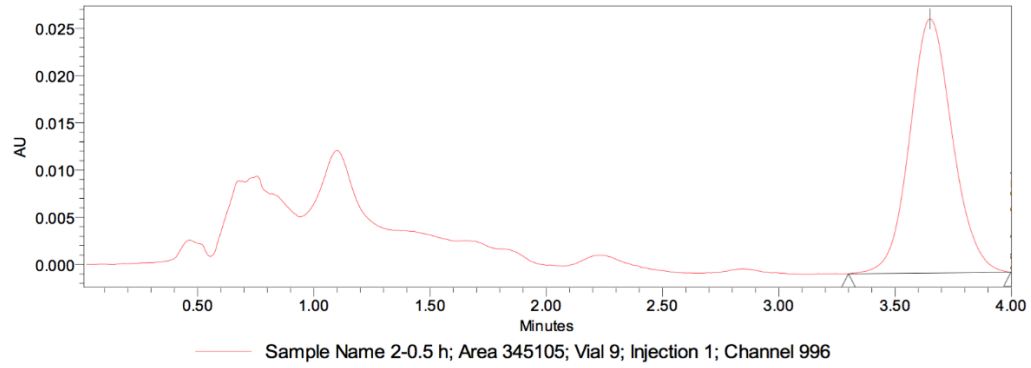

Sample Name 2-0.5 h; Area 345105; Vial 9; Injection 1; Channel 996

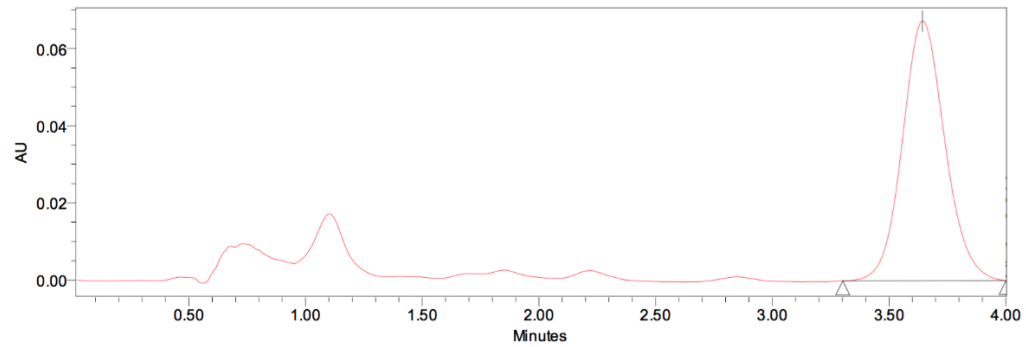

Sample Name 2-1 h; Area 853214; Vial 10; Injection 1; Channel 996

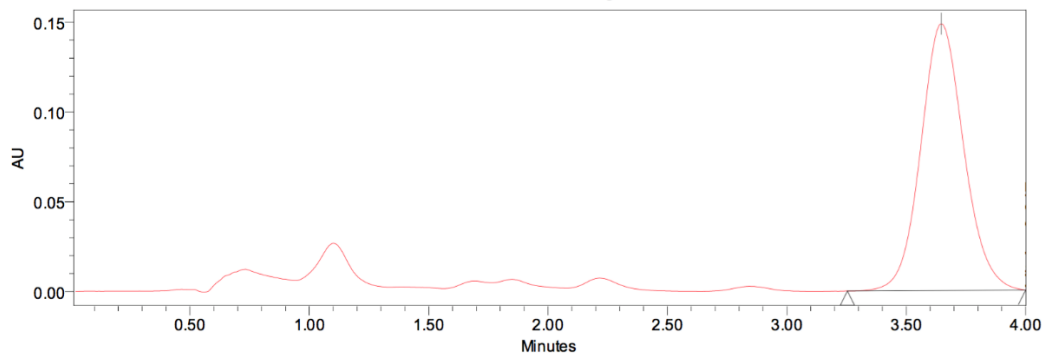

Sample Name 2-2 h; Area 1868164; Vial 11; Injection 1; Channel 996

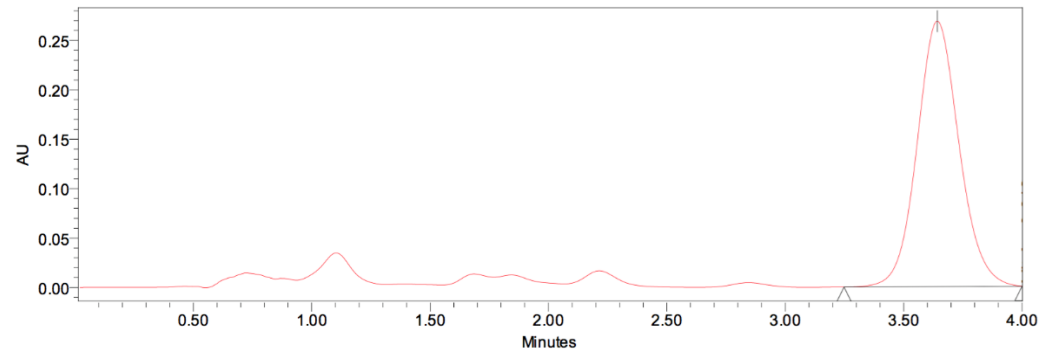

Sample Name 2-4 h; Area 3322598; Vial 12; Injection 1; Channel 996

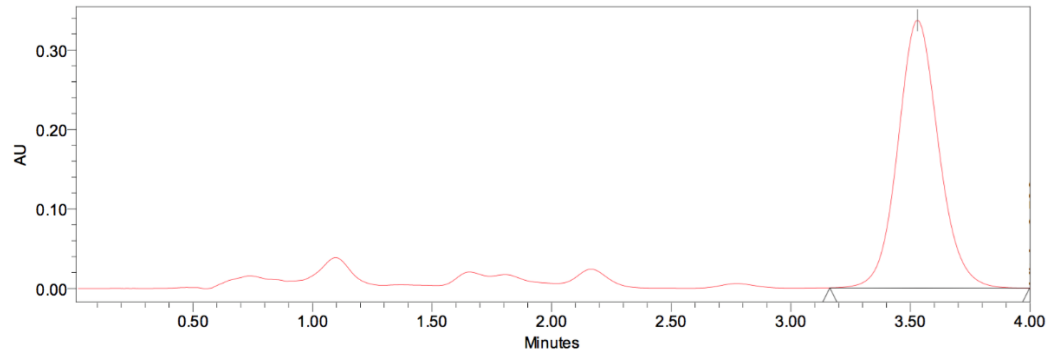

Sample Name 2-6 h; Area 4008678; Vial 13; Injection 1; Channel 996

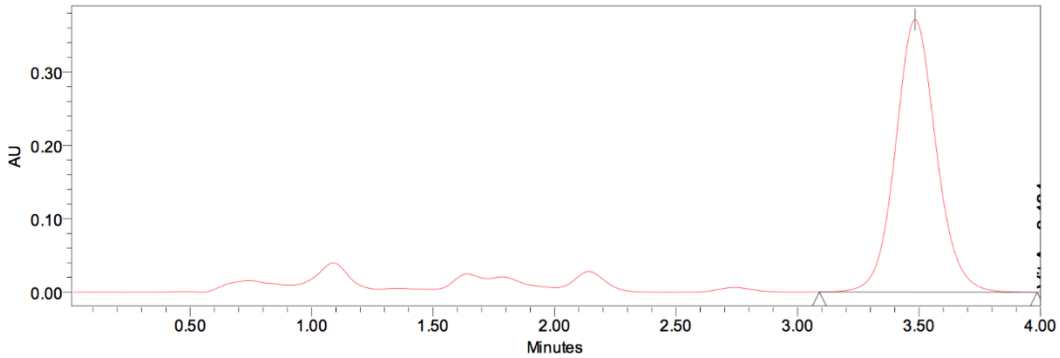

Sample Name 2-8 h; Area 4339845; Vial 14; Injection 1; Channel 996

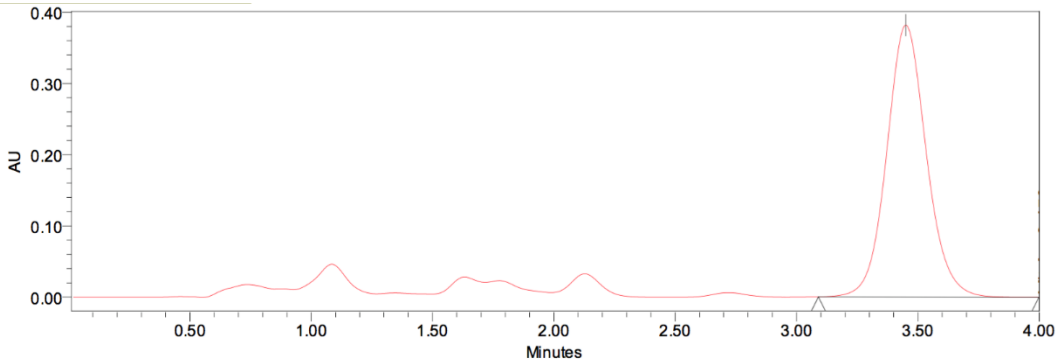

Sample Name 2-12 h; Area 4347266; Vial 15; Injection 2; Channel 996

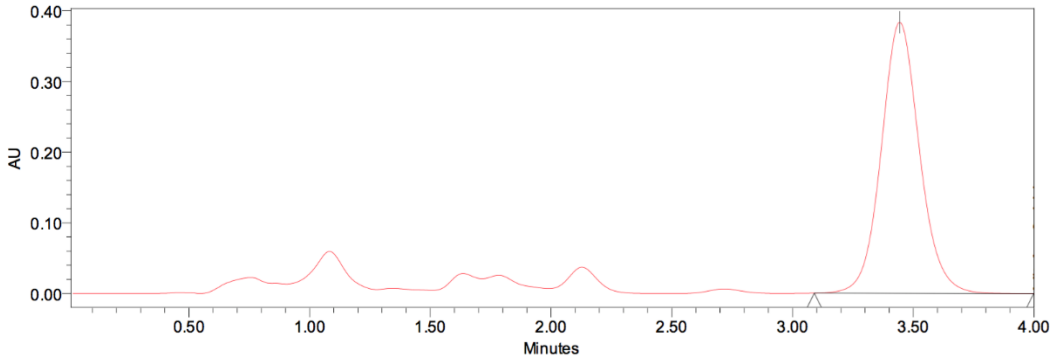

Sample Name 2-24 h; Area 4236294; Vial 16; Injection 2; Channel 996

Chromatograms of *in-vitro* release for T3:

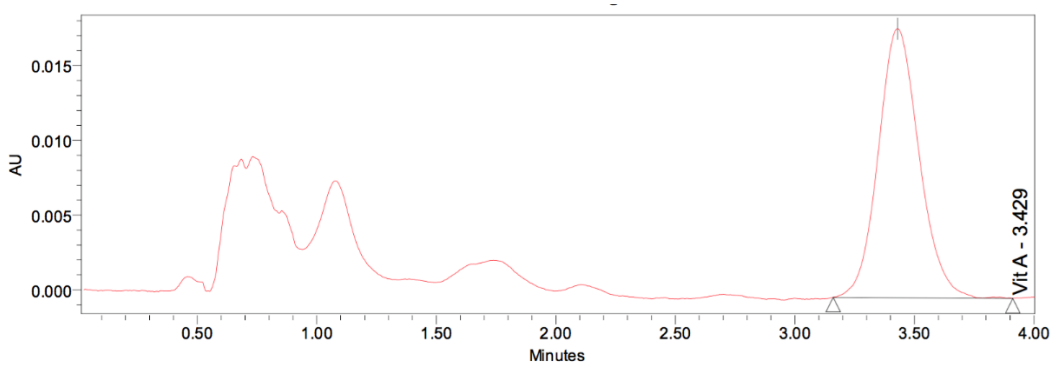

Sample Name 3-0.5 h; Area 214844; Vial 17; Injection 1; Channel 996

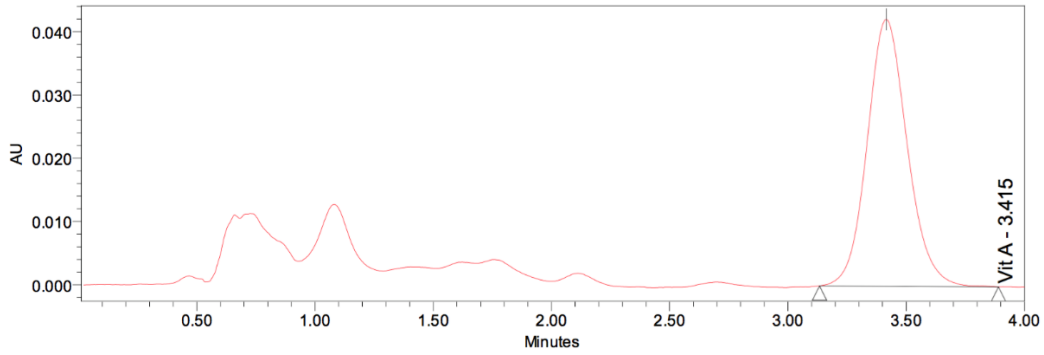

Sample Name 3-1 h; Area 497973; Vial 18; Injection 1; Channel 996

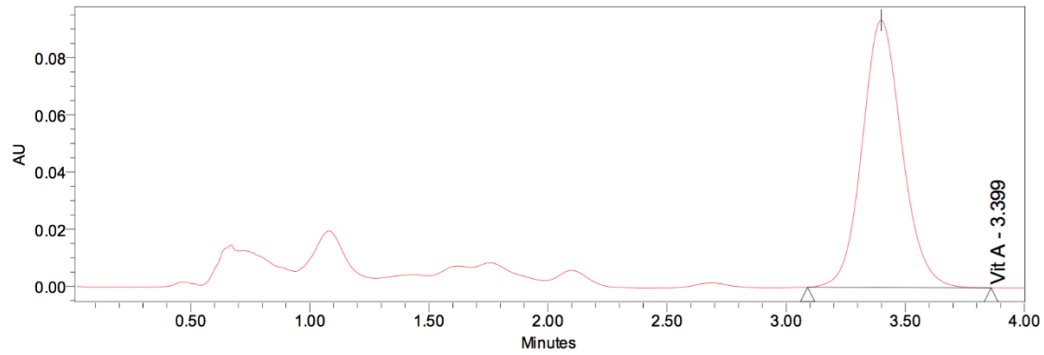

Sample Name 3-2 h; Area 1087708; Vial 19; Injection 1; Channel 996

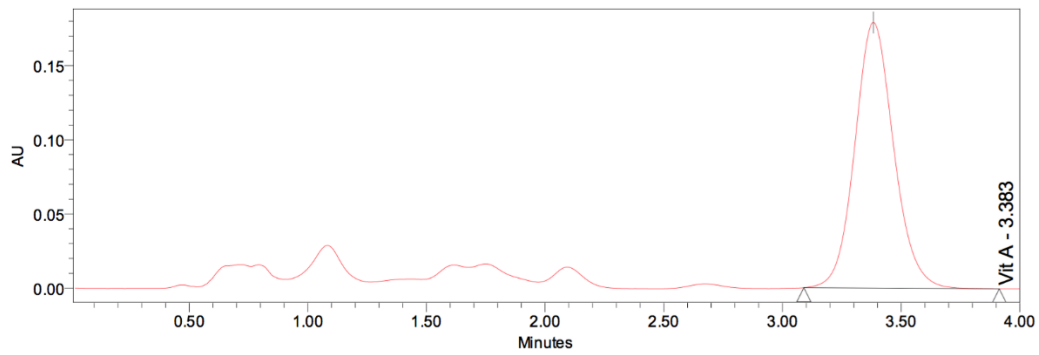

Sample Name 3-4 h; Area 2044036; Vial 20; Injection 2; Channel 996

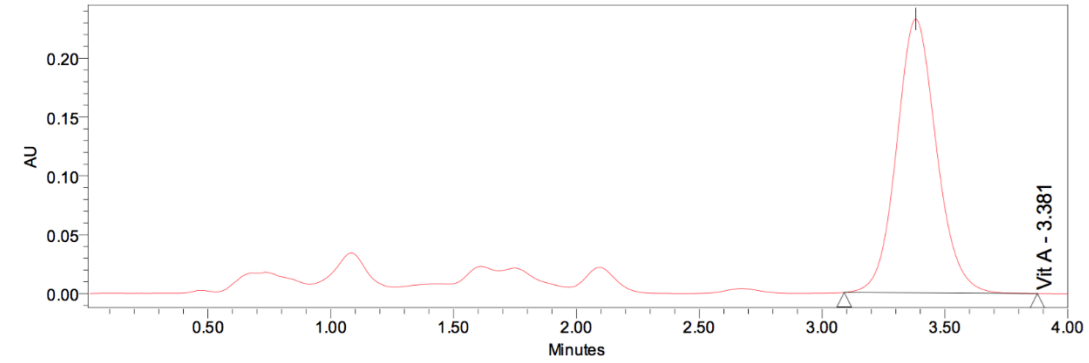

Sample Name 3-6 h; Area 2631036; Vial 21; Injection 1; Channel 996

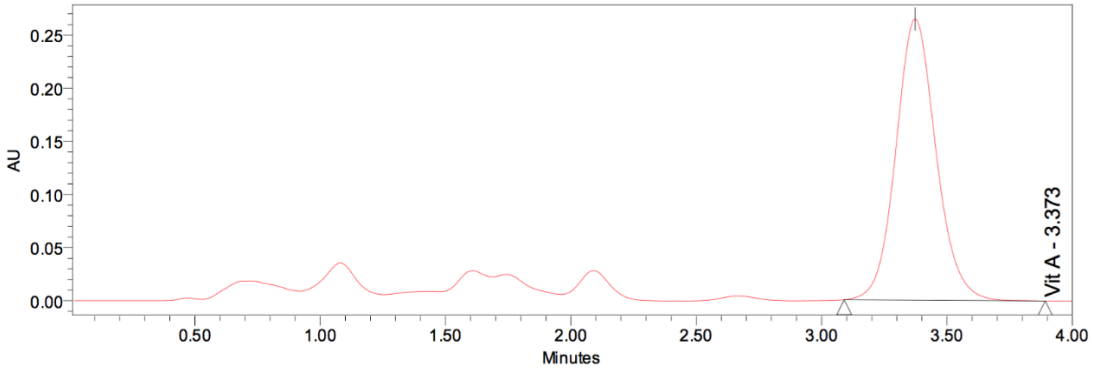

Sample Name 3-8 h; Area 2953857; Vial 22; Injection 1; Channel 996

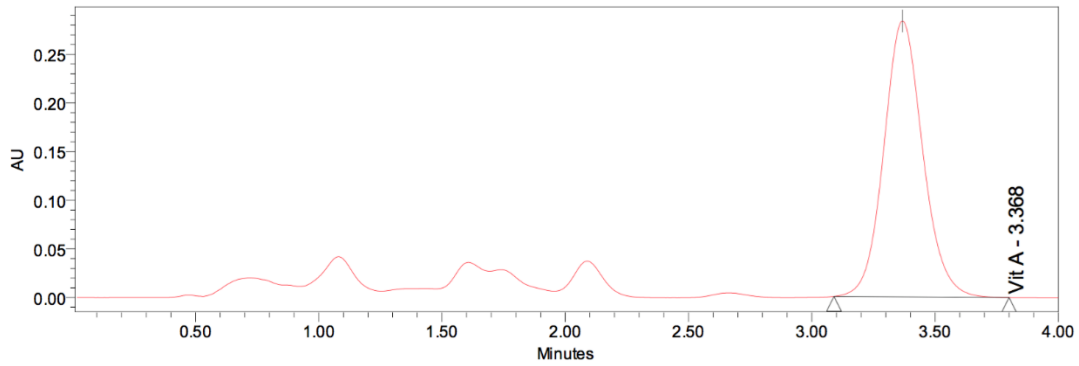

Sample Name 3-12 h; Area 3125081; Vial 23; Injection 2; Channel 996

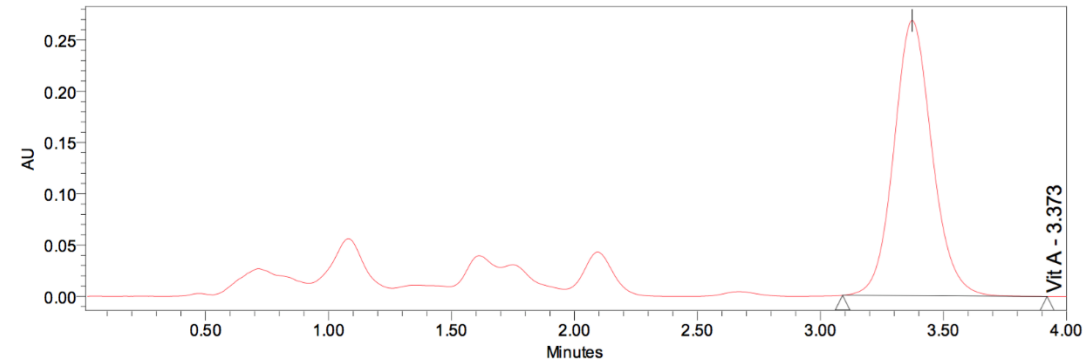

Sample Name 3-24 h; Area 2912207; Vial 24; Injection 1; Channel 996

Chromatograms of *in-vitro* release for T4:

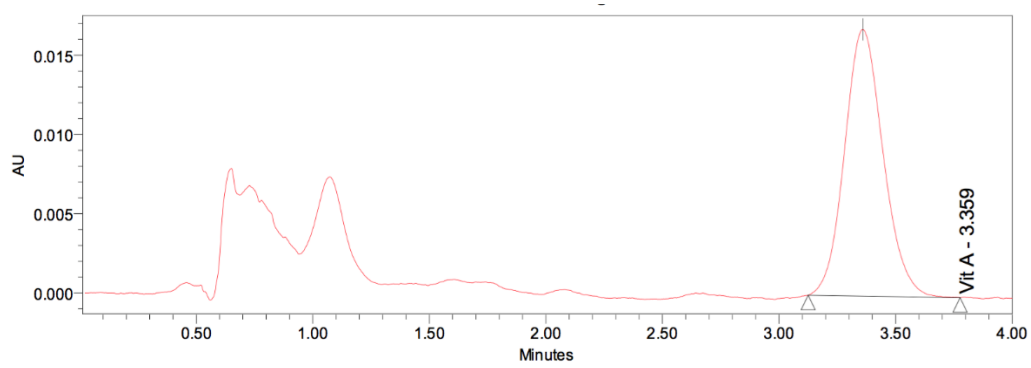

Sample Name 4-0.5 h; Area 194207; Vial 25; Injection 2; Channel 996

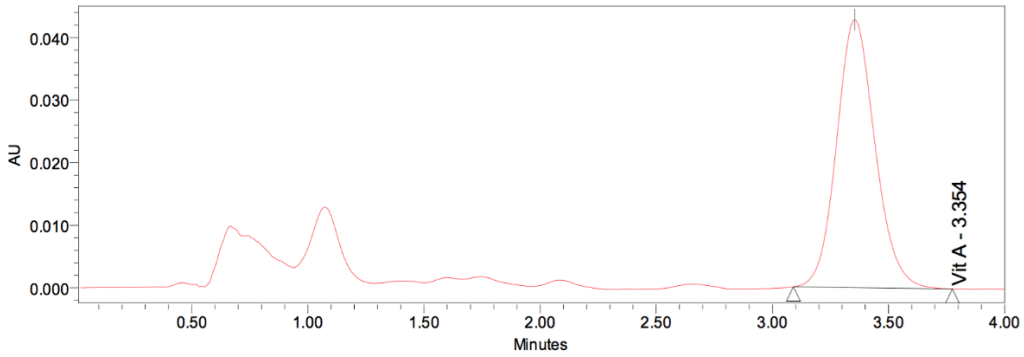

Sample Name 4-1 h; Area 493650; Vial 26; Injection 1; Channel 996

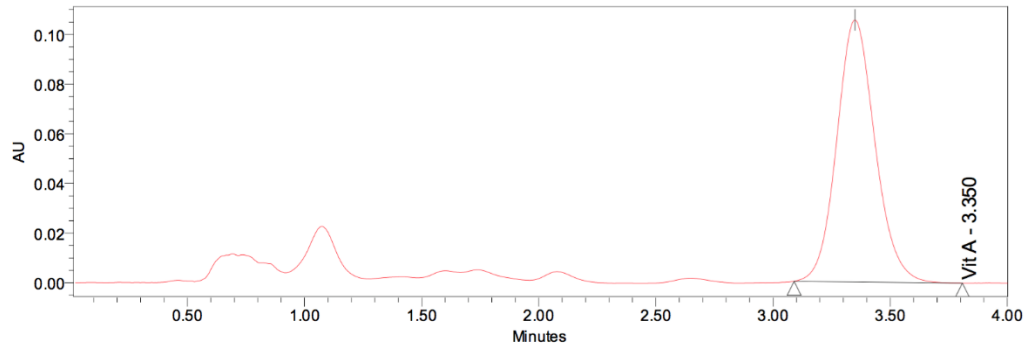

Sample Name 4-2 h; Area 1200479; Vial 27; Injection 1; Channel 996

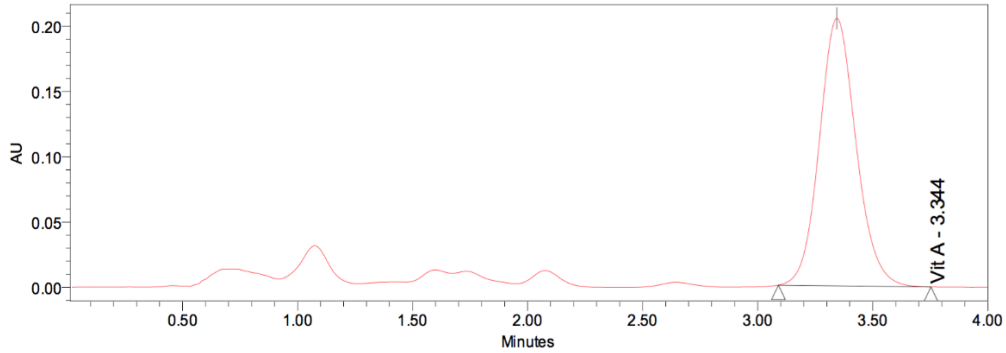

Sample Name 4-4 h; Area 2277999; Vial 28; Injection 1; Channel 996

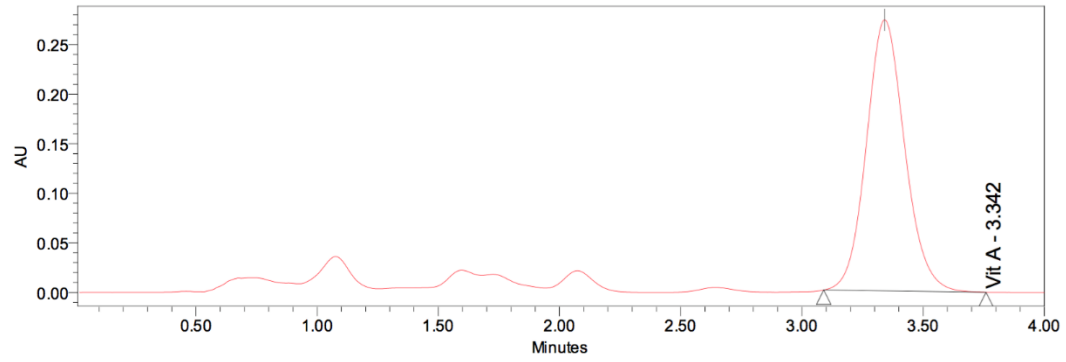

Sample Name 4-6 h; Area 3018530; Vial 29; Injection 2; Channel 996

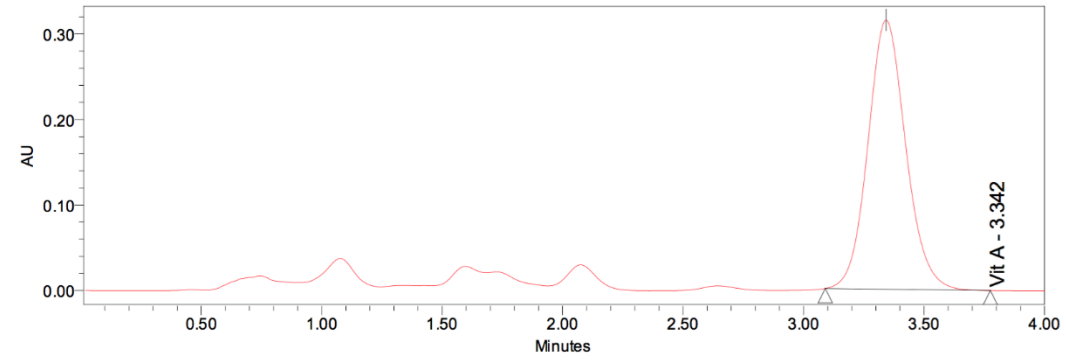

Sample Name 4-8 h; Area 3443226; Vial 30; Injection 1; Channel 996

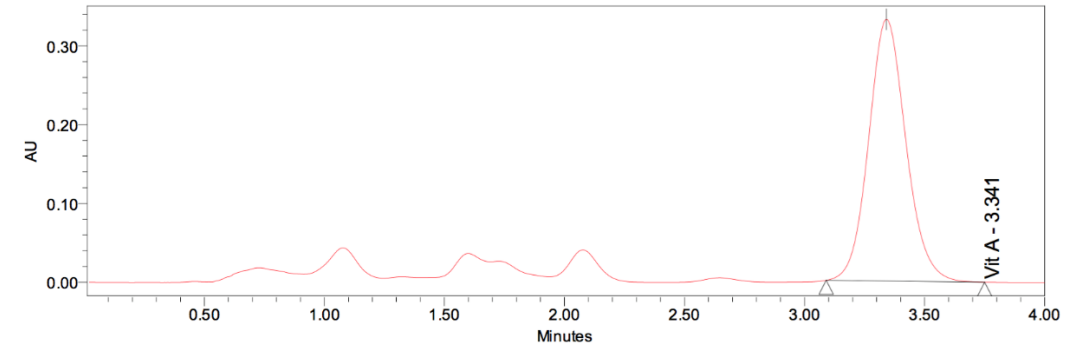

Sample Name 4-12 h; Area 3597642; Vial 31; Injection 2; Channel 996

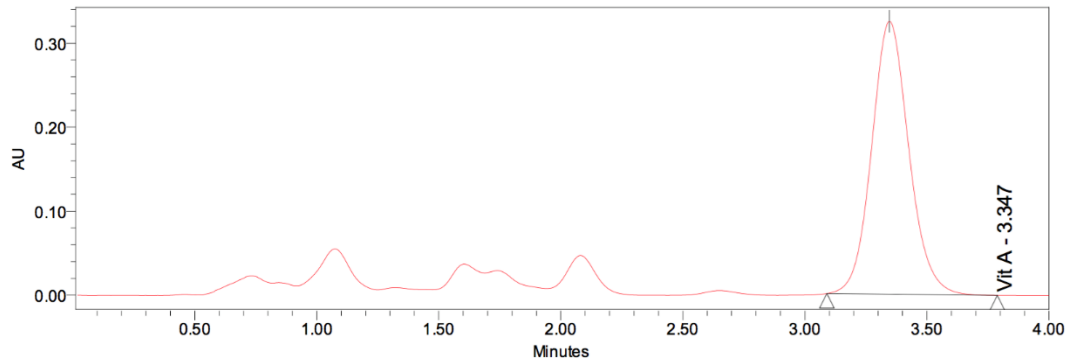

Sample Name 4-24 h; Area 3454338; Vial 32; Injection 1; Channel 996

Chromatograms of *in-vitro* release for T5:

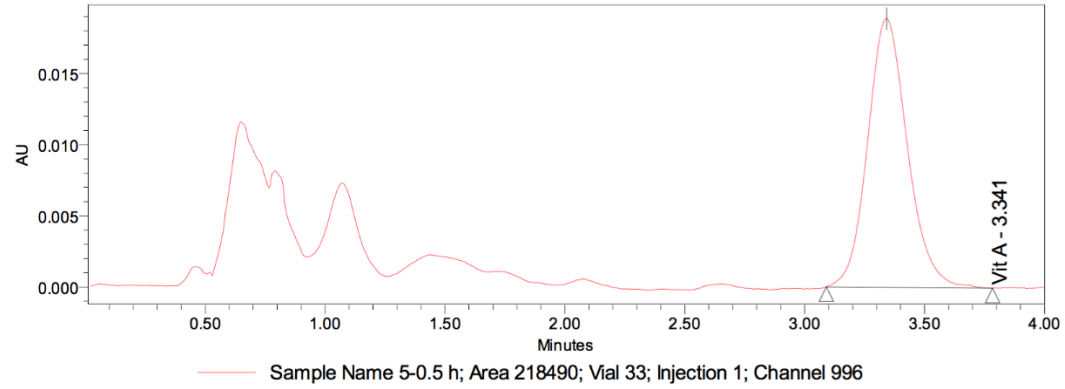

Sample Name 5-0.5 h; Area 218490; Vial 33; Injection 1; Channel 996

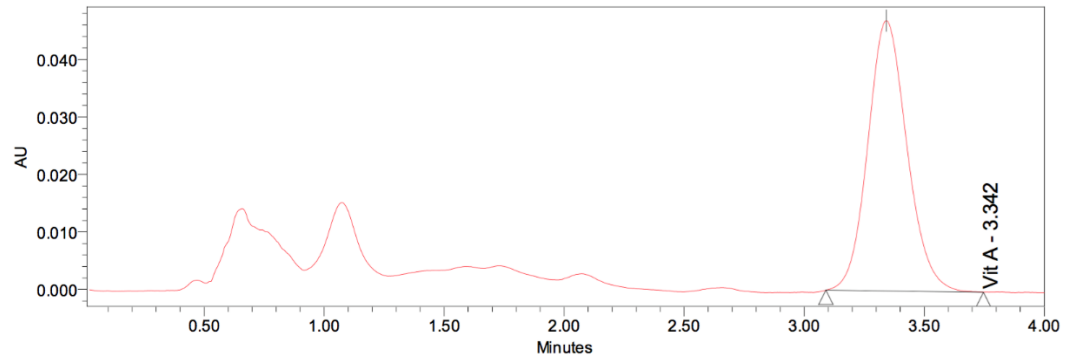

Sample Name 5-1 h; Area 534535; Vial 34; Injection 2; Channel 996

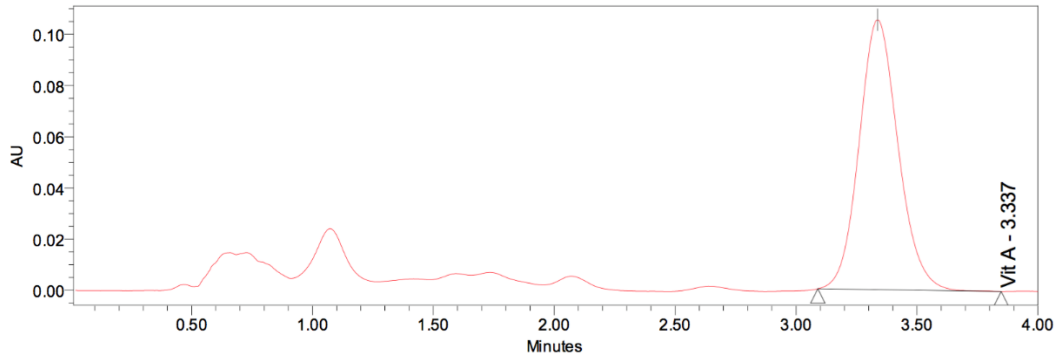

Sample Name 5-2 h; Area 1184074; Vial 35; Injection 1; Channel 996

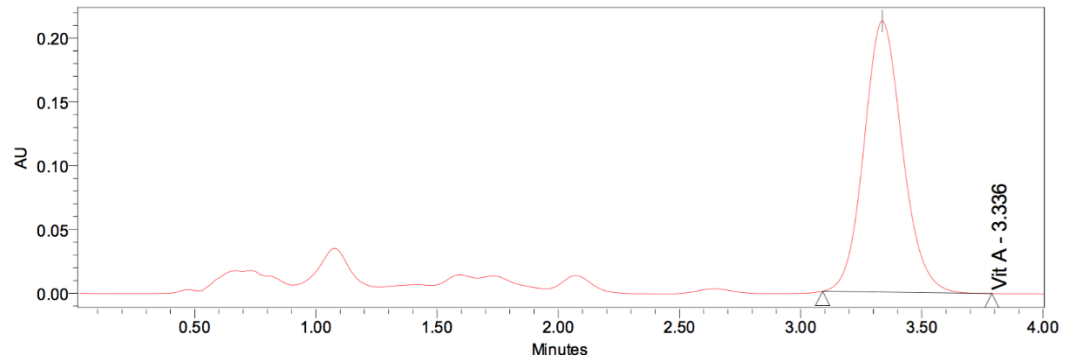

Sample Name 5-4 h; Area 2344073; Vial 36; Injection 1; Channel 996

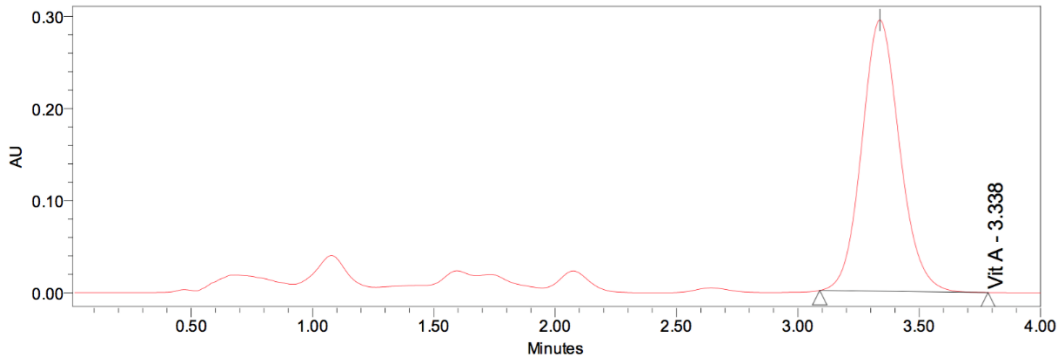

Sample Name 5-6 h; Area 3207213; Vial 37; Injection 2; Channel 996

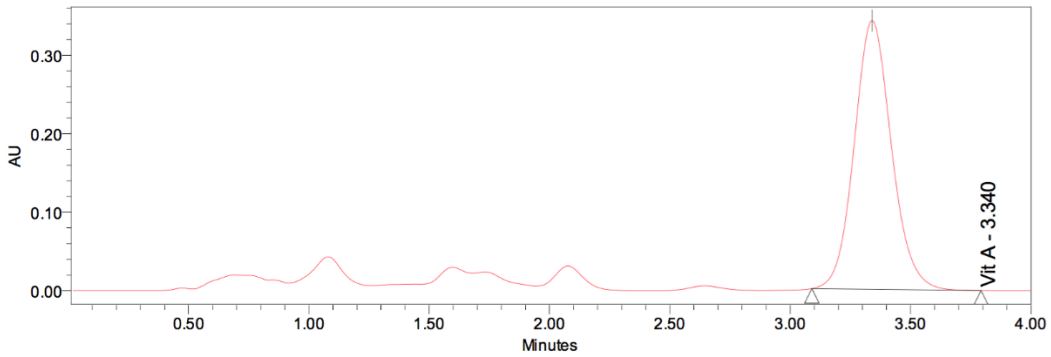

Sample Name 5-8 h; Area 3692295; Vial 38; Injection 2; Channel 996

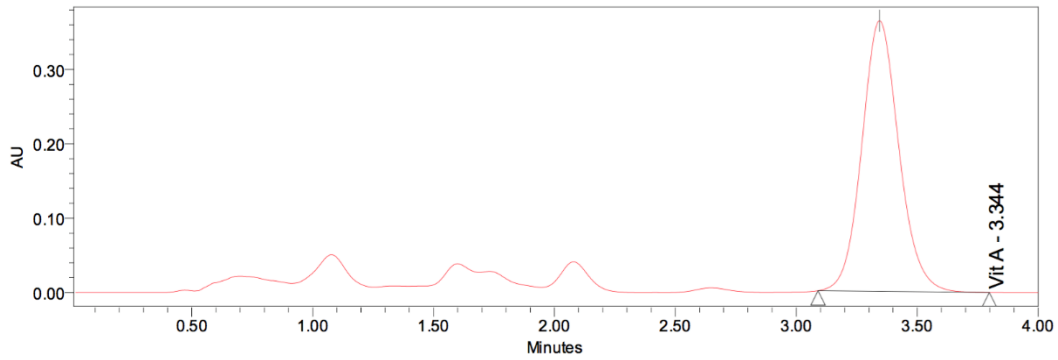

Sample Name 5-12 h; Area 3890519; Vial 39; Injection 2; Channel 996

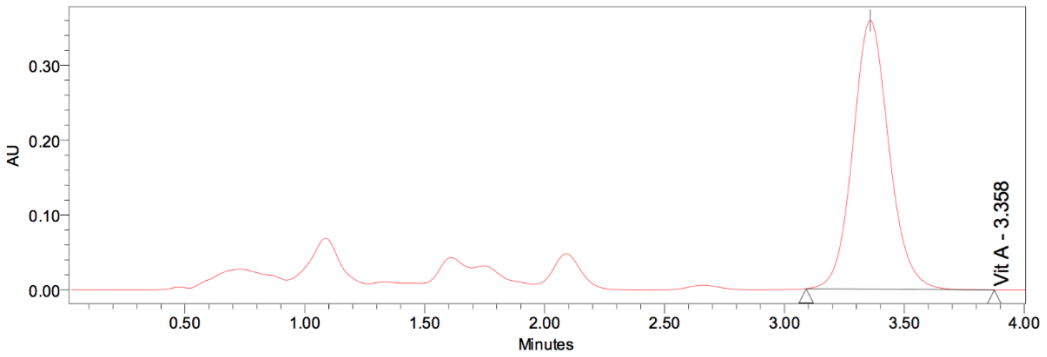

Sample Name 5-24 h; Area 3767237; Vial 40; Injection 2; Channel 996

Chromatograms of *in-vitro* release for T6:

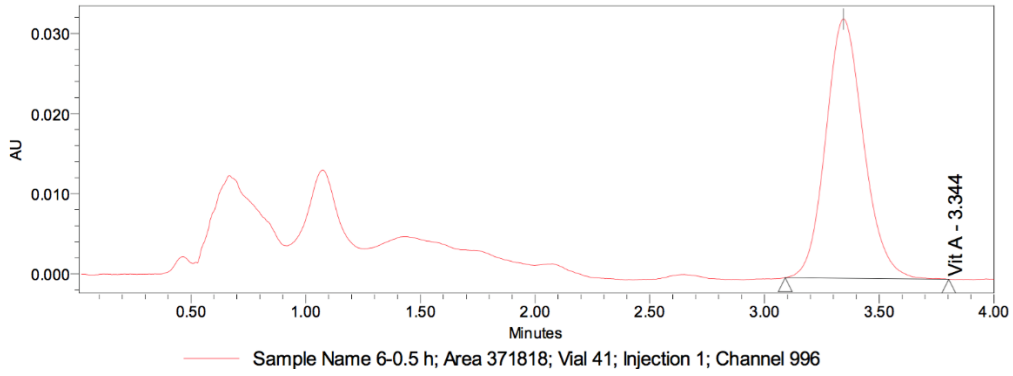

Sample Name 6-0.5 h; Area 371818; Vial 41; Injection 1; Channel 996

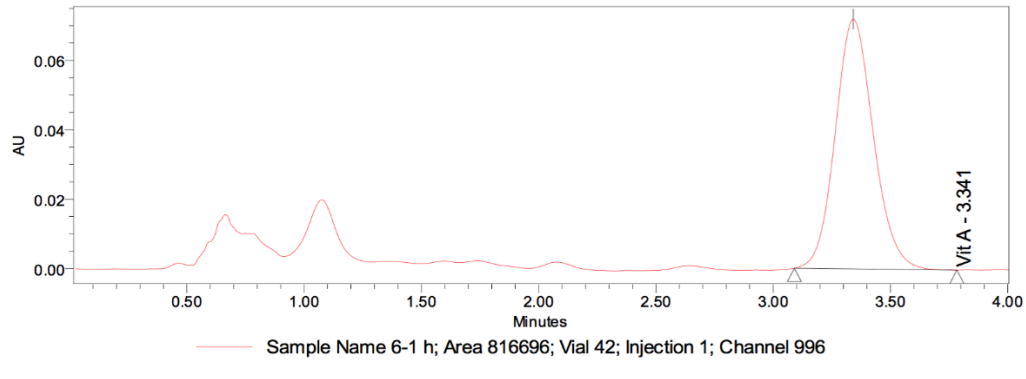

Sample Name 6-1 h; Area 816696; Vial 42; Injection 1; Channel 996

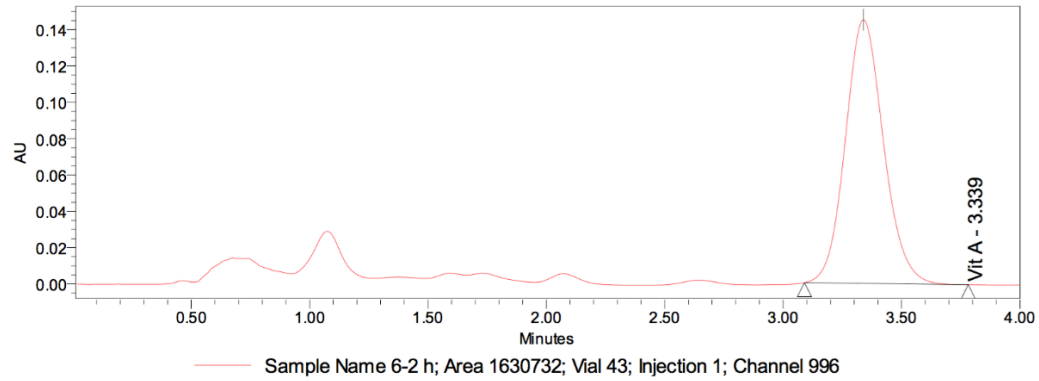

Sample Name 6-2 h; Area 1630732; Vial 43; Injection 1; Channel 996

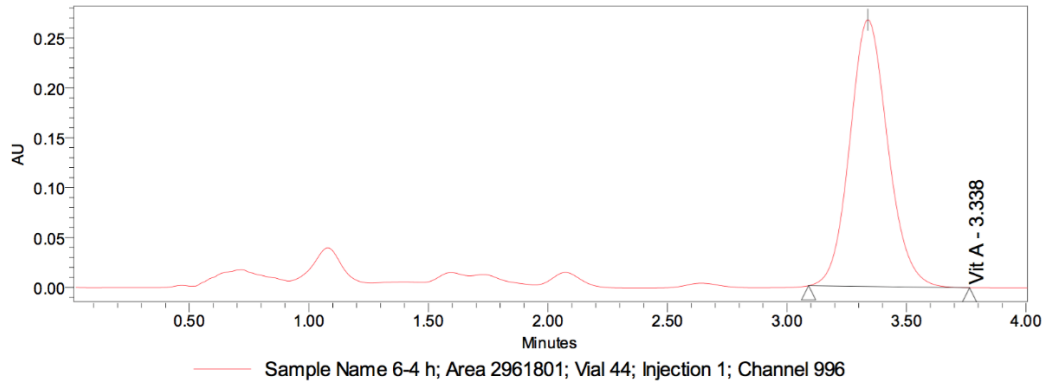

Sample Name 6-4 h; Area 2961801; Vial 44; Injection 1; Channel 996

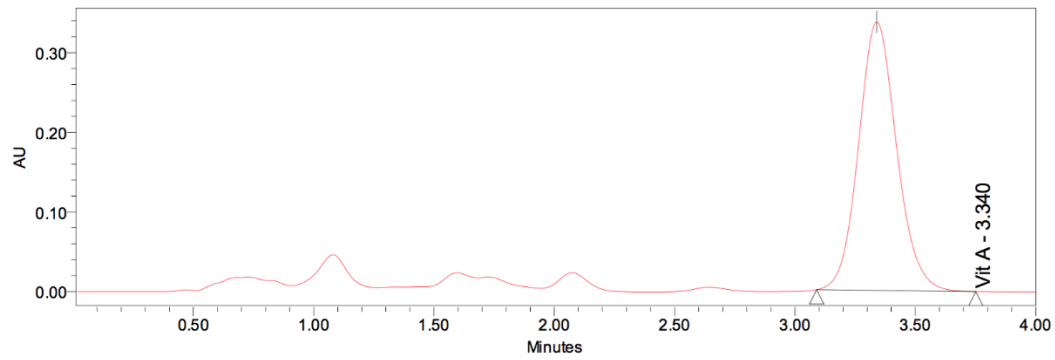

Sample Name 6-6 h; Area 3712987; Vial 45; Injection 2; Channel 996

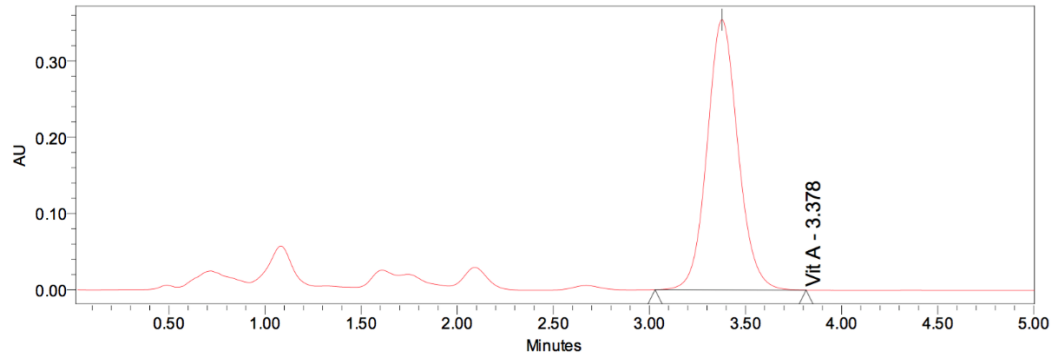

Sample Name 6-8 h; Area 3969593; Vial 46; Injection 2; Channel 996

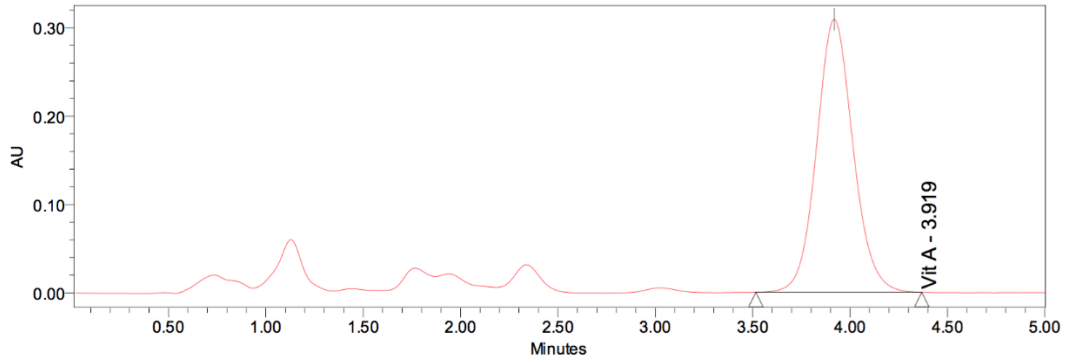

Sample Name 6-12 h; Area 4039689; Vial 47; Injection 2; Channel 996

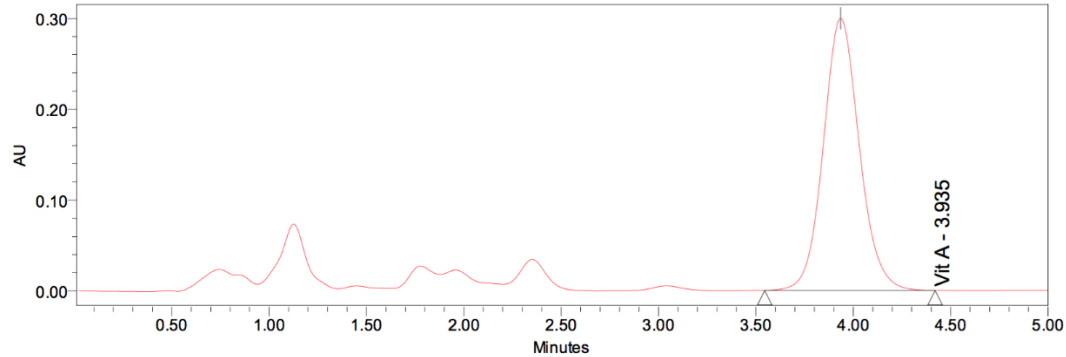

Sample Name 6-24 h; Area 3860786; Vial 48; Injection 1; Channel 996

Chromatograms of *in-vitro* release for T7:

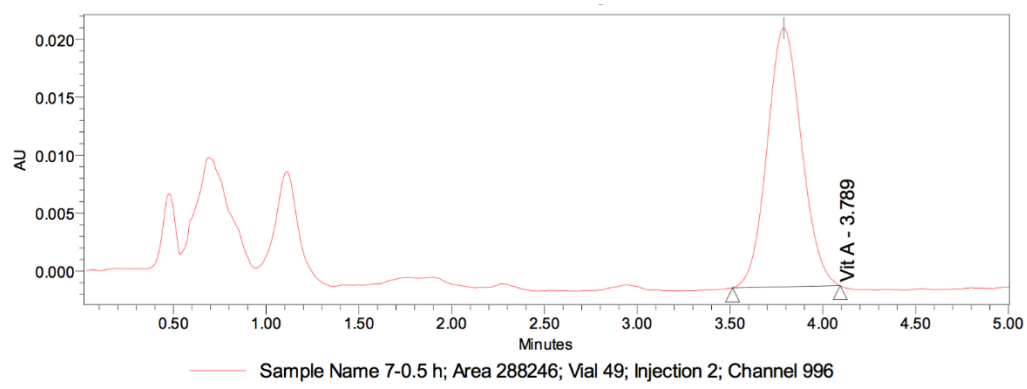

Sample Name 7-0.5 h; Area 288246; Vial 49; Injection 2; Channel 996

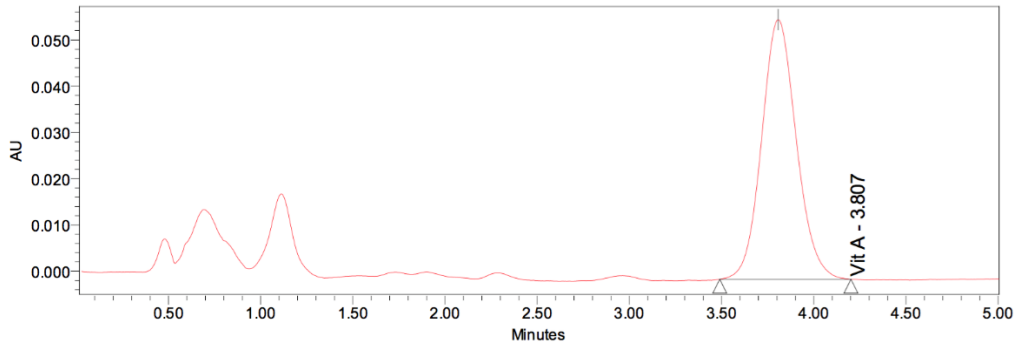

Sample Name 7-1 h; Area 734654; Vial 50; Injection 1; Channel 996

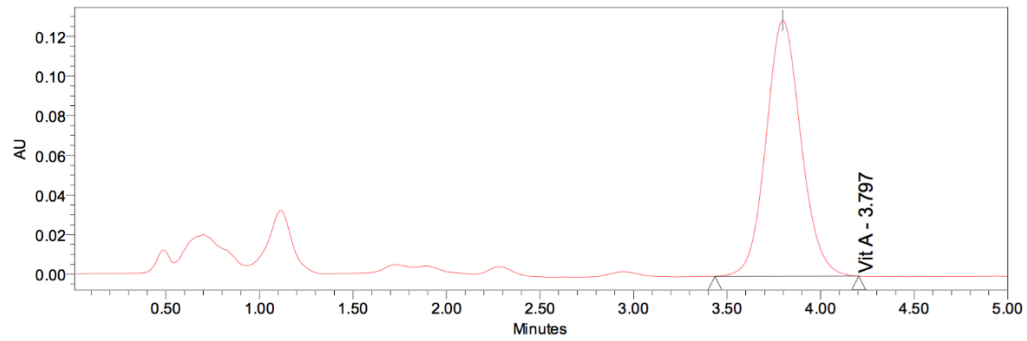

Sample Name 7-2 h; Area 1677455; Vial 51; Injection 2; Channel 996

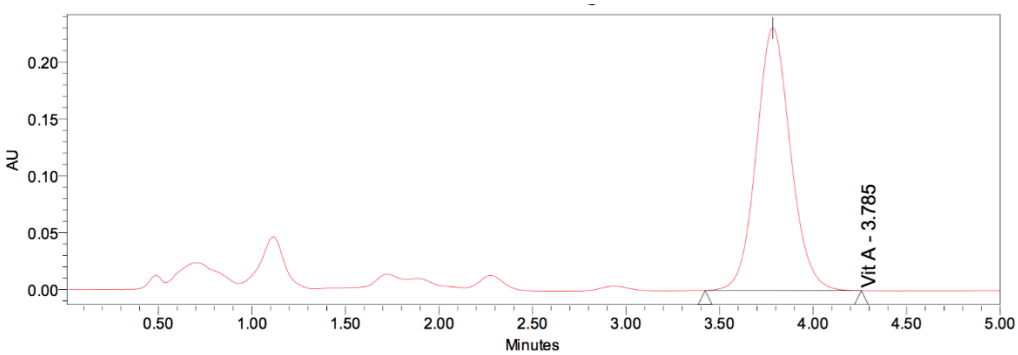

Sample Name 7-4 h; Area 2942433; Vial 52; Injection 2; Channel 996

Chromatograms of *in-vitro* release for T8:

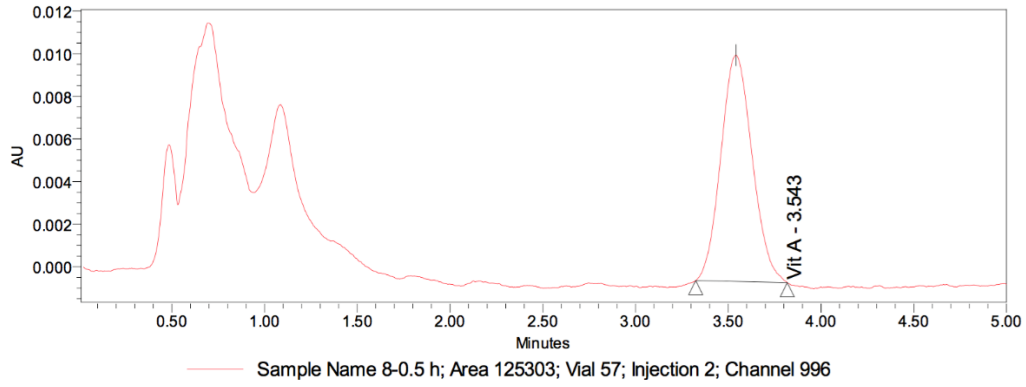

Sample Name 8-0.5 h; Area 125303; Vial 57; Injection 2; Channel 996

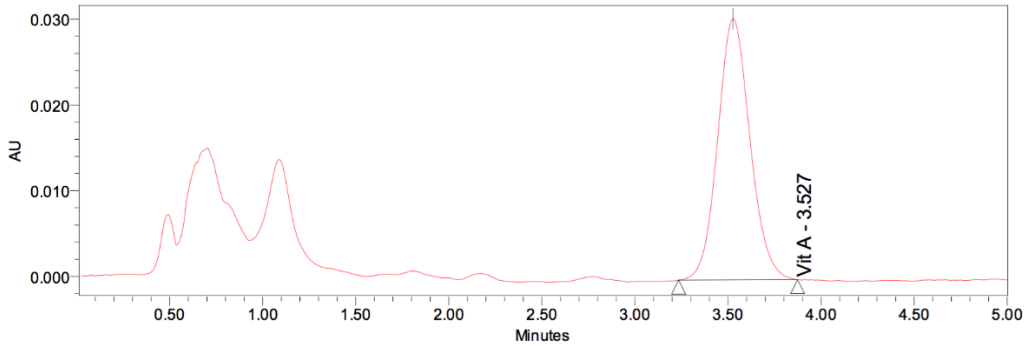

Sample Name 8-1 h; Area 368463; Vial 58; Injection 1; Channel 996

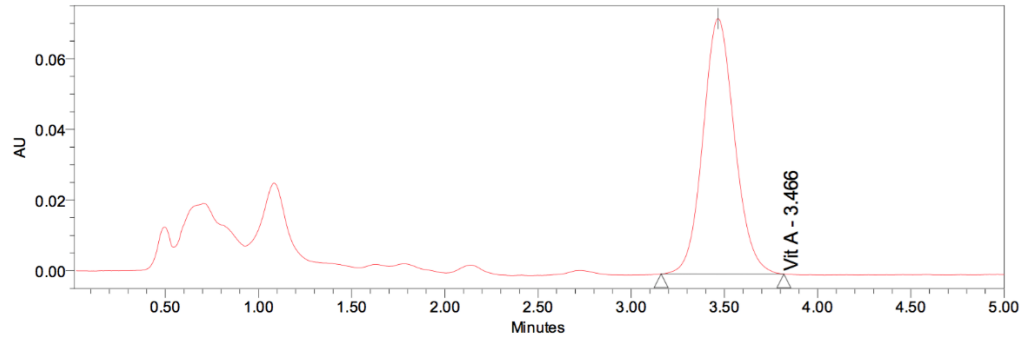

Sample Name 8-2 h; Area 855130; Vial 59; Injection 2; Channel 996

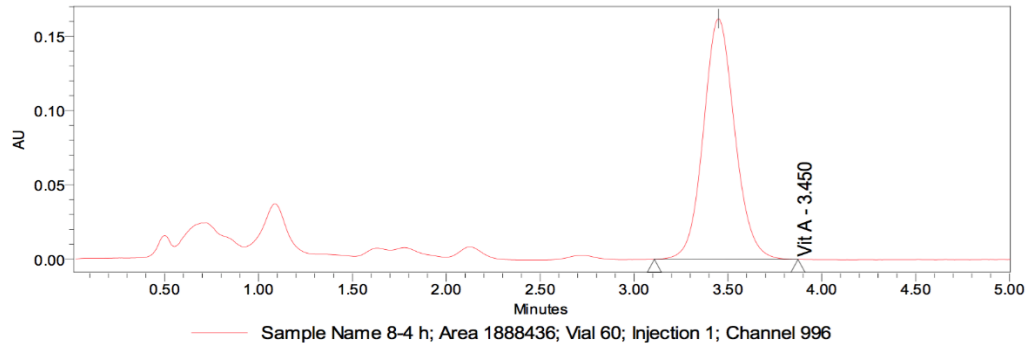

Sample Name 8-4 h; Area 1888436; Vial 60; Injection 1; Channel 996

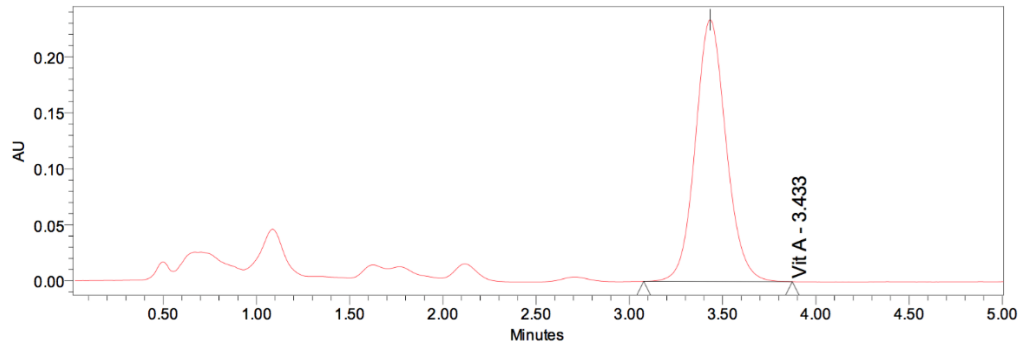

Sample Name 8-6 h; Area 2688460; Vial 61; Injection 1; Channel 996

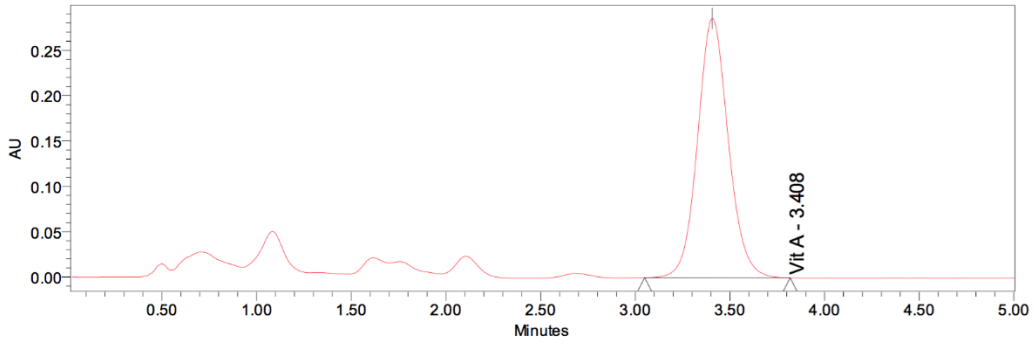

Sample Name 8-8 h; Area 3233850; Vial 62; Injection 2; Channel 996

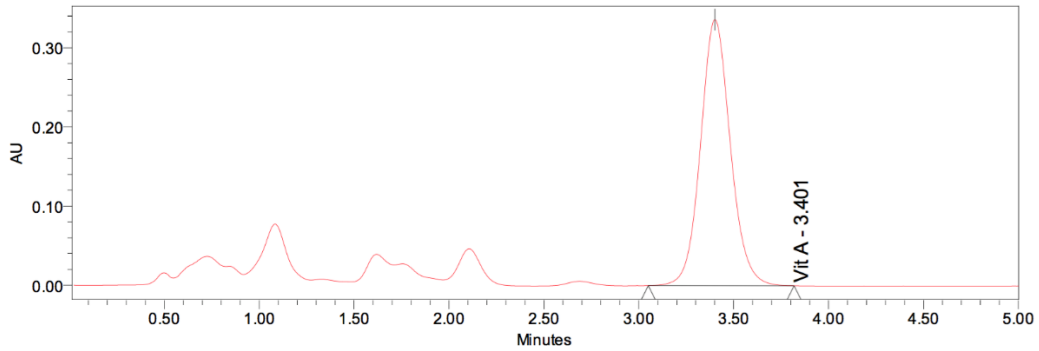

Sample Name 8-12 h; Area 3676033; Vial 64; Injection 1; Channel 996

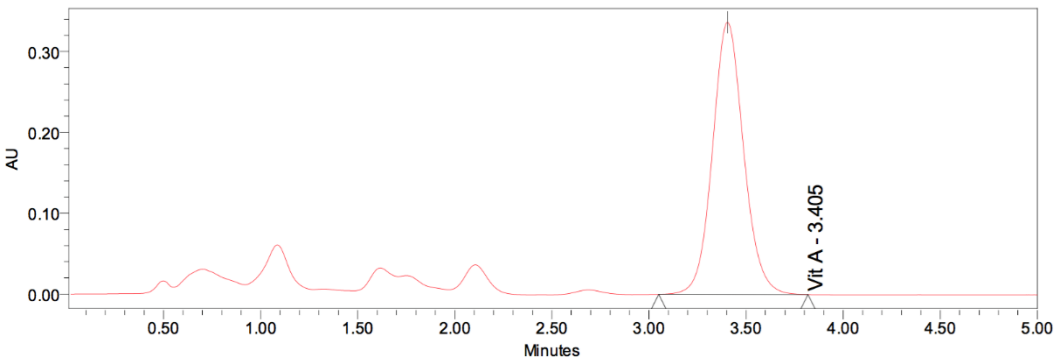

Sample Name 8-12 h; Area 3758566; Vial 63; Injection 1; Channel 996

Chromatograms of *Ex-Vivo* Permeation for T2:

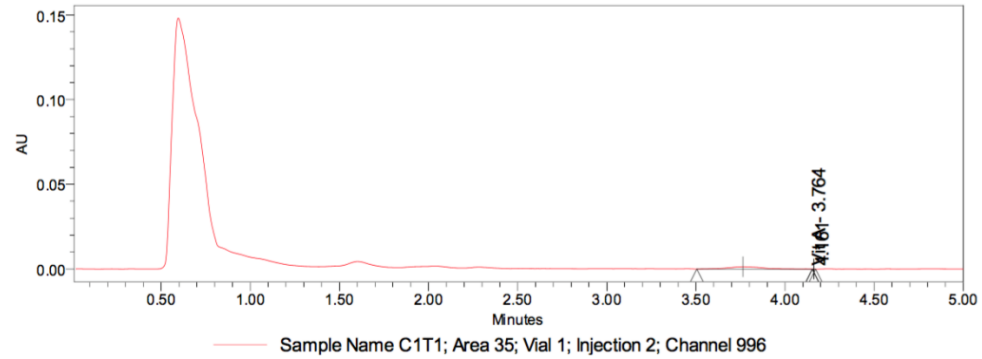

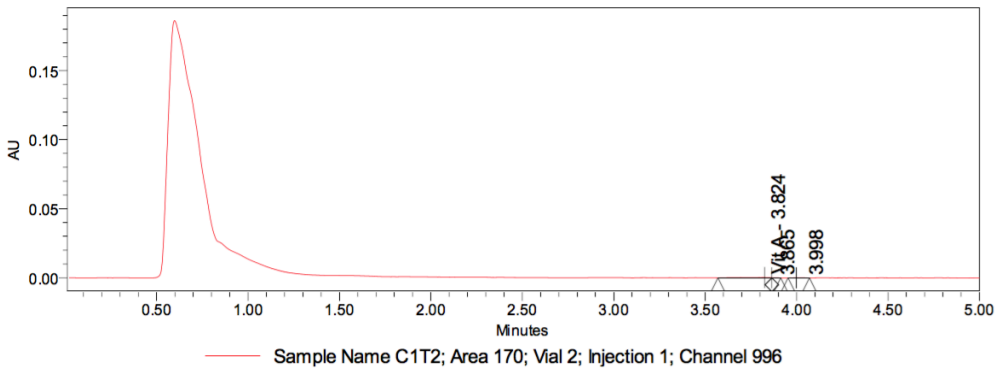

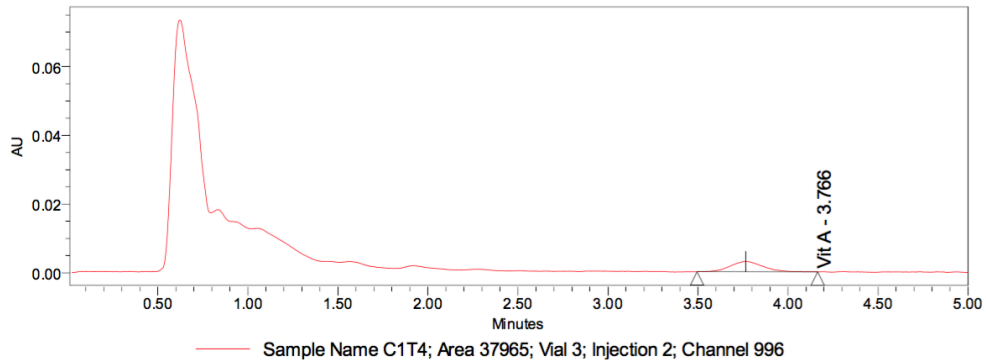

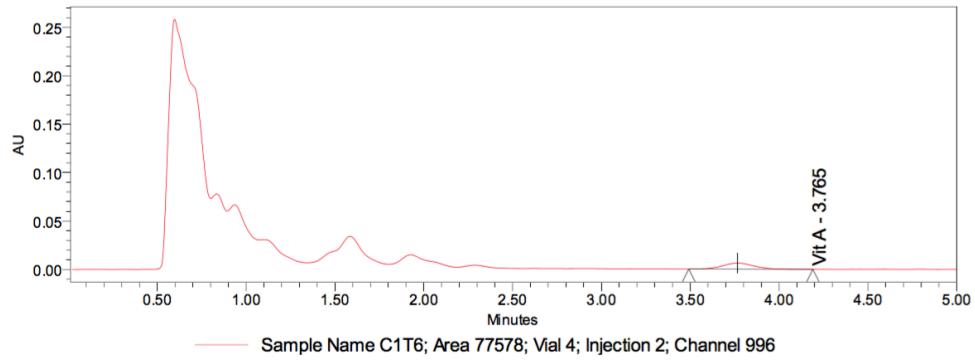

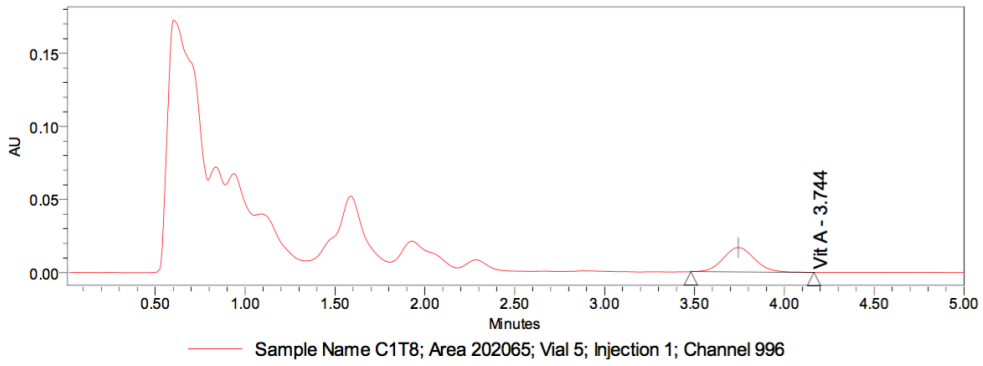

Sample Name C1T8; Area 202065; Vial 5; Injection 1; Channel 996

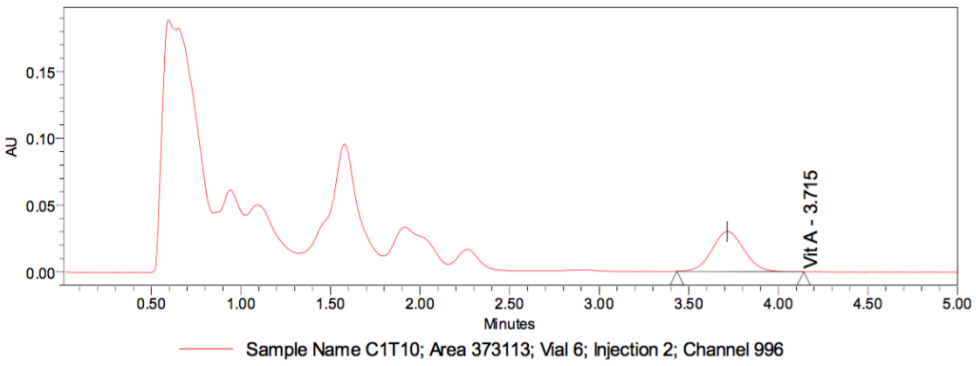

Sample Name C1T10; Area 373113; Vial 6; Injection 2; Channel 996

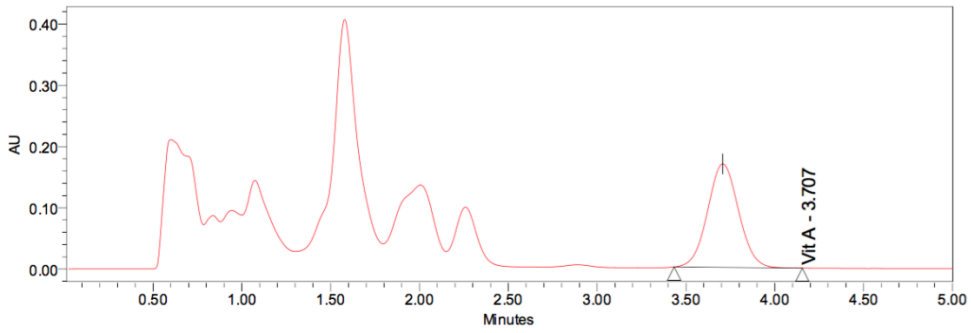

Sample Name C1T24; Area 2046123; Vial 8; Injection 1; Channel 996

Chromatograms of *Ex-Vivo* Permeation T6:

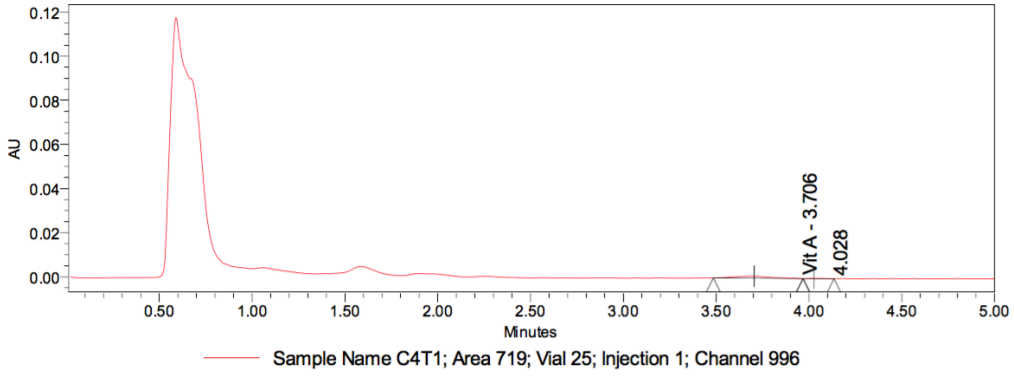

Sample Name C4T1; Area 719; Vial 25; Injection 1; Channel 996

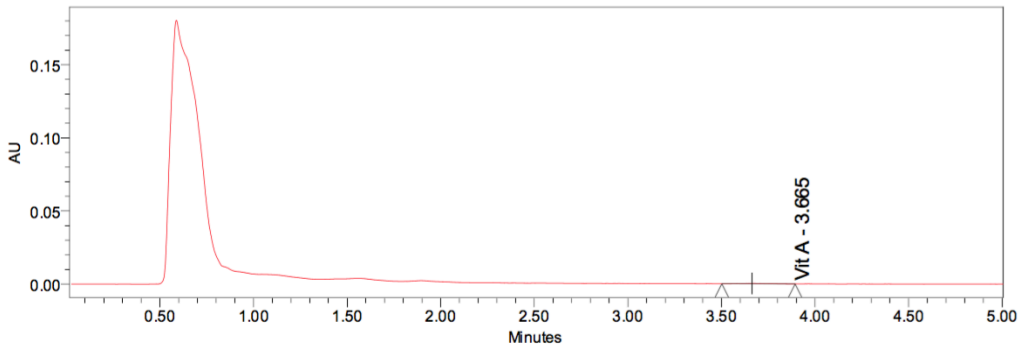

Sample Name C4T2; Area 4262; Vial 26; Injection 2; Channel 996

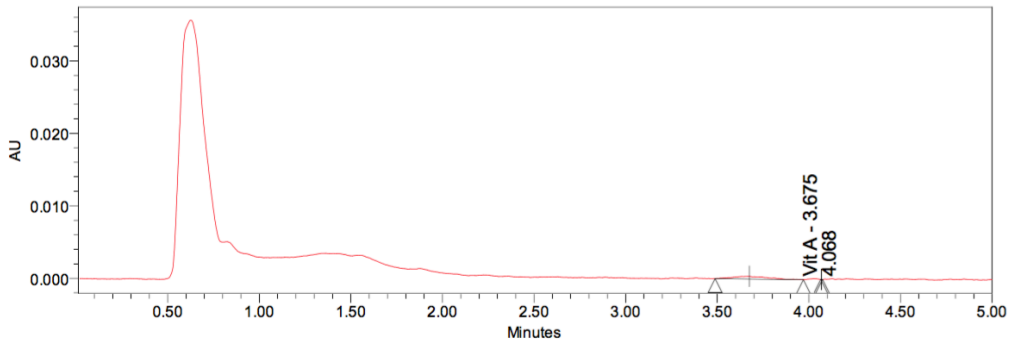

Sample Name C4T4; Area 4; Vial 27; Injection 1; Channel 996

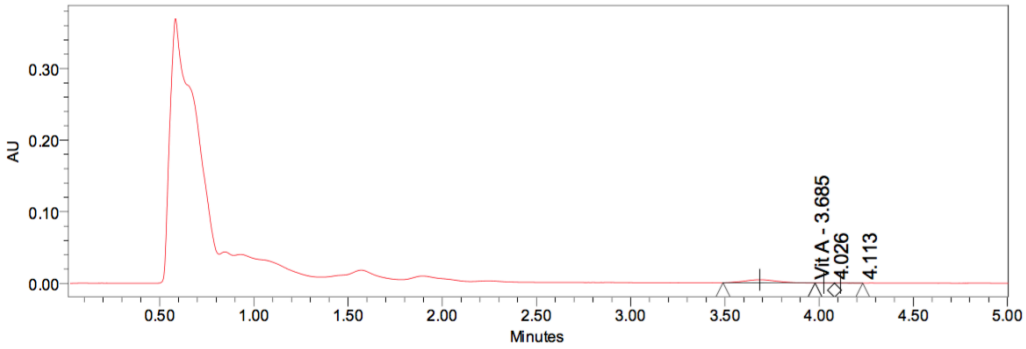

Sample Name C4T6; Area 464; Vial 28; Injection 2; Channel 996

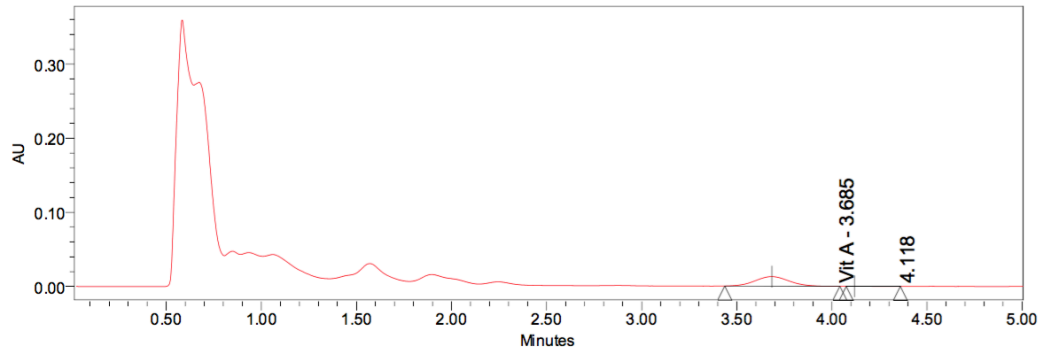

Sample Name C4T8; Area 1096; Vial 29; Injection 1; Channel 996

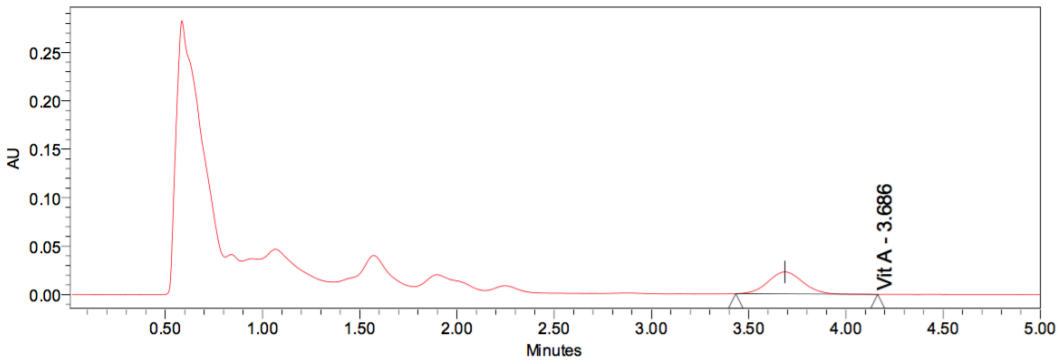

Sample Name C4T10; Area 280736; Vial 30; Injection 2; Channel 996

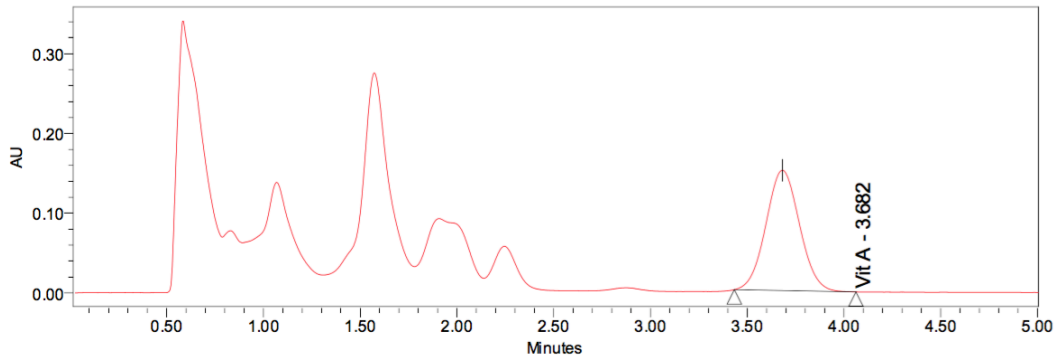

Sample Name C4T24; Area 1819956; Vial 32; Injection 1; Channel 996

Chromatograms of Skin Retention Studies of T2:

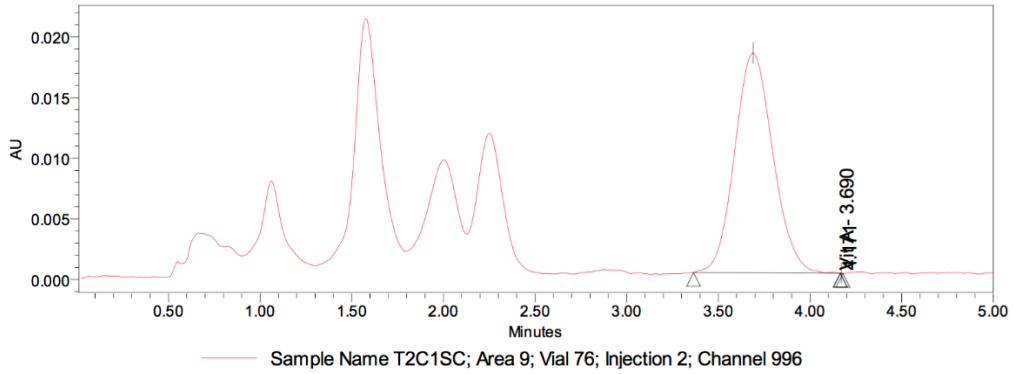

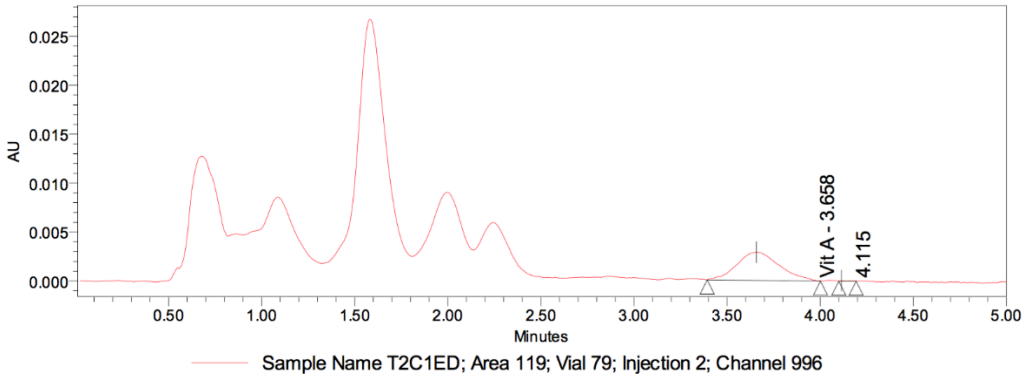

Chromatograms of Skin Retention Studies of T6:

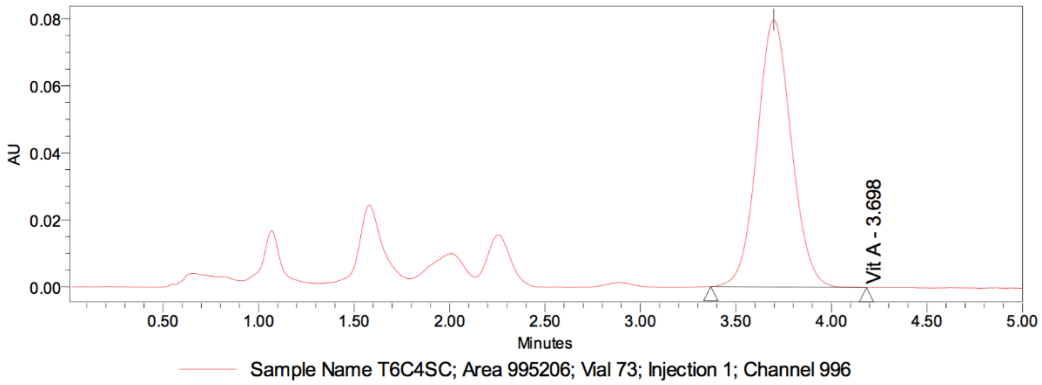

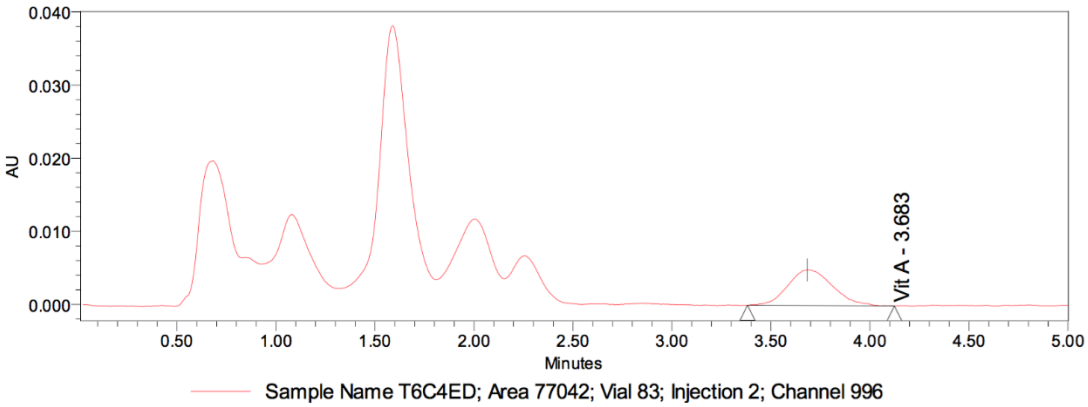

References

References

(1) Bello, S. "Cosmeceticals: A Review". *Afr. J. Pharm. Pharmacol.* **2010**, *4* (4), 127-129.

(2) Piga, A.; D'Aquino, S.; Agabbio, M.; M. Schirra. "Storage life and Quality Attributes of Cactus Pears cv "Gialla" as Affected by Packaging". *Agr. Med.* **1996**, *126* (1), 423–427.

(3) This is the reason Cleopatra and ancient Egyptians used essential oils every single day | The Hearty Soul https://theheartysoul.com/ancient-egyptian-essential-oils/ (accessed Nov 21, 2017).

(4) Raj, S.; Jose, S.; Sumod, U. S.; Sabitha, M. *J. Pharm.* "Nanotechnology in Cosmetics: Opportunities and Challenges". *Bioallied Sci.* **2012**, *4* (3), 186–193.

(5) Patravale, V. B.; Mandawgade, S. D. "Novel Cosmetic Delivery Systems: an Application Update". *Int. J. Cosmet. Sci.* **2008**, *30* (1), 19–33.

(6) Uchechi, O.; Ogbonna, J. D. N.; Attama, A. A. "Nanoparticles for Dermal and Transdermal Drug Delivery". In *Application of Nanotechnology in Drug Delivery*; Sezer, A. D., Ed.; InTech, **2014**. 194–223.

(7) Wikramanayake, T. C.; Stojadinovic, O.; Tomic-Canic, M. "Epidermal Differentiation in Barrier Maintenance and Wound Healing". *Adv. Wound Care* **2014**, *3* (3), 272–280.

(8) Oh, Y. K.; Kim, M. Y.; Shin, J.-Y.; Kim, T. W.; Yun, M.-O.; Yang, S. J.; Choi, S. S.; Jung, W.-W.; Kim, J. A.; Choi, H.-G. "Skin permeation of retinol in Tween 20-based deformable liposomes: in-vitro evaluation in human skin and keratinocyte models". *J. Pharm. Pharmacol.* **2006**, *58* (2), 161–166.

(9) Hua, S. "Lipid-based nano-delivery systems for skin delivery of drugs and bioactives". *Front. Pharmacol.* **2015**, *6*, 219-223.

(10) Sapino, S.; Carlotti, M. E.; Pelizzetti, E.; Vione, D.; Trotta, M.; Battaglia, L."Protective Effect of SLNs Encapsulation on the Photodegradation and Thermal Degradation of Retinyl Palmitate Introduced in Hydroxyethylcellulose Gel". *J. Drug Deliv. Sci. Technol.* **2005**, *15* (2), 159–165.

(11) Müller, R. H.; Mäder, K.; Gohla, S. "Solid lipid Nanoparticles (SLN) for Controlled Drug Delivery – a Review of the State of the Art". *Eur. J. Pharm. Biopharm.* **2000**, *50* (1), 161–177.

(12) Eldem, T.; Speiser, P.; Hincal, A. "Optimization of Spray-Dried and -Congealed Lipid Micropellets and Characterization of their Surface Morphology by Scanning Electron Microscopy". *Pharm. Res.* **1991**, *8* (1), 47–54.

(13) Pardeike, J.; Hommoss, A.; Müller, R. H. "Lipid Nanoparticles (SLN, NLC) in Cosmetic and Pharmaceutical Dermal Products". *Int. J. Pharm.* **2009**, *366* (1), 170–184.

(14) Müller, R. H.; Radtke, M.; Wissing, S. A. "Nanostructured Lipid Matrices for Improved Microencapsulation of Drugs". *Int. J. Pharm.* **2002**, *242* (1), 121–128.

(15) Naseri, N.; Valizadeh, H.; Zakeri-Milani, P. "Solid Lipid Nanoparticles and Nanostructured Lipid Carriers: Structure, Preparation and Application". *Adv. Pharm. Bull.* **2015**, *5* (3), 305–313.

(16) Jenning, V.; Schäfer-Korting, M.; Gohla, S. "Vitamin A-loaded Solid Lipid Nanoparticles for Topical Use: Drug Release Properties". *J. Control. Release.* **2000**, *66* (2), 115–126.

(17) Brantner, A.; Grein, E. "Antibacterial Activity of Plant Extracts Used Externally in Traditional Medicine". *J. Ethnopharmacol.* **1994**, *44* (1), 35–40.

(18) Thring, T. S.; Hili, P.; Naughton, D. P. "Anti-collagenase, Anti-Elastase and Anti-Oxidant Activities of Extracts from 21 Plants". *BMC Complement. Altern. Med.* **2009**, *9*. DOI: 10.1186/1472-6882-9-27.

(19) Estevez, A. Y.; Miller, S.; Self, Q. R.; Erlichman, J. S. "Assessment of Catalytic Activity and Oxidation-Reduction Potential of Custom-Synthesized Cerium Oxide Nanoparticles in Cell-Free Systems and Tissue". *Free Radic. Biol. Med.* **2014**, *76*, S80–S81.

(20) Get to Know Cactus Oil, the Natural Beauty Ingredient That Will Completely Transform Your Skin http://www.elle.com/beauty/makeup-skin-care/news/a27040/cactus-oil-for-skin/ (accessed Sep 6, 2017).

(21) Gustavo Barja. " Free Radicals and Aging". *Trends Neurosci.* **2004**, *27* (10), 595–600.

(22) Hoff, V. D. Why We Recommend Putting Cactus All Over Your Face http://www.elle.com/beauty/makeup-skin-care/news/a27040/cactus-oil-for-skin/ (accessed Nov 18, 2017).

(23) Morales, J. O.; Valdés, K.; Morales, J.; Oyarzun-Ampuero, F. "Lipid Nanoparticles for the Topical Delivery of Retinoids and Derivatives". *Nanomed.* **2015**, *10* (2), 253–269.

(24) Liu, J.; Hu, W.; Chen, H.; Ni, Q.; Xu, H.; Yang, X. "Isotretinoin-loaded Solid Lipid Nanoparticles with Skin Targeting for Topical Delivery". *Int. J. Pharm.* **2007**, *328* (2), 191–195.

(25) Carlotti, M. E.; Sapino, S.; Trotta, M.; Battaglia, L.; Vione, D.; Pelizzetti, E. "Photostability and Stability over Time of Retinyl Palmitate in an O/W Emulsion and in SLN Introduced in the Emulsion". *J. Dispers. Sci. Technol.* **2005**, *26* (2), 125–138.

(26) Mukherjee, S.; Ray, S.; Thakur, R. S. "Solid lipid nanoparticles: a modern formulation approach in drug delivery system". *Indian J. Pharm. Sci.* **2009**, *71* (4), 349–358.

(27) Jee, J.-P.; Lim, S.-J.; Park, J.-S.; Kim, C.-K. " Stabilization of all-trans Retinol by Loading Lipophilic Antioxidants in Solid Lipid Nanoparticles". *Eur. J. Pharm. Biopharm.* **2006**, *63* (2), 134–139.

(28) Akhavan, A.; Levitt, J. "Assessing retinol stability in a hydroquinone 4%/retinol 0.3% cream in the presence of antioxidants and sunscreen under simulated-use conditions: a pilot study". *Clin. Ther.* **2008**, *30* (3), 543–547.

(29) Ito, N.; Hirose, M.; Imaida, K. " Antioxidants: Carcinogenic and Chemopreventive Properties". In *Encyclopedia of Cancer (Second Edition)*; Bertino, J. R., Ed.; Academic Press: New York, 2002; pp 89–101.

(30) Prickly Pear Seed Oil and the Skin https://aromaticstudies.com/prickly-pear-seed-oil/ (accessed Sep 3, 2017).

(31) Melo, A.; Amadeu, M. S.; Lancellotti, M.; Hollanda, L. M. de; Machado, D.; Melo, A.; Amadeu, M. S.; Lancellotti, M.; Hollanda, L. M. de; Machado, D. "The Role of Nanomaterials in Cosmetics: National and International Legislative Aspects". *Quím. Nova* **2015**, *38* (4), 599–603.

(32) Mehnert, W.; Mäder, K. "Solid Lipid Nanoparticles: Production, Characterization and Applications". *Adv. Drug Deliv. Rev.* **2001**, *47* (2), 165–196.

(33) Weiss, J.; Decker, E. A.; McClements, D. J.; Kristbergsson, K.; Helgason, T.; Awad, T. "Solid Lipid Nanoparticles as Delivery Systems for Bioactive Food Components". *Food Biophys.* **2008**, *3* (2), 146–154.

(34) Unera, M.; Yener, G.; Erguven, M.; Karaman, E. F.; Gozde Utku, E. "Solid Lipid Nanoparticles and Nanostructured Lipid Carriers of Celecoxib for Topical Application – Preparation, Characterization and Drug Penetration Through Rat Skin". *Curr. Nanosci.* **2014**, *10* (4). DOI: 10.2174/15734137106661402182313O7.

(35) Jin Zhang; Purdon, C. H.; Smith, E. W. " Solid Lipid Nanoparticles for Topical Drug Delivery". *Am. J. Drug Deliv.* **2006**, *4* (4), 215–220.

(36) López-García, R.; Ganem-Rondero, A. "Solid Lipid Nanoparticles for Topical Drug Delivery". *J. Cosmet. Dermatol. Sci. Appl.* **2015**, *05* (02), 62–72.

(37) Liu, C.-H.; Wu, C.-T.; Fang, J.-Y. "Characterization and Formulation Optimization of Solid Lipid Nanoparticles in Vitamin K1 Delivery". *Drug Dev. Ind. Pharm.* **2010**, *36* (7), 751–761.

(38) Müller, R. H.; Radtke, M.; Wissing, S. A. "Solid Lipid Nanoparticles (SLN) and Nanostructured Lipid Carriers (NLC) in Cosmetic and Dermatological Preparations". *Adv. Drug Deliv. Rev.* **2002**, *54*, S131–S155.

(39) Ghanbarzadeh, S.; Hariri, R.; Kouhsoltani, M.; Shokri, J.; Javadzadeh, Y.; Hamishehkar, H. "Enhanced Stability and Dermal Delivery of Hydroquinone Using Solid Lipid Nanoparticles". *Colloids Surf. B.* **2015**, *136*, 1004–1010.

(40) Kushwaha, A. K.; Vuddanda, P. R.; Karunanidhi, P.; Singh, S. K.; Singh, S. "Development and Evaluation of Solid Lipid Nanoparticles of Raloxifene Hydrochloride for Enhanced Bioavailability". *BioMed Res. Int.* **2013**, *2013*, 584549.

(41) Müller, R. H.; Petersen, R. D.; Hommoss, A.; Pardeike, J. "Nanostructured Lipid Carriers (NLC) in Cosmetic Dermal Products". *Adv. Drug Deliv. Rev.* **2007**, *59* (6), 522–530.

(42) Fang, J.-Y.; Fang, C.-L.; Liu, C.-H.; Su, Y.-H. "Lipid Nanoparticles as Vehicles for Topical Psoralen Delivery: Solid Lipid Nanoparticles (SLN) Versus Nanostructured Lipid Carriers (NLC)". *Eur. J. Pharm. Biopharm.* **2008**, *70* (2), 633–640.

(43) Souto, E. B.; Wissing, S. A.; Barbosa, C.; Müller, R. H. "Development of a Controlled Release Formulation Based on SLN and NLC for Topical Clotrimazole Delivery". *Int. J. Pharm.* **2004**, *278*, 71–77.

(44) Argimón, M.; Romero, M.; Miranda, P.; Mombrú, Á.; Miraballes, I.; Zimet, P.; Pardo, H. "Development and Characterization of Vitamin A-Loaded Solid Lipid Nanoparticles for Topical Application". *J. Braz. Chem. Soc.* **2016**. *28* (7), 1177-1183.

(45) Jenning, V.; Gysler, A.; Schäfer-Korting, M.; Gohla, S. H. " Vitamin A Loaded Solid Lipid Nanoparticles for Topical Use: Occlusive Properties and Drug Targeting to the Upper Skin". *Eur. J. Pharm. Biopharm.* **2000**, *49* (3), 211–218.

(46) Jenning, V.; Gohla, S. "Encapsulation of Retinoids in Solid Lipid Nano-particles (SLN)". *J. Microencapsul.* **2000**, *18*, 149–158.

(47) Beatriz, C. "Nanoemulsions (NEs), Liposomes (LPs) and Solid Lipid nanoparticles (SLNs) for Retinyl Palmitate: Effect on Skin Permeation". *Int. J. Pharm.* **2014**, *473* (1–2), 591–598.

(48) Melot, M.; Pudney, P. D. A.; Williamson, A.-M.; Caspers, P. J.; Van Der Pol, A.; Puppels, G. J. "Studying the Effectiveness of Penetration Enhancers to Deliver Retinol through the Stratum Cornum by in Vivo Confocal Raman Spectroscopy". *J. Control. Release* **2009**, *138* (1), 32–39.

(49) Teixeira, Z.; Zanchetta, B.; Melo, B. A. G.; Oliveira, L. L.; Santana, M. H. A.; Paredes-Gamero, E. J.; Justo, G. Z.; Nader, H. B.; Guterres, S. S.; Durán, N. " Retinyl Palmitate Flexible Polymeric Nanocapsules: Characterization and Permeation Studies". *Colloids Surf. B.* **2010**, *81* (1), 374–380.

(50) Oliveira, M. B.; Prado, A. H. do; Bernegossi, J.; Sato, C. S.; Lourenço Brunetti, I.; Scarpa, M. V.; Leonardi, G. R.; Friberg, S. E.; Chorilli, M. "Topical Application of Retinyl Palmitate-Loaded Nanotechnology-Based Drug Delivery Systems for the Treatment of Skin Aging". *BioMed Res. Int.* **2014**, *2014*, 1–7.

(51) Pezeshki, A.; Ghanbarzadeh, B.; Mohammadi, M.; Fathollahi, I.; Hamishehkar, H. "Encapsulation of vitamin A palmitate in nanostructured lipid carrier (NLC)-effect of surfactant concentration on the formulation properties". *Adv. Pharm. Bull.* **2014**, *4* (Suppl 2), 563–568.

(52) Jeon, H. S.; Seo, J. E.; Kim, M. S.; Kan, M. H. "A Retinyl Palmitate-Loaded Solid Lipid Nanoparticle System: Effect of Surface Modification with Dicetyl Phosphate on Skin Permeation in Vitro and Anti-Wrinkle Effect in Vivo". *Int. J. Pharm.* **2013**, *452* (1–2), 311–320.

(53) Kikuchi, K.; Suetake, T.; Kumasaka, N.; Tagami, H. "Improvement of Photoaged Facial Skin in Middle-Aged Japanese Females by Topical Retinol (vitamin A alcohol): A Vehicle-Controlled, Double-Blind Study". *J. Dermatol. Treat.* **2009**, *20* (5), 276–281.

(54) Babamiri, K.; Nassab, R. "Cosmeceuticals: The Evidence Behind the Retinoids". *Aesthet. Surg. J.* **2010**, *30* (1), 74–77.

(55) Raza, K.; Singh, B.; Lohan, S.; Sharma, G.; Negi, P.; Yachha, Y.; Katare, O. P. "Nano-lipoidal Carriers of Tretinoin with Enhanced Percutaneous Absorption, Photostability, Biocompatibility and Anti-Psoriatic Activity". *Int. J. Pharm.* **2013**, *456* (1), 65–72.

(56) Ennouri, M.; Evelyne, B.; Laurence, M.; Hamadi, A. "Fatty Acid Composition and Rheological Behaviour of Prickly Pear Seed Oils". *Food Chem.* **2005**, *93* (3), 431–437.

(57) Chougui, N.; Tamendjari, A.; Hamidj, W.; Hallal, S.; Barras, A.; Richard, T.; Larbat, R. "Oil Composition and Characterization of Phenolic Compounds of Opuntia Ficus-Indica Seeds". *Food Chem.* **2013**, *139* (1–4), 796–803.

(58) El-Mostafa, K.; El Kharrassi, Y.; Badreddine, A.; Andreoletti, P.; Vamecq, J.; El Kebbaj, M. S.; Latruffe, N.; Lizard, G.; Nasser, B.; Cherkaoui-Malki, M. "Nopal Cactus (Opuntia ficus-indica) as a Source of Bioactive Compounds for Nutrition, Health and Disease". *Molecules.* **2014**, *19* (9), 14879–14901.

(59) Vinardell, M. P.; Mitjans, M. "Nanocarriers for Delivery of Antioxidants on the Skin". *Cosmetics* **2015**, *2* (4), 342–354.

(60) Carmo, C. S. do; Serra, A. T.; Duarte, C. M. M. "Recovery Technologies for Lipophilic Bioactives". In *Eng. Food for Bioac. Stab. and Del.*; Springer, New York, NY, **2017**; pp 1–49.

(61) Lasic, D. D. "Applications of Liposomes". *Handb. Biol. Phys.* **1995**, *1*, 491–519.

(62) Touitou, E.; Junginger, H. E.; Weiner, N. D.; Nagai, T.; Mezei, M. "Liposomes as Carriers for Topical and Transdermal Delivery". *J. Pharm. Sci.* **1994**, *83* (9), 1189–1203.

(63) Lopes, S. C. de A.; Giuberti, C. dos S.; Rocha, T. G. R.; Ferreira, D. dos S.; AmaralLeite, E.; Oliveira, M. C. "Liposomes as Carriers of Anticancer Drugs". *Cancer Treat. - Con. and Inn. App.* **2013**, 83-113. DOI 10.5772/55290.

(64) Akbarzadeh, A.; Rezaei-Sadabady, R.; Davaran, S.; Joo, S. W.; Zarghami, N.; Hanifehpour, Y.; Samiei, M.; Kouhi, M.; Nejati-Koshki, K. " Liposome: Classification, Preparation, and Applications". *Nanoscale Res. Lett.* **2013**, *8* (1), 102-111.

(65) Grit, M.; Crommelin, D. J. A. "Chemical Stability of Liposomes: Implications for their Physical Stability". *Chem. Phys. Lipids* **1993**, *64* (1), 3–18.

(66) Gregoriadis, G.; Florence, A. T.; Patel, H. M. *Liposomes in Drug Delivery*; Harwood Academic Publishers, **1993**, 15-28.

(67) Choi, M. J.; Maibach, H. I. "Liposomes and Niosomes as Topical Drug Delivery Systems". *Skin Pharmacol. Physiol.* **2005**, *18* (5), 209–219.

(68) Liers, H. Benefits of Liposomal Nutrients http://www.integratedhealthblog.com/benefits-of-liposomal-nutrients-liposomes-2/ (accessed Oct 16, 2017).

(69) Emulsion - Uses Of Emulsions http://science.jrank.org/pages/2461/Emulsion-Uses-emulsions.html (accessed Oct 30, 2017).

(70) Liberman, H. A.; Rieger, M. M.; Banker, G. S. *Pharmaceutical Dosage Forms - Disperse Systems*; Marcel Dekker Inc: New York, **1989**, pp 335-378.

(71) Hommos, A. Nanostructured Lipid Carriers (NLC) in Dermal and Personal Formulations. PhD. Dissertation, Freie Universitat Berlin, **2008**.

(72) Coelho, J. *Drug Delivery Systems: Advanced Technologies Potentially Applicable in Personalised Treatment*; Springer Science & Business Media, **2013**, 35–43.

(73) Gupta, A.; Eral, H. B.; Hatton, T. A.; Doyle, P. S. "Controlling and Predicting Droplet Size of Nanoemulsions: Scaling Relations with Experimental Validation." *Soft Matter* **2016**, 12 (11), 2826–2841.

(74) Benita, S.; Friedman, D.; Weinstock, M. "Pharmacological Evaluation of an Injectable Prolonged Release Emulsion of Physostigmine in Rabbits". *J. Pharm. Pharmacol.* **1986**, *38* (9), 653–658.

(75) Kligman, A. M. "The growing importance of topical retinoids in clinical dermatology: a retrospective and prospective analysis". *J. Am. Acad. Dermatol.* **1998**, *39* (2 Pt 3), S2-7.

(76) Chevalier, Y.; Bolzinger, M.-A. "Emulsions stabilized with solid nanoparticles: Pickering emulsions". *Colloids Surf. Physicochem. Eng. Asp.* **2013**, *439* (Supplement C), 23–34.

(77) Sacanna, S. " Thermodynamically Stable Pickering Emulsions". *Phys. Rev. Lett.* **2007**, *98* (15). DOI: 10.1103/PhysRevLett.98.158301.

(78) Soviapriya, S.; Daisy, P.A; Boby, J. G.; Praveen, R. R.; Thomas, N.; Carla, B. "Multiple Emulsions: A Comprehensive Review". *World J. Pharm. Med. Res.* **2016**, *2* (5), 83–88.

(79) McClements, D. J. " Nanoemulsions versus Microemulsions: Terminology, Differences, and Similarities". *Soft Matter* **2012**, *8* (6), 1719–1729.

(80) Euler, M. "Nanomaterials and Cosmetics". In *Nanotechnology in a Nutshell*; Ngô, C.; Voorde, M. H. V. Atlantis Press, Paris, **2014**; pp 311–319.

(81) Sanad, R. A. "Lipid Nanoparticles (SLNs and NLCs): Wide Range of Application from Cosmetics to Cancer Chemotherapy". *J. Drug Res. Egypt* **2014**, *35* (1), 73-78.

(82) Lucks, S.; Müller, R. Medication vehicles made of solid lipid particles (solid lipid nanospheres - SLN). EP0605497 B1, March 20, **1996**.

(83) Hussein, L.; Elsabee, M. Z.; Ismail, E. A.; Naguib, H. F.; Aziz, H. A.; Elsawy, M. A. "Transesterification of Jojoba Oil-Wax Using Microwave Technique". *Int J Env. Earth Sci Eng* **2014**, *8*, 248–252.

(84) E. Carlotti, M.; Sapino, S.; Vione, D.; Pelizzetti, E.; Ugazio, E.; Morel, S. "Study on the Photostability of Octyl-p-Methoxy Cinnamate in SLN". *J. Dispers. Sci. Technol.* **2005**, *26*, 809–816.

(85) Severino, P.; Andreani, T.; Macedo, A. S.; Fangueiro, J. F.; Santana, M. H.; Silva, A. M.; Souto, E. B. "Current State-of-Art and New Trends on Lipid Nanoparticles (SLN and NLC) for Oral Drug Delivery". *J. Drug Deliv.* **2012**. DOI: 10.1155/2012/750891

(86) Nikam, S.; Chavan, M.; Sharma, P. H. "Solid Lipid Nanoparticles: A Lipid Based Drug Delivery". *IPP.* **2014**, *2* (3), 365-376.

(87) Kammari, R.; Das, N. G.; Das, S. K. In *Emerging Nanotechnologies for Diagnostics, Drug Delivery and Medical Devices*; Micro and Nano Technologies; Elsevier: Boston, **2017**; pp 105-144.

(88) Shidhaye, S.; Vaidya, R.; Sutar, S.; Patwardhan, A.; Kadam, V. "Solid Lipid Nanoparticles and Nanostructured Lipid Carriers d-pharmaceutical-science/solid-lipid-nanoparticle" *J. Curr. Drug Deliv.* **2008**, *5*, 324-331.

(89) Abdelbary, G.; Fahmy, R. H. " Diazepam-Loaded Solid Lipid Nanoparticles: Design and Characterization". *AAPS PharmSciTech* **2009**, *10* (1), 211–219.

(90) Jafari, S. M. *Nanoencapsulation Technologies for the Food and Nutraceutical Industries*; Academic Press, **2017**; pp. 115-129.

(91) Muller, R.; Petersen, R.; Hommoss, A.; Pardeike, J. " Nanostructured Lipid Carriers (NLC) in Cosmetic Dermal Products". *Adv. Drug Deliv. Rev.* **2007**, *59* (6), 522–530.

(92) Pardeike, J.; Hommoss, A.; Müller, R. H. "Lipid Nanoparticles (SLN, NLC) in Cosmetic and Pharmaceutical Dermal Products". *Int. J. Pharm.* **2009**, *366* (1–2), 170–184.

(93) Kim, D.-G.; Jeong, Y.-I.; Choi, C.; Roh, S.-H.; Kang, S.-K.; Jang, M.-K.; Nah, J.-W. " Retinol-Encapsulated Low Molecular Water-Soluble Chitosan Nanoparticles". *Int. J. Pharm.* **2006**, *319* (1), 130–138.

(94) Ro, J.; Kim, Y.; Kim, H.; Park, K.; Lee, K.-E.; Khadka, P.; Yun, G.; Park, J.; Chang, S. T.; Lee, Jonghwi.; Jeong, J. H.; Lee, Jaehwi. "Pectin Micro- and Nano-capsules of Retinyl

Palmitate as Cosmeceutical Carriers for Stabilized Skin Transport". *Korean J. Physiol. Pharmacol.* **2015**, *19* (1), 59–64.

(95) Retinol - Chemistry Encyclopedia - structure, examples, number, molecule http://www.chemistryexplained.com/Pr-Ro/Retinol.html (accessed Sep 6, 2017).

(96) Liu, J.; Hu, W.; Chen, H.; Ni, Q.; Xu, H.; Yang, X. " Isotretinoin-Loaded Solid Lipid Nanoparticles with Skin Targeting for Topical Delivery". *Int. J. Pharm.* **2007**, *328* (2), 191–195.

(97) Bolomey, R. A. " Oxidative Decomposition of Vitamin A; Absorption Spectrophotometry of Oxidized Vitamin A". *J. Biol. Chem.* **1947**, *169* (2), 331–335.

(98) Arayachukeat, S.; Wanichwecharungruang, S. P.; Tree-Udom, T. " Retinyl Acetate-Loaded Nanoparticles: Dermal Penetration and Release of the Retinyl Acetate". *Int. J. Pharm.* **2011**, *404* (1), 281–288.

(99) Advanced Skin Technology http://www.advancedskintech.com/GCScience.htm (accessed Oct 30, 2017).

(100) Granger, S. P.; Scott, I. R.; Donovan, R. M.; Iobst, S. T.; Licameli, L. Method for treating skin with retinoids and retinoid boosters. US8409550 B2, April 2, 2013.

(101) Tolleson, W. H.; Cherng, S.-H.; Xia, Q.; Boudreau, M.; Yin, J. J.; Wamer, W. G.; Howard, P. C.; Yu, H.; Fu, P. P. " Photodecomposition and Phototoxicity of Natural Retinoids". *Int. J. Environ. Res. Public. Health* **2005**, *2* (1), 147–155.

(102) Ramadan, M. F.; Mörsel, J.-T. " Analysis of Glycolipids from Black cumin (Nigella sativa L.), Coriander (Coriandrum sativum L.) and Niger (Guizotia abyssinica Cass.) Oilseeds". *Food Chem.* **2003**, *80* (2), 197–204.

(103) Coşkuner, Y. n; Tekin, A. " Monitoring of Seed Composition of Prickly Pear (Opuntia ficus-indica L) Fruits During Maturation Period". *J. Sci. Food Agric.* **2003**, *83* (8), 846–849.

(104) Özcan, M. M.; Juhaimi, F. Y. A. " Nutritive Value and Chemical Composition of Prickly Pear Seeds (Opuntia ficus indica L.) Growing in Turkey". *Int. J. Food Sci. Nutr.* **2011**, *62* (5), 533–536.

(105) Fawzy Ramadan, M.; Mörsel, J.-T. " Phospholipid Composition of Niger (Guizotia Abyssinica Cass.) Seed Oil". *LWT - Food Sci. Technol.* **2003**, *36* (2), 273–276.

(106) Emerit, I. "Free Radicals and Aging of the Skin". *EXS* **1992**, *62*, 328-341.

(107) What Is Homogenization? https://www.pharmaceuticalonline.com/doc/what-is-homogenization-0001 (accessed Oct 30, 2017).

(108) Nano & the top 10 big cosmetics companies : L'Oréal, Procter & Gamble and Henkel on the podium for patents. *Nanocolors - the Nanotech 2.0 hub*, 2009.

(109) Jie Liu; Wen Hu; Huabing Chen; Qian Ni; Huibi Xu; Xiangliang Yang. " Isotretinoin-loaded Solid Lipid Nanoparticles with Skin Targeting for Topical Delivery". *Cosmetics.* **2007**, *328* (2), 191–195.

(110) Hu, F.-Q.; Jiang, S.-P.; Du, Y.-Z.; Yuan, H.; Ye, Y.-Q.; Zeng, S. "Preparation and Characteristics of Monostearin Nanostructured Lipid Carriers". *Int. J. Pharm.* **2006**, *314* (1), 83–89.

(111) Pople, P. V.; Singh, K. K. "Development and Evaluation of Topical Formulation Containing Solid Lipid Nanoparticles of Vitamin A". *AAPS PharmSciTech* **2006**, *7* (4), E63–E69.

(112) Sheikh, M. H. Separation of Copper-oxide Nanoparticles from Nanoparticle Enhanced Phase Change Material. MSc. Dissertation, The University of Alabama, **2013**.

(113) Pall, NANOSEP 3K, Omega membrane (end 9/27/2017 2:15 PM) https://www.lelong.com.my/pall-nanosep-3k-omega-membrane-mylaboratories-183388526-2017-09-Sale-P.htm (accessed Oct 21, 2017).

(114) Spectroscopy - Types of electromagnetic-radiation sources | science | Britannica.com https://www.britannica.com/science/spectroscopy/Types-of-electromagnetic-radiation-sources (accessed Dec 27, 2017).

(115) Daniel C. Harris. *Quantitative Chemical Analysis*, 7th ed.; W.H. Freeman and Company: New York, **2007**; pp. 380-387.

(116) Pavia, D. L.; Lampman, G. M.; Kriz, G. S.; Vyvyan, J. A. *Introduction to Spectroscopy*; Cengage Learning, **2014**; pp. 353-385.

(117) Double beam - UV-VIS-NIR Spectrophotometer http://www.holmarc.com/spectrophotometer_uv_vis.php (accessed Nov 1, 2017).

(118) Spectrophotometry https://www.slideshare.net/suniu/spectrophotometry-16091660 (accessed Nov 1, 2017).

(119) Coskun, O. "Separation techniques: Chromatography". *North. Clin. Istanb.* **2016**, *3* (2), 156-160.

(120) Lakshmi, S.. "A Review on Chromatography with High Performance Liquid Chromatography (HPLC) and its Functions". *Res. Rev. J. Pharm. Anal.* **2015**, *4* (1), 1-15.

(121) What is the Difference Between UHPLC and UPLC? Chromatography Today https://www.chromatographytoday.com/news/hplc-uhplc-lc-ms/31/breaking_news/what_is_the_difference_between_uhplc_and_uplc/30754 (accessed Nov 24, 2017).

(122) Savarala, S. Controlling DNA compaction with cationic amphiphiles for efficient delivery systems A step forward towards non-viral Gene Therapy. PhD. Dissertation, Temple University, **2012**.

(123) Thermal Analysis Solutions and Beyond https://www.perkinelmer.com/lab-solutions/resources/docs/BRO_DSCFamilyBrochure.pdf (accessed Dec 27, 2017).

(124) Chiu, M. H.; Prenner, E. J. " Differential Scanning Calorimetry: An Invaluable Tool for a Detailed Thermodynamic Characterization of Macromolecules and their Interactions". *J. Pharm. Bioallied Sci.* **2011**, *3* (1), 39-59.

(125) Transmission Electron Microscopy | Central Microscopy Research Facility https://cmrf.research.uiowa.edu/transmission-electron-microscopy (accessed Nov 1, 2017).

(126) Fultz, B.; Howe, J. *Transmission Electron Microscopy and Diffractometry of Materials | Brent Fultz* Springer; **2013**; pp. 59-115.

(127) Sheikh, L. Study of Novel Nanomagnetic Hydroxyapatite as a Potent Biomedical System. MSc. Dissertation, North Orissa University, Baripada, **2012**.

(128) Backscattered Electrons • Materials Science and Engineering • Iowa State University https://www.mse.iastate.edu/research/laboratories/sem/microscopy/how-does-the-sem-work/high-school/how-the-sem-works/backscattered-electrons/ (accessed Nov 1, 2017).

(129) Spotlight on Science: Scanning Electron Microscopy | Out of the Depths: a Paleontologist's Adventures at Sea https://geologelizabeth.wordpress.com/2014/03/26/spotlight-on-science-scanning-electron-microscopy/ (accessed Nov 1, 2017).

(130) Zhou, W.; Apkarian, R.; Wang, Z. L.; Joy, D. "Fundamentals of Scanning Electron Microscopy". In *Scanning microscopy for nanotechnology*; Zhou, W; Wang, Z. L. Springer, 2006; pp 1–40.

(131) Transmission Electron Microscope (TEM) - Uses, Advantages and Disadvantages http://www.microscopemaster.com/transmission-electron-microscope.html (accessed Dec 30, 2017).

(132) Atomic World - Transmission electron microscope (TEM) - Principle of TEM http://www.hk-phy.org/atomic_world/tem/tem02_e.html (accessed Nov 1, 2017).

(133) Transmission Electron Microscope (TEM) http://www.saha.ac.in/web/index.php?option=com_content&view=article&id=1729&Itemid=2682 (accessed Nov 1, 2017).

(134) Hanson, R.; Heaney, J. "A Primer on Automating the Vertical Diffusion Cell (VDC)" *Dissolution Technol.* **2013**, *20* (2), 40–43.

(135) Kaszuba, M.; McKnight, D.; Connah, M. T.; McNeil-Watson, F. K.; Nobbmann, U. "Measuring Sub Nanometre Sizes Using Dynamic Light Scattering". *J. Nanoparticle Res.* **2008**, *10* (5), 823–829.

(136) Salminen, H.; Gömmel, C.; Leuenberger, B. H.; Weiss, J. " Influence of Encapsulated Functional Lipids on Crystal Structure and Chemical Stability in Solid Lipid Nanoparticles: Towards Bioactive-Based Design of Delivery Systems". *Food Chem.* **2016**, *190* (Supplement C), 928–937.

(137) Lu, G. W.; Gao, P. In *Handbook of Non-Invasive Drug Delivery Systems*; Kulkarni, V. S., Ed.; Personal Care & Cosmetic Technology; William Andrew Publishing: Boston, 2010; pp 59part

(138) Carneiro-da-Cunha, M. G.; Cerqueira, M. A.; Souza, B. W. S.; Teixeira, J. A.; Vicente, A. A. " Influence of Concentration, Ionic Strength and pH on Zeta Potential and Mean Hydrodynamic Diameter of Edible Polysaccharide Solutions Envisaged for Multinanolayered Films Production". *Carbohydr. Polym.* **2011**, *85* (3), 522-528.

(139) Glyceryl Stearate | Cosmetics Info http://www.cosmeticsinfo.org/ingredient/glyceryl-stearate (accessed Oct 14, 2017).

(140) CETEARYL ALCOHOL || Skin Deep® Cosmetics Database | EWG https://www.ewg.org/skindeep/ingredient/701236/CETEARYL_ALCOHOL/#.WeKYpNwstp8 (accessed Oct 14, 2017).

(141) Labuschagne, M. t.; Hugo, A. "Oil Content and Fatty Acid Composition of Cactus Pear Seed Compared with Cotton and Grape Seed". *J. Food Biochem.* **2010**, *34* (1), 93–100.

(142) STEARETH-21 || Skin Deep® Cosmetics Database | EWG https://www.ewg.org/skindeep/ingredient/724159/STEARETH-21/#.WeLEtleQJp8 (accessed Oct 15, 2017).

(143) Brij™ S721 by Croda Inc. - Personal Care & Cosmetics https://www.ulprospector.com/en/na/PersonalCare/Detail/134/50801/Brij-S721 (accessed Oct 15, 2017).

(144) Dow Answer Center https://dowac.custhelp.com/app/answers/detail/a_id/3277/~/surfactant-basics---definition-of-hlb%2C-and-how-it-applies-to-emulsions (accessed Oct 15, 2017).

(145) Phosphatidylcholine - Scientific Review on Usage, Dosage, Side Effects | Examine.com https://examine.com/supplements/phosphatidylcholine/ (accessed Oct 14, 2017).

(146) Lecithin and Phospholipids: A Simple Guide to Use and Selection http://www.ethorn.com/ssw/files/American%20Lecithin%20Company.pdf (accessed Dec 27, 2017).

(147) Aykas, D. P.; Barringer, S. "The Effect of Temperature, Lecithin Content and Voltage on Droplets/cm2 during Electrostatic Spraying of Oil". *J. Food Process. Preserv.* **2014**, *38* (1), 484–492.

(148) Carafa, M.; Marianecci, C.; Salvatorelli, M.; Di Marzio, L.; Cerreto, F.; Lucania, G.; Santucci, E. "Formulations of Retinyl Palmitate included in Solid Lipid Nanoparticles: Characterization and influence on Light-induced Vitamin Degradation". *J. Drug Deliv. Sci. Technol.* **2008**, *18* (2), 119–124.

(149) Jung, Y. J.; Truong, N. K. V.; Shin, S.; Jeong, S. H. "A Robust Experimental Design Method to Optimize Formulations of Retinol Solid Lipid Nanoparticles". *J. Microencapsul.* **2013**, *30* (1), 1–9.

(150) Pal, R. *Rheology of Particulate Dispersions and Composites*; CRC Press, 2006; pp 5–7.

(151) Montgomery, D. C. *Design and Analysis of Experiments*; John Wiley & Sons, 2008; pp 233–252.

(152) Kielhorn, J.; Mangelsdorf, I. *Dermal Absorption*; World Health Organization, 2006; pp 38–78.

(153) Dickel, H.; Goulioumis, A.; Gambichler, T.; Fluhr, J. W.; Kamphowe, J.; Altmeyer, P.; Kuss, O. "Standardized Tape Stripping: a Practical and Reproducible Protocol to Uniformly Reduce the Stratum Corneum". *Skin Pharmacol. Physiol.* **2010**, *23* (5), 259–265.

(154) Akbari, J.; Saeedi, M.; Morteza-Semnani, K.; Rostamkalaei, S. S.; Asadi, M.; Asare-Addo, K.; Nokhodchi, A. "The Design of Naproxen Solid Lipid Nanoparticles to Target Skin Layers". *Colloids Surf. B.* **2016**, *145*, 626–633.

(155) Kashanian, S.; Azandaryani, A. H.; Derakhshandeh, K. "New Surface-Modified Solid Lipid Nanoparticles Using N-glutaryl Phosphatidylethanolamine as the Outer Shell". *Int. J. Nanomedicine.* **2011**, *6*, 2393–2401.

(156) Pathak, P.; Nagarsenker, M. "Formulation and Evaluation of Lidocaine Lipid Nanosystems for Dermal Delivery". *AAPS PharmSciTech.* **2009**, *10* (3), 985–992.

(157) Ibrahim, W. M.; AlOmrani, A. H.; Yassin, A. E. "Novel sulpiride-loaded solid lipid nanoparticles with enhanced intestinal permeability". *Int. J. Nanomedicine.* **2014**, *9*, 129–144.

(158) Hanumanaik, M.; Sree, R.; Patel, S. K. "Solid Lipid Nanoparticles: a Review". *Int J Pharm Sci and Res* **2013**, *4* (3), 928–940.

(159) Zirak, M. B.; Pezeshki, A. "Effect of Surfactant Concentration on the Particle Size, Stability and Potential Zeta of Beta carotene Nano Lipid Carrier". *Int J Curr Microbiol App Sci* **2015**, *4* (9), 924–932.

(160) Jenning, V.; Thünemann, A. F.; Gohla, S. H. "Characterisation of a novel solid lipid nanoparticle carrier system based on binary mixtures of liquid and solid lipids". *Int. J. Pharm.* **2000**, *199* (2), 167–177.

(161) Mitra, A. K.; Cholkar, K.; Mandal, A. *Emerging Nanotechnologies for Diagnostics, Drug Delivery and Medical Devices*; William Andrew, 2017; pp 105-121.

(162) Jores, K.; Mehnert, W.; Drechsler, M.; Bunjes, H.; Johann, C.; Mäder, K. "Investigations on the Structure of Solid Lipid Nanoparticles (SLN) and Oil-Loaded Solid Lipid Nanoparticles by Photon Correlation Spectroscopy, Field-Flow Fractionation and Transmission Electron Microscopy". *J. Control. Release* **2004**, *95* (2), 217–227.

(163) Kulkarni, V. S.; Shaw, C. *Essential Chemistry for Formulators of Semisolid and Liquid Dosages*; Academic Press: Amsterdam, 2015; pp 5–28.

(164) Thassu, D.; Chader, G. J. *Ocular Drug Delivery Systems: Barriers and Application of Nanoparticulate Systems*; CRC Press/Taylor & Francis: Boca Raton, 2012; pp 3–10.

(165) Pamudji, J. S.; Mauludin, R.; Indriani, N. "Development of Nanostructured Lipid Carrier Formulation Containing of Retinyl Palmitate". *Int. J. Pharm. Pharm. Sci.* **2016**, *8* (2), 256–260.

(166) Freitas, C.; Müller, R. H. "Effect of Light and Temperature on Zeta Potential and Physical Stability in Solid Lipid Nanoparticle (SLN™) Dispersions". *Int. J. Pharm.* **1998**, *168* (2), 221–229.

(167) Ekambaram, P.; Abdul, H. S. A. "Formulation and Evaluation of Solid Lipid Nanoparticles of Ramipril". *J. Young Pharm. JYP* **2011**, *3* (3), 216–220.

(168) Bardow, A.; Göke, V.; Koß, H.-J.; Lucas, K.; Marquardt, W. "Concentration-Dependent Diffusion Coefficients from a Single Experiment using Model-based Raman Spectroscopy". *Fluid Phase Equilibria* **2005**, *228–229*, 357–366.

(169) Trommer, H.; Neubert, R. H. H. "Overcoming the Stratum Corneum: The Modulation of Skin Penetration". *Skin Pharmacol. Physiol.* **2006**, *19* (2), 106–121.

(170) Ibrahim, S. A.; Li, S. K. "Efficiency of Fatty Acids as Chemical Penetration Enhancers: Mechanisms and Structure Enhancement Relationship". *Pharm. Res.* **2010**, *27* (1), 115–125.

(171) Jeon, H. S.; Seo, J. E.; Kim, M. S.; Kang, M. H.; Oh, D. H.; Jeon, S. O.; Seong Hoon Jeong; Choi, Y. W.; Lee, S. "A Retinyl Palmitate-Loaded Solid Lipid Nanoparticle System: Effect of Surface Modification with Dicetyl Phosphate on Skin Permeation in Vitro and Anti-Wrinkle Effect in Vivo". *Int. J. Pharm.* **2013**, *452* (1), 311–320.

(172) Mason, T. G. "New Fundamental Concepts in Emulsion Rheology". *Curr. Opin. Colloid Interface Sci.* **1999**, *4* (3), 231–238.